DEVELOPMENT OF IMPROVED LOX COMPATIBLE LAMINATED GASKET COMPOSITE

By Don Marano and William G. Scheck

Prepared under Contract No. NAS 8-5053 by
WHITTAKER CORPORATION
Narmco Research & Development Division
San Diego, Calif.

for

NATIONAL AERONAUTICS AND SPACE ADMINISTRATION

WHITTAKER CORPORATION
Narmco Research & Development Division
San Diego, Calif.

DEVELOPMENT OF IMPROVED LOX COMPATIBLE LAMINATED GASKET COMPOSITE

16 June 1965 – 16 June 1966

By Don Marano and William G. Scheck

FINAL SUMMARY REPORT
Contract NAS 8-5053
Control No. 1-5-54-01170-01 (1F), and S1 (1F)

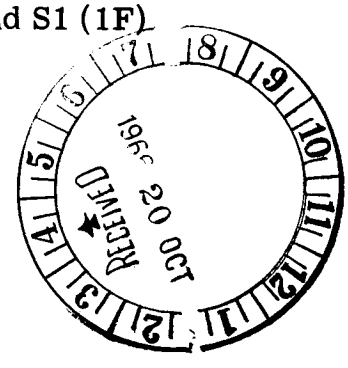

August 1966

Nonmetallic Materials Branch
Materials Division
Propulsion and Vehicle Engineering Laboratory
National Aeronautics and Space Administration
George C. Marshall Space Flight Center
Huntsville, Alabama

PREFACE

This report was prepared by Whittaker Corporation, Narmco Research & Development Division, San Diego, California, under Contract NAS 8-5053, "Development of Improved LOX-Compatible Laminated Gasket Material," for the George C. Marshall Space Flight Center of the National Aeronautics and Space Administration. The work was administered under the technical direction of the Nonmetallic Materials Branch, Materials Division, Propulsion and Vehicle Engineering Laboratory of the George C. Marshall Space Flight Center with Mr. James E. Curry acting as project manager.

ABSTRACT

Various testing procedures, including load decay, compressive modulus, and leak, were made to develop a new cryogenic gasket compatible with liquid oxygen (LOX). These testing procedures were also employed to demonstrate shortcomings of existing cryogenic gaskets, including fiberglass-filled Teflon, encapsulated, and impregnated asbestos. Data are presented indicating that cold flow is the major problem of fluorocarbon polymers, which are frequently considered because of the LOX compatibility. Attempts were made to restrict the cold flow of the fluorocarbon materials by utilizing various fillers and encapsulated configurations. Conventional fillers, reinforcements, and encapsulation techniques were not effective in minimizing cold flow to the required extent. Further consideration of the need to overcome this problem led to the development of a glass fabric laminated structure in which the glass fiber bundle was not completely saturated with fluorocarbon polymer binder. This permitted mechanical compressibility, not subject to drastic changes in compressive modulus when exposed to cryogenic temperatures.

Some design criteria data are presented along with a theoretical analysis for predicting flange loads and internal pressure sealing capabilities.

Various configurations utilizing the flat gasket concept are described, including O-rings, chevron seals, lip seals, ball seals, diaphragms, and flexible tubing. Process techniques are described for all configurations.

Leak test data and compression versus deflection data are presented for the configurations showing promise.

Also discussed are the studies conducted for specific applications of the composite gasket material.

The program has resulted in the development of a LOX compatible composite gasket material for use at temperatures as low as -423°F which does not require lengthy torquing sequences to effect a gasket seal, is reusable, and does not exhibit cold flow. The composite material can also be fabricated into various configurations, retaining most of the desirable properties.

TABLE OF CONTENTS

TABLE OF CONTENTS (Continued)

LIST OF ILLUSTRATIONS

LIST OF ILLUSTRATIONS (Continued)

LIST OF ILLUSTRATIONS (Continued)

LIST OF ILLUSTRATIONS (Continued)

LIST OF ILLUSTRATIONS (Continued)

LIST OF ILLUSTRATIONS (Continued)

LIST OF ILLUSTRATIONS (Continued)

LIST OF TABLES

LIST OF TABLES (Continued)

LIST OF TABLES (Continued)

LIST OF TABLES (Continued)

NOMENCLATURE

A	area, $in.^2$
B	bolt force, lb
C	defined parameter
E	modulus of elasticity, $lb/in.^2$
F	force applied to gasket, lb
K	experimental constant
L	length, in.
N	number of bolts
a	gasket inside radius, in.
b	gasket outside radius, in.
d	nominal bolt diameter, in.
g	gasket thickness (uncompressed), in.
h	flange thickness (assumed the same for both flanges)
p	pressure (i, inside; o, outside), psia
t	temperature, °F
α	coefficient of linear expansion, in./in./°F
δ	compressed gasket thickness, in.
Δ	increment
ϵ	strain, in./in.
σ	normal stress, $lb/in.^2$

Subscripts:

a	ambient
b	bolt
c	cryogenic
f	flange
g	gasket
t	total
1	unpressurized
2	pressurized

DEVELOPMENT OF IMPROVED LOX-COMPATIBLE LAMINATED GASKET MATERIAL

By Don Marano and William G. Scheck
Whittaker Corporation
Narmco Research & Development Division

SUMMARY

The overall objective of this program was to develop, fabricate, and test a new LOX compatible sealing concept for utilization on the Saturn vehicle system. An encapsulated laminated composite of Teflon and glass was developed and utilized for the fabrication of various types of seals. The type of seals developed include flat gaskets, O-rings, chevron, and lip seals. These seals have proven applicability at temperatures of -297°F, -320°F, and -423°F. The flat laminated gasket composite is currently being utilized for critical applications on the Saturn vehicle system.

INTRODUCTION

Cryogenic engineering technology is continually being expanded to keep pace with the development and refinement of aerospace vehicles that use cryogenic fluids. One of the more critical areas of concern today is the gasketing of cryogenic fuel lines in rockets and missiles. The work described in this report, while sponsored by the National Aeronautics and Space Administration specifically for the Saturn V launch vehicle, has application wherever liquid oxygen (LOX) and liquid hydrogen gaskets are required.

Program Objectives

Only one composite gasket material is presently qualified for use in the LOX system of the Saturn space vehicle. This material, Allpax 500 Superheat Sheet, is a styrene-butadiene copolymer reinforced with asbestos fiber. In order to render it satisfactory in terms of LOX compatibility, it must be impregnated with Fluorolube, a chlorofluorocarbon. This is a tedious process, requiring batch-to-batch LOX compatibility testing for quality control. Furthermore, this gasket material occasionally leaks.

Other gasket materials with satisfactory LOX compatibility include:

1. Braided Teflon
2. Bleached fluorocarbon felt
3. Teflon and asbestos fibers

4. Teflon and ceramic fibers

5. Teflon and glass fibers

6. Viton A and asbestos

7. Chrome tanned leather and Fluorolube

However, none of these proprietary gasket materials has the proper combination of physical properties that would make it suitable for use with the existing flanges in the Saturn LOX systems.

Narmco Research & Development therefore proposed to develop suitable gasket materials having satisfactory LOX compatibility without requiring special treatment. In addition, the physical properties of the developed materials were to equal or exceed those of the materials now used in this application. To satisfy these objectives, the following criteria had to be met:

1. The materials had to be capable of maintaining a tight seal under helium gas pressure up to 200 psi at temperatures below -297°F.

2. Compression properties had to be adequate for this application.

3. The materials had to be compatible with LOX, such that there would be no ignition, explosion, charring, or other evidence of chemical reaction during LOX-impact testing.*

Additional program objectives, which evolved as the work progressed, included optimization of the developed Teflon-glass laminate concept, encapsulation of individual gaskets, the determination of physical properties and leak-sealing capabilities of the gasket composite, and the development of analytical methods for predicting gasket performance.

The gasket composite concept was finally utilized with the object of developing processing techniques for seal configurations other than flat gaskets, including O-rings, chevron, lip and ball valve seals, control valve diaphragms, and flexible tubing.

Program Approach

Before investigating new gasket materials, the existing material was extensively evaluated in order to establish a point of reference. Fluorocarbon, oil-treated Allpax 500 was the logical choice because of its current use in LOX systems. Data on this gasket would enable more effective evaluation of the improvement in each of the several gasket properties desired, including

1. Little or no cold flow or creep at ambient temperature

* This test is delineated in Reference 1.

2. Little or no compression set at ambient temperature

3. Retention of some degree of flexibility at cryogenic temperatures

4. Generally good sealing characteristics at ambient and cryogenic temperatures

5. Complete lack of reaction upon impact in LOX

6. Reusability

In selecting materials, one of the most restrictive of the above requirements was LOX compatibility. This requirement eliminated binder materials which were not of a highly halogenated nature. Highly fluorinated resins were the only materials with a proven capability of fulfilling this need.

Several tests were designed to evaluate the properties listed above. All tests initially conceived were employed for a more comprehensive evaluation of Allpax 500. To avoid duplicating the evaluation of a critical property, or one which was not the crux of performance shortcomings, several tests, such as stress relaxation, were not continued for all the materials under study.

Other tests, including load cycling and leak tests, were modified to make them more meaningful. This was accomplished by changing either the equipment or the procedure. The latter method was used in the leak test, where the minimal flange pressure necessary to prevent leakage was found to be quite similar for most materials. The data also provided a test value more descriptive of the differences between good and poor gaskets. It was called "flange deflection to leak," and actually measured the distance a flange could be removed from its original sealing position before leakage occurred.

Examination of commerical cryogenic gaskets revealed that most of the design concepts were directed toward containing or restricting cold flow by confining the polyfluorocarbon, filling it with solids, or using it as an encapsulating material for another system which may or may not have LOX compatibility. All of these concepts were investigated in this program. One of the most informative tests carried out on the specimens was that of load cycling. Results from this single test were used to evaluate cold flow, compression set, relaxation, and reusability. They were also applicable to the calculation of the relative degree of compressibility at room temperature and at -320°F.

Results of the load cycling tests pointed the way to an ideal cryogenic gasket concept. Allpax 500 is well reinforced with asbestos fibers. Under testing, it was found that the material had a cold flow problem and also did not have cryogenic flexibility. On the other hand, some measure of cryogenic

flexibility was attained by moderate reinforcement of fluorocarbons with short fiberglass segments, but the restriction of cold flow was insufficient. This suggested the design concept of using long glass fibers for the reinforcement of polyfluorocarbons and then using the fibers in the form of woven fabrics, which were combined with the binder in a conventional laminated configuration. Thus, the fiber bundle in the fabric restricted cold flow by effective reinforcement.

Although the glass fabric provided reinforcement, it did not seriously decrease the compressibility of the laminate. This was a principal result of the method chosen for fabrication, which prevented complete wetting of the fiber bundle. This resulted in a mechanical compressibility best suited for cryogenic applications, one that was not drastically affected by the decrease in temperature.

Thus, a gasket design was conceived utilizing a Teflon-glass fabric laminate.

An extensive process technology evaluation of two different polytetrafluoroethylene material suppliers and both the lamination and encapsulation processing was conducted. In order to determine the effects of the various processing variables, a simple, inexpensive test (compression versus deflection) was utilized as the response item to changes in processing. The secondary evaluation of a particular fabrication process was a leak test with helium gas at -320°F with a small (2 $in.^2$) gasket. The final proof of any of the processes evaluated was a helium gas leak test with 4-, 8-, and 12-in. diameter gaskets at 75°F and -320°F.

The physical and mechanical properties (i.e., coefficient of thermal expansion, Poisson's ratio, and Young's compressive modulus of elasticity) of the laminated gasket composite were determined at 75°F, -320°F, and -423°F. These property values were required for use in the analytical expressions.

The newly developed laminated gasket composite was tested only at 75°F and -320°F early in the program. Since portions of the Saturn launch system use liquid hydrogen, the leak-sealing capability of the gasket composite had to be determined at this temperature. A special test fixture for use at -423°F was developed which measured helium gas leakage, if any, on the 2 $in.^2$ gasket at 75°F and -423°F.

In some sections of the Saturn vehicle, the sealing agent will conceivably be at some elevated temperature before the passage of the cryogenic fluid. The effects of thermal cycling were determined by developing a test fixture that maintained the flange pressure and measured helium gas leakage at both the elevated and cryogenic test temperatures.

An additional task of this program was to fabricate laminated gasket composites for specific applications. Several of these applications are discussed in this report.

MATERIALS INVESTIGATION AND DEVELOPMENT

Various testing procedures, including those for load decay, compressive modulus, and leakage, were devised to develop a new cryogenic gasket compatible with LOX and to demonstrate shortcomings of existing cryogenic gaskets. Data on fluorocarbon polymers, which are frequently given consideration because of their LOX compatibility, indicated that there is a cold flow problem with these materials. Attempts were made to restrict this cold flow by utilizing various fillers and encapsulated configurations. The problem was not solved, however, as the gasket continued to lose compressibility when the cold flow was controlled. This problem led to the development of a glass fabric laminated structure in which the glass fiber bundle was not completely saturated with fluorocarbon polymer binder. This permitted mechanical compressibility without a drastic change in compressive modulus during exposure to cryogenic temperatures. Sealing studies demonstrated the ability of the laminated gasket to maintain flange sealing pressure even though the flange was moved an appreciable distance. This is expressed as a coefficient, describing permissible flange deflection per unit thickness of the gasket before a leak occurs.

Stress-Relaxation Studies

These studies were carried out with Allpax 500 at low load levels and under cyclic loading. Loading levels of 2250 psi, 1500 psi, and 1000 psi were used to investigate relaxation properties. Tests were made using the fixture shown in Figures 1 through 3.

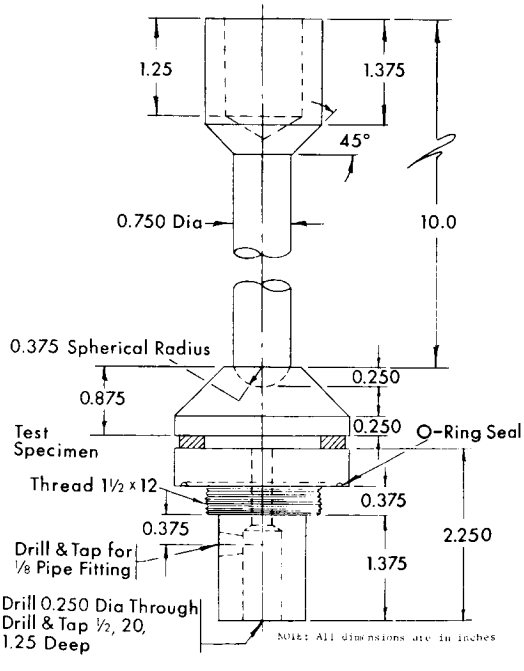

Figure 1. Test Fixture for Cryogenic Gaskets

Specimens for these tests and subsequent tests discussed in this report were circular, flat gaskets with an outside diameter of 2.06 in. and an inside diameter of 1.31 in., resulting in an area of 2 in^2. When flat sheet stock was tested, a specimen was cut with the die depicted in Figure 4. All specimens of Allpax 500 were Fluorolube-treated.

The sample was installed in the fixture and the fixture assembled in the cryostat. A slight load (50 psi) was then applied. Liquid nitrogen was added and the system allowed to reach equilibrium. The sample was then loaded to the test pressure. The decrease in load due to gasket deformation was recorded for 20 minutes. The load was then reduced to 125 psi. After approximately 1 minute, the specimen was again loaded to the test pressure. The

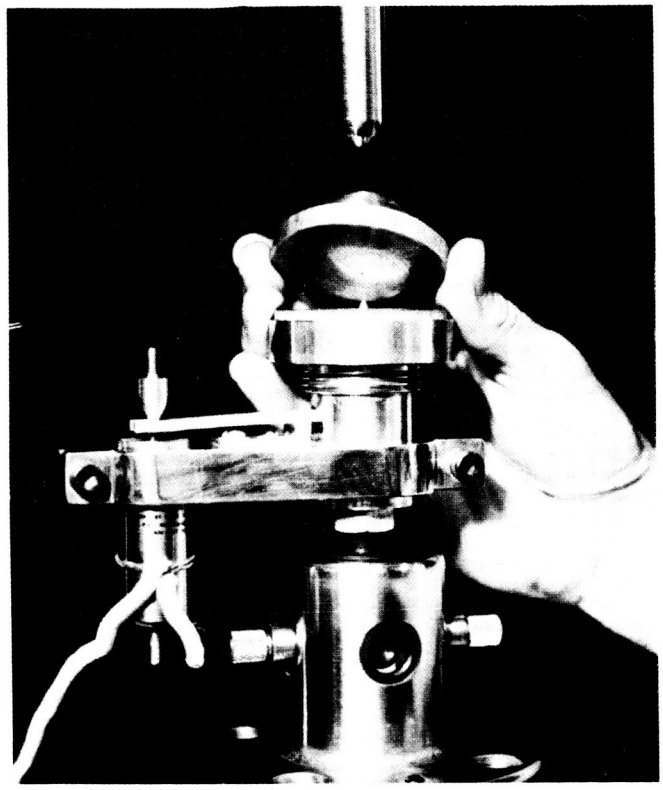

Figure 2. Test Fixture with Extensometer Installed, and 1/8-in. Thick Sample Prepared for a Room Temperature Test

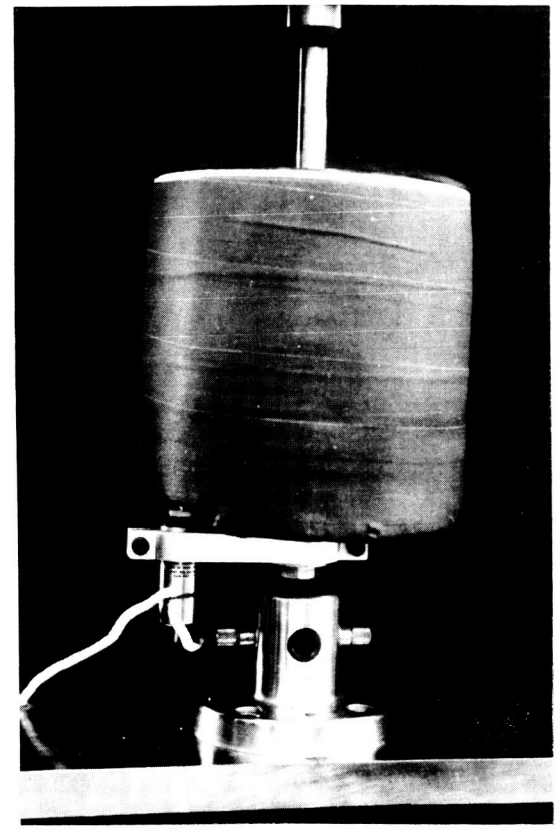

Figure 3. Test Fixture with Insulated Cryostat for Low Temperature Tests

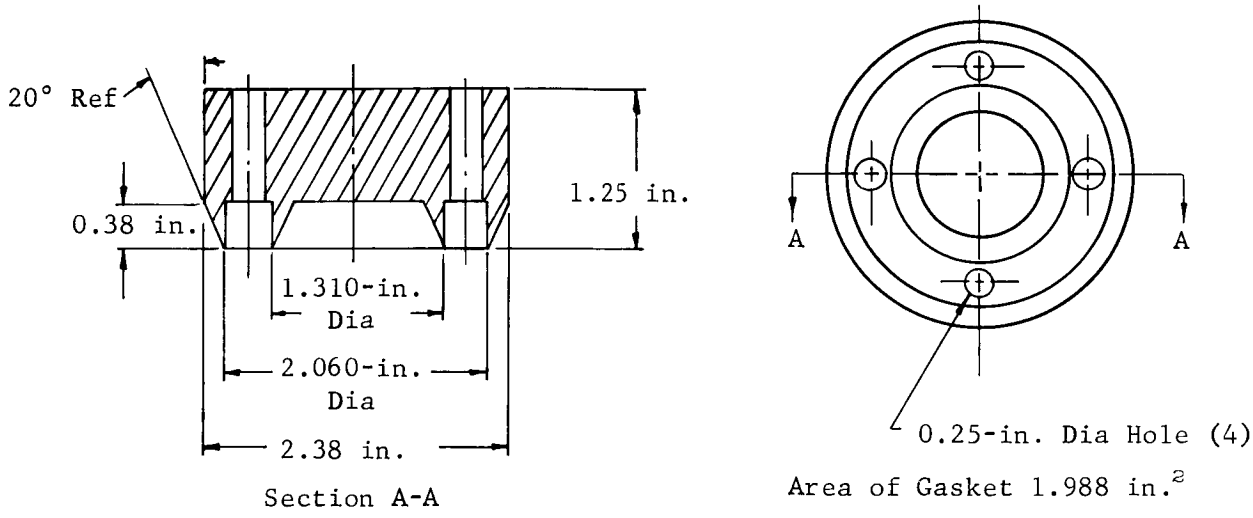

Figure 4. Gasket Die

procedure was repeated for ten cycles. These tests were performed only on 1/8-in. thick samples of Fluorolube-treated Allpax 500.

A chart was obtained showing the decrease in load versus time, affording a direct comparison between different materials and between different numbers of cycles.

Stress-relaxation data revealed the behavior of Allpax 500. At reduced temperatures, the material was quite hard and upon cycling no great change in stress was observed. Because of the slight deflection of the material at low temperatures, accurate measurements with the extensometer were difficult.

The cycling procedure at room temperature revealed fatigue in the recovery of the gasket upon repeated cycling. Typical curves are shown in Figure 5. Most of the relaxation

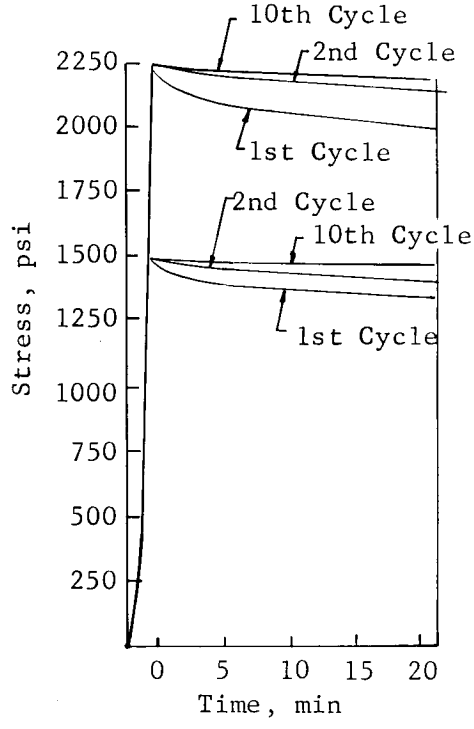

Figure 5. Stress-Relaxation Curves for Allpax 500 at Room Temperature

occurred in the first few minutes, but the indication was that cycling had only a slight effect after the first compression. In reality, this was an important feature, but a material which displays little change in the first and second cycle would be even more desirable. It was believed, however, that similar information could be obtained on materials utilizing the load decay procedure (described below). Consequently, the stress-relaxation studies at these stress levels were not pursued. An additional test of gasket materials was made at room temperature at high stress levels. This test was termed "load decay," and was carried out in the following manner:

1. The thickness of the standard test gasket specimen (2 $in.^2$) was recorded.

2. The gasket was placed between two flat steel surfaces and quickly loaded to 30,000 lb (15,000 psi) in a hydraulic press.

3. A graph was obtained of the load decay versus time for a period of 30 minutes.

4. After 30 minutes, the thickness under load was measured.

5. The load was then released, and 24 hours later the thickness of the gasket was again recorded.

The compression set under these conditions, as well as the compressibility, was determined directly from the data obtained. In addition, the load decay curve showed the physical characteristic of the material and gave some indication of how the gasket will perform in a seal. Its creep properties were obtained, and the resulting graph indicated whether or not the material became stabilized after this arbitrary period of time.

Figure 6 is the load decay curve of Allpax 500. Figures 7 and 8 are curves for filled Viton A systems. Compare the load decay and creep of the three systems. The nature of the filler has an important effect, indicated by the curve for the 37% Plastibest in Viton A and the family of curves for zinc oxide in Viton A. At the same filler level, there is considerable difference in stress-relaxation behavior.

Some studies were carried out to establish the general compression properties resulting from changes in filler content. Figure 9 gives typical results, in this case with a Plastibest 20 or zinc oxide filled Viton A. At some level of filler content, regardless of the type of filler, virtually all of the compressibility is an irreversible set. The situation, as shown for zinc oxide in Viton A, where compression set increased very slowly, was determined to be more desirable for a gasket material.

Another type of filled system, chopped fiberglass-filled tetrafluoroethylene (Teflon TFE), was investigated by the load decay procedure. This material was studied in detail because of the interest shown in this composition by commercial cryogenic gasket suppliers.

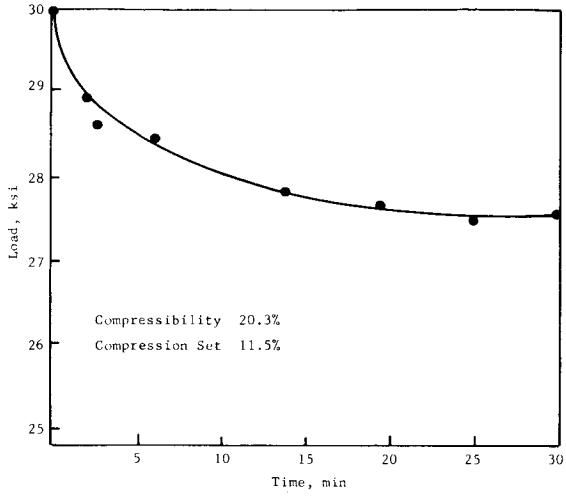

Figure 6. Load Decay Curve for Fluorolube Impregnated Allpax 500

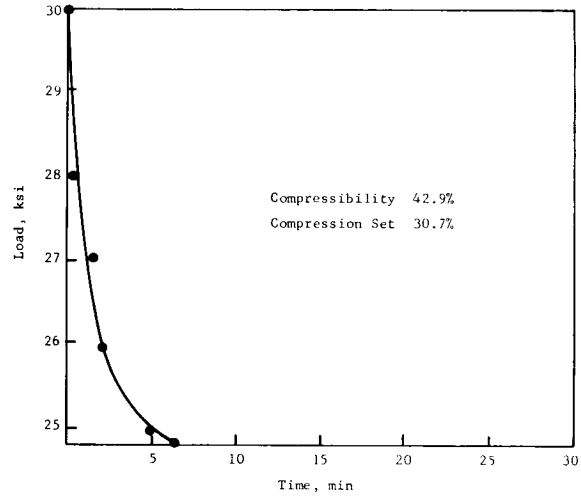

Figure 7. Load Delay Curve for Viton A; 37% Plasti-best 20

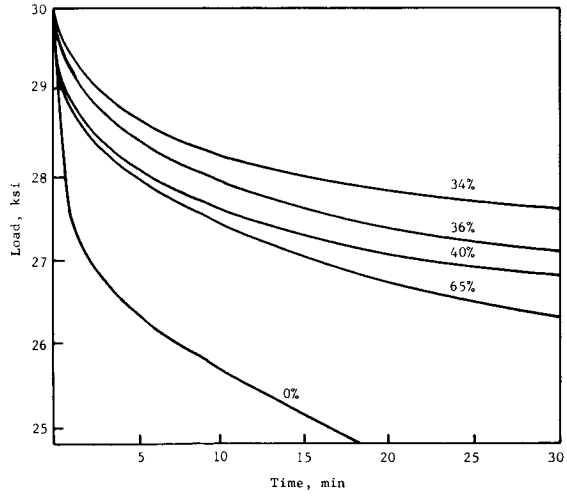

Figure 8. Family of Load Decay Curves for Zinc Oxide Filled Viton A

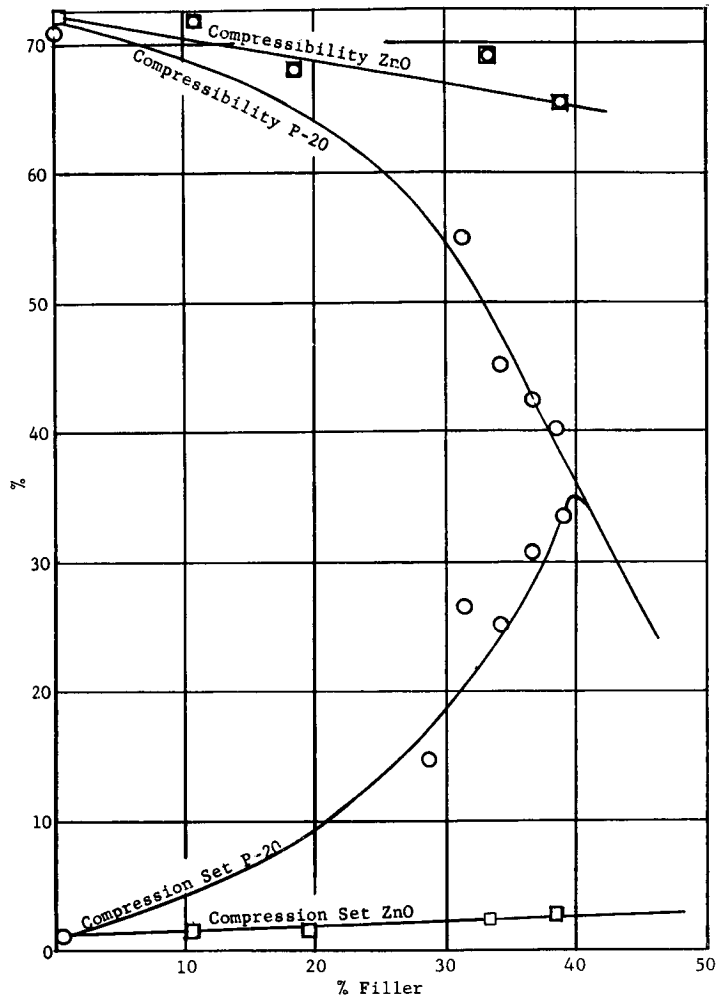

Figure 9. Effect of Filler Content on Room Temperature Compression Properties for Viton A

Specimens for this study were prepared by cold-molding premixed powdered Teflon TFE and the appropriate filler. The mold depicted in Figure 10 was filled with the powdered mixture and a billet was formed at 15,000 psi and ambient temperature. The mold was removed from the press, and the inner section of the mold was removed from the barrel. Figure 11 is a photograph of the billet still in place on the inner shaft after removal from the barrel. A number of billets were rapidly prepared in this manner (Figure 12) and subsequently "free sintered" by a stepwise postcure to 740°F, followed by a stepwise cool-down. The billets were then sliced into a number of gaskets with a nominal thickness of 0.090 in. (see Figure 13). Specific gravity of the "free sintered" gaskets was measured and revealed that the void content was equal to or less than was previously reported (Reference 2). For example, at a level of 35% glass fiber, the void-free specific gravity was 2.29 with actual billets measured at a reported maximum of 2.19. Specimens prepared for this program at the same filler level had a specific gravity of 2.1-2.3 (see Table 1).

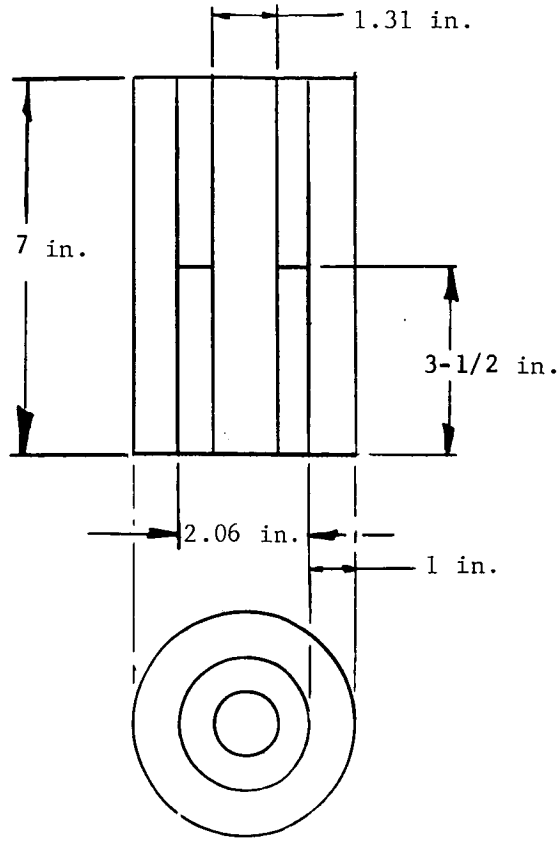

NOTE: 0.0015-in. clearance on each mold surface.

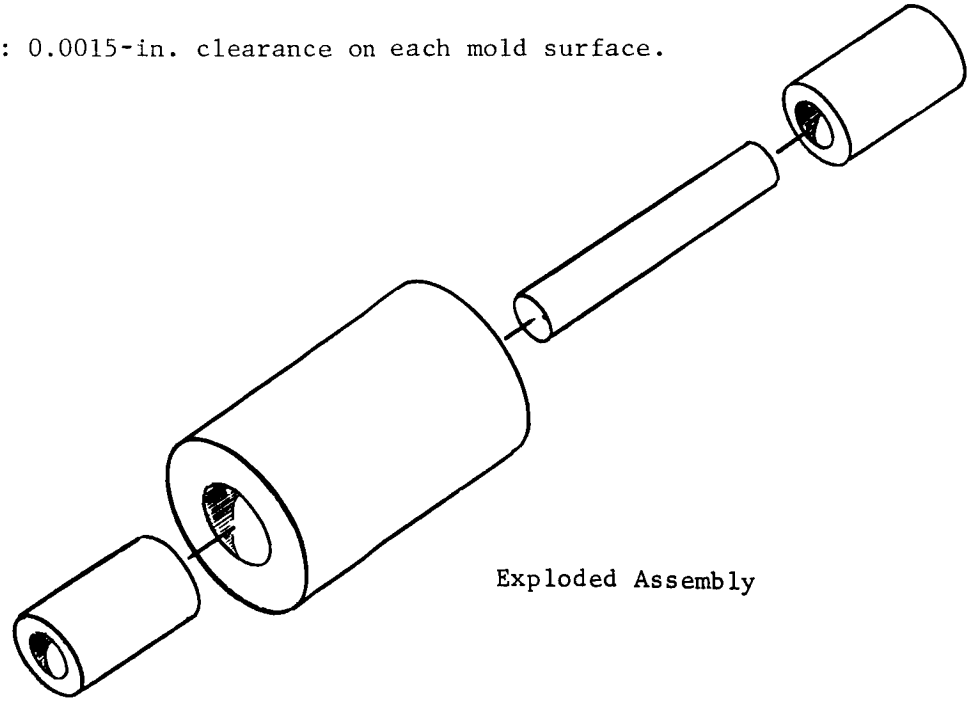

Figure 10. Compression Mold for Cylindrical Gasket Stock

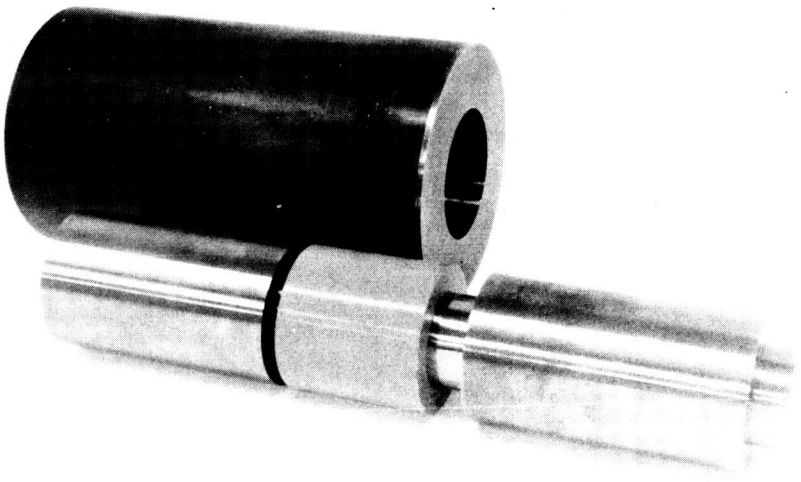

Figure 11. Billet Shown after Molding

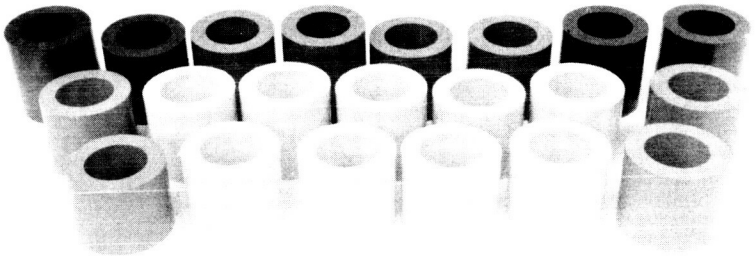

Figure 12. Test Billets Ready for Slicing

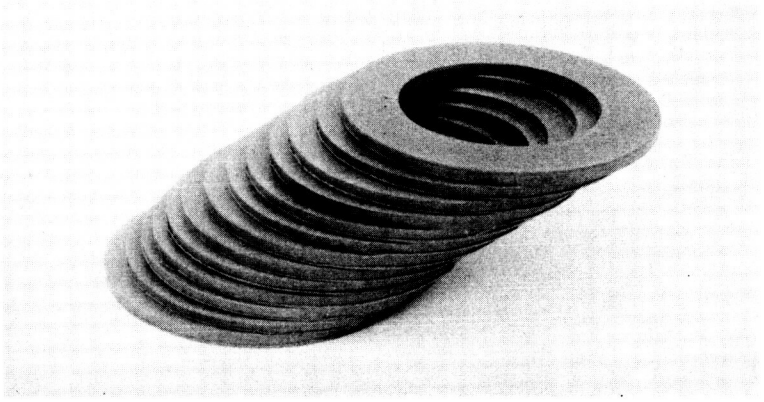

Figure 13. Sliced Billet

TABLE 1

SPECIFIC GRAVITY OF FIBERGLASS-FILLED
TEFLON GASKETS

Gasket Designation	Filler Level	Sp Gr
1A	20% unpigmented	2.233
2A	40% unpigmented	2.212
6A	20% pigmented*	2.234
7A	40% pigmented*	2.205
Fluorogold (OF)	20% pigmented**	2.161
Fluorogreen (E-600)	16% pigmented**	2.235
HS-10 (88)	25% unpigmented	2.098
HS-10 (B)	40% unpigmented	2.160

* Filler level does not include 2% LNP 201 orange pigment.

** Burnout values which include pigment.

Table 2 is a tabulation of the data obtained from the load decay curves for chopped fiberglass-filled TFE. Notice that compression set is high and that most of the compressibility is a compression set. Most specimens suffered a compression set of about 35%-40% in this test. The two materials with the lowest values for compression set were the specimens produced commercially: Fluorogold and Fluorogreen.†

The actual load decay curves for several compositions are shown in Figure 14. Notice how increasing fiberglass content influenced the load decay curve. Here, again, it appeared that Fluorogold and Fluorogreen were unique in that they had the least load decay of this group. DuPont HS-10, with only 25% fiberglass, had less load decay than the molded specimen at the same filler level, apparently because of special processing which oriented the glass fibers.

It might be pointed out here that the pigmentation reduced the load decay, probably as a result of the reduction in compression set. The curves in Figure 14 are for pigmented systems, except the HS-10. Another point of interest was the actual change in size suffered during the load decay test, as shown in Figure 15. The grey area is the size before the test, and the white area indicates the degree of flow which occurred during the test.

† Products of Fluorocarbon Co., Inc. and John L. Doré Co. respectively.

TABLE 2

COMPRESSIBILITY AND COMPRESSION SET OF FILLED TEFLON SYSTEMS

Code	Filler	% by Wt	Pigment	Compressibility, %	Compression Set, %
6B	Fiberglass	20	LNP 201 (2%)	45.5	36.7
8A		25	LNP 201 (2%)	44.0	36.3
9A		30	LNP 201 (2%)	54.5	36.5
10A		35	LNP 201 (2%)	46.2	36.3
7A		40	LNP 201 (2%)	46.7	37.8
1A		20	None	47.7	41.2
5A		30	None	48.9	42.2
3A		35	None	44.0	35.7
2A		40	None	50.0	40.0
0F		20*	Fluorogold	52.3	23.7
E-600		16*	Fluorogold	46.8	30.0
HS-10-88	HS-10 fiberglass	25	DuPont	48.9	37.5
11	MoS_2 fiberglass	5 15	None	48.9	43.4
12	MoS_2 fiberglass	20 20	None	51.1	34.8

* Values obtained by burnout and include pigment.

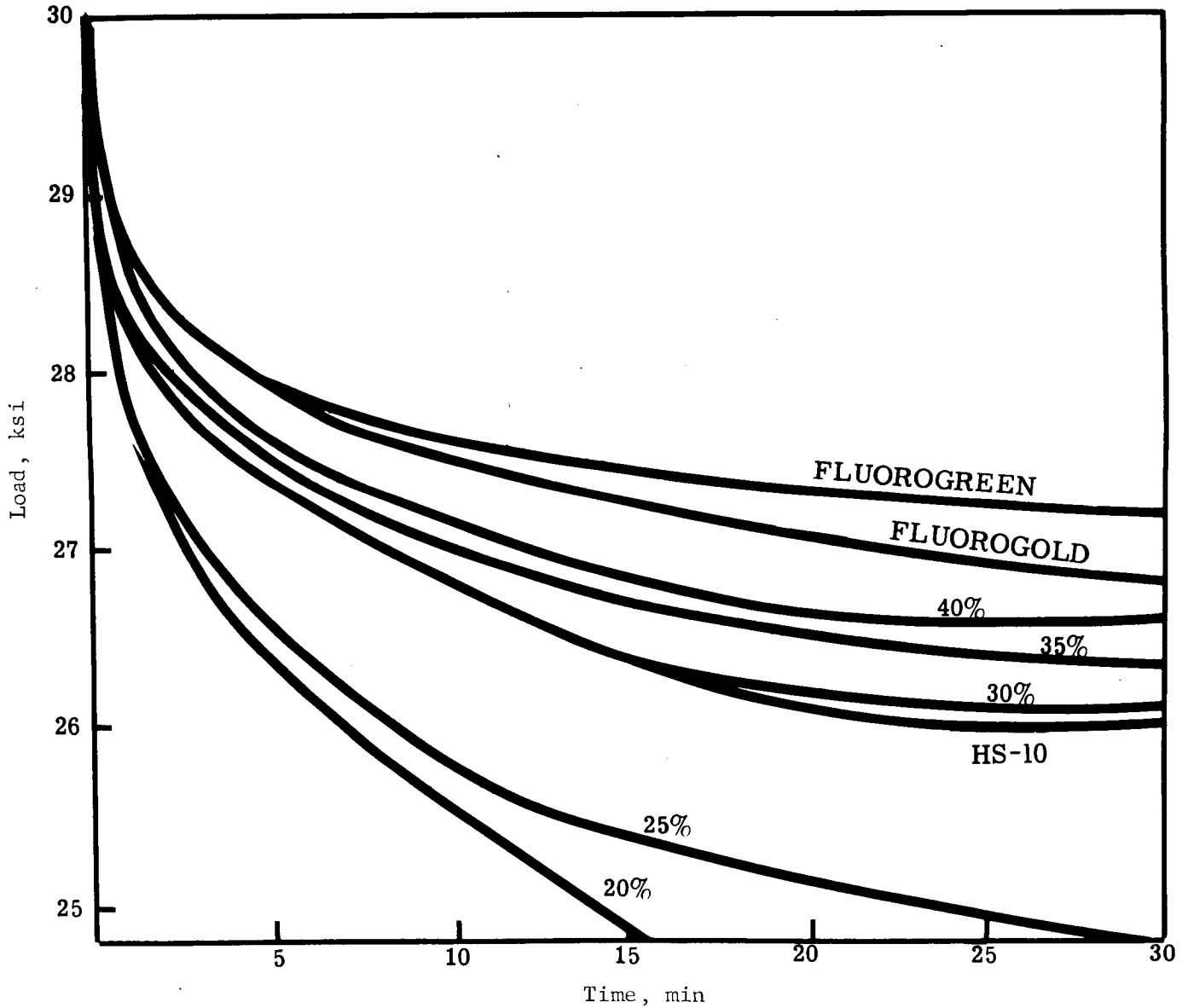

Figure 14. Family of Load Decay Curves for Various Filler Levels of Fiberglass-Teflon Gaskets

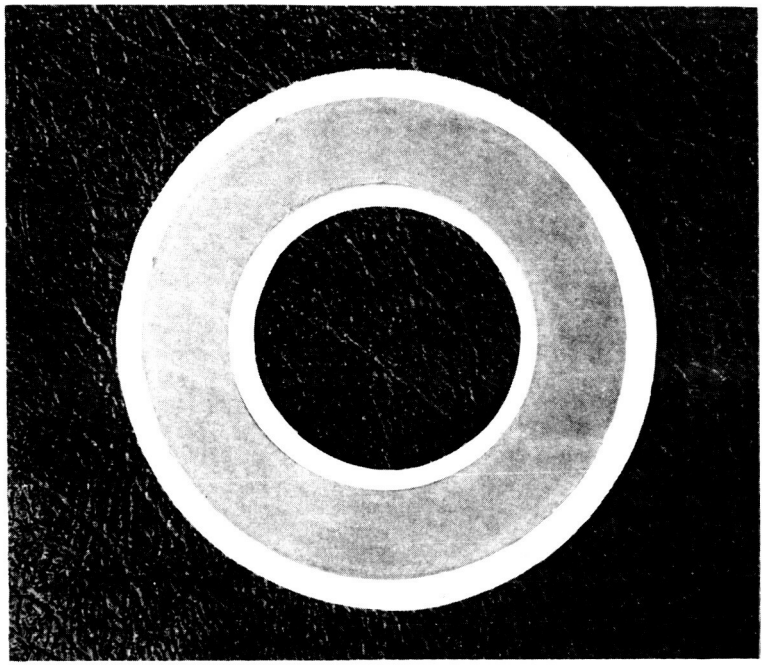

Figure 15. Change in Gasket Size after Loading

The conclusion drawn from the above tests is that the filled Teflon materials were not acceptable because of high compression set.

Laminated gasket materials were also studied in load decay tests. These studies revealed an excellent ability to maintain pressure against a gasket flange. Laminates were fabricated by laying up alternate plies of the fabric and the binder. The binder was used in the form of a film, which flowed to a certain extent during the pressing at elevated temperatures. For example, a single ply of 5-mil Teflon FEP film was used between each fabric ply. Pressing was carried out at temperatures from 500°-700°F at pressure of 100 psi for 10 minutes. Binders for these laminates were selected from fluorinated ethylene-propylene (Teflon FEP), polychlorotrifluoroethylene films (Aclar — Kel F), and fluorocarbon elastomers (Viton A — Fluorel, etc.). The latter two material types have pressing temperatures of 400°-450°F. Therefore, it was possible to use both materials in the same laminate. By varying the ratio of materials, it was possible to control the flexibility characteristics of the laminate.

In the layup of woven fabrics, it was found that when biaxial fiber orientation was used, the physical properties were not uniform in all directions and, in particular, the tensile strength on the bias was low. Consequently, laminates were constructed by alternating one-half of the fabric plies at 45° angles to the other half. Errors in the layup angle actually contributed to a more desirable multiaxial orientation. The tensile strength of such a laminate was fairly uniform in all directions.

The load decay curve shown in Figure 16 was obtained with a gasket prepared from Aclar 22C and asbestos paper. The compressibility was low, but it was quite similar in load decay to Fluorolube-treated Allpax 500. A laminate of Teflon FEP and 112 glass fabric (Figure 17) showed even better performance. Data from a number of exploratory laminates are presented in Table 3. A summary of typical data from all types is shown in Table 4.

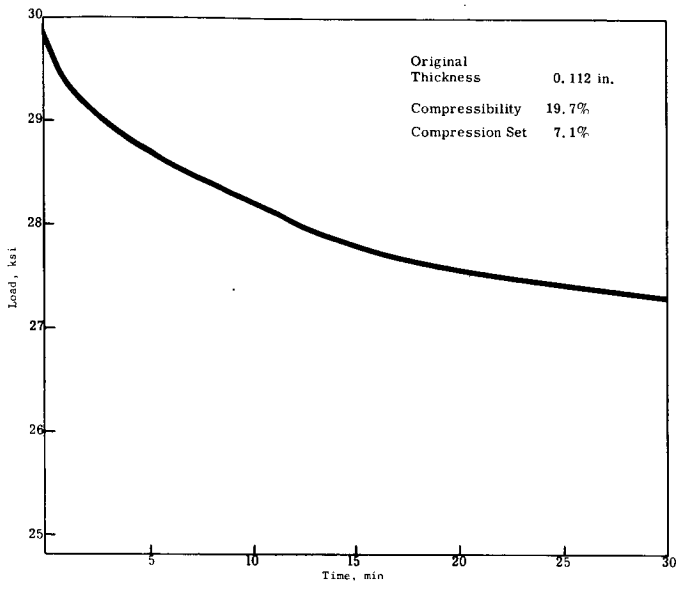

Figure 16. Load Decay Curve for Aclar 22C-Asbestos Laminate OU-1

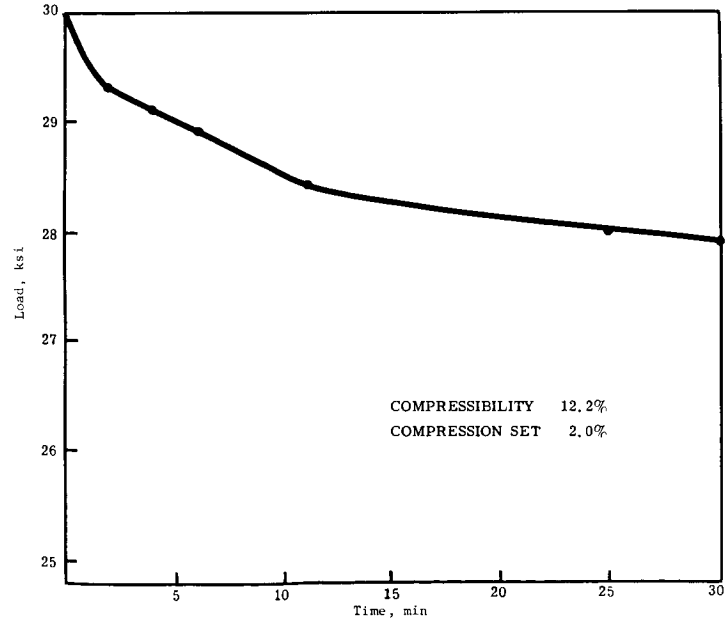

Figure 17. Load Decay Curve of Teflon and 112 Glass Fabric Laminate

TABLE 3

COMPRESSIBILITY AND COMPRESSION SET OF LAMINATES

Code	Material	Compressibility %	Compression Set, %
PE	10-ply glass 112 laminate 6-ply 33 C (5 mil) 5-ply Viton A	38.0	15.2
PB	11-ply glass 112 12-ply 33 C (5 mil)	7.5	0.5
PF	11-ply asbestos 8-ply 33 C 4-ply Viton A	9.2	1.3
PG	15-ply 112 glass 16-ply Teflon FEP (5 mil)	12.2	2.0
OU	13-ply asbestos 14-ply 22 C (5 mil) 100 psi	12.7	2.0
OU1	13-ply asbestos 14-ply 22 C (5 mil) 50 psi	19.7	7.1
OW	11-ply asbestos 12-ply Viton A (9 mil)	33.9	11.7
OO	13-ply asbestos 14-ply polyethylene 150 psi (5 mil)	19.6	6.5
OT	13-ply asbestos 14-ply Kynar (5 mil)	5.2	0.5
OG	19-ply asbestos 20-ply polyethylene	8.6	1.5
OR	13-ply asbestos 14-ply polyethylene 85 psi	24.0	9.6
PD	11-ply asbestos 4-ply 33 C 8-ply Viton A 300 psi	14.1	4.3
OX	11-ply asbestos 4-ply 33 C 8-ply Viton A 200 psi	14.0	3.1
PC	11-ply 112 glass 12-ply Viton A	45.6	71.0
OV	11-ply asbestos 12-ply 33 C	12.5	1.56
OI	15-ply asbestos 16-ply Teflon FEP	9.1	1.00

* Material failure.

TABLE 4

TYPICAL COMPRESSIBILITY AND COMPRESSION SET DATA FOR VARIOUS GASKET TYPES

Composition	Compressibility %	Compression Set, %
Allpax 500	20	12
20%-40% fiberglass teflon	47	35
65% ZnO in Viton A	46	4
Teflon FEP — 112 glass fabric	12	2
Encapsulated types:		
CG-12 (Fluorocarbon Co.)	46	34
Taskline (Duriron Co.)	34	22

Stress-Strain Studies

Stress-strain cycling data were obtained on gasket candidates. Information of this type was most helpful in evaluating compression properties at room temperature and at cryogenic temperature.

A maximum load on the test gasket was established at 6000 lb, or 3000 psi. In most cases, the stress-strain curve was nearly a straight line, but it did depart sufficiently to require some arbitrary point to be selected for the calculation of a compressive modulus. This was done by using the slope of the curve at 1500 psi.

At -320°F, inferior quality gasketing materials behave quite similarly. For example, the filled Teflon systems have steep slopes, with corresponding high modulus and low deflection. In this test, the gasket was cycled 10 times and a record kept of the stress-strain relationship on each cycle. Because most of the change took place after the first cycle, modulus values were tabulated after the first, second, and tenth cycle. A typical set of stress-strain curves is shown for Allpax 500 at room temperature in Figure 18. Considerable change took place after the first cycle, as shown by the curves of Figures 19 and 20. These curves are of the first, second, and tenth cycles of a set of stress-strain curves similar to those shown in Figure 18. A tabulation of the compressive modulus, obtained from the stress-strain curves of Allpax 500 of various thicknesses, is presented in Table 5.

Stress-strain data were obtained for various filled Teflon systems and Viton A systems. The compressive moduli of filled Teflon systems at room temperature and -320°F are presented in Tables 6 and 7. The compressive moduli of filled Viton A systems at -320°F are tabulated in Table 8. The specimens extruded from the flange when the Viton A specimens were tested at room temperature.

Complete data on compressive moduli at room temperature and at -320°F for various laminated composites are presented in Tables 9 and 10 respectively. The data are grouped in divisions representing the same type of composite.

The fluorocarbon resin-fabric laminates presented some unusual and promising results. Their behavior at cryogenic temperatures was excellent, and the original concept of reinforcement, in the direction of creep, was successful at room temperature.

The ability of the laminated gasket to retain a major portion of its compressibility was due to its structure and the unconventional lamination procedure. By using films at the binder between fabric plies, all fiber bundle wetting took place during the actual pressing step. Because the viscosity of the resin at the laminating temperature was high, the flow was limited, and fiber bundle wetting was incomplete. The unsaturated fiber bundle in the final gasket material could be compressed under load, resulting in a compressive deflection of the gasket. Because this compressibility was mechanical in nature, the force required to bring about compression was fairly constant with

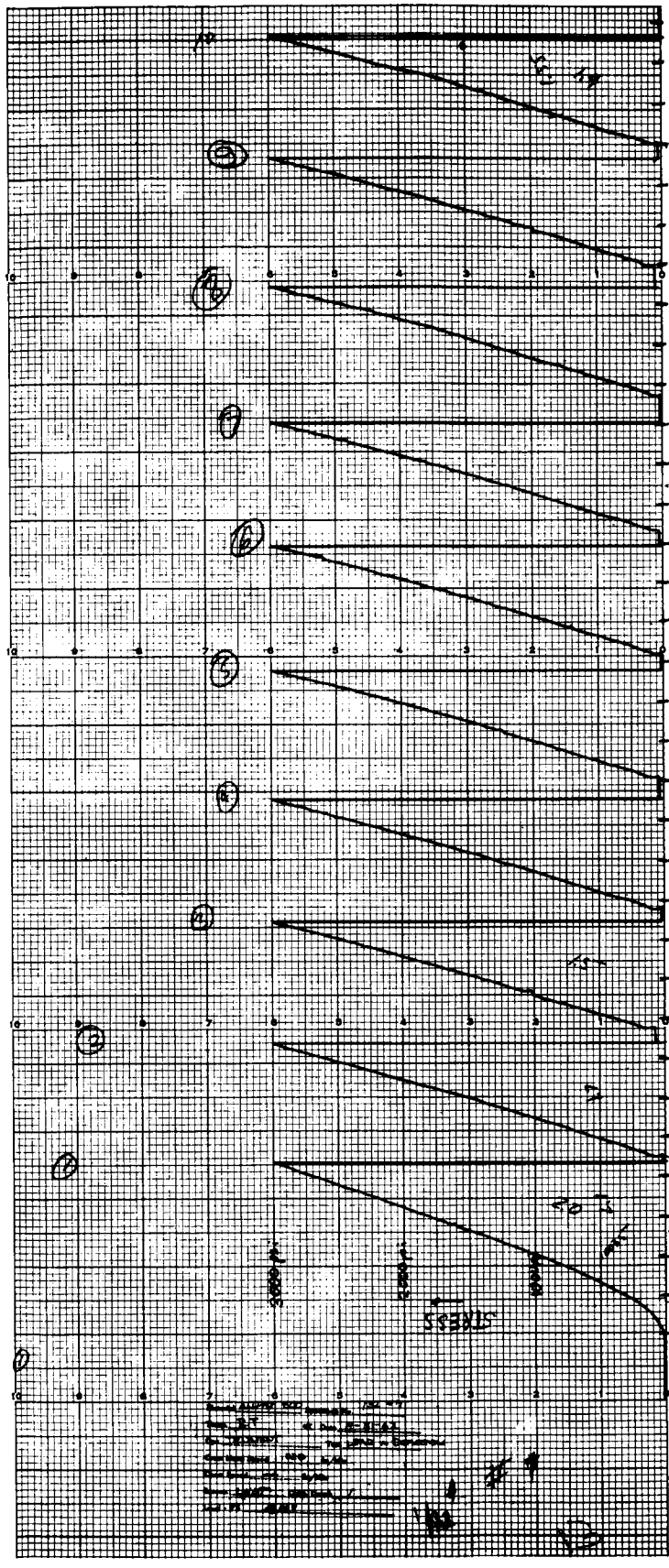

Figure 18. Instron Record of Stress-Strain for Allpax 500 at Room Temperature

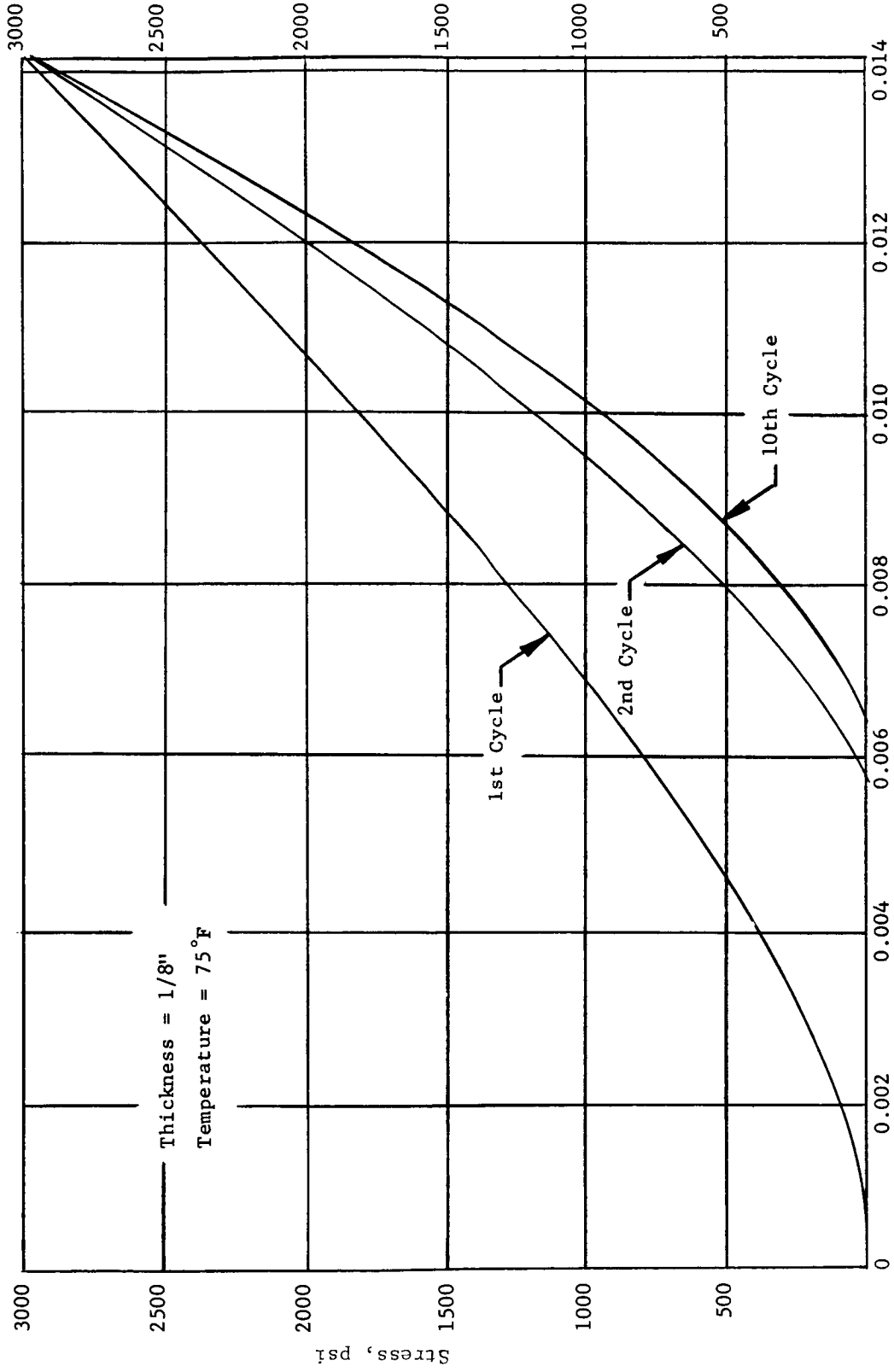

Figure 19. Stress-Strain Curves for Allpax 500 upon Cycling at Room Temperature

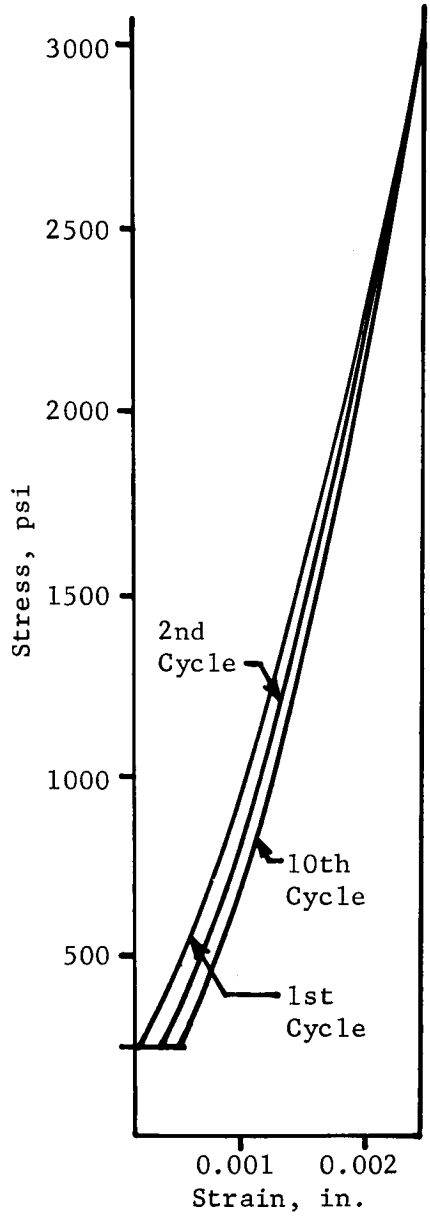

NOTE: 1/8-in. thickness; gasket preloaded @ 250 psi to seal cryostat.

Figure 20. Stress-Strain Curves for Allpax 500 upon Cycling at -320°F

TABLE 5

MODULUS OF ALLPAX 500

Thickness, in.	Temp, °F	Modulus @ 1500 psi Stress		
		1st Cycle	2nd Cycle	10th Cycle
1/32	RT	29,400	33,400	33,400
		28,500	32,800	33,900
		25,800	31,900	35,000
1/16	RT	24,400	43,400	50,500
		27,400	44,200	49,200
		24,300	34,300	48,100
1/8	RT	38,400	52,700	56,200
		31,500	53,400	60,000
		38,700	57,600	60,800
1/32	-320	35,200	38,700	49,400
		47,400	51,700	66,200
		34,000	45,200	60,300
1/16	-320	8,3600	108,500	114,000
		103,000	108,000	135,000
		94,000	98,600	128,000
1/8	-320	175,000	190,000	199,000
		190,000	190,000	199,000
		155,000	175,000	182,000

TABLE 6

COMPRESSIVE MODULI OF FILLED TEFLON SYSTEMS AT ROOM TEMPERATURE

Code	Filler, wt %	Modulus, psi		
		1st cycle	2nd cycle	10th cycle
1A	20% Fiberglass	77,900	105,700	102,900
4A	25% Fiberglass	56,100	67,100	75,600
5A	30% Fiberglass	57,100	72,100	72,100
3A	35% Fiberglass	58,000	72,800	74,900
2A	40% Fiberglass	55,500	71,400	77,900
6A	20% Fiberglass 2% Pigment	57,600	68,900	71,400
8A	35% Fiberglass 2% Pigment	57,500	80,200	81,700
9A	30% Fiberglass 2% Pigment	80,100	91,000	92,000
10A	35% Fiberglass 2% Pigment	74,300	89,000	93,000
7A	40% Fiberglass 2% Pigment	61,300	83,000	87,000
E-600	16% Fluorogreen + pigment	55,500	62,700	67,100
OF	20% Fluorogold + pigment	51,500	60,800	66,000
HS-10 -88	25% DuPont Fiberglass	50,000	63,000	70,100
HS-10B	40% DuPont Fiberglass	24,900	47,900	57,500
11A	15% Fiberglass 5% MoS_2	66,200	72,800	75,300
12A	20% Fiberglass 20% MoS_2	106,800	110,000	119,000

TABLE 7

COMPRESSIVE MODULI OF FILLED TEFLON SYSTEMS AT -320°F

Code	Filler, wt %	Modulus, psi		
		1st cycle	2nd cycle	10th cycle
1A	20% Fiberglass	143,000	175,000	173,000
4A	25% Fiberglass	108,000	156,000	156,000
5A	30% Fiberglass	140,000	154,000	154,000
3A	35% Fiberglass	151,000	159,000	168,000
2A	40% Fiberglass	179,000	184,000	206,000
6A	20% Fiberglass 2% Pigment	188,000	179,000	186,000
8A	25% Fiberglass 2% Pigment	137,000	173,000	197,000
9A	30% Fiberglass 2% Pigment	110,000	107,000	113,000
10A	35% Fiberglass 2% Pigment	142,000	149,000	142,000
7A	40% Fiberglass 2% Pigment	140,260	151,200	150,000
E-600	16% Fluorogreen + pigment	95,000	123,000	126,000
OF	20% Fluorogold + pigment	132,000	136,000	130,000
HS-10 -88	25% DuPont Fiberglass	113,000	113,000	118,000
HS-10B	40% DuPont Fiberglass	89,300	89,300	89,300
12A	20% Fiberglass 20% MoS_2	141,000	149,000	152,000

TABLE 8

COMPRESSIVE MODULI OF FILLED VITON SYSTEMS AT -320°F

Code	Filler, Wt %	Modulus, psi		
		1st Cycle	2nd Cycle	10th Cycle
OM-1	34% ZnO	134,000	136,000	140,000
OL-1	36% ZnO	135,000	135,000	126,000
OK-1	38% ZnO	127,000	163,000	161,000
OJ-2	50% ZnO	161,000	151,000	161,000
OK-2	55% ZnO	109,000	109,000	112,000
OL-2	60% ZnO	131,000	109,000	118,000
OM-2	65% ZnO	218,000	210,000	204,000
PZ	60% MgO	104,000	130,000	134,000
QA	60% $CaCO_3$	173,000	144,000	163,000
QC	73% Copper powder	115,000	147,000	158,000
QD	73% Steel powder	115,000	144,000	134,000
QE	60% Teflon powder	135,000	132,000	128,000

NOTE: At room temperature, all of these specimens extruded from the flange.

TABLE 9

COMPRESSIVE MODULI OF LAMINATES AT ROOM TEMPERATURE

Code	Composition	Modulus, psi		
		1st Cycle	2nd Cycle	10th Cycle
OH	13-ply asbestos (sized) 14-ply polyethylene	67,600	75,800	79,800
OS	13-ply asbestos (sized) 14-ply Teflon	52,100	63,900	67,700
OW	11-ply asbestos (sized) 12-ply Viton A	47,200	55,500	60,700
PH	13-ply 112 glass 14-ply Aclar 33C	69,200	76,600	78,300
PI	11-ply asbestos (sized) 14-ply Teflon	56,100	65,800	65,200
PJ	12-ply asbestos (sized) 13-ply Aclar 33C	55,800	71,100	69,800
PK	10-ply 112 glass 4-ply Viton A 9-ply Aclar 33C	58,600	61,000	63,400
PQ	13-ply asbestos (unsized) 14-ply Teflon	69,000	76,000	74,000
PT	9-ply stainless steel fabric 0.002 in. 200-mesh 10-ply Aclar 33C	84,000	84,100	92,300
PV	11-ply 0.005 in. aluminum 12-ply Teflon	--	--	76,000
181-A	7-ply 181 glass fabric 8-ply Teflon	60,700	60,800	65,000

TABLE 10

COMPRESSIVE MODULI OF LAMINATES AT -320°F

Code	Composition	Modulus, psi		
		1st Cycle	2nd Cycle	10th Cycle
OH	13-ply asbestos (sized) 14-ply polyethylene	62,700	83,700	80,800
OS	13-ply asbestos (sized) 14-ply Teflon	87,600	89,600	93,900
OW	11-ply asbestos (sized) 12-ply Viton A	73,000	76,000	86,000
PH	13-ply 112 glass 14-ply Aclar 33C	66,500	73,600	71,300
PI	11-ply asbestos (sized) 14-ply Teflon	77,700	73,900	73,000
PJ	12-ply asbestos (sized) 13-ply Aclar 33C	53,800	60,000	59,600
PK	10-ply 112 glass 4-ply Viton A 9-ply Aclar 33C	96,000	98,300	100,800
PQ	13-ply asbestos (unsized) 14-ply Teflon	118,000	106,000	118,000
PT	9-ply stainless steel fabric 0.002 in. 200-mesh 10-ply Aclar 33C	64,000	97,000	107,000
PU	11-ply 0.005-in. aluminum 12-ply Teflon	54,000	100,000	134,000
181-A	7-ply 181 glass fabric 8-ply Teflon	77,400	77,900	78,800

changing temperature. (This took place, fortunately, even though sufficient bonding to the fiber bundle enabled the bundles to restrict flow of resin between one another.)

Comparative compressive moduli of three fluorocarbon composite types are shown in Figure 21. Regardless of test condition or temperature, the laminate construction had the smallest change in performance when compared to the two other types of materials tested.

Additional evidence of improved performance of laminated materials was obtained by examination of hysteresis loops. The loops for a 25% fiberglass-filled Teflon gasket are shown in Figure 22. These curves demonstrated flow problems not observed in the hysteresis loops obtained on a Teflon-112 glass fabric laminate, as shown in Figure 23. The latter curves were nearly Hookian, and did not change appreciably upon cycling at room temperature.

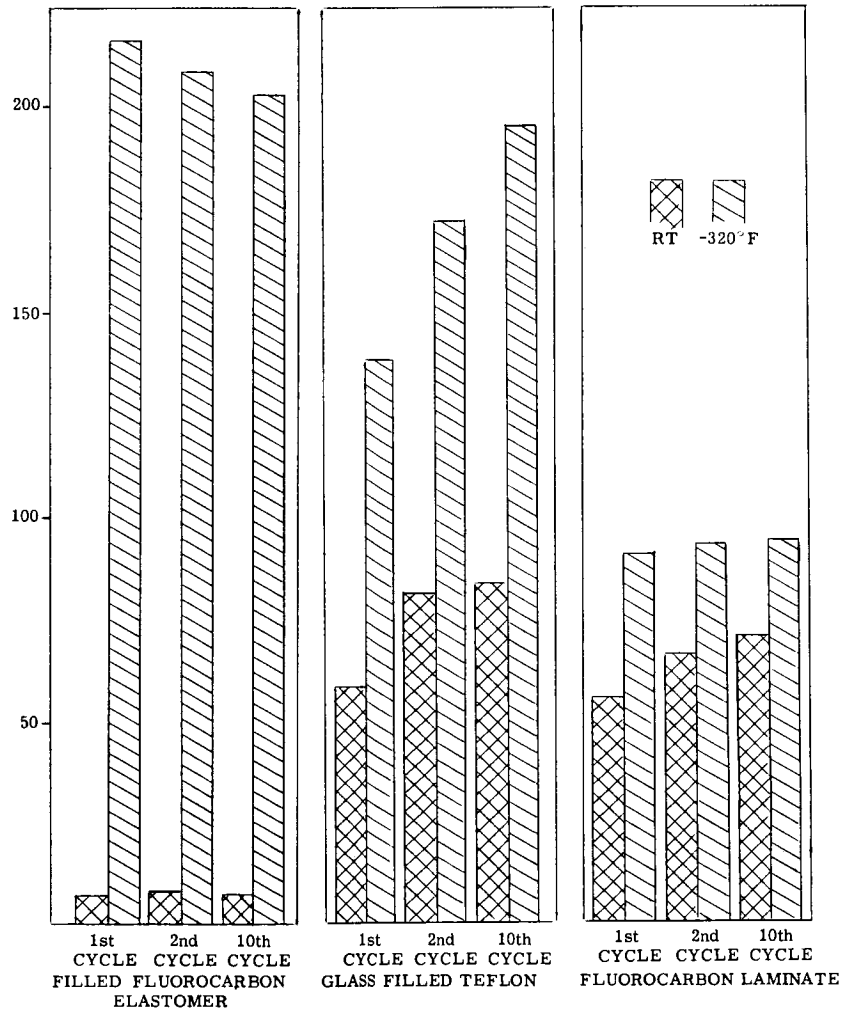

Figure 21. Comparative Compressive Moduli of Three Types of Fluorocarbon Composites upon Cycling at Room Temperature and -320°F

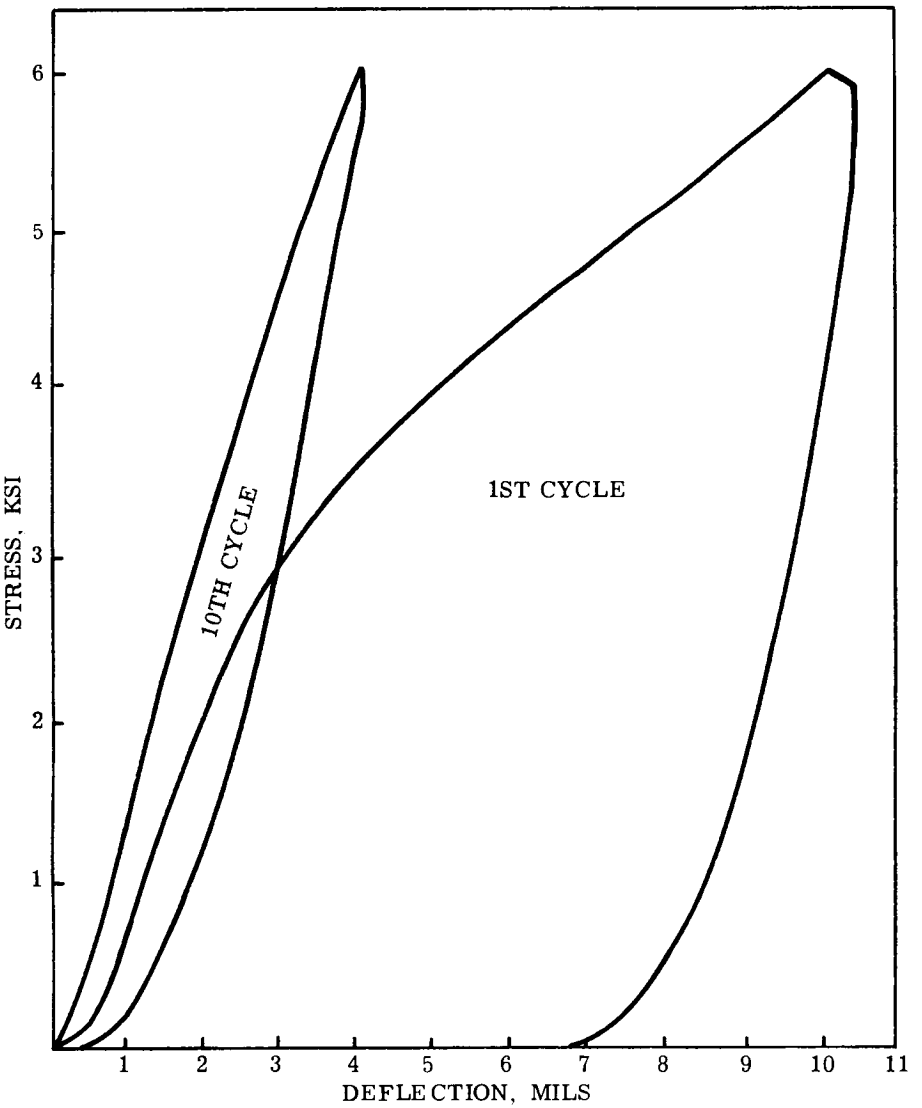

Figure 22. Compressive Hysteresis Curves for 25% Glass Filled Teflon at Room Temperature

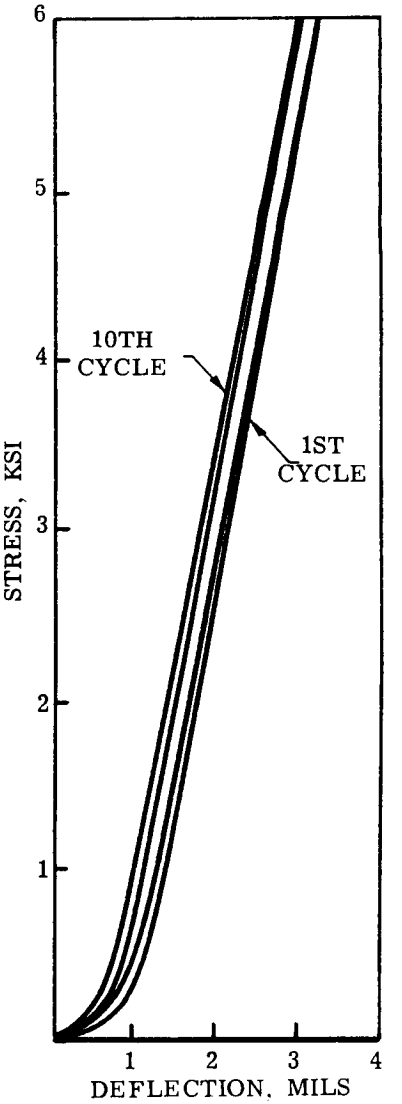

Figure 23. Compressive Hysteresis Curves for Teflon – 112 Glass Laminate at Room Temperature

Sealing Studies

The test fixture used for the stress-strain studies was also used, with internal pressurization, for sealing studies. The equipment with the cryostat in place is shown in Figure 24.

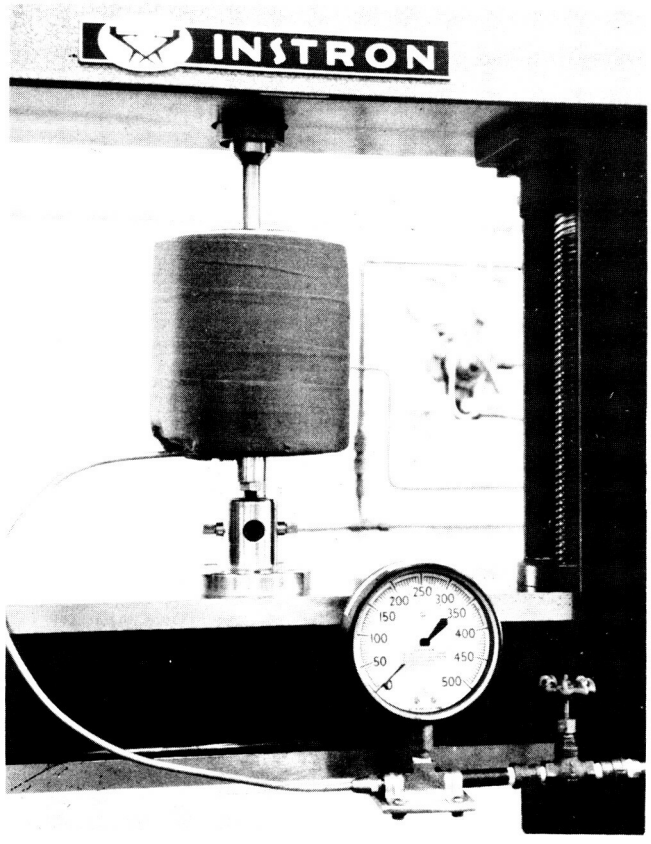

Figure 24. Test Fixture Assembled for Determination of Low Temperature Sealing Characteristics

The test procedure involved loading the gasket to 1500 psi, pressurizing the internal volume to 200 psig in nitrogen, then gradually decreasing the load on the gasket until a leak occurred, as evidenced by a drop in internal pressure.

Because of the small internal volume, it was felt that a slight leak would be easily detected on the pressure gage. Some interesting and anomalous data were obtained, suggesting careful interpretation and modification of the test.

The most surprising observation was that some materials exhibited lower sealing flange pressure at -320°F than at room temperature. This can be

explained by the fact that the test gasket was loaded at room temperature and then the temperature lowered to -320°F. This procedure accurately reproduced a real application, and also introduced a gasket behavior which did not give data too useful for comparative purposes. Under these loading conditions, the gasket at -320°F was perfectly mated to the flange, due to a "freezing" of the surface, to form a matched surface. When the pressure exerted by the flange was reduced, it was easy to see how the two perfectly mated surfaces sealed at a low flange pressure. This was not the case at room temperature.

It appeared that the actual sealing pressure was not as important as the distance the flange had to be withdrawn before the gasket no longer exerted its sealing pressure. In the data tabulated in Tables 11 through 14, this information is called the flange deflection-to-leak, and is expressed in terms of inches per inch of gasket thickness.

Ideally, at -320°F a good gasketing material has a high value for its flange deflection-to-leak. According to the data, laminate systems have the highest deflections at -320°F of all the materials tested. Note that the filled Teflon gaskets and the filled Viton A gaskets in most cases have flange deflections-to-leak of less than 0.020 in./in. at -320°F. Values two to three times higher were observed with laminated gaskets.

In reality, the flange deflection-to-leak is directly related to compressive modulus. Knowing the latter, it could be accurately predicted which materials would have the highest values for the flange deflection-to-leak. This holds true because the variation in leak pressure from one gasket to another is small in comparison to the maximum load applied in the test.

The value for the -320°F flange deflection-to-leak for the E-600 material is 0.025 in./in. Consideration of the -320°F modulus for this material upon cycling brings out another point. This flange deflection is obtained on the first cycle. In this particular case, the modulus increased upon cycling, so that for a complete analysis of any material, the modulus appears to be more important than flange deflection-to-leak, and more specifically the change in the modulus value upon cycling.

Notably, the value for the flange deflection at -320°F for Allpax 500 is one of the lowest of all materials tested. See Table 14.

Optimization of Laminating Variables

Most of the laminated gasket studies previously discussed were exploratory in nature and demonstrated the feasibility of this type of composite in cryogenic, LOX-compatible gaskets. A number of processing variables were indicated, but little effort was made to optimize these variables. Accepting the fact that the laminated composite has considerable potential in cryogenic gasketing, careful study should follow regarding the fabrication of the laminate in order to achieve the best possible combination of variables resulting in a optimum gasket. Variables that should be considered are the resin, pressing time and temperature, laminating pressure, interlaminar separation,

TABLE 11

LEAK DATA FOR FILLED VITON SYSTEMS

Code	Filler Wt %	RT Leak Flange Pressure, psi	RT Flange Deflection-to-Leak in./in.	-320°F Leak Flange Pressure, psi	-320°F Flange Deflection-to-Leak in./in.
OM-1	34% ZnO	275	No test	650	0.021
OL-1	26% ZnO	250	↓	550	0.017
OK-1	38% ZnO	250	↓	675	0.020
OJ-2	50% ZnO	↓	↓	375	0.015
OK-2	55% ZnO	250	↓	575	0.018
OL-2	60% ZnO	300	↓	600	0.016
OM-2	65% ZnO	275	0.330	600	0.011
PZ	60% MgO	No test	No test	1000	0.016
QA	60% $CaCO_3$	↓	↓	850	0.012
QD	73% Steel powder	↓	↓	475	0.023
QE	60% Teflon powder	↓	↓	750	0.015
QC	73% Copper powder	↓	↓	500	0.022

TABLE 12

LEAK DATA FOR GLASS-FILLED TEFLON SYSTEMS

Code	Filler, Wt %	RT Leak Flange Pressure, psi	RT Flange Deflection-to-Leak in./in.	-320°F Leak Flange Pressure, psi	-320°F Flange Deflection-to-Leak in./in.
1A	20% Fiberglass	325	0.046	575	0.017
4A	25% Fiberglass	500	0.068	375	0.022
5A	30% Fiberglass	400	0.062	375	0.020
3A	35% Fiberglass	455	0.058	350	0.018
2A	40% Fiberglass	340	0.061	550	0.015
6A	20% Fiberglass, 2% pigment	375	0.080	525	0.015
8A	25% Fiberglass, 2% pigment	400	0.080	450	0.018
9A	30% Fiberglass, 2% pigment	300	0.035	450	0.018
10A	35% Fiberglass, 2% pigment	325	0.047	325	0.020
7A	40% Fiberglass, 2% pigment	250	0.056	350	0.019
E-600	16% Doré filler (Fiberglass + pigment)	425	0.056	550	0.025
OF	20% Fluorogold filler (Fiberglass + pigment)	385	0.064	300	0.018
HS-10-88	25% Fiberglass, DuPont	300	0.059	500	0.023
HS-10-B	40% Fiberglass, DuPont	275	0.116	275	0.031
11A	5% Molydisulfide, 15% fiberglass	325	0.069	600	0.016
12A	20% Molydisulfide, 20% fiberglass	300	0.055	375	0.019

TABLE 13

LEAK DATA FOR LAMINATES

Code	Filler, Wt %	RT Leak Flange Pressure, psi	RT Flange Deflection-to-Leak in./in.	-320°F Leak Flange Pressure, psi	-320°F Flange Deflection-to-Leak in./in.
PO	11-ply 112 glass 14-ply Teflon	500	0.041	700	0.034
PP	10-ply 112 glass 9-ply Aclar 14-ply Teflon	450	0.032	975	0.015
PK	Repeat PP	325	0.047	300	0.027
PQ	11-ply asbestos (sized) 14-ply Teflon	250	0.038	450	0.024
PI	Repeat PQ	255	0.056	700	0.030
PR	11-ply 112 glass 12-ply Viton	250	0.046	1250	0.012
PS	11-ply asbestos (unsized) 12-ply Viton	250	0.058	1025	0.014
OW	Repeat PS	250	0.076	300	0.037
OH	13-ply asbestos (sized) 14-ply polyethylene	350	0.061	350	0.042
OS	13-ply asbestos (sized) 14-ply Teflon	375	0.057	300	0.027
PT	9-ply 200-mesh stainless steel 12-ply Aclar	400	--	375	0.038
PU	11-ply 0.0005-in. aluminum 12-ply Teflon	400	--	450	0.046
QH	14-ply 0.002-in. aluminum 15-ply Teflon	325	--	400	0.032
PH	13-ply 112 glass 14-ply Aclar	300	0.062	275	0.041
PJ	12-ply asbestos (sized) 13-ply Aclar	275	0.091	250	0.048

TABLE 14

LEAK DATA

Code	Filler, Wt %	RT Leak Flange Pressure, psi	RT Flange Deflection-to-Leak in./in.	-320°F Leak Flange Pressure, psi	-320°F Flange Deflection-to-Leak in./in.
CG12	Fluorocarbon Co. Inc.	300	0.035	375	0.021
CG24	Fluorocarbon Co. Inc.	275	0.051	450	0.023
PX	DuPont SP	500	0.021	600	0.022
TF	Teflon	425	0.064	650	0.026
OY	Allied Halon TVS – 300	> 650	--	> 650	--
OZ	Allied Halon VK – 300	> 650	--	> 650	--
PA	Allied Halon VK – 270	> 650	--	> 650	--
	Allpax 500 1/8 in. (Fluorolube treated)	300	0.079	550	0.014

and fabric type and style. If compression of the fiber bundle is the factor responsible for the ability of the fluorocarbon laminates to maintain their compressibility at low temperatures, then any of the variables affecting fiber bundle wetting are of importance.

The effect of temperature was studied by preparing laminates at temperatures from 550°F to 650°F. Results of these tests are shown in Tables 15 and 16.

Both temperature and pressure have an effect on fiber bundle wetting, so a slightly different approach was used to determine the effect of resin content by changing the distance between glass fabric plies. These results are shown in Table 17.

Considering the data in Tables 15 through 17, it is apparent that the effects of these variables are more subtle than the gross differences in material composition. These gross differences allow a comparison of compressive stress-strain data, but the more subtle variables in the preparation of laminates require more accuracy and reliability than Narmco's stress-strain equipment setup could deliver. Because of scatter, it was difficult to form any conclusions from data presented in Tables 15 through 17. Because of the difficulties inherent in compression measurements of the materials, a great deal of effort was applied to the improvement of measuring equipment and techniques.

A conclusive indication that one of the processing variables does effect laminate characteristics was obtained by using a penetrant dye solution. In this case, wetting of the fiber bundle was demonstrated to be influenced by the laminating temperature.

Wicking of the laminates prepared at temperatures ranging from 550°F to 650°F was investigated by immersing a polished edge of each laminate in a penetrant dye solution. After 20 minutes, the specimens were removed and wiped dry. Results of the wicking are tabulated in Table 18. Notice the change in the degree of wicking. In other words, when the laminating temperature was reduced, the resin viscosity was increased and fiber wetting was more difficult. This resulted in a more extensive penetration of the test dye into the edge of the laminate. Note that even at 650°F there was slight wicking.

It is easily understood how the laminating temperature can have an effect on other previously mentioned variables, due to the change in resin flow characteristics with temperature change. Probably the most important of these variables is the interlaminar separation. The effect of temperature can be readily observed by examining the photomicrographs of the polished edges of two laminates shown in Figures 25 and 26. The laminate in Figure 26 was prepared at 550°F, and greater interlaminar separation is apparent compared with the laminate prepared at 650°F. The lower viscosity of the resin at the higher temperature allowed the laminate plies to be pressed closer together, although actual laminating pressure was the same in both cases.

Further efforts to optimize the laminate approach departed from the use of glass fabric as the reinforcement. Some work was carried out during the

TABLE 15

CORRELATION OF PRESSING TEMPERATURE, INTERLAMINAR SEPARATION, AND COMPRESSIVE MODULUS FOR TEFLON-112 GLASS LAMINATE

Pressing Temp, °F	Overall Laminate Thickness, in.	Avg Interlaminar Separation, mils	Compressive Modulus @ RT, psi			% Increase on Cycling @ RT	Compressive Modulus @ -320°F, psi			% Increase on Cycling @ -320°F
			1st Cycle	2nd Cycle	10th Cycle		1st Cycle	2nd Cycle	10th Cycle	
650	60	1.0	69,500	77,000	79,100	14	78,900	78,900	84,000	6.4
625	82	2.9	81,000	90,600	91,800	13	80,000	86,000	87,500	9.4
600	87	3.3	83,100	87,000	96,200	16	170,000	85,000	93,000	33.0
575	85	3.3	76,900	90,300	106,300	38	82,000	94,000	97,200	19.0
550	92	3.5	76,800	92,900	100,000	30	77,500	95,200	97,900	27.0

TABLE 16

EFFECT OF LAMINATION PRESSURE
112 GLASS-TEFLON PRESSED AT 650°F

Gasket No.	Thickness, mils	Laminate Pressure, psi	RT Modulus, psi			-320°F Modulus, psi		
			1st Cycle	2nd Cycle	10th Cycle	1st Cycle	2nd Cycle	10th Cycle
D19	92	25	79,400	88,600	93,900	107,000	134,000	128,000
D18	82	50	86,500	86,500	89,700	63,000	107,000	112,000
D17	81	75	80,600	85,200	84,200	90,600	112,500	126,000
D16	78	100	74,700	80,000	80,000	79,000	90,600	99,000
D23	67	150	67,000	71,800	73,500	80,400	94,800	97,500
D24	68	200	65,600	73,100	73,100	85,000	85,000	94,400
D25	71	250	72,500	75,100	75,500	65,700	85,200	96,800

TABLE 17

EFFECT OF INTERLAMINAR FILM THICKNESS ON COMPRESSIVE MODULUS
112 GLASS-TEFLON PRESSED AT 650°F

Gasket No.	Overall Thickness, mils	Teflon Film Thickness, mils	RT Modulus, psi			-320°F Modulus, psi		
			1st Cycle	2nd Cycle	10th Cycle	1st Cycle	2nd Cycle	10th Cycle
D5	92	5	76,800	92,900	100,000	72,500	95,200	97,900
D12	110	6	91,200	102,000	101,000	89,600	91,600	103,000
D11	112	7	93,700	98,500	98,500	114,000	111,000	117,000
D13	123	8	100,000	106,000	110,000	103,000	136,000	140,000
D9	130	9	103,000	112,000	109,000	115,000	126,000	128,000
D8	151	10	106,000	111,000	113,000	103,000	112,000	133,000

TABLE 18

EFFECT OF PRESSING TEMPERATURE ON WICKING
TEFLON-112 GLASS LAMINATE

Pressing Temp, °F	Extent of Wicking,* mm
650	4
625	8
600	9
575	18
550	20

* Determined by exposure of laminate edge to penetrant dye solution for 20 minutes.

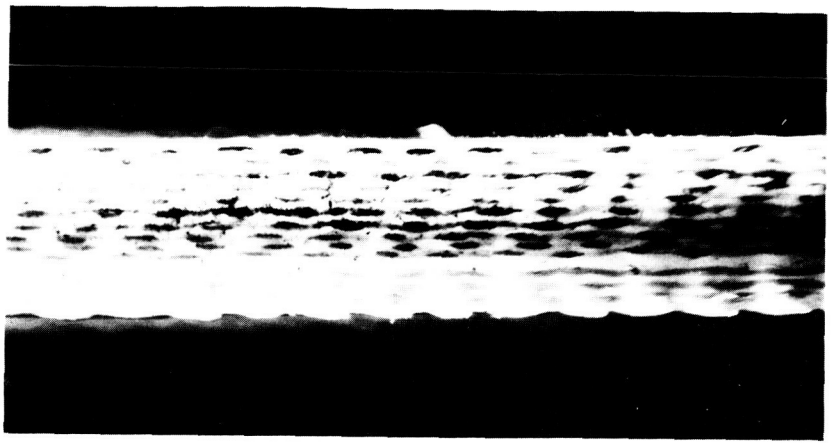

Figure 25. Edge of 13-ply, 64-mil Thick Teflon-112 Glass Laminate Pressed at 650°F

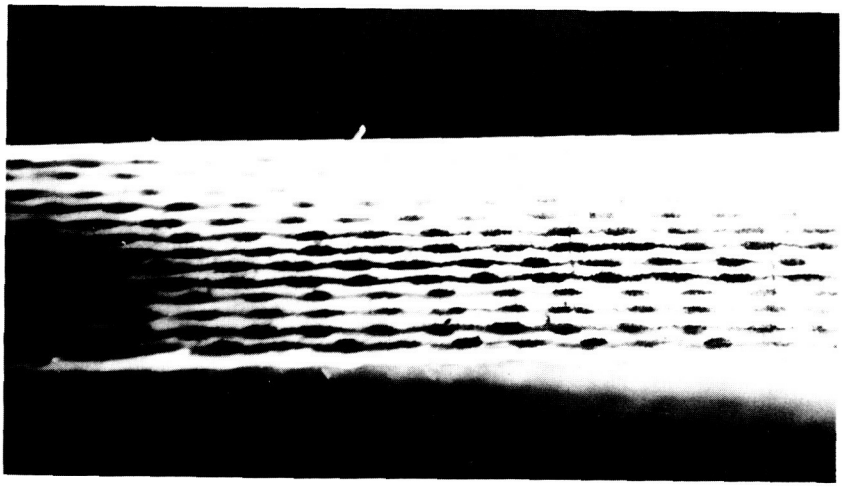

Figure 26. Edge of 13-ply, 12-mil Thick Teflon-112 Glass Laminate Pressed at 550°F

program using laminates of asbestos paper, but no actual optimization of variables was attempted. This was also the case with laminates prepared with fabrics woven from metal wire. The modulus appeared to be slightly higher than that for similar gaskets using glass fabric.

LOX-Impact Testing

With very little LOX compatibility information available on laminated composites, it was believed advisable to submit a fairly complete sampling of all laminate types to George C. Marshall Space Flight Center (MSFC) for LOX-impact testing. Samples were cut from various laminates in the form of disks of 11/16-in. diameter. Results of testing at MSFC are recorded in Table 19.

TABLE 19

LIQUID OXYGEN IMPACT SENSITIVITY OF LAMINATED GASKETS

Laminate Code No.	Composition	Reactions/ Tests
PP	10-ply asbestos paper, 4-ply Viton A, and 9-ply Aclar 33C	0/20
PR	11-ply 112 glass fabric, 12-ply Viton A	0/20
PS	11-ply asbestos paper, 12-ply Viton A	0/20
PQ	11-ply unsized asbestos paper, 12-ply Teflon	0/20
PU	11-ply 0.75-mil aluminum foil, 12-ply Teflon	0/20
QK	7-ply 2-mil aluminum foil, 10-ply Viton A	7/20
PG	15-ply 112 glass and 16-ply 5-mil FEP Teflon, 700°F press @ 300 psi	0/20
PO	13-ply 112 glass and 14-ply 5-mil FEP Teflon, 700°F press @ 300 psi, slow cool-down	1/20
PH	13-ply 112 glass 14-ply 5-mil Allied Aclar 33C, 425°F press @ 300 psi	0/20
PI	11-ply sized asbestos paper 12-mil and 14-ply 5-mil FEB Teflon (double outside plies) pressed 15 min @ 700°F @ 300 psi	0/20
PJ	12-ply sized asbestos paper 12-mil and 13-ply 5-mil Allied Aclar 33C pressed 15 min @ 425°F @ 300 psi	0/20
PK	10-ply 112 glass, 4-ply Viton A, 9-ply 5-mil Allied Aclar 33C	0/20

All tests were carried out at MSFC using equipment and procedure described in MSFC Specification 106.

These tests indicated that all laminates, except QK and PO, were acceptable. The laminate QK was a composite of aluminum foil and Viton A, which was most reactive. Viton A was used on the outside plies. This raised a question regarding the compatibility of Viton A, although no other laminate incorporating this material displayed any reaction (see PR and PS). The Teflon-glass fabric laminate, PO, was prepared at 300 psi and 700°F with a slow cooldown. This resulted in a dense laminate with very little compressibility. It was observed that very hard materials sometimes caused flashes arising from the aluminum test cup. Laminates PG and PO were similarly prepared, except that PG remained in the press for 10 minutes only.

From this series of tests, it appeared that the laminated composites utilizing a polyfluorocarbon binder were LOX compatible; the aluminum-Viton A composite, QK, was an exception.

Improved Compression-Deflection Measurements

The test fixture shown in Figure 1 was unsuitable for the optimization studies, which required the detection of more subtle differences in compressive deflection. The compression and flexing of the fixture between the bottom flange and the point of attachment of the extensometer just below the pipe fitting on the lower shaft was one source of difficulty. To avoid this, the fixture was revised so that the extensometer was mounted on an extension of the bottom flange.

Mounting the extensometer in this fashion solved the problem of deflection below the flange. However, there was play in the extensometer and the fixture was abandoned even though it had been used to obtain all the preceding data.

Attention was then directed to the ASTM-type fixture, a circular ram of small diameter which was impinged on the sample, and the cross-head travel recorded at given loads (see Reference 3).

The ASTM procedure does not allow the use of an extensometer, and cross-head travel must be used for deflection. A correction can be applied for flexing of the cross-head, but this leads to serious problems because the deflection of gaskets at -320°F is considerably less than the distortion of the cross-head beam.

Further consideration of the extensometer method of measurement resulted in an improved fixture (Figure 27) that demonstrated excellent sensitivity and reliability. The extensometer was installed in the bottom of the fixture, with its centerline coinciding with that of the fixture. The extensometer armature bore directly on the top portion of the fixture, eliminating the need for a linkage system. The bottom flange was of heavy steel mounted directly on the cross-head. At -320°F, the bottom flange was placed in the cryostat, which was mounted on insulating material between the bottom of the cryostat and the cross-head. Deflection of the insulating material was of no consequence (if the cross-head loading speed were increased to account for deflection in the

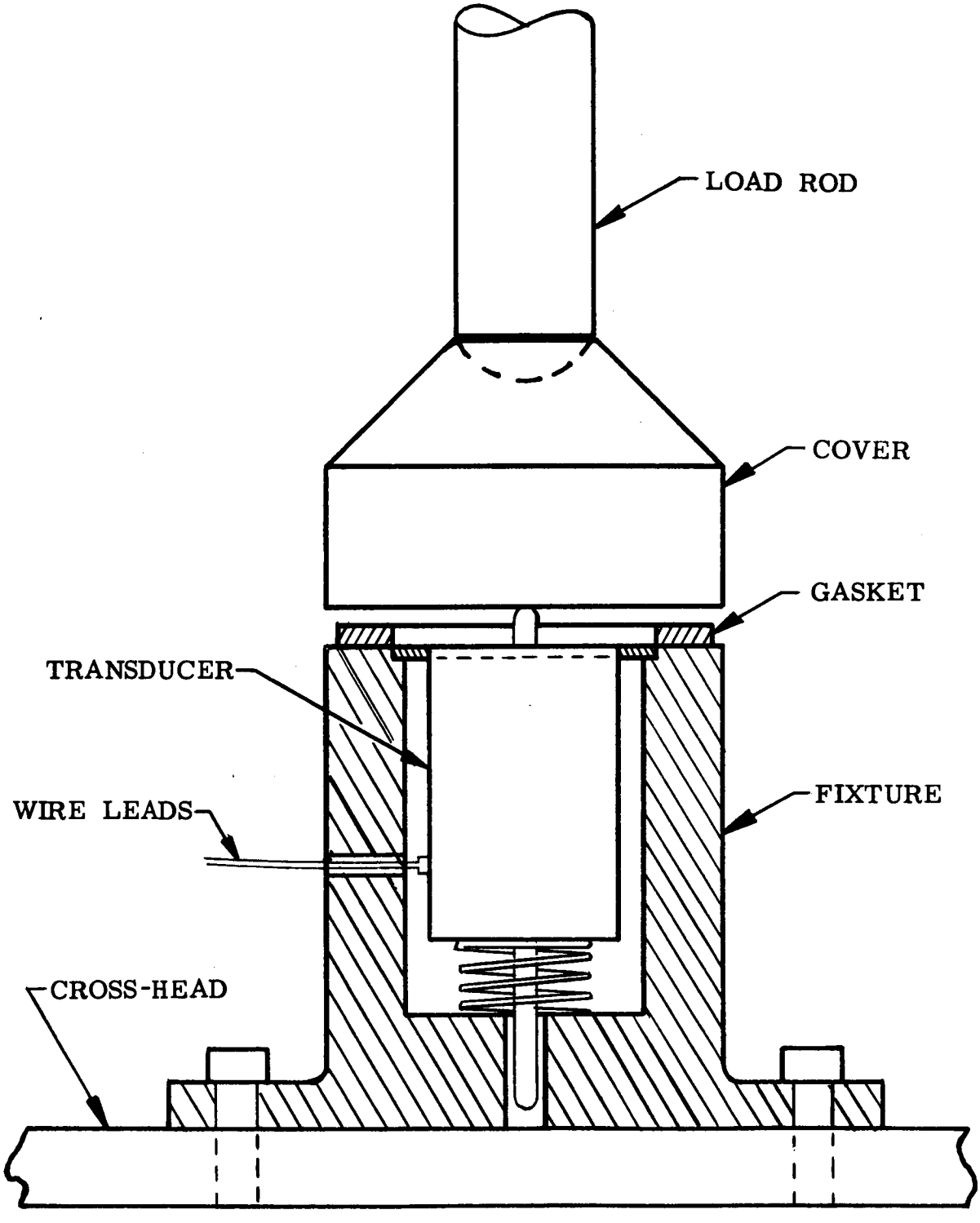

Figure 27. Compression versus Deflection Test Fixture

insulation). One disadvantage of this fixture was the loss of sensitivity of the extensometer. Previously, there was a mechanical multiplication of deflection; in the new fixture there was a 1:1 ratio of gasket deflection to core displacement. This resulted in a lower chart movement per unit deflection (chart movement was controlled by the extensometer). The recorder was used with the highest gear ratio, and the chart deflection was considerably less than previous stress-strain curves. The coil in the present fixture is being used with the maximum applied voltage to obtain the greatest chart movement per unit deflection.

A number of other gasket materials have been tested at room temperature with the improved equipment. The data obtained at room temperature are tabulated in Table 20, with values given for the deflection per unit of gasket thickness. Notice that trends in a given series are much more discernible than with previous compressive modulus values.

TABLE 20

DEFLECTION OF GASKET MATERIALS AT ROOM TEMPERATURE

Material	Deflection,* in./in.	Remarks
Allpax 500	0.0277	Fluorolube treated
Teflon FEP	0.0235	
Filled Teflon	0.0116	Fiberglass + pigment: 20%
	0.0119	25%
	0.0110	30%
	0.0094	35%
	0.0100	40%
Fluorogreen	0.0156	
Taskline	0.0237	Duriron Co. product
Fluorogold	0.0220	
CG-24	0.0205	
CG-12	0.0258	
Teflon 112 laminates		
5-mil film	0.0165	Cure: 550°F @ 100 psi
	0.0154	575°F @ 100 psi
	0.0148	625°F @ 100 psi
	0.0134	700°F @ 100 psi
8-mil film	0.0152	550°F
10-mil film	0.0154	550°F
5-mil film	0.0168	650°F @ 25 psi
	0.0268	650°F @ 50 psi
	0.0194	650°F @ 150 psi
	0.0060	650°F @ 200 psi
	0.0067	650°F @ 250 psi

* Determined during tenth cycle.

Preliminary Large Laminate Preparation

At the request of the Contracting Agency's technical representative, efforts were directed toward the preparation of large laminates. These laminates were needed to demonstrate feasibility of laminated gaskets in large static test flanges. Because more information had been collected on the Teflon-glass fabric laminates, these were selected for size scale-up to 24 in. x 24 in.

A Dake 100-ton press (Figure 28) was modified to increase the temperature capability to 700°F. The press could be heated from room temperature to 700°F in 30 minutes, but an additional 10 minutes assured even platen temperature.

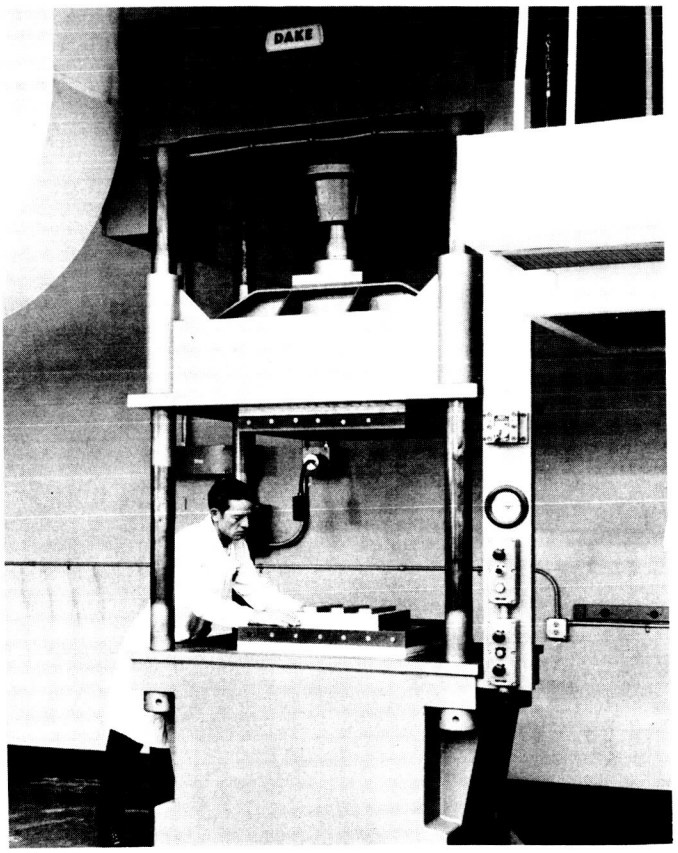

Figure 28. 100-ton 700°F Press for Large Laminates

The heavy-duty heaters gave very uniform platen temperature, which is indicated by the thickness profile diagram of the best laminate prepared (181-3) in Figure 29. The thickness sought was 1/16 in.

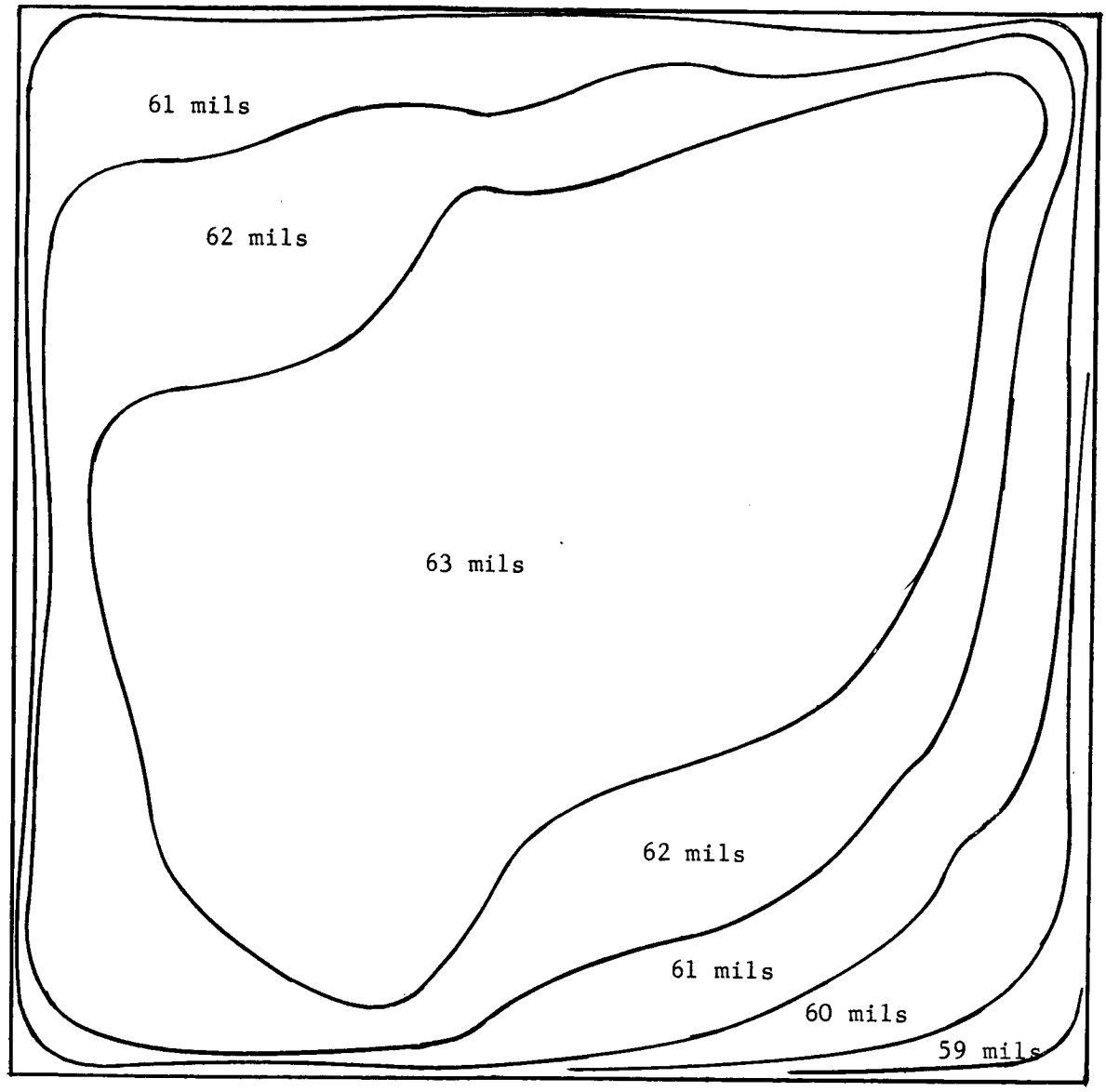

Figure 29. Isometric Diagram of 181-3 Laminate

Several problems were encountered before the 181-3 laminate was obtained. Separator problems necessitated the lamination direction between caul plates. It was desirable to use a fluorocarbon release for LOX considerations; however, it is easy to see why this type of release was not effective. Under the lamination conditions, the adhesion of Teflon to metals becomes a significant

problem. Excellent aluminum-aluminum bonds can be prepared by an equivalent process. A compromising solution was found using a very thin film of wax release agent, Poly-lease 77, but "puddling" and bleeding through the outer Teflon plies was present. This resulted in small, dark areas of mold release trapped just under the laminate surface. The only way to avoid this was to use an absolute minimum amount of mold release.

Edge seizure on the 24-in. x 24-in. cauls gave laminate failures. This was circumvented by reducing the size of the laminate by 0.5 in. less than the caul plates on all four sides.

The large laminates shown in Table 21 were prepared at 600°F, but in contrast to all previous equivalent laminates, they would not be removed after a 10-minute pressing. The large press was not equipped with a water cooling system, and forced-air cooling required several hours. This process exposed the laminate to elevated temperatures for a considerably longer time, and consequently resulted in more complete bundle wetting. The laminates were not as compressible as the previous small laminates which were cooled quickly.

TABLE 21

LARGE LAMINATE DATA

Order of Preparation and Designation (Fabric Style)	No. Glass Plies	% Resin Content (Approx)	Avg Thickness, mils	Mold Release	Remarks
1(181-2)	5	55	63.5	GS-3*	Release failure.
2(112-2)	8	80	61.0	Poly-lease 77**	Release effective but "puddles" and bleeds into outer plies.
3(112-1)	8	80	63.0		
4(18101)	5	55	62.5		
5(181-3)	5	55	62.5		Release effective but "puddles" and bleeds into outer plies. Size reduced to 23 in. x 23 in. to eliminate edge seizure.

NOTE: All laminates are Teflon FEP binder, multiaxial fabric, laminated 10 minutes @ 600°F with slow cooldown.

* Fluorocarbon release produced by Ram Chemicals, Inc.

** Wax release produced by Allied Chemical Company.

OPTIMIZATION OF THE TEFLON-GLASS LAMINATE CONCEPT AND PRELIMINARY PERFORMANCE CRITERIA

As was discovered early in this program, one of the main problems with cryogenic gasketing is that materials become harder with decreasing temperature. Their moduli increase greatly. For a flanged joint to maintain a seal, however, the gasket should retain some flexibility or compressibility. The increasing moduli result in decreasing compressibilities. In addition, the shrinkage of most gasket materials, when subjected to cryogenic temperatures, is greater than that of the bolt material, causing a drop-off in bolt load and consequently a decrease in flange pressure. This increases the possibility of a leak developing.

Existing liquid oxygen gaskets are undesirable because of cold flow and/or poor sealing ability. This section deals with the development of the Teflon-glass laminate concept and the subsequent material optimization. The need for encapsulation of individual gaskets is shown.

Some design criteria are presented as well as the results of a brief investigation into possible application of the newly developed gasket material to liquid hydrogen service.

General Teflon-Glass Laminate Development

Some cryogenic gasket suppliers add short chopped filaments to their material but, for the most part, these filaments tend to flow with the resin and only moderately restrict creep. The longer interconnected fibers of a glass fabric, however, do not flow. Knowing this, Narmco developed a gasket design utilizing a Teflon film – glass fabric combination. The effectiveness of this design in reducing cold flow was demonstrated by stress-relaxation tests, a measure of the reduction in compression load with time for the solid resin and a glass reinforced laminate. The reinforced laminate withstood more stress, as shown in Figure 30. Furthermore, the small amount of relaxation that did occur took place within the first 30 minutes; the solid resin specimen was still relaxing when the test was terminated after 2 hours. Creep rate was less at lowered temperatures but was still present (Reference 4). The indication of this test was that laminate construction is preferable because it induces a lower amount of bolt load drop-off than does solid resin construction. Other investigators also give indication that laminated gasket designs show promise for cryogenic applications (Reference 5).

There are two types of Teflon resins: TFE and FEP. Reference 6 indicates that both have satisfactory LOX-compatibility ratings. Besides the difference in appearance (TFE is opaque, while FEP is transparent), many of the properties of these materials are dissimilar. One of the most important properties for the gasket application is the modulus of elasticity, since good compressibility is quite desirable. FEP possesses a higher modulus than TFE (Reference 4),

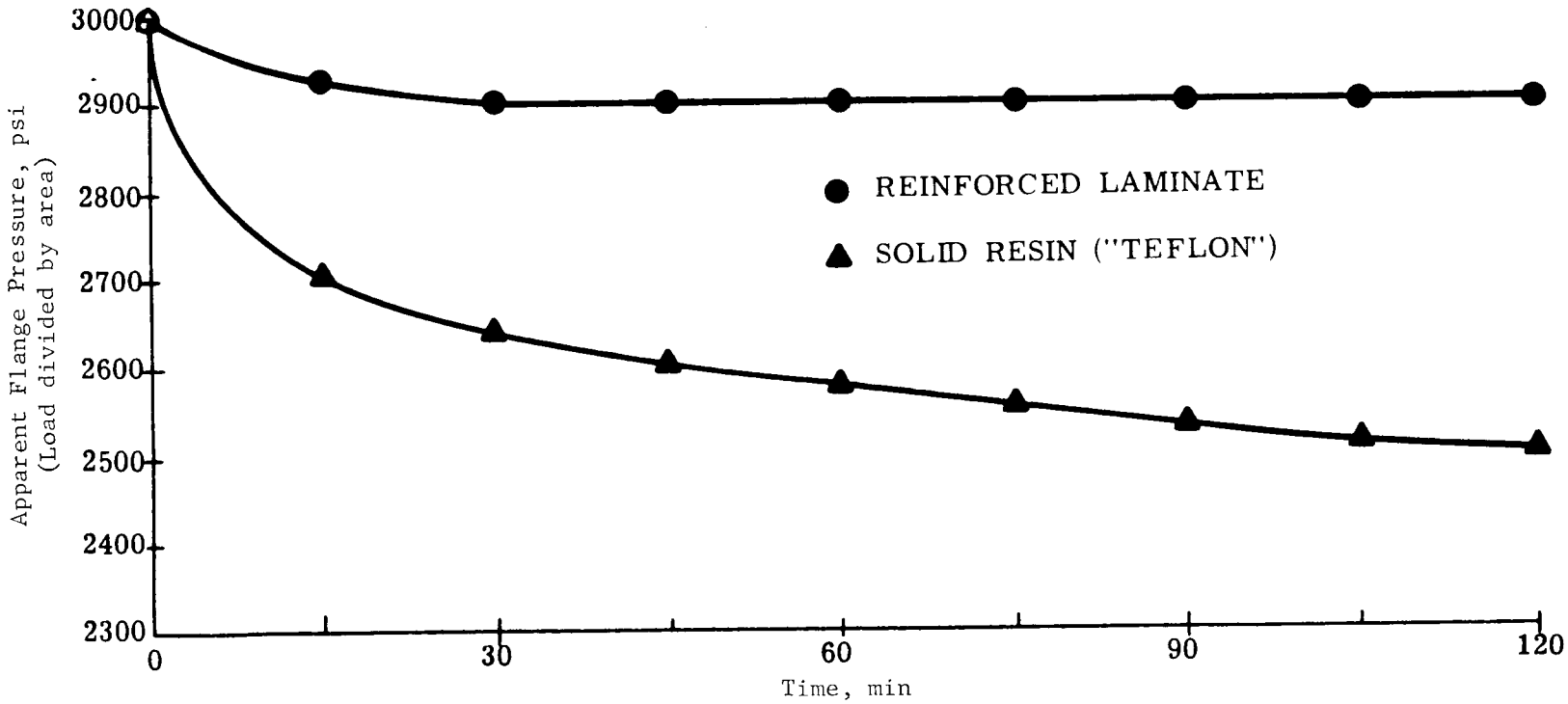

Figure 30. Stress Relaxation Curves

making it less desirable from a compressibility standpoint. The compressive moduli of both greatly increases with decreasing temperatures, as shown in Figure 31 (Reference 7).

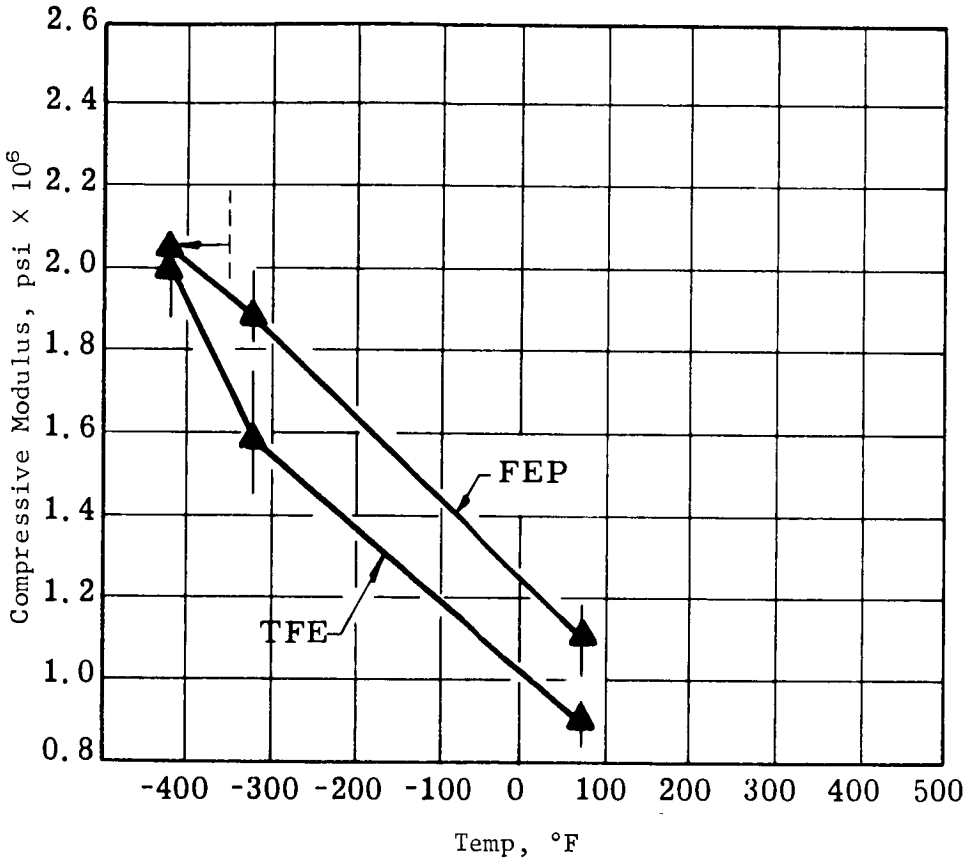

Figure 31. Effect of Temperature on the Compressive Modulus of Glass Fabric Reinforced Teflon

Another important difference between TFE and FEP greatly affects laminate fabrication. FEP is a true thermoplastic, and melts. This results in relatively easy lamination between FEP and the substrate (the reinforcement material). As FEP melts, it wets the glass fiber to form a relatively strong bond, whereas the TFE forms only a mechanical interlock. TFE, however, does not melt: at 621°F, it undergoes transition into a gel state, but never melts regardless of temperature or pressure. Therefore, the lamination technique developed involved a relatively high lamination pressure, which served to drive the substrate into the soft resin. The mechanical bond thus obtained was quite strong, although not as good as that obtainable with the FEP laminates. Figures 32 and 33 show that the FEP melted and was absorbed in part by the glass substrate and that this did not occur with TFE. Besides the superior compressibility of TFE resin, TFE glass laminates were also more compressible than FEP laminates, because the TFE did not melt and the glass substrate remained completely dry. Therefore, more of the mechanical compressibility

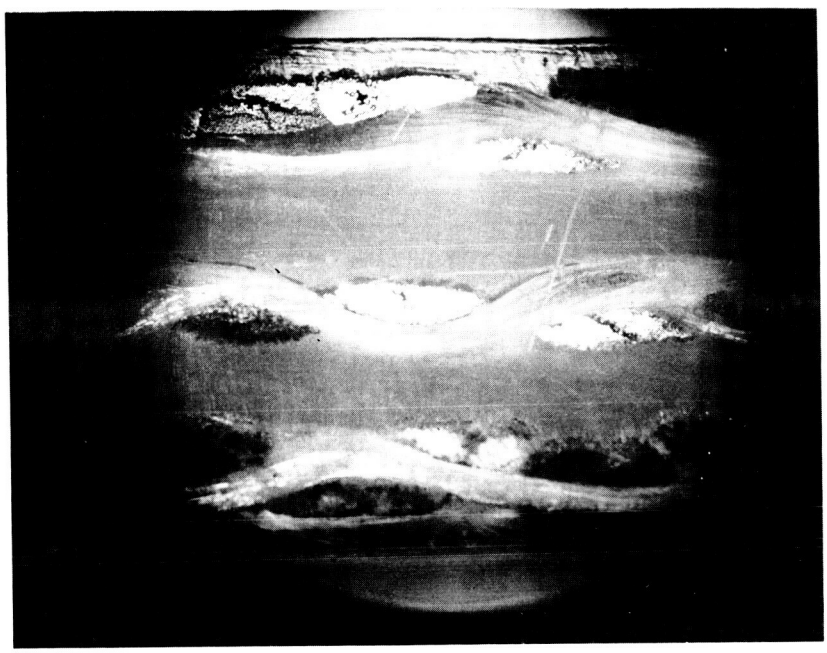

Figure 32. TFE-Glass Laminate

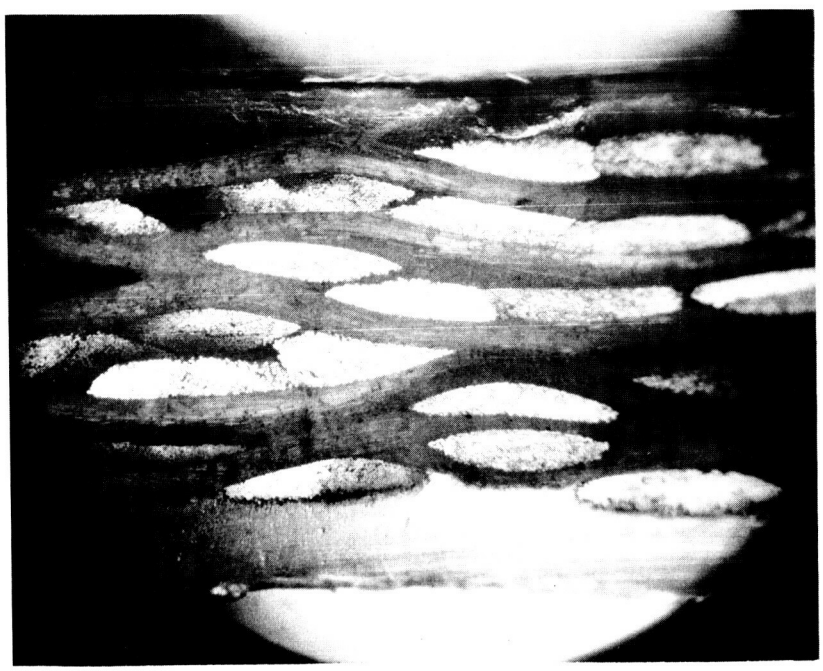

Figure 33. FEP-Glass Laminate

of the glass fabric was retained. One of the major advantages of the glass reinforced laminate design is that the mechanical compressibilitv of the glass fabric is relatively unaffected by temperature. Hence, these laminates perform very well in the cryogenic condition.

Various candidate laminate constructions were compared on the basis of compressibility and compression set. The test devised for these comparisons (called the compression versus deflection test) consisted of preloading a specimen to 1500-psi flange pressure at room temperature, cooling it to -320°F with liquid nitrogen, then varying the flange pressure from 0 to 3000 psi for 10 cycles. An extensometer measured the gasket deflection. Figure 27 is a sketch of the test fixture (without the cryostat). An x-y plotter recorded the data on tape (see Figure 18 for a typical set of curves).

Since the load can easily be converted to stress and the deflection to strain, the compression-deflection curves also represent stress-strain curves. As such, the slope of the curve should be the compressive modulus. Due to the nonlinearity of the curves, however, there is no single slope for a particular cycle. This did not allow the modulus determination in the classic manner. Nevertheless, it was reasoned that the area under the curves, representing the amount of energy absorbed, could be just as useful a standard of comparison. Therefore, these areas were measured and energy absorption figures calculated for the first, second, and tenth cycles to determine the effects of short- and long-time cycling. Candidates showing higher energy absorption values with minimum falloff with cycling were judged superior in compressibility.

Different substrates were considered for reinforcement in the laminate: glass fabrics, knit glass, a few metals in various shapes, and spirally wound glass. Because it performs so well, most of the investigation was concerned with glass fabrics.

Various weaves of fabric were considered and tested. Although the fabric weave did not appear to greatly influence the characteristics of the laminate, the weave called crowfoot satin yielded the most compressible laminates; consequently, its use was indicated. The glass fabric used in fabricating laminates must be heat-cleaned (destarched) to be LOX-compatible. As mentioned earlier, the lower modulus of TFE made it the preferred resin.

Testing was performed to determine the optimum thickness of the resin and glass plies; a resin thickness of about 0.005-in. TFE film and about 0.010-in. thick crowfoot satin glass fabric were determined to be the best combination. The fabrication technique involved rotating successive layers of fabric, producing a multiaxial laminate (see Figures 34 through 39). Such rotation, in addition to strengthening the laminate, also improved compression properties. The compressibilities of the optimum construction and of a less-than-optimum glass reinforced laminate are shown in Figure 40. Here, the energy absorption, which is a measure of compressibility, is plotted for 1, 2, and 10 load cycles.

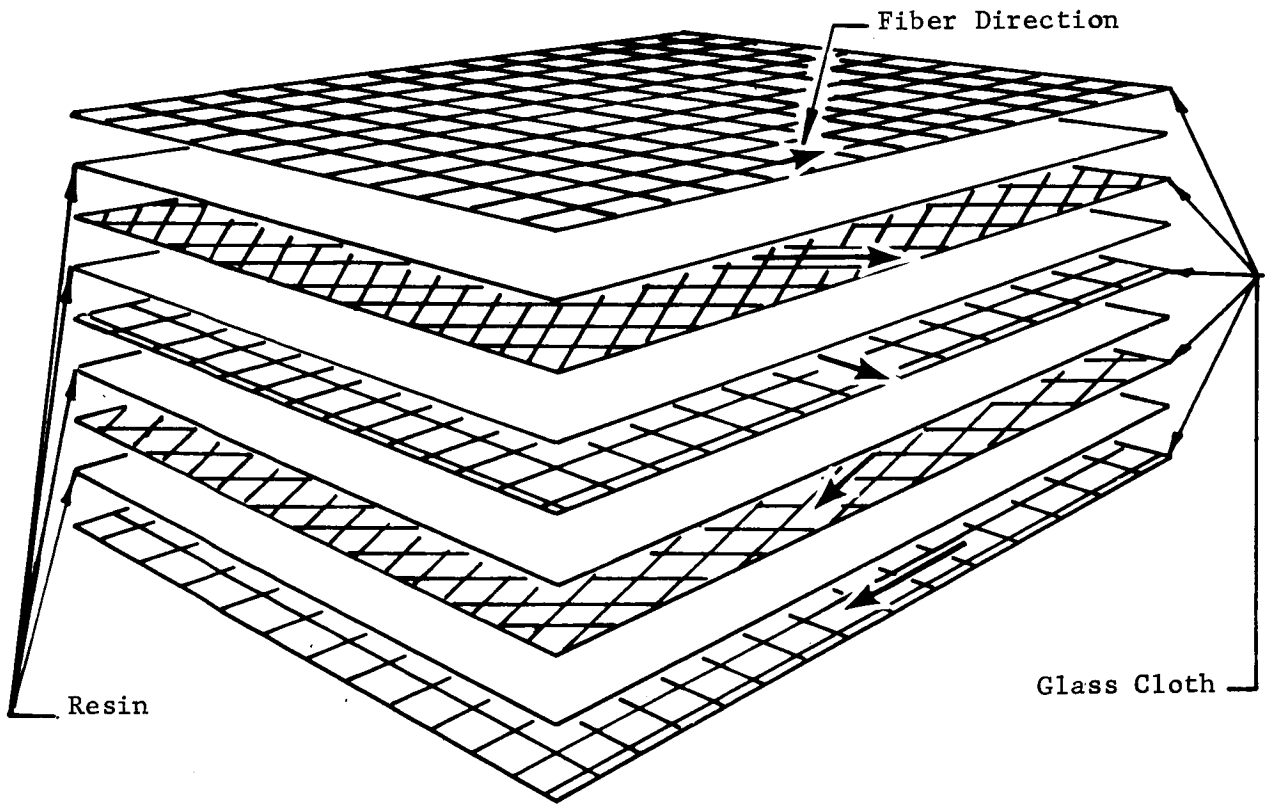

Figure 34. Laminate Layup

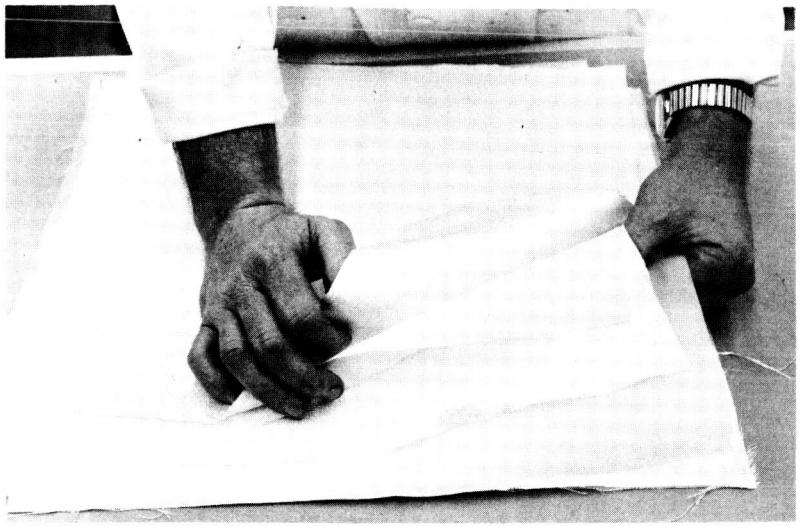

Figure 35. Interleaving the Plies

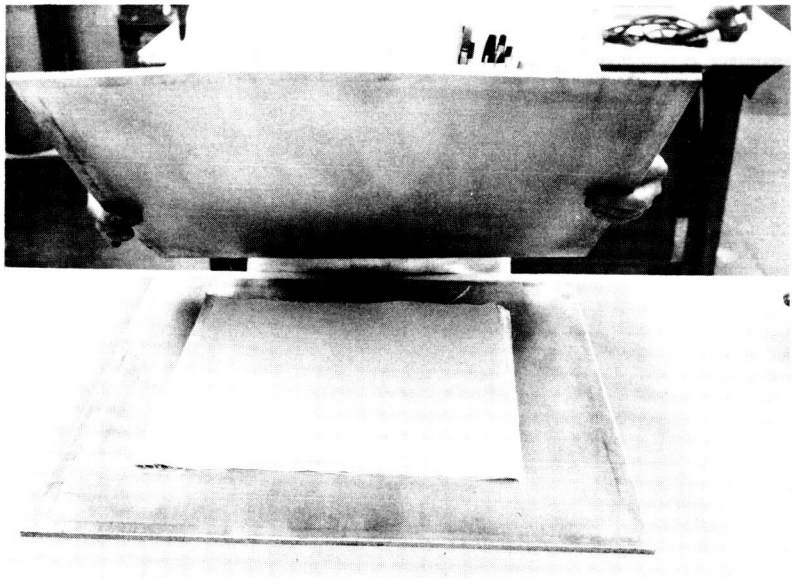

Figure 36. Layup between Caul Plates

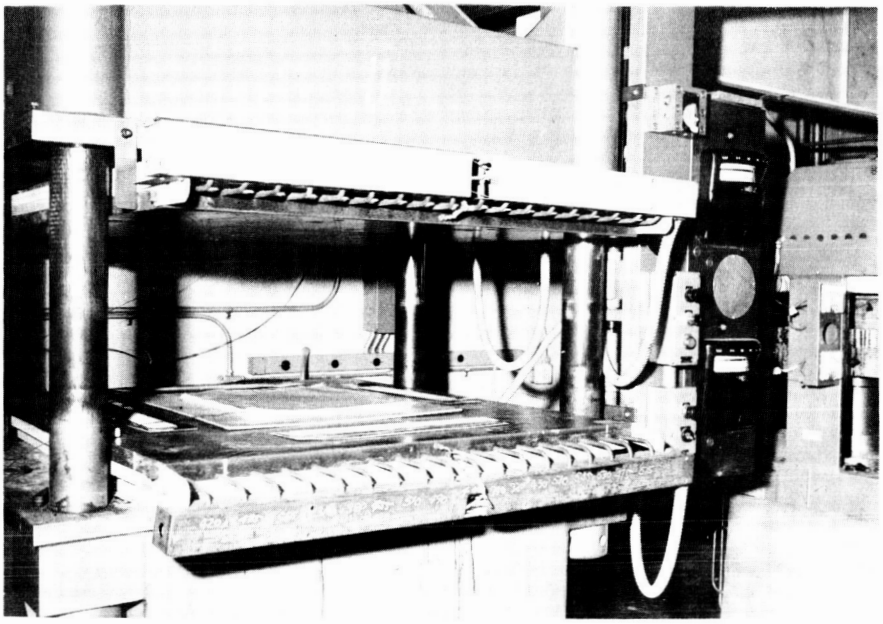

Figure 37. Lamination Press

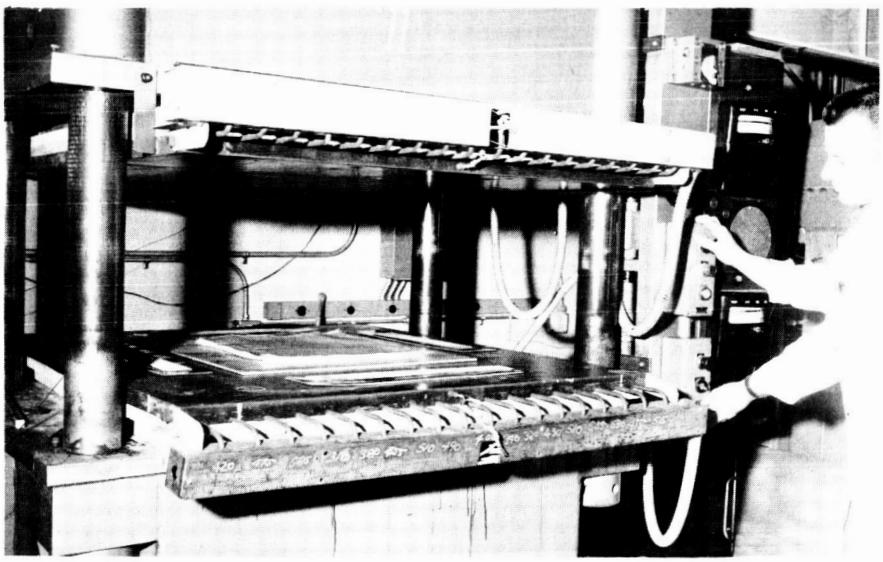

Figure 38. Closing the Press on Layup

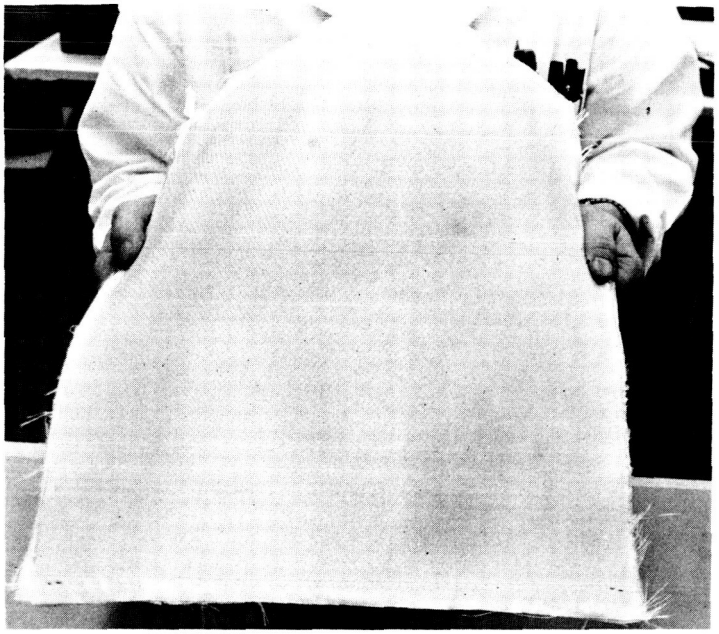

Figure 39. Finished Laminate

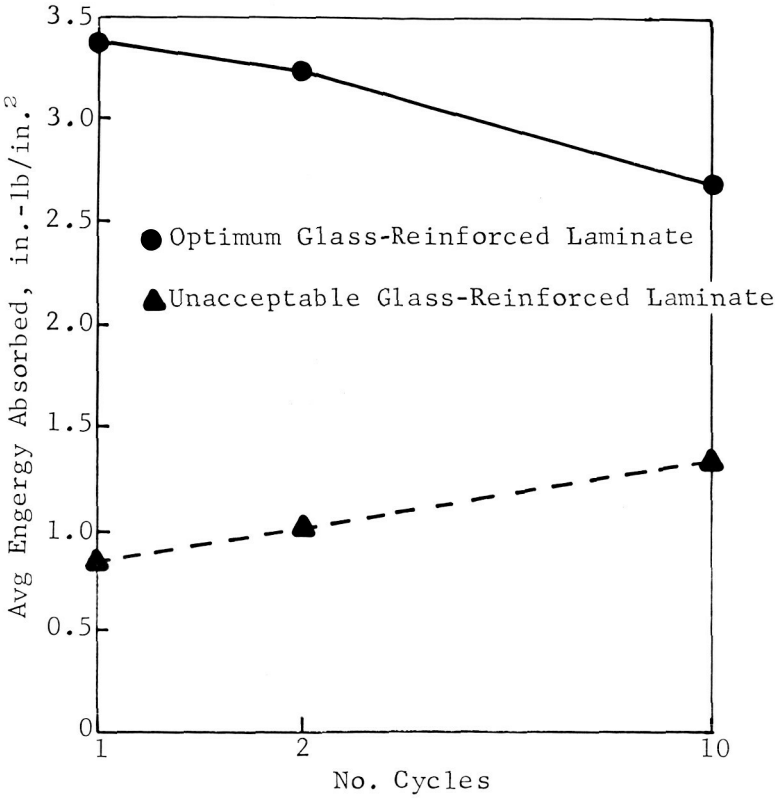

Figure 40. Energy Absorption of Glass-Reinforced Laminates

The material currently being used for LOX service, Allpax 500, is a styrene-butadiene copolymer reinforced with asbestos fiber. The performance of this material, compared with the optimum glass reinforced laminate, is shown in Figure 41. Note the superior compressibility characteristics of the newly developed material.

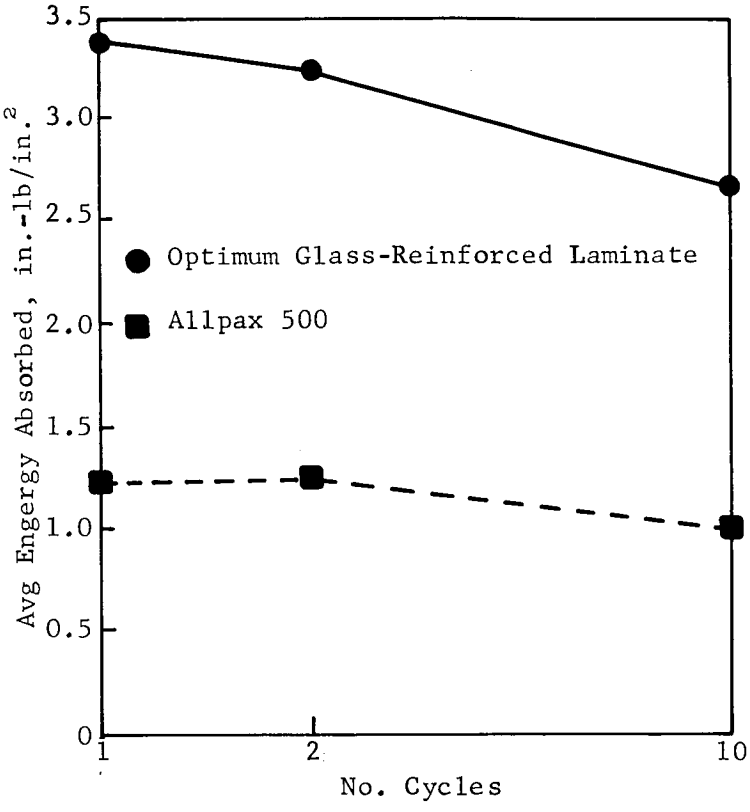

Figure 41. Energy Absorption of Glass-Reinforced Laminate and Allpax 500

When specimens were cut from a glass reinforced TFE laminate, glass fibers were exposed on the inner and outer circumference surfaces. Because the resin did not melt, the glass was still dry. This would have allowed the contained gas or liquid to soak through the gasket radially. To prevent this, encapsulation of the inside circumference surface was attempted. The easier fabricability of FEP meant that it was preferred for encapsulation. Moisture and contamination still had access to the gasket, however, through the outside circumference surface. Tests confirmed the hypothesis that moisture would reduce the compressibility at cryogenic conditions. Therefore, encapsulation of both circumferential surfaces, locking out all moisture and contamination, was adopted. Laminates were fabricated with glass fabric plies on the outer layers. Specimens were then cut from the laminates and all exposed surfaces

covered with FEP resin. Totally encapsulated gaskets were thus developed (see Figures 42 through 45). Figure 46 is a photograph of an encapsulated gasket and Figure 47 is a photograph of an enlarged cross section of a gasket, showing the TFE and glass plies totally encapsulated with FEP resin.

The leak-sealing ability of the various candidate constructions was measured at room temperature by inserting the test specimen between flanges and increasing the load to 3000 psi. The gasket was then internally pressurized to 200 psi with gaseous nitrogen, the pressure source locked off, and the flange load dropped until a leak occurred. Figure 1 is a sketch of the test fixture and Figure 24 is a photograph of the experimental setup. The flange pressure at initial leak divided by the internal pressure gave the ASME gasket m factor. The m factors smaller than one were considered attainable only by pressure-energized or bonded gaskets, neither of which was considered during this program. The leak-sealing ability of the gaskets was measured at cryogenic temperatures in the same fashion, except that after loading the gasket to 3000 psi at room temperature, the gasket and fixture were cooled to -320°F with liquid nitrogen. The remaining procedure was unchanged. With these tests, m factors as low as 1.31 at room temperature and as low as 1.56 at -320°F were obtained from Teflon-glass gaskets. The gasket material currently being used, Allpax 500, yielded an m factor of 1.30 at room temperature. At -320°F, no seal was obtained at a flange pressure of 3000 psi.

In each of these tests, a drop of 5 psi in internal pressure was considered the leak point; however, since the pressurized volume of the gasket, tubing, and valves was only 0.4 $in.^3$, the actual gaseous leakage was quite small.

Because both leak tests were concerned only with gross leakage, and because a gasket with repeatable high energy absorption characteristics normally exhibited the best leak-sealing ability, the energy absorption test was given added weight for the purpose of selecting the optimum combination of materials.

As the m factor is the ratio of flange pressure at the point of leak to the internal pressure, it cannot be used to predict a gasket material's leak-sealing ability. An approach was desired which would take into consideration the size of the gasket, the pressure to be sealed, and the physical properties of the material under consideration. The investigation into this area is presented in a later section.

Scale-up Studies for Large Diameter Gaskets

All the work performed up to this point involved a standard size test gasket with a flange area of 2 in^2. Figure 43 shows one of these gaskets being placed in the encapsulation fixture.

The behavior of the newly developed gasket material in larger size gaskets was also investigated. A series of three gasket sizes was established (see Table 22).

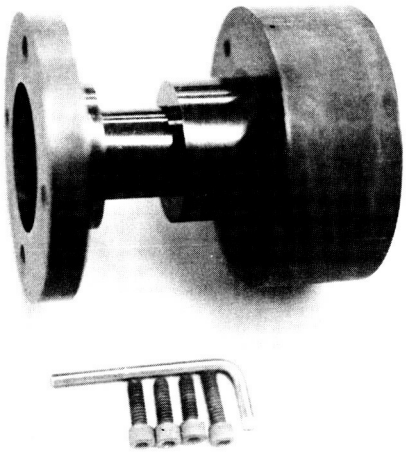

Figure 42. Test Gasket Encapsulation Fixture

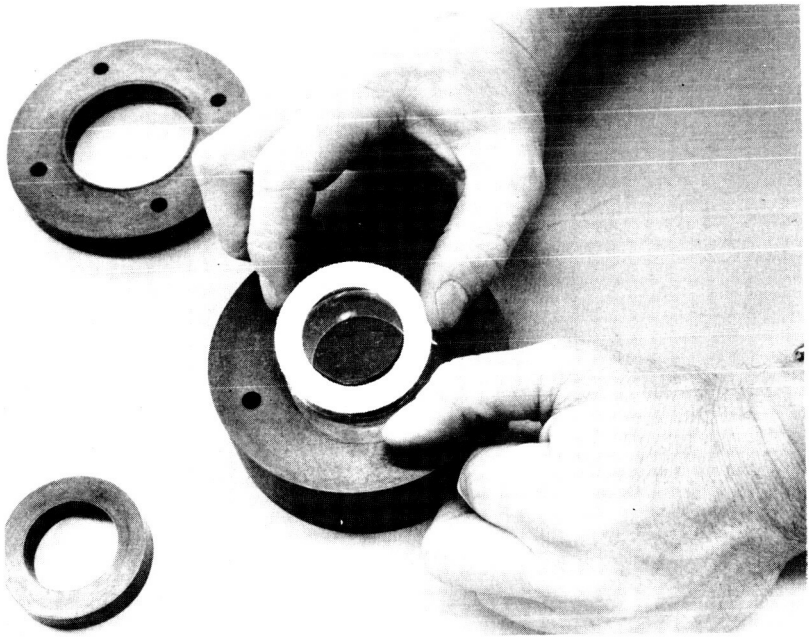

Figure 43. Laying Up the Material for Encapsulating the Test Gasket

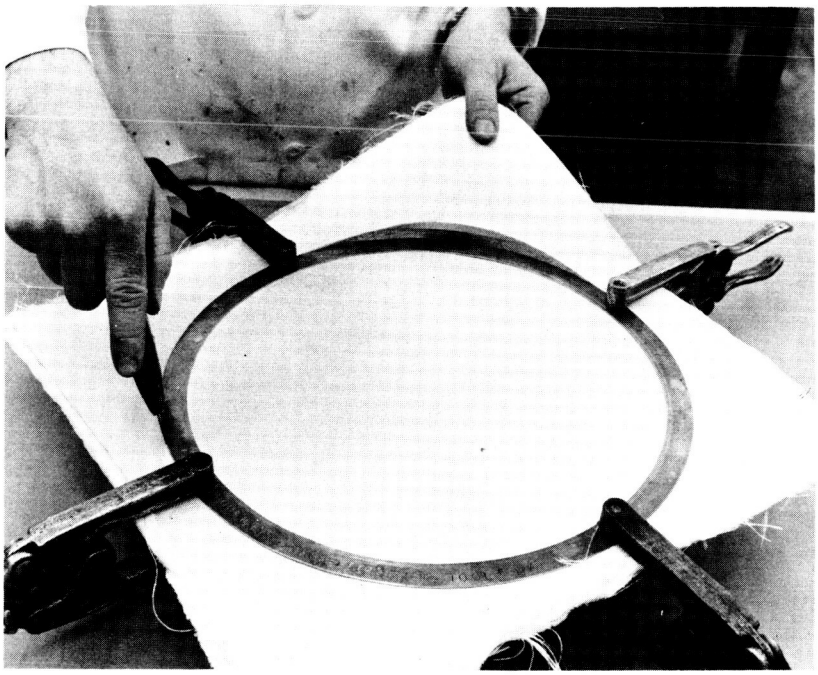

Figure 44. Large Specimen Being Cut from a Laminate

Figure 45. Laying Up the Material for Encapsulating Three Gaskets

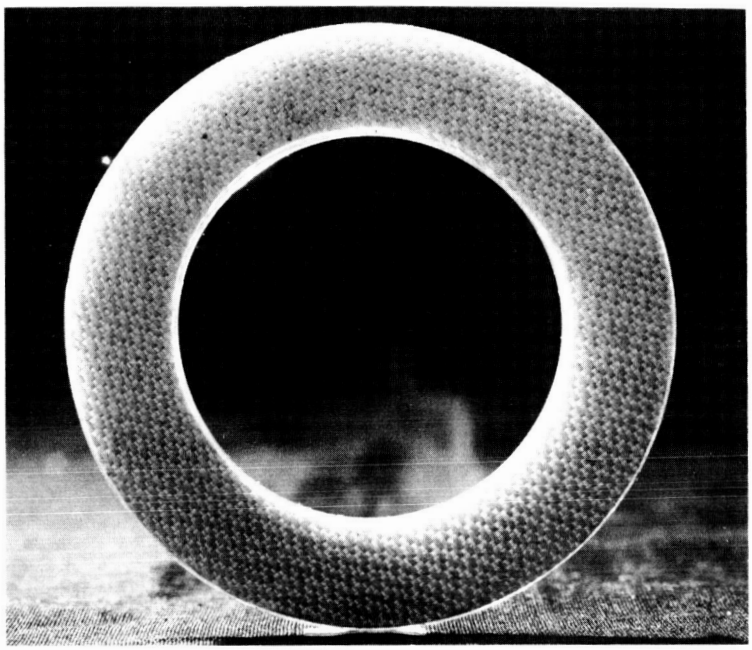

Figure 46. Encapsulated Gasket

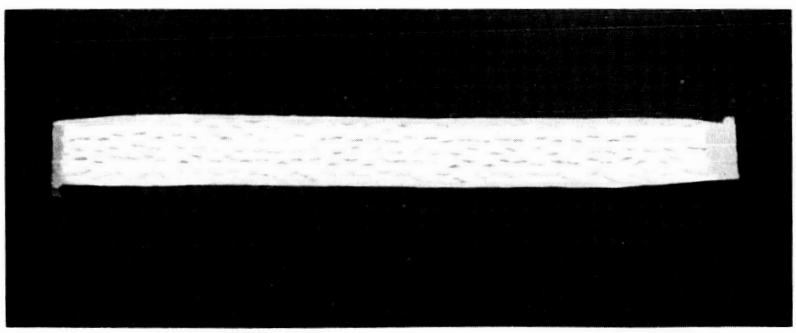

Figure 47. Gasket Cross Section

TABLE 22

LARGE DIAMETER GASKET DIMENSIONS

Gasket Size	ID, in.	OD, in.	Desired Thickness, in.
I	4	5-1/2	1/16
II	8	9-1/2	1/16
III	12	13-1/2	1/16

To fabricate the large diameter gaskets, a special encapsulation fixture capable of simultaneously encapsulating a set of three gaskets was used (see Figure 48). Unfortunately, the mating of this two-part tool could not maintain the close tolerances that existed in the small multipart fixture. Consequently, many difficulties were encountered in the encapsulation of the large gaskets. The completeness of the encapsulations was determined by spraying each specimen with a liquid dye penetrant. If a laminate were not completely encapsulated, the penetration of the dye into the glass fabric would be easily observed through the transparent FEP Teflon encapsulation (see Figure 49). Any such gaskets were reworked (reheated in the encapsulation fixture to reflow the FEP and/or applied additional FEP material). Regrettably, the addition of the excessive resin content undoubtedly affected gasket compressibility in an adverse way: the "dry" glass in the laminate absorbed more of the FEP each time it was melted. Nevertheless, 10 leakproof* specimens in each of the 3 sizes was fabricated. The performance of these specimens was to be compared with that of Allpax 500. (Narmco was supplied with six Allpax 500 specimens in each of the three sizes.)

A testing procedure was conceived and approved by the Contracting Officer's Technical Representative. As the testing progressed, modifications to this procedure became necessary.

Pairs of flanges for each of the three sizes were fabricated. A cryostat capable of holding even the largest pair was built. Figure 50 is a sketch of the experimental setup.

* Determined using the liquid dye penetrant test.

Figure 48. Set of Large Diameter Gaskets

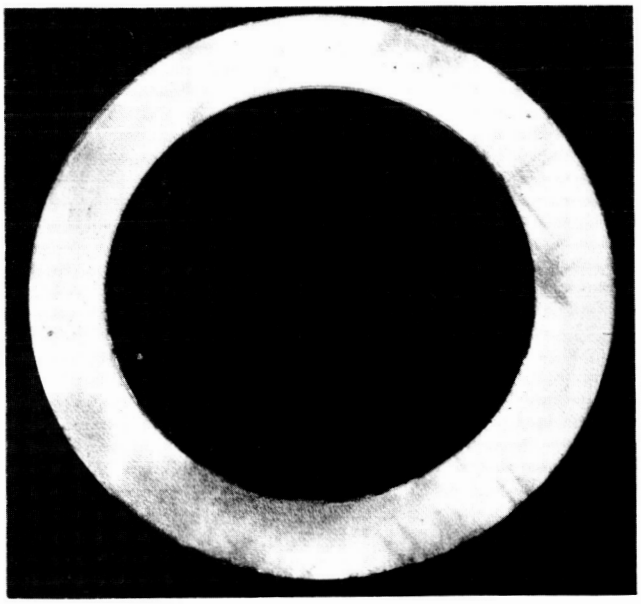

Figure 49. Dye Penetrated into Poorly Encapsulated Gasket

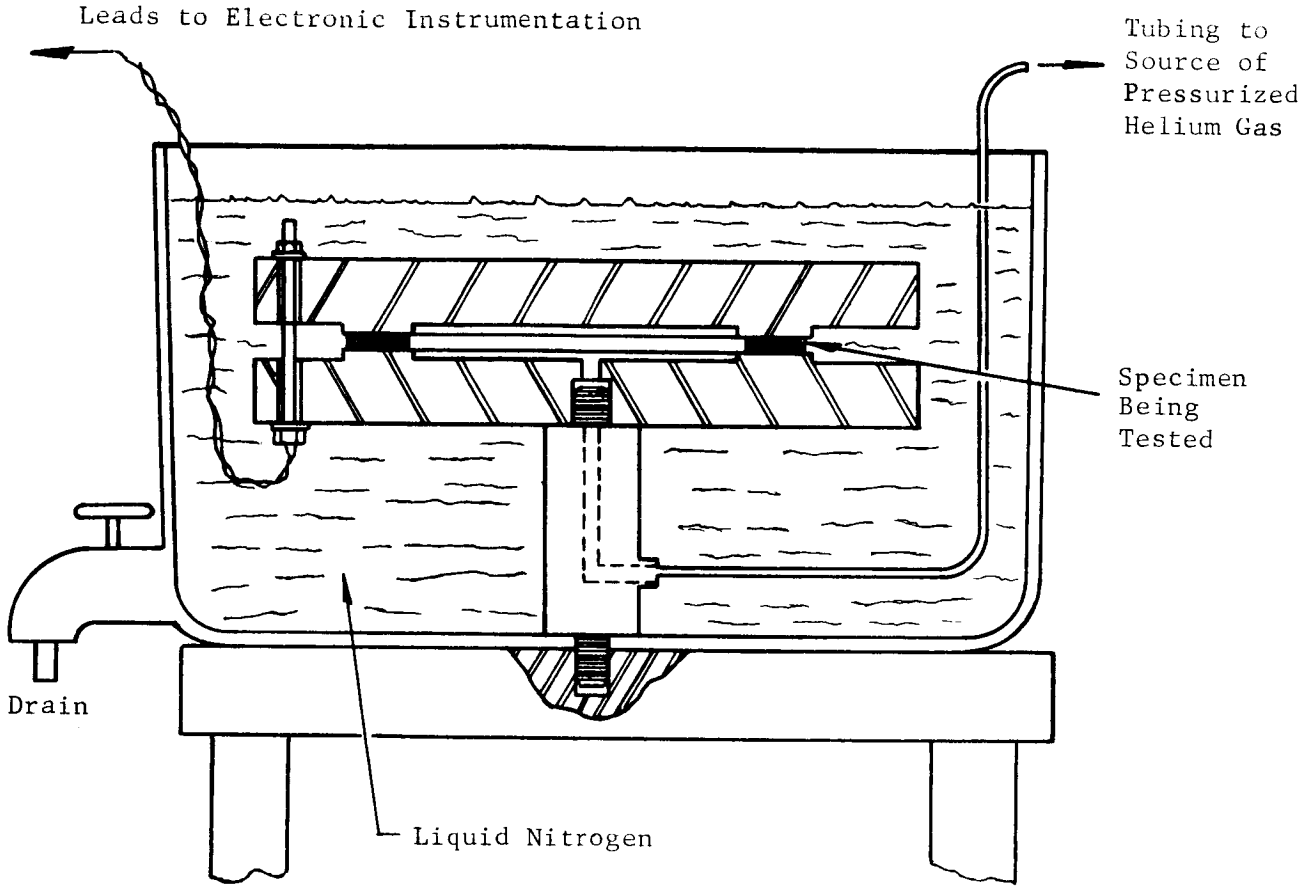

Figure 50. Experimental Setup for Large Diameter Gaskets

Strain gage bolts were utilized to determine the bolt loads and also to evaluate the technique of determining bolt loads with a torque wrench. The torque wrench technique was found to have acceptable accuracy and repeatability when used by trained personnel. It was decided that the large number of bolts required (24 for the largest gasket size) did not all have to be of the expensive load-indicating type but rather that three or four of these, distributed among conventional bolts, would suffice.

The technique employed in the clamping down operation then involved tightening down the load-indicating bolts until the bolt load desired was obtained, noting the torque value associated with this load, averaging these torques from all of the load-indicating bolts, and then applying this average torque to the other (nonindicating) bolts. This operation was performed in stages (i.e., a desired bolt load could not be arrived at directly but was approached in increments) and retorquing was required because changing the loading in any bolt changed the loading on all bolts.

The test procedure is described below:

1. The fixture itself was leak-tested. This was accomplished by inserting a plug in the bottom flange at the gas inlet location and then pressurizing the system. The pressure was shut off at 500 psi. The system was considered leakproof if it maintained this pressure for a length of time.

2. The plug was removed and a gasket installed (see Figures 51 and 52). The top flange was put in place. Cap screws, nuts and washers were then assembled in place and the torque wrench used to obtain the desired bolt loading (see Figure 53). The helium gas was again introduced to check the room temperature leak-sealing ability (see Figure 54). The specimen had to contain 100 psi for the test to proceed. The gas was then relieved.

3. Liquid nitrogen was added to the cryostat until the entire test fixture became submerged (see Figure 55). After temperature equilibrium was reached, the bolts were retorqued to the level desired.

4. The helium gas was then reintroduced, first to 50 psi, then in 20-psi increments. After each pressure was obtained, the system was sealed off (see Figure 56). Any drop-off in pressure (as shown by a pressure gage) indicated a leak. The pressure was then relieved and the "leak point" again approached, only in smaller increments. In this manner, the maximum pressure contained at a bolt load level was determined within 5 psi.

5. After relieving the pressure, the bolts were torqued down to the next bolt load level desired and the procedure described in Item 4 repeated. In this manner, the maximum pressure contained by each specimen at three different load levels was obtained.

The initially conceived load levels were gasket flange pressures of 1500, 2000, and 2500 psi. When the testing started on the smallest size gaskets, however, it was discovered that these levels resulted in pressure containment in excess of the 500-psi limit of the pressure gage. Therefore, the gasket flange pressure levels were lowered to 500, 1000, and 1500 psi. Unfortunately, these levels were too low for the largest gaskets, and levels of 3000, 3500, and 4000 psi were employed. Therefore, evaluation of the effect of gasket size was impeded because of the different loading used.

The test results are presented in Tables 23 through 28. Note the variation in thicknesses of the laminated gaskets due to the encapsulation rework.

The spread of test results for the laminated gaskets is quite large. However, this large spread is also present in the Allpax test results.

The superiority of the laminated gasket over the Allpax 500 was less noticeable in these large diameter gaskets than it was with the 2 $in.^2$ test

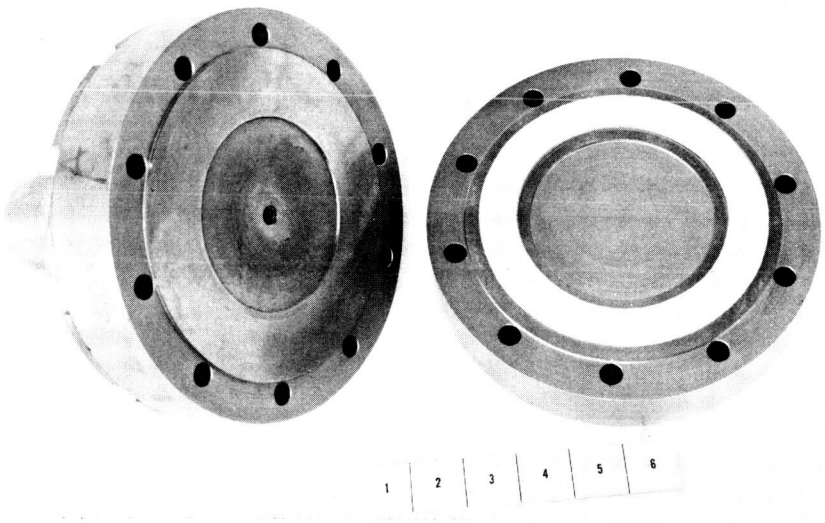

Figure 51. Smallest (Size I) Gasket and Fixture

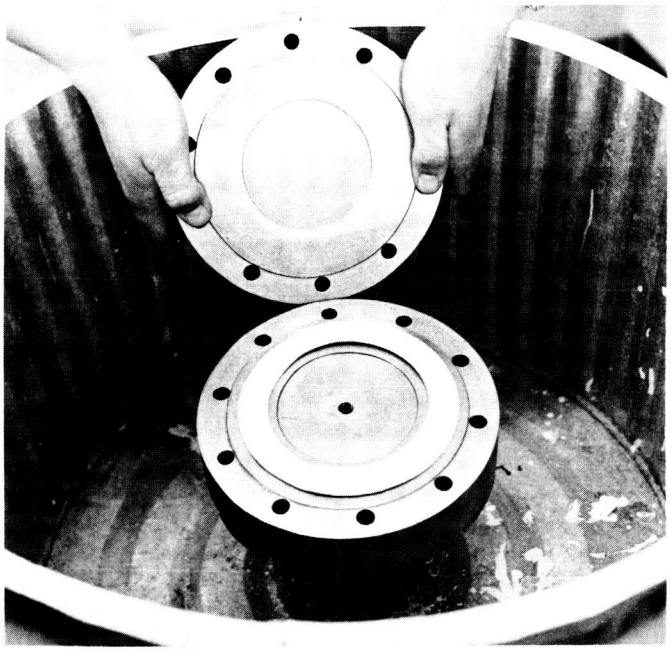

Figure 52. Assembling the Gasket Test Fixture

Figure 53. Bolting Gasket Test Fixture

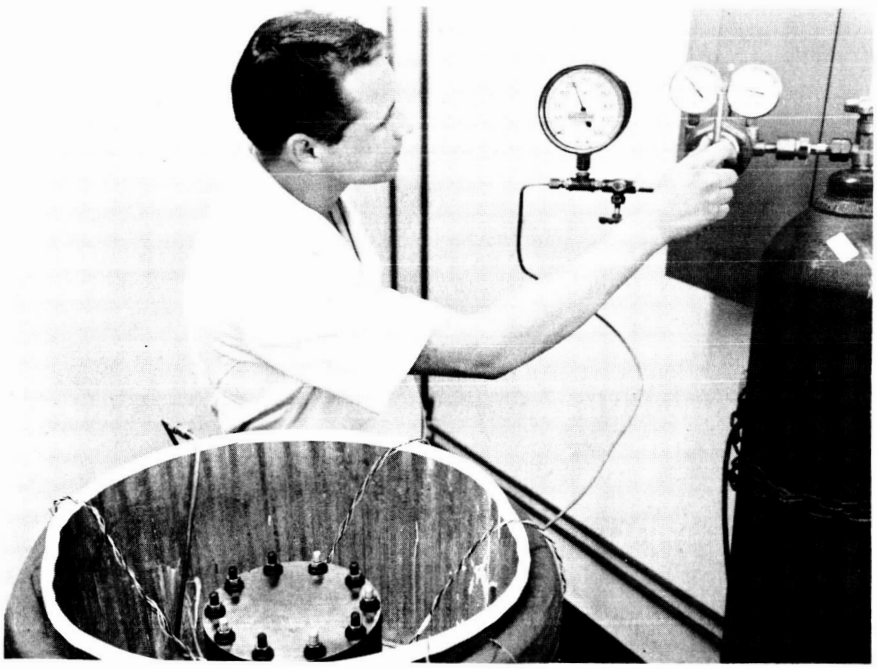

Figure 54. Room Temperature Leak Testing

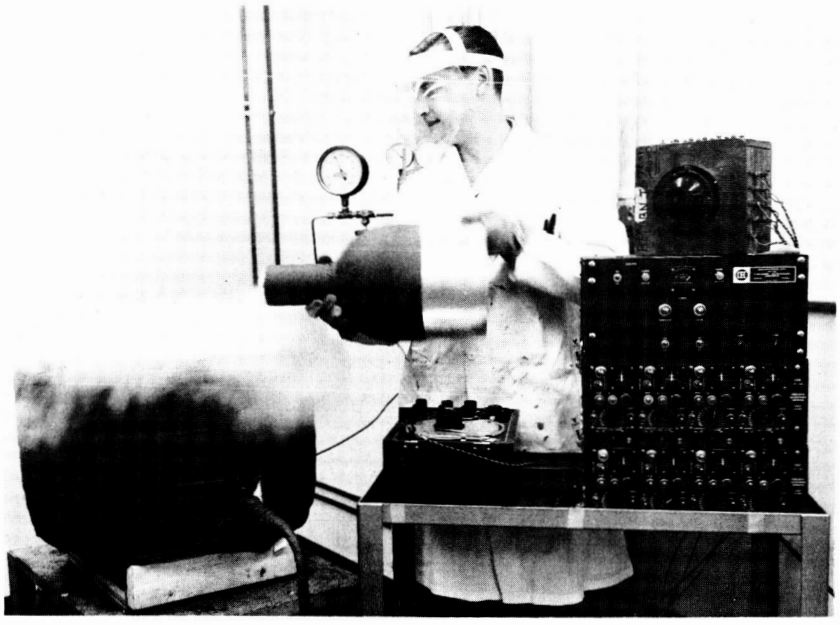

Figure 55. Adding the Cryogen

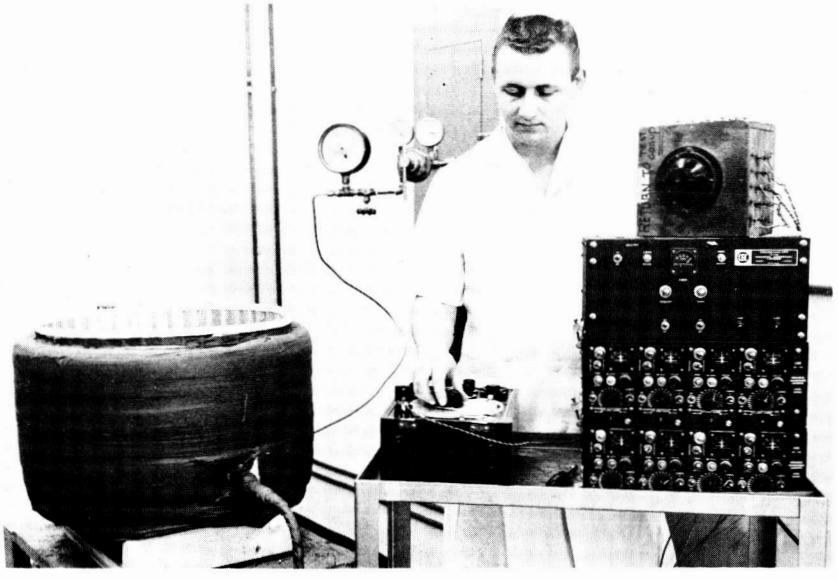

Figure 56. Gasket Testing

TABLE 23

TEST RESULTS OF SIZE I LAMINATED GASKETS

(4-in. Inside Diameter)

Specimen No.	Specimen Thickness, in.	Gasket Flange Pressure, psi	Torque, in.-lb	Contained Pressure, psi
4-1	0.078	500 1000 1500	65 110 160	400 380 500+
4-2	0.095	500 1000 1500	55 95 135	40 60 80
4-3	0.078	500 1000 1500	35 70 115	110 185 230
4-4	0.085	500 1000 1500	50 90 135	125 200 270
4-5	0.075	500 1000 1500	50 90 125	30 50 75
4-6	0.075	500 1000 1500	45 95 130	100 120 160
4-7	0.078	500 1000 1500	45 90 125	100 150 160
4-8	0.090	500 1000 1500	55 95 130	95 130 165
4-9	0.090	500 1000 1500	50 90 130	100 225 300
4-10	0.091	500 1000 1500	50 90 125	70 80 90

TABLE 24

TEST RESULTS OF SIZE I ALLPAX 500 GASKETS

(4-in. Inside Diameter)

Specimen No.	Specimen Thickness, in.	Gasket Flange Pressure, psi	Torque, in.-lb	Contained Pressure, psi
4-11	0.060	500 1000 1500	80 145 185	85 100 200
4-12	0.060	500 1000 1500	45 90 135	60 100 150
4-13	0.060	500 1000 1500	45 100 155	75 150 170
4-14	0.060	500 1000 1500	50 90 135	110 200 200
4-15	0.060	500 1000 1500	50 95 140	145 250 250
4-16	0.060	500 1000 1500	65 120 165	110 190 225

TABLE 25

TEST RESULTS OF SIZE II LAMINATED GASKETS

(8-in. Inside Diameter)

Specimen No.	Specimen Thickness, in.	Gasket Flange Pressure, psi	Torque, in.-lb	Contained Pressure, psi
8-1	0.080	500 1000 1500	55 95 140	75 110 125
8-2	0.090	500 1000 1500	55 100 140	20 50 100
8-3	0.080	500 1000 1500	55 95 135	110 150 175
8-4	0.088	500 1000 1500	50 100 140	100 160 200
8-5	0.096	500 1000 1500	45 95 135	0 0 0
8-6	0.074	500 1000 1500	60 100 140	70 70 80
8-7	0.095	500 1000 1500	55 100 145	110 130 160
8-8	0.075	500 1000 1500	60 95 145	60 60 70
8-9	0.089	500 1000 1500	60 105 140	60 100 140
8-10	0.092	500 1000 1500	70 120 180	165 250 325

TABLE 26

TEST RESULTS OF SIZE II ALLPAX 500 GASKETS

(8-in. Inside Diameter)

Specimen No.	Specimen Thickness, in.	Gasket Flange Pressure, psi	Torque, in.-lb	Contained Pressure, psi
8-11	0.060	500 1000 1500	50 95 130	80 110 160
8-12	0.060	500 1000 1500	60 105 140	60 100 125
8-13	0.060	500 1000 1500	50 100 140	75 140 180
8-14	0.060	500 1000 1500	65 120 155	80 150 170
8-15	0.060	500 1000 1500	65 100 140	55 70 100
8-16	0.060	500 1000 1500	60 100 140	90 125 170

TABLE 27

TEST RESULTS OF SIZE III LAMINATED GASKETS

(12-in. Inside Diameter)

Specimen No.	Specimen Thickness, in.	Gasket Flange Pressure, psi	Torque, in.-lb	Contained Pressure, psi
12-1	0.084	3000 3500 4000	330 380 440	225 220 280
12-2	0.098	3000 3500 4000	305 365 430	75 85 125
12-3	0.081	3000 3500 4000	305 370 445	75 130 200
12-4	0.095	3000 3500 4000	330 420 450	80 80 110
12-5	0.084	3000 3500 4000	330 375 420	80 100 100
12-6	0.101	3000 3500 4000	330 375 420	100 120 150
12-7	0.085	3000 3500 4000	320 380 425	140 220 245
12-8	0.083	3000 3500 4000	320 365 440	70 75 80
12-9	0.093	3000 3500 4000	310 350 390	65 70 100
12-10	0.093	3000 3500 4000	325 395 500	75 120 270

TABLE 28

TEST RESULTS OF SIZE III ALLPAX 500 GASKETS

(12-in. Inside Diameter)

Specimen No.	Specimen Thickness, in.	Gasket Flange Pressure, psi	Torque, in.-lb	Contained Pressure, psi
12-11	0.060	3000 3500 4000	360 400 460	50 70 120
12-12	0.061	3000 3500 4000	330 375 425	80 80 110
12-13	0.060	3000 3500 4000	340 380 450	70 100 115
12-14	0.060	3000 3500 4000	345 440 550	90 90 110
12-15	0.060	3000 3500 4000	330 380 430	80 105 110
12-16	0.060	3000 3500 4000	330 370 420	100 120 175

gasket (see Figure 41). However, it is believed that most of this reduction in superiority was due to encapsulation difficulties. However, it should be repeated that even with the difficulties experienced, the large diameter laminated gaskets still were superior to the Allpax 500. This fact, together with the better LOX-compatibility properties, gave indication that the laminated gasket would be the preferred material.

Performance Criteria Investigation

A major requirement of any gasket is that it be leakproof. Completely leakproof connections are not always required, however. A pipeline transmitting a heavy oil and a line containing helium have vastly different sealing requirements. Therefore, the material to be contained must be specified before leakage requirements are known. It is generally accepted that LOX systems can operate with around 0.0 to 3.0 std cc/second leakage (Reference 5, p. 14). While some experimental work has been done with mass spectrometer measurements and helium gas (Reference 8), the testing performed in this program dealt only with gross leakage. However, it was felt that testing with gaseous nitrogen at the cryogenic condition was more severe than the actual application (containment of the cryogenic liquid). Also, leak tests were performed at both ambient and cryogenic conditions.

The flange pressure loading on a gasket can be obtained in the following manner: the torque applied to the bolts can be used to find the load in the bolts by the involved equations given in most textbooks (e.g., Reference 9) or handbooks (Reference 10), or by using the approximate formula that torque is equal to two-tenths of the product of the bolt diameter and bolt load (Reference 11). The total bolt load divided by the gasket flange area yields an apparent flange pressure. If all threads are well lubricated, this is the actual flange pressure. If not, some of the torque is lost in friction and the apparent flange pressure value is higher than the actual value. Use of Figure 2 of Reference 12 then yields actual flange pressure from the calculated apparent flange pressure.

The thickness of a gasket must be enough to allow plastic flow of the outer surfaces into the irregularities of the flanges, as normal stress alone is not sufficient to effect a seal. In addition, the thickness must be enough to retain the seal after the relative displacement of the flange faces caused by different thermal contractions of the joint elements during large temperature changes. At the same time, however, a gasket must be as thin as possible to reduce the chance of gasket extrusion and to minimize torque losses in the bolting (Reference 13). For this particular program, the gasket thickness was specified, so it could not be considered variable.

Various gasket designs have evolved with time. For example, a group referred to as pressure-energized seals have been developed. These seals have cross sections such that increasing internal pressure increases the flange pressure, improving the seal. Constrained gaskets, where the gasket is confined in a groove in one of the flanges, have been shown to be superior to

unconstrained ones (References 8 and 14). However, the flat gasket materials developed for this program were specified by the customer, so other configurations were not considered during the early part of the program.

The relation between minimum sealing stress and the internal pressure contained by the joint is linear (see Figure 1 of Reference 15). In addition to the pressure differential across the seal and the flange stress, the following parameters affect the leakage phenomenon: the yield strengths and strain hardening characteristics of the gasket and flange materials, and the surface finish of the mating surfaces (Reference 8).

The relative displacement of the flange faces when the connection is made cryogenic is due to the difference in thermal contractions between the bolts and gasket. Usually, the gasket shrinks more than the bolts, so the flange faces tend to approach each other. The usual net result of these shrinkages is a reduction in the bolt load and hence a reduction in the gasket flange pressure. If the initial loading were not high enough to allow for this, it is possible that the reduction in gasket flange pressure would be sufficient to allow leakage. This problem is compounded by the fact that gasket materials harden when cooled, so that increased flange pressure should be applied to maintain a seal. If excess load is applied initially to allow for these two factors, it is possible that the gasket material could be extruded and flattened so much that the shrinkage problem could still lead to leakage. Therefore, the required bolting for a specific gasket material in a particular joint for a given environmental condition is an important factor and one that does not allow too much latitude.

One of the advantages offered by the glass reinforced laminate gasket material recently developed is that, although its modulus is relatively high at ambient temperature and, like almost everything else, it increases with decreasing temperatures, the modulus changes less with temperature than many gasket materials. Therefore, the changing load requirements with changing temperatures are minimized.

The increase in modulus with decreasing temperature can be explained by the fact that a polymer goes through a glass transition stage (from a rubberlike material to a glasslike material) when it is cooled. This increasing of moduli with decreasing temperature can also be explained by treating organic gasket materials as two-phase: elastic and viscoelastic (where stress-strain relationships are time-dependent). Above the transition temperature, the elastic phase dominates; below, the viscoelastic, with its higher modulus. The viscoelastic phase could also explain the creep, or cold flow, phenomenon.

The previous discussion dealt with cryogenic gasket sealing in general. At this point in the program, a theoretical analysis was completed which predicted the torque required on a gasket joint to seal a given internal pressure. The derivation of the theoretical relationship is presented in detail in Appendix A. A comparison of this relationship and another relationship which was developed at a later date is also presented in this section and in Appendix B.

Liquid Hydrogen Performance Studies

A series of encapsulated gaskets with the optimum Teflon-glass laminate construction was fabricated. Five of these specimens were tested in a special fixture in liquid hydrogen (the existing fixture and cryostat, used throughout the program with liquid nitrogen, could not be used with liquid hydrogen — see Figures 57 through 59). The average of the test results is presented in Figure 60, along with results for Laminate 48, the same (optimum) construction, obtained earlier in liquid nitrogen. Note that the temperature difference did not appreciably change the behavior. The warmer liquid nitrogen environment gave better compressibility, but liquid hydrogen provided results which were also satisfactory.

To verify that consistent results were being obtained, adjacent specimens were cut from the same laminate and arbitrarily identified T-1 and T-2. These unencapsulated specimens were tested at liquid nitrogen in the liquid nitrogen fixture (see Figure 61). The almost identical results confirmed the reproducibility of the test. To check the liquid hydrogen fixture versus the liquid nitrogen fixture, Specimen T-2 was tested in the liquid hydrogen fixture with liquid nitrogen fluid. The similarity of the two curves for T-2 in Figure 62 demonstrated that compatible results were obtainable from the two fixtures.

Specimen T-1 was also run in liquid hydrogen. The comparison of test results at the two temperatures is shown in Figure 63. It is believed that the superior compressibility at liquid hydrogen was due to the fact that the specimen was run at this condition first, then rerun at liquid nitrogen. Some of the specimen's compressibility was expended in the initial test, so that the first cycle at liquid nitrogen was actually the eleventh cycle the specimen experienced.

The main conclusion of the liquid hydrogen investigation was that the more severe environment (about 100°F colder) only slightly diminished the compressibilities of the newly designed gasket.

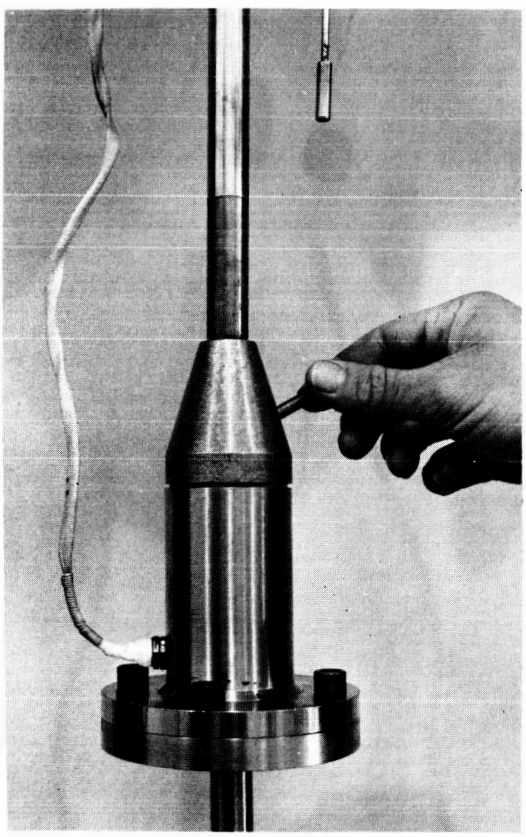

Figure 57. Liquid Hydrogen Test Fixture

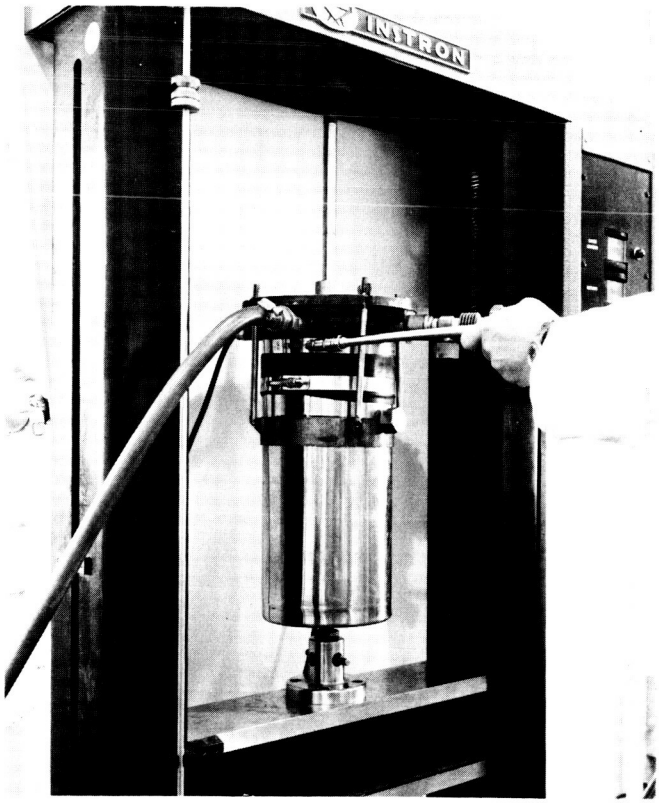

Figure 58. Liquid Hydrogen Cryostat Being Assembled

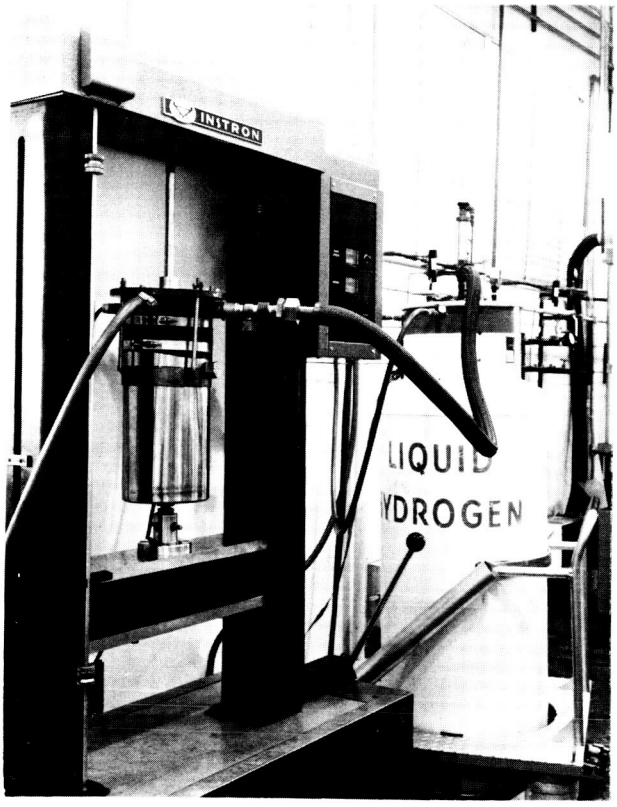

Figure 59. Liquid Hydrogen Testing

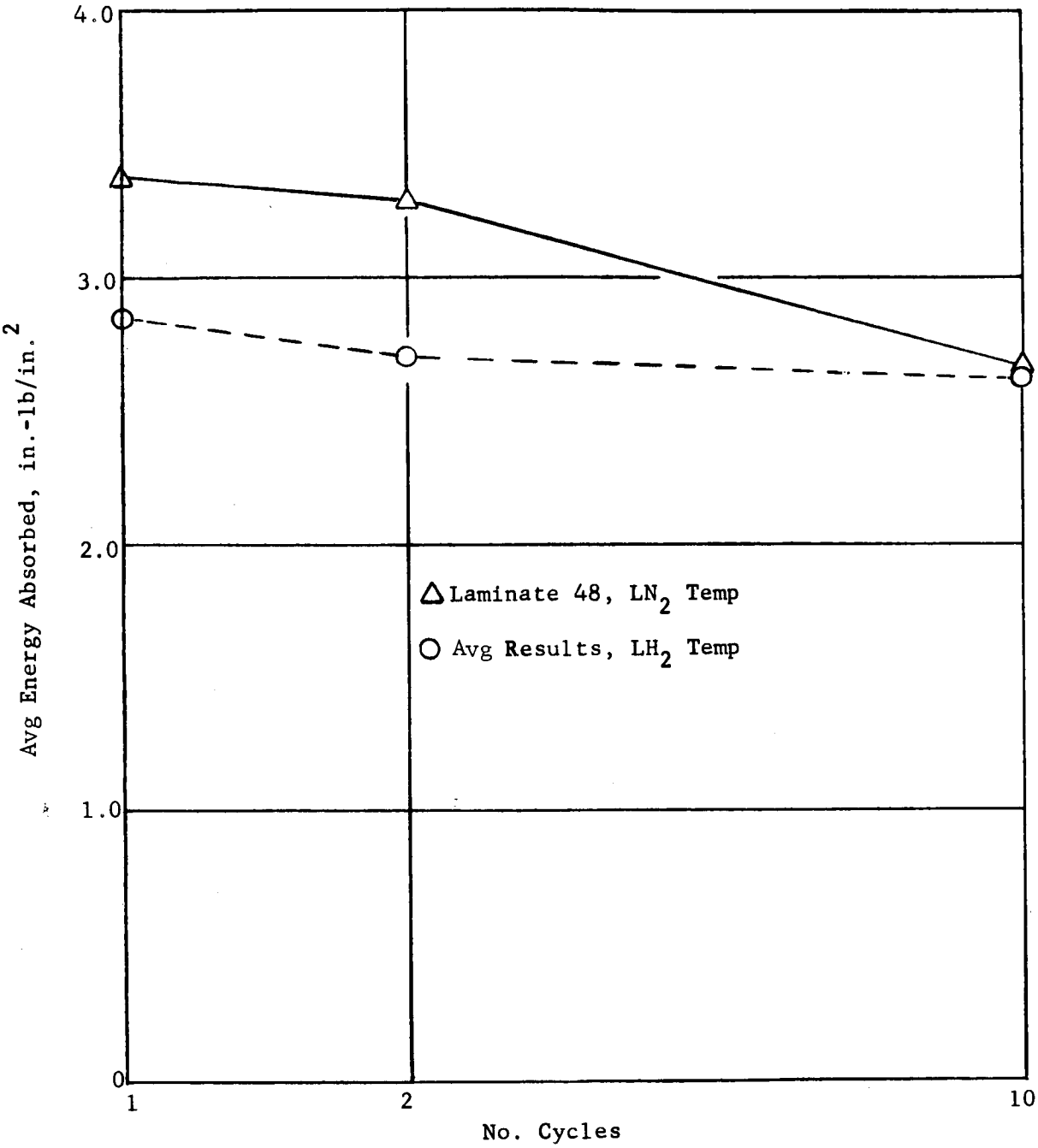

Figure 60. Energy Absorptions of Laminate Design at Liquid Nitrogen and Liquid Hydrogen Temperatures

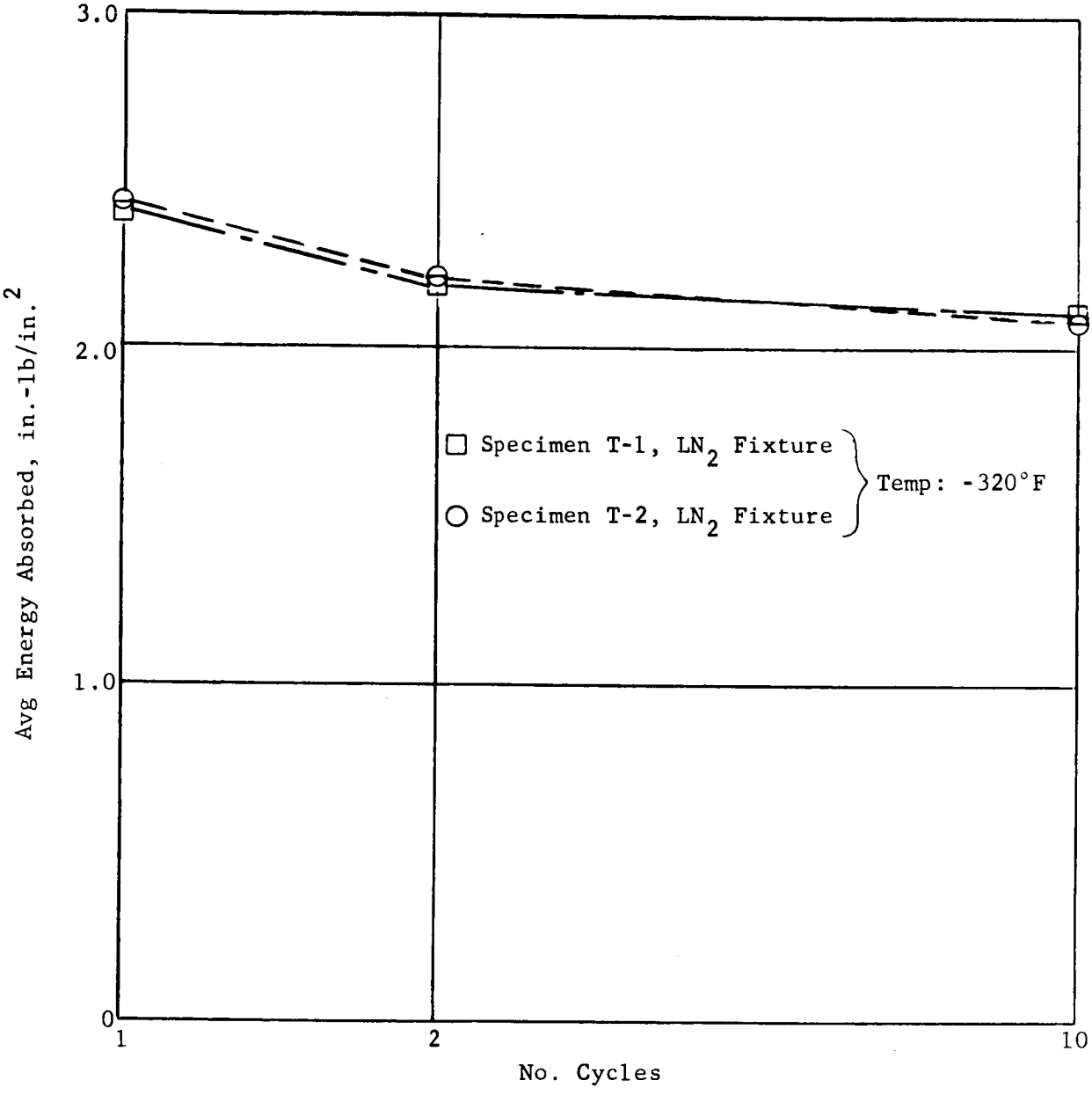

Figure 61. Energy Absorptions of Teflon-Glass Laminate at Liquid Nitrogen Temperature

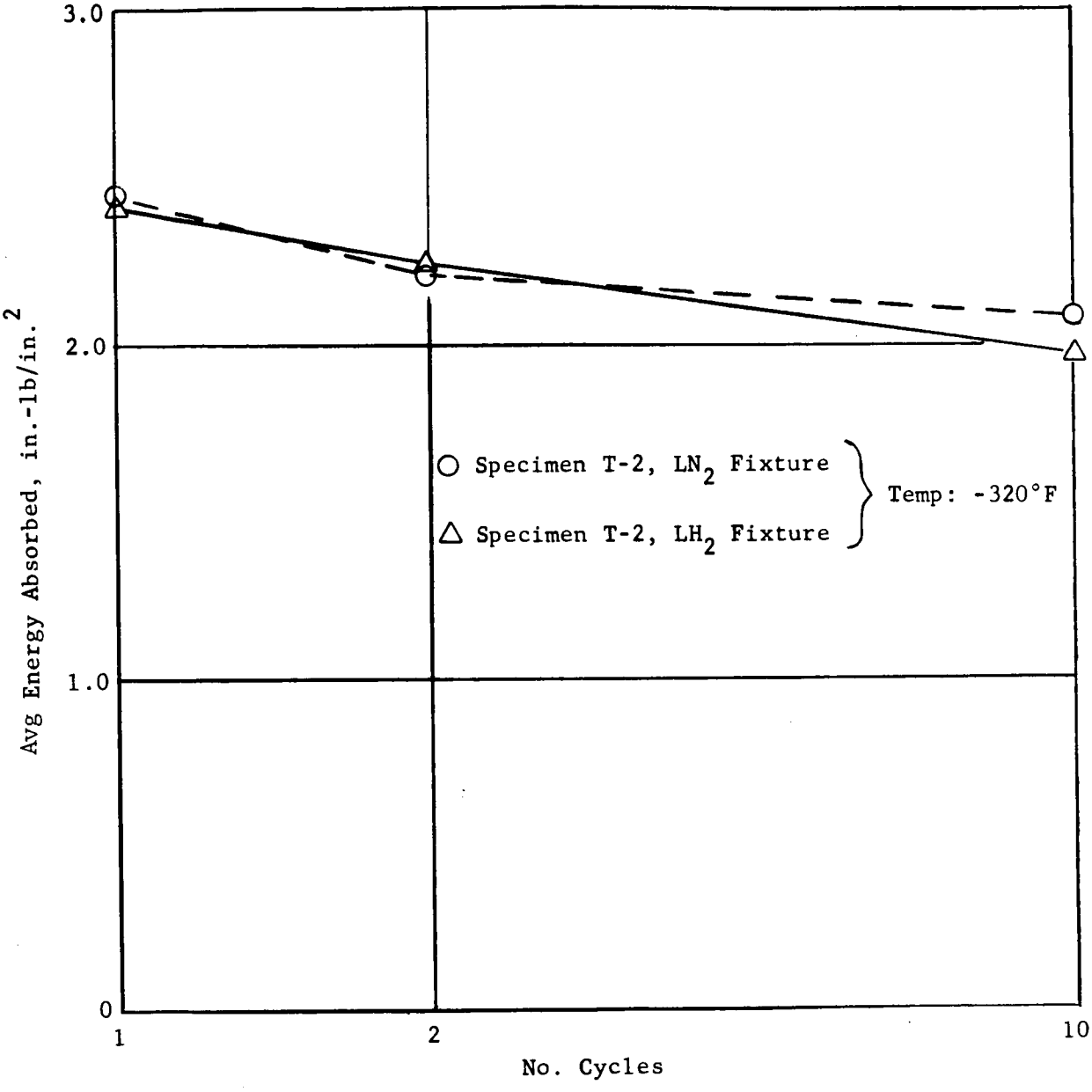

Figure 62. Energy Absorptions of Specimen T-2 in Different Fixtures

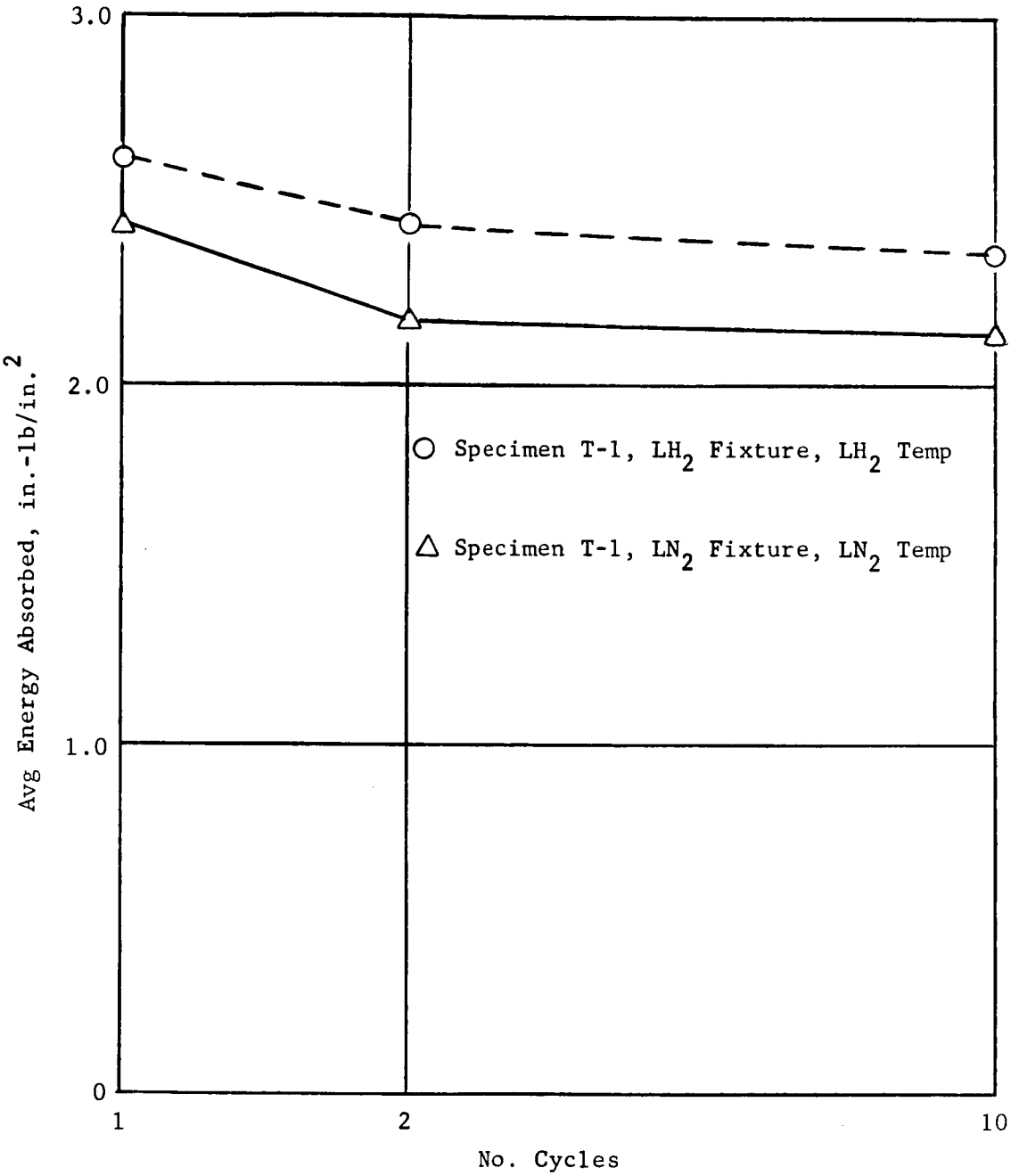

Figure 63. Energy Absorptions of Specimen T-1 at Liquid Nitrogen and Liquid Hydrogen Temperatures

OPTIMIZATION OF GASKET MANUFACTURING AND DETERMINATION OF PHYSICAL PROPERTIES AND DESIGN CRITERIA

Specimen-to-specimen variations exist for gaskets utilizing both the laminated gasket composite material and the presently used production gasket material, Allpax 500, which is an item of high quality control.

A manufacturing technology study was conducted to coordinate material and processing optimization in order to provide minimum specimen-to-specimen variation.

The optimized gasket processing was utilized to fabricate specimens so that various gasket performance criteria could be determined. The physical and mechanical properties of the laminated gasket composite were determined at 75°F, -320°F, and -423°F. Additional leak-sealing capability data were obtained at 75°F, -320°F, and -423°F.

In some applications in the Saturn vehicle, a seal may be subjected to an elevated temperature; it was therefore necessary to determine the performance of the laminated gasket at an elevated temperature. Also investigated were the effects of thermally cycling the gasket composite from an elevated temperature to -320°F.

Finally, the physical properties data and the leak sealing data were utilized for comparison with the analytical methods which were developed to predict the performance of a gasketed joint.

Manufacturing Technology Study

An extensive process technology evaluation of two different TFE material suppliers and both the lamination and encapsulation processing was conducted. In order to determine the effects of the various processing variables, a simple, inexpensive test (compression versus deflection) was utilized as the response item to changes in processing. The secondary evaluation of a particular fabrication process was a leak test with helium gas at -320°F with a small (2-in.^{2}) gasket. The final proof of any of the processes evaluated was a helium gas leak test with 4-, 8-, and 12-in. diameter gaskets at 75°F and -320°F.

During the initial phases of the work, quality control specifications were developed for the receiving inspection of materials to be used in fabricating the newly developed laminated gasket composite. This was done in an effort to more closely control the materials received and thus possibly decrease the variation in compression versus deflection properties. These specifications are shown in Appendixes C through E for TFE resin, FEP resin, and style 401 glass cloth. It is believed that materials received throughout the program were of high quality and did not contribute to the variation in physical properties of the laminated gasket composite.

The process developed previously included a glass cloth and fluorocarbon film layup technique, a lamination technique, and an encapsulation technique. Initial compression versus deflection screening tests indicated that the various phases of the fabrication process, when followed as developed (Reference 6), were not causing the variation in physical properties of the laminated gasket composite; instead, the quality of tooling used during the encapsulation phase caused this variation. This was verified by conducting compression versus deflection tests on a number of encapsulated and unencapsulated gaskets. Two types of polytetrafluoroethylene resin were used to fabricate the gaskets: DuPont's TFE Teflon and Allied Chemical's Halon G-80 resin. All gaskets fabricated from either resin were encapsulated with DuPont's FEP Teflon resin.

Results obtained from tests conducted at room temperature and -320°F are listed in Tables 29 through 34, with average values (at room temperature and -320°F) shown in Table 35. A typical set of data is shown in Figure 18. The area under the curve for cycles 1, 2, and 10 was measured and reported as energy absorbed by the gasket.

This test is delineated in a later section, when statistical analysis of variation in properties of three types of gaskets is presented. The coding used consisted of a laminate number and an alphabetical suffix to identify the individual specimen. Laminates were fabricated using lamination and encapsulation techniques previously determined (Reference 6) and all used the same glass cloth. Comparison of cryogenic values for each laminate design of the unencapsulated and encapsulated forms show that encapsulation reduced compressibility only slightly. This led to modification of the existing small encapsulation tool to the point where finished thickness tolerances were ±0.003 in. Additionally, a definite fabrication process as developed in the previous study was used to investigate the effects of tooling and two types of laminating resins. A short description of the fabrication process is provided below; a detailed, step-by-step process specification is presented as Appendix F.

The first step in fabricating the newly developed laminated gasket composite involved lamination of TFE resin films with style 401 heat-cleaned glass cloth. For a finished gasket size of 1/16-in. thickness, five layers of glass cloth and four sheets of TFE film were cut. Three plies of glass cloth were cut with the fiber direction parallel to the cuts, and two plies were cut with the fibers inclined at a 45-degree angle. These plies were interleaved with alternate layers of resin, so that each successive layer of glass was rotated 45 degrees (see Figures 34 and 35). This produced a multiaxial laminate. The outer layers of the laminate were not resin but glass cloth, a design which evolved from an attempt to solve the following problem.

During lamination with resin on the outer layers, the stainless steel or aluminum foil sheets (used to protect the sandwich from the caul sheets) bonded to the laminate by the resin. This problem was solved by placing the glass on the outer layers (see Figure 36); however, the gaskets were covered during encapsulation, as these surfaces should not be unprotected. This technique is actually preferred for encapsulation, because the FEP resin bonds quite well to the exposed substrate and to the inside and outside diameter of the gasket.

TABLE 29

ENERGY ABSORPTION VALUES OF NARMCO UNENCAPSULATED GASKETS AT ROOM TEMPERATURE WITH TFE LAMINATING RESIN

Specimen No.	Type Resin	Thickness, in.	Cycle No.	Energy Absorption, in.-lb/in.^{3}
101-C	DuPont TFE	0.058	1 2 10	79.6 55.9 19.6
102-C	DuPont TFE	0.057	1 2 10	110.9 48.8 36.8
103-C	DuPont TFE	0.057	1 2 10	82.4 35.4 15.6
104-C	DuPont TFE	0.051	1 2 10	70.0 30.4 19.8
105-C	DuPont TFE	0.058	1 2 10	93.6 42.1 26.4
106-C	DuPont TFE	0.053	1 2 10	74.0 46.6 34.0
114-C	DuPont TFE	0.050	1 2 10	70.2 47.2 35.2
115-C	DuPont TFE	0.052	1 2 10	59.6 42.9 31.3
116-C	DuPont TFE	0.054	1 2 10	81.8 52.2 37.4

TABLE 30

ENERGY ABSORPTION VALUES OF NARMCO UNENCAPSULATED GASKETS AT ROOM TEMPERATURE WITH HALON G-80 LAMINATING RESIN

Specimen No.	Type Resin	Thickness in.	Cycle No.	Energy Absorption, in.-lb/in.^{3}
107-C	Halon G-80	0.042	Equipment failure nullified the test of this specimen	
108-C	Halon G-80	0.048	1 2 10	80.4 28.8 31.7
109-C	Halon G-80	0.044	1 2 10	63.2 19.1 15.9
110-C	Halon G-80	0.043	1 2 10	50.2 27.9 20.0
111-C	Halon G-80	0.043	1 2 10	65.8 34.9 32.1
112-C	Halon G-80	0.053	1 2 10	73.2 48.7 35.8
113-C	Halon G-80	0.048	1 2 10	71.7 43.3 37.1

TABLE 31

ENERGY ABSORPTION VALUES OF NARMCO UNENCAPSULATED GASKETS AT LIQUID NITROGEN TEMPERATURE WITH TFE LAMINATING RESIN

Specimen No.	Type Resin	Thickness, in.	Cycle No.	Energy Absorption, in.-lb/in.^{3}
101-B	DuPont TFE	0.055	1 2 10	33.5 34.7 28.0
102-B	DuPont TFE	0.058	1 2 10	45.9 46.2 41.0
103-B	DuPont TFE	0.057	1 2 10	34.6 38.4 35.3
104-B	DuPont TFE	0.054	1 2 10	45.6 42.2 38.0
105-B	DuPont TFE	0.053	1 2 10	46.4 42.3 40.9
106-B	DuPont TFE	0.051	1 2 10	33.3 33.7 29.4
114-B	DuPont TFE	0.048	1 2 10	35.4 35.4 33.5
115-B	DuPont TFE	0.052	1 2 10	44.0 32.7 29.4
116-B	DuPont TFE	0.049	1 2 10	27.8 24.9 25.3

TABLE 32

ENERGY ABSORPTION VALUES OF NARMCO UNENCAPSULATED GASKETS AT LIQUID NITROGEN TEMPERATURE WITH HALON G-80 LAMINATING RESIN

Specimen No.	Type Resin	Thickness, in.	Cycle No.	Energy Absorption, $in.\text{-}lb/in.^3$
107-B	Halon G-80	0.043	1 2 10	28.8 26.0 21.9
108-B	Halon G-80	0.049	1 2 10	54.3 46.5 39.0
109-B	Halon G-80	0.044	1 2 10	25.4 27.7 29.1
110-B	Halon G-80	0.045	1 2 10	35.1 37.3 33.3
111-B	Halon G-80	0.042	1 2 10	20.0 19.5 23.1
112-B	Halon G-80	0.052	1 2 10	29.4 29.2 31.0
113-B	Halon G-80	0.047	1 2 10	41.3 37.4 34.7

TABLE 33

ENERGY ABSORPTION VALUES OF NARMCO ENCAPSULATED GASKETS
AT LIQUID NITROGEN TEMPERATURE WITH TFE LAMINATING RESIN

Specimen No.	Type Resin	Thickness, in.	Cycle No.	Energy Absorption, in.-lb/in.^{3}
101-A	DuPont TFE	0.069	1 2 10	41.2 42.9 38.6
102-A	DuPont TFE	0.073	1 2 10	40.3 37.0 35.9
103-A	DuPont TFE	0.077	1 2 10	35.8 35.3 34.5
104-A	DuPont TFE	0.074	1 2 10	34.3 34.6 36.8
105-A	DuPont TFE	0.080	1 2 10	34.0 33.5 30.8
106-A	DuPont TFE	0.073	1 2 10	37.3 41.1 33.4
114-A	DuPont TFE	0.067	1 2 10	31.9 30.4 34.5
115-A	DuPont TFE	0.074	1 2 10	28.6 28.4 27.0
116-A	DuPont TFE	0.074	1 2 10	29.2 27.3 25.7

TABLE 34

ENERGY ABSORPTION VALUES OF NARMCO ENCAPSULATED GASKETS
AT LIQUID NITROGEN TEMPERATURE WITH HALON G-80 LAMINATING RESIN

Specimen No.	Type Resin	Thickness, in.	Cycle No.	Energy Absorption, in.-lb/in.^{3}
107-A	Halon G-80	0.062	1 2 10	27.7 28.7 27.7
108-A	Halon G-80	0.074	1 2 10	37.6 37.3 34.6
109-A	Halon G-80	0.066	1 2 10	29.5 27.3 28.3
110-A	Halon G-80	0.068	1 2 10	31.6 28.4 32.2
111-A	Halon G-80	0.062	1 2 10	26.3 25.6 26.3
112-A	Halon G-80	0.075	1 2 10	32.8 33.6 31.5
113-A	Halon G-80	0.071	1 2 10	31.4 30.1 29.8

TABLE 35

AVERAGE VALUES OF ENERGY ABSORPTIONS

Material	Test Temp, °F	Avg Value, in.-lb/in.^{3}		
		1st Cycle	2nd Cycle	10th Cycle
Unencapsulated laminate*	RT	80.2	44.6	28.4
	-320	38.5	36.7	33.4
Encapsulated laminate*	-320	35.8	34.5	33.0
Unencapsulated laminate**	RT	67.4	33.8	28.8
	-320	33.5	31.9	30.3
Encapsulated laminate**	-320	31.0	30.1	30.0

* TFE resin

** G-80 resin

Therefore, this design alleviates the need for bonding the two types of Teflon (TFE and FEP) together, which is a troublesome operation.

The entire layup, between stainless steel foil sheets, was placed between aluminum caul sheets in a press (see Figures 37 and 38). A thermocouple was inserted at the edge of the laminate so that the temperature at the laminate rather than at the platen was obtained. Lamination then took place under the following optimum conditions: 720°F and 500 psi for 5 minutes. The laminate was cooled under pressure to 400°F, removed from the press, and quick-quenched with water while still between the caul sheets. The rough laminate is shown in Figure 39.

Cleanliness was an important factor after lamination and before encapsulation, which was the critical phase of the process. Extreme care was exercised with the laminates, as the glass cloth was on the outer layers, making them vulnerable to contamination.

The entire surface area of the rough laminate was then covered with FEP Teflon which was cured at 550°F and 100 psi for 2 minutes. This step in the processing enabled a clean, sharp edge on the gasket to be obtained when cut from the laminate.

To fabricate a finished gasket, an encapsulation fixture, a laminate cutter, and an FEP Teflon film cutter are required. During the program, for

example, three small gasket encapsulation tools were fabricated since rough gaskets can be cut from the laminate much faster than they can be encapsulated. Typical tools required for the encapsulation of the small gasket are shown in Figures 42 and 64.

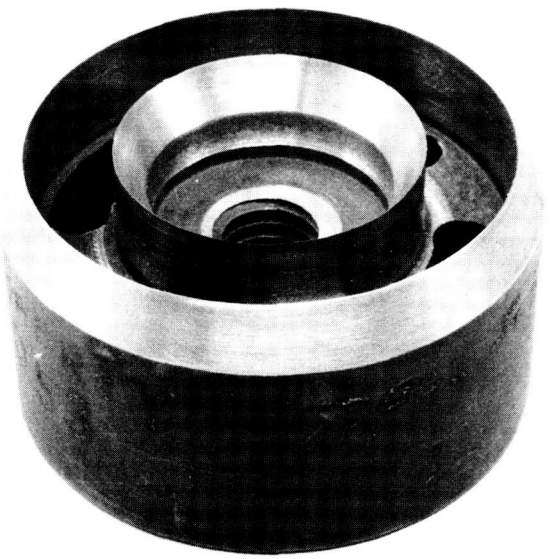

Figure 64. Test Gasket Laminate and Film Cutter

Specimens were cut from the laminate using a laminate cutter. They were cut undersize in comparison with the finished gasket dimensions; i.e., the specimen outside diameter was less than that of the desired gasket, while the specimen inside diameter was larger. The amount of undercutting was determined by the amount of encapsulation material desired. A minimum amount was used, because of the cold flow and poor compressibility of the solid resin, while employing sufficient material to guarantee encapsulation. It was determined that 0.010 in. of FEP Teflon was sufficient for encapsulation.

The cut laminate specimen was assembled with the surrounding layers of resin in the encapsulating fixture (see Figure 43). The fixture was previously chemically nickeled and then sprayed with a releasing agent (Ram Chemicals' GS-3). This served as a good parting agent as it prevented the FEP from bonding to the fixture; the encapsulation temperature was low enough that the release agent did not bond to either the FEP or the fixture.

The completely assembled fixture was then placed in a press. Encapsulation is best achieved with 500°F and 100 psi for 2 minutes. The fixture for small test gaskets could be immediately quick-quenched in water, but the larger

encapsulation fixtures required cooling under pressure to 500°F before water quenching: handling of the hot large tool while the encapsulation resin was liquid could have resulted in poor encapsulation.

The laminated gasket composite was extensively evaluated and compared to the specially processed Allpax 500 material by the use of a compression versus deflection test. Figure 18 is representative of the resulting curves. The area under the curves, representing the amount of energy absorbed, was measured and energy absorption figures calculated for the first, second, and tenth cycles to determine the effects of short- and long-time cycling. Candidate materials showing higher energy absorption values with minimum decrease with cycling were judged superior in compressibility.

During the first few months of the manufacturing technology studies, Halon G-80, DuPont TFE, and Allpax 500 were extensively investigated. Compression versus deflection tests were conducted at room temperature, -320°F, and -423°F to provide data that could be utilized in the development of a reliable material and fabricating process. Small (2-in.^{2}) gaskets were fabricated from the Allpax 500 material supplied by NASA. Laminates were fabricated either with G-80 or TFE resins by applying 500-psi pressure at 800°F. Each one of the gaskets, regardless of whether G-80 or TFE resin was used, was encapsulated with FEP resin at 500°F with 100-psi pressure applied to the gasket.

Two gaskets from each laminate of each material were tested at room temperature and at -320°F; a fifth gasket from the TFE laminate was tested at -423°F. The data obtained were reproduced in the form of frequency charts (see Figures 65 through 67). These charts show the distribution or spread of test data obtained for each material at each test temperature. The average values obtained for each group of data are given in Table 36.

The average values obtained for the energy absorption at 75°F and -320°F of G-80 and TFE by themselves suggest that these two materials are very similar. When the distribution of data for both materials is considered, however, TFE is superior in that it displays the higher degree of consistency. This is illustrated by Figures 66 and 67, which show that the G-80 gaskets had a spread from -40% to +30% on the tenth energy absorption cycle at room temperature, compared to ±20% for the TFE material. At -320°F, the TFE material had a spread of ±30% on the tenth energy absorption cycle compared to -30% to +40% for the G-80 material. On this basis, the TFE material was selected for further evaluation at 75°F, -320°F, and -423°F.

The Allpax 500 material submitted by NASA met the requirements for testing at 75°F and -320°F only. Therefore, comparisons between the Allpax and TFE materials could be made only at these temperatures. At room temperature, the spread of data obtained for Allpax 500 was slightly less than that for TFE. At -320°F, however, the TFE was considerably more consistent in energy absorption properties than the Allpax 500, as shown in Figures 65 and 67. The average values given in Table 36 indicate that the Allpax material had a slightly higher value at room temperature but a 300% lower value at -320°F than the TFE material. This would indicate that Allpax 500 had become very hard and brittle

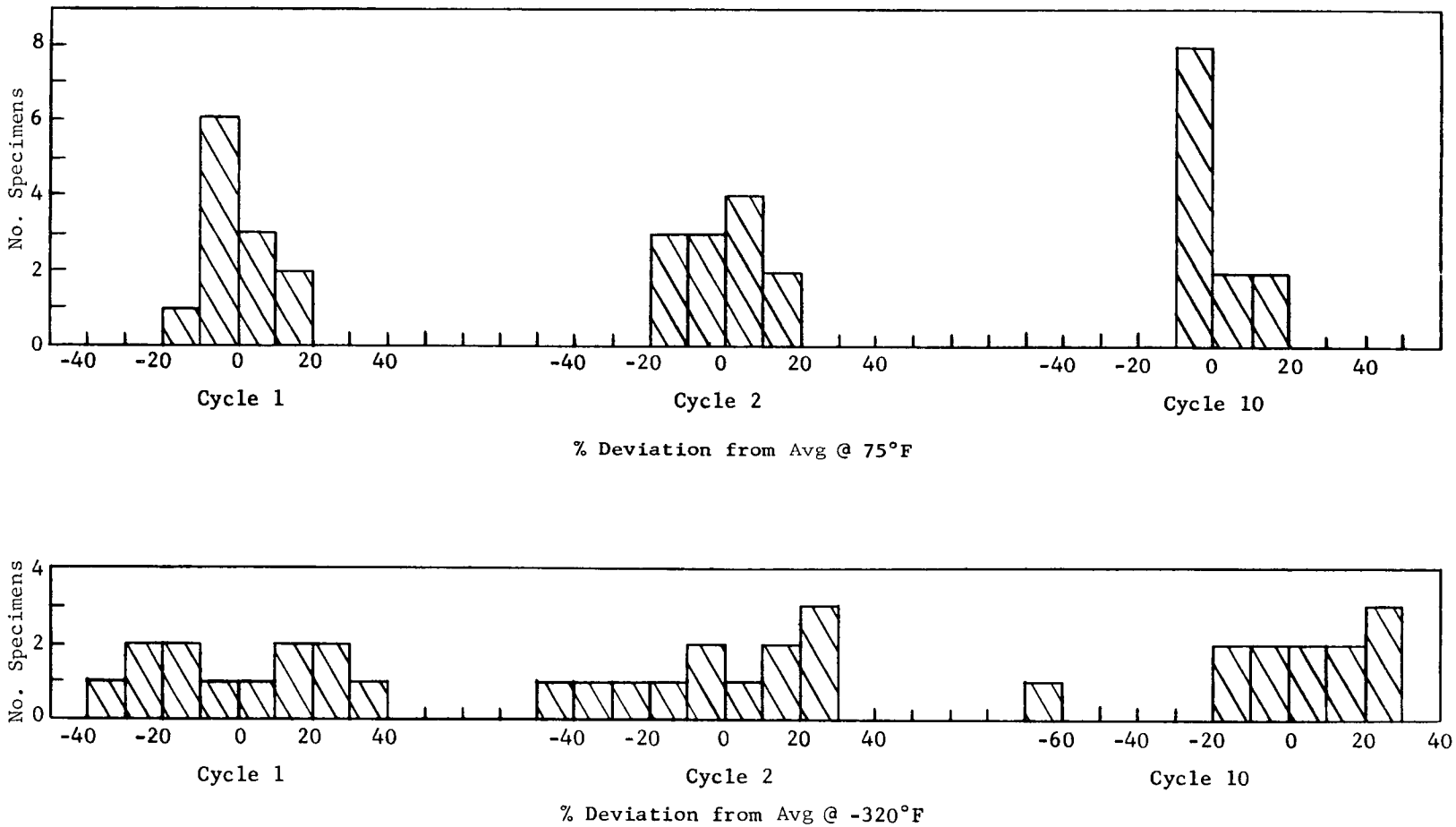

Figure 65. Frequency Distribution of Energy Absorption Data Obtained for Styrene-Butadiene Copolymer Reinforced with Asbestos Tested at 75°F and -320°F

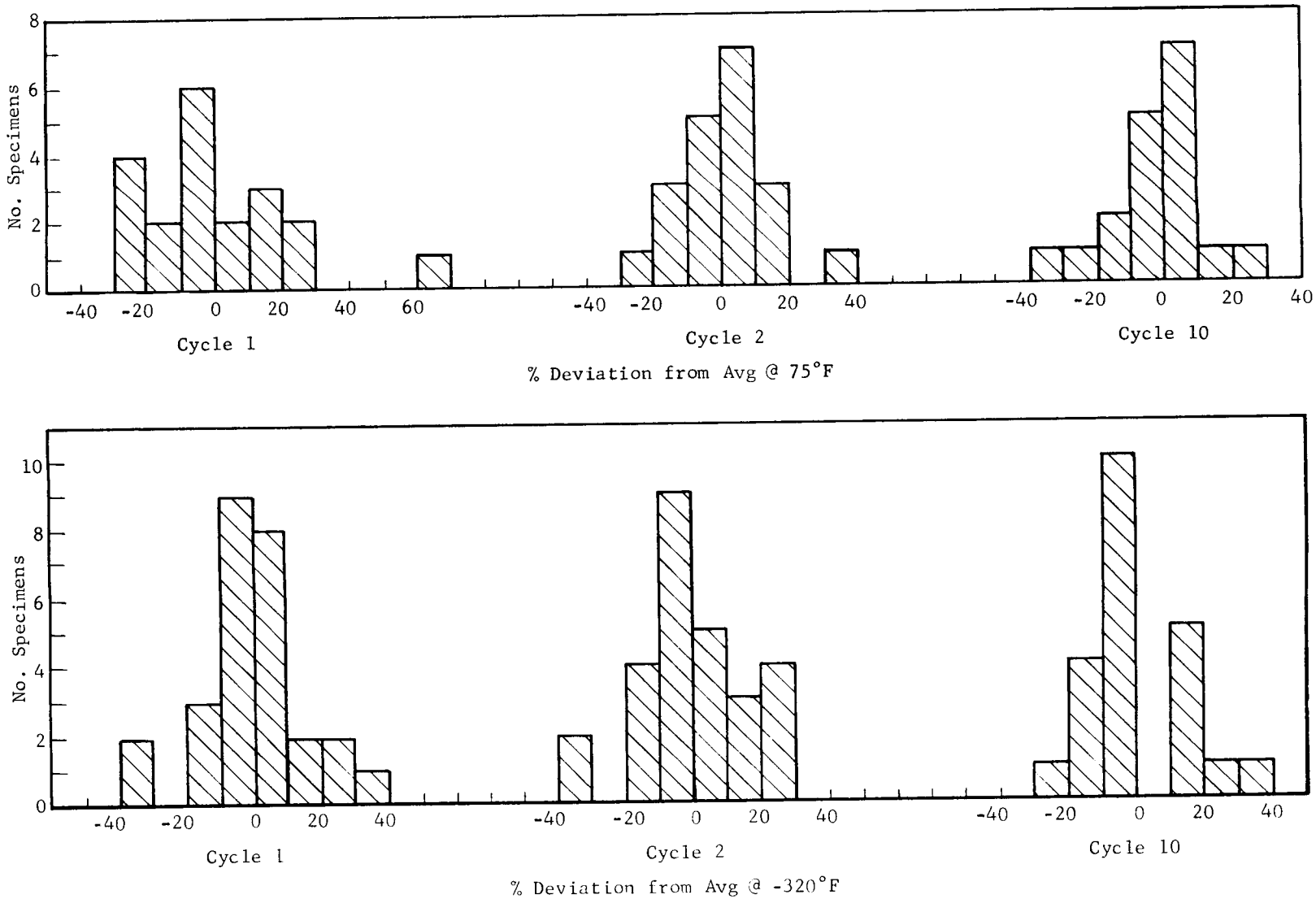

Figure 66 Frequency Distribution of Energy Absorption Data Obtained for Narmco-Laminated Gasket Composite Using Allied Chemical's Halon G-80 Material Tested at 75°F and -320°F

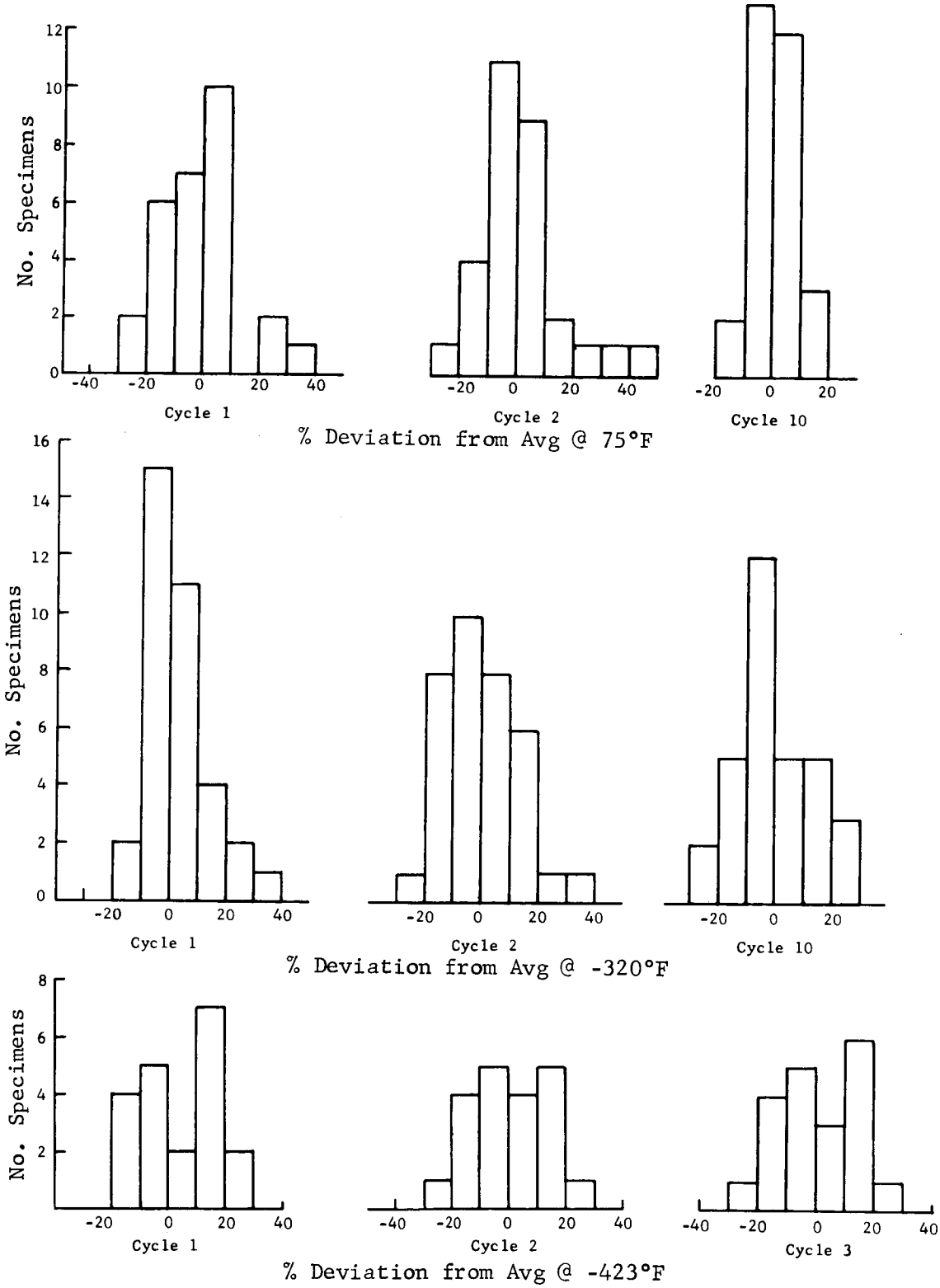

Figure 67. Frequency Distribution of Energy Absorption Data Obtained for Narmco-Developed Laminated Gasket Composite with DuPont TFE Material Tested at 75°F, -320°F, and -423°F

TABLE 36

AVERAGE VALUES OF ENERGY ABSORPTION FOR NARMCO LAMINATED GASKET COMPOSITE USING HALON G-80 RESIN, TEFLON TFE RESIN, AND STYRENE-BUTADIENE RUBBER ASBESTOS REINFORCED GASKETS

Type of Material	Test Temp, °F	Cycle No.	Avg Value, X
Narmco laminated gasket composite with Halon G-80 resin*	75	1	84.6
		2	51.4
		10	38.5
	-320	1	30.0
		2	29.5
		10	36.1
Narmco laminated gasket composite with DuPont's TFE resin	75	1	89.4
		2	53.9
		10	36.1
	-320	1	33.7
		2	31.9
		10	30.1
	-423	1	32.5
		2	30.9
		10	26.9
Styrene-butadiene asbestos reinforced	75	1	87.2
		2	58.8
		10	48.6
	-320	1	9.9
		2	9.8
		10	11.4

* Allied Chemical Corporation's trade name for polytetrafluoroethylene.

when tested at -320°F. On the basis of the data obtained, the TFE gasket composite was determined to be considerably superior to the Allpax material for use in cryogenic gaskets.

The TFE gasket was tested at 75°F, -320°F, and -423°F for its energy absorption properties. As shown in Table 36, the energy absorption of the TFE gasket at -320°F and -423°F is nearly the same. In fact, when the frequency distribution given in Figure 67 is examined, the energy absorption at -423°F is slightly more consistent than the energy absorption values obtained at -320°F. The data obtained during the course of this program indicate that the TFE gasket meets the requirements of the secondary objective of this program; i.e., that the compression versus deflection properties of separate TFE laminates be reproducible within the batch-to-batch percent deviation of the compression properties of the treated Allpax 500 product now used.

Upon conclusion of the screening tests, the materials chosen for further process refinement and testing were

1. 401 crowfoot glass cloth (Reinforcement)

2. 0.005-in. TFE (Lamination)

3. 0.005-in. FEP (Encapsulation)

The leak-sealing ability of the Narmco-developed gasket composite was measured initially at 75°F, -320°F, and -423°F by inserting a small (2-in.^{2}) test specimen between flanges and increasing the load to 2000 psi. A sketch of the test fixture used is shown in Figure 1. The gasket was then internally pressurized to 600 psi with gaseous helium, the pressure source disconnected, and if any leak developed after 5 minutes it was measured and recorded. The leak-sealing ability of the gaskets was measured at cryogenic temperatures in the same fashion, except that after loading the gasket to 2000 psi at room temperature, the gasket and fixture were cooled to -320°F with liquid nitrogen or -423°F with liquid hydrogen. In each of these tests, a drop of 2 psi in internal pressure was considered to be a leak. Since the pressurized volume of the entire test assembly was only 0.4 in.^{3}, the actual gaseous leakage was quite small.

The test results (Table 37) show that 16 of 18 gaskets retained the maximum internal pressure of 600 psi. The other two gaskets retained internal pressures of 552 and 596 psi respectively. At -320°F, 10 of 18 gaskets retained the maximum internal pressure of 600 psi, and the remaining 8 gaskets all held pressures in excess of 500 psi. At -423°F, 6 gaskets retained the maximum internal pressure of 600 psi, and the remaining 12 gaskets all held helium gas pressures in excess of 450 psi.

Leak tests were conducted with helium gas at room temperature and -320°F, and at internal pressures as high as 200 psi on 4- and 8-in. diameter gaskets in order to experimentally determine the required flange pressures. These gaskets were first tested at room temperature and -320°F in unbolted flanges. A constant external load was applied to flanges at room temperature by a

TABLE 37

TEST RESULTS FOR 2-IN.^{2} NARMCO LAMINATED GASKET
COMPOSITE TESTED WITHOUT BOLTS

Specimen No.	RT Flange Pressure, psi	-320°F Flange Pressure, psi	-423°F Flange Pressure, psi	Max.* Internal Pressure @ 75°F psi	Max.* Internal He Pressure @ -320°F psi	Max.* Internal He Pressure @ -423°F psi
1	2000	2000	2000	600	600	600
2	↓	↓	↓	600	600	528
3	↓	↓	↓	600	600	580
4	↓	↓	↓	552	589	560
5	↓	↓	↓	596	576	578
6	↓	↓	↓	600	562	480
7	↓	↓	↓	↓	600	600
8	↓	↓	↓	↓	600	600
9	↓	↓	↓	↓	600	600
10	↓	↓	↓	↓	600	595
11	↓	↓	↓	↓	582	472
12	↓	↓	↓	↓	600	600
13	↓	↓	↓	↓	600	600
14	↓	↓	↓	↓	600	600
15	↓	↓	↓	↓	523	465
16	↓	↓	↓	↓	544	460
17	↓	↓	↓	↓	600	584
18	↓	↓	↓	↓	521	485

* Pressure held for 5 minutes after reaching steady state at test temperature.

Universal testing machine and then the load was allowed to fall off as the temperature was decreased to -320°F. Experimental results obtained for the two different sizes of gaskets are listed in Tables 38 and 39.

The 4-in. diameter gaskets were tested to an internal pressure of 200 psi at room temperature with an indicated flange load of 1787 psi. All 12 of the gaskets tested retained the 200-psi helium gas pressure for 5 minutes. The test fixture was cooled to -320°F, where the apparent flange load decreased to 858 to 920 psi due to the thermal contraction of the metal flanges. The test results obtained (see Table 38) show that seven of the eight gaskets tested maintained an internal pressure in excess of the 200 psi goal specified.

When the flange load was increased to approximately 1775 psi, the minimum internal pressure, held for 5 minutes at -320°F, was increased to 300 psi. The test results indicated that a flange load of approximately 2000 psi at -320°F would be required to contain an internal pressure of 500 psi at -320°F.

The testing of the 8-in. diameter gasket was limited to the capacity of the testing machine; therefore, a room temperature flange load of only 970 psi could be applied and the internal pressure retained was the maximum pressure (200 psi). At -320°F, the retained internal pressure varied from 130 to

TABLE 38

NARMCO-LAMINATED GASKETS OF 4-IN. INSIDE DIAMETER TESTED WITHOUT BOLTS

Specimen No.	RT Flange Pressure, psi	-320°F Flange Pressure, psi	Max.* Internal He Pressure @ 75°F, psi	Max.* Internal He Pressure @-320°F, psi
1	1787	858	200	295
2	↓	875	↓	325
3		920		148
4		900		245
5		920		270
6		875		350
7		903		270
8		894		345
9		1778		395
10		1778		423
11		1769		470
12		1769		300

*Pressure held for 5 minutes after reaching steady state at test temperature.

TABLE 39

NARMCO-LAMINATED GASKETS OF 8-IN. INSIDE DIAMETER TESTED WITHOUT BOLTS

Specimen No.	RT Flange Pressure, psi	-320°F Flange Pressure, psi	Max.* Internal He Pressure @ 75°F, psi	Max.* Internal He Pressure @ -320°F, psi
1	970	970	200	150
2	↓	↓	↓	155
3	↓	↓	↓	170
4	↓	↓	↓	195
5	↓	↓	↓	195
6	↓	↓	↓	150
7	↓	↓	↓	165
8	↓	↓	↓	130
9	↓	↓	↓	130
10	↓	↓	↓	150

* Pressure held for a period of 5 minutes after reaching steady state at test temperature.

195 psi. The somewhat lower values of the internal pressure at -320°F were due to the low initial flange load. The tests conducted on the 8-in. diameter gaskets would hold helium gas pressure at -320°F with an initial flange load applied at room temperature.

A test procedure was conceived utilizing the strain gage bolts as previously discussed. The test procedure for the 4-, 8-, and 12-in. diameter gaskets is given below.

1. The fixture itself was leak-tested. This was accomplished by inserting a plug in the bottom flange at the gas inlet location and then pressurizing the system. The pressure was shut off at 500 psi and maintained for a length of time, which indicated that the system was leakproof.

2. The plug was removed and a gasket installed as shown in Figures 51 and 52. The top flange was put in place. Cap screws, nuts, and washers were then assembled in place, and the torque wrench used to obtain the desired bolt loading. The helium was again introduced to check the room temperature leak-sealing ability (Figures 53 and 54). The specimen had to contain 500 psi for the test to proceed. The gas was then relieved.

3. Liquid nitrogen was added to the cryostat until the entire test fixture became submerged (Figure 55).

4. The helium gas was then increased to 500 psi (Figure 56). After pressure was obtained, the system was sealed off. Any drop-off in pressure (detected by a pressure gage) indicated a leak. The pressure was then relieved and the "leak point" again approached, only in smaller increments. In this manner, the maximum pressure contained at a bolt load level was determined within 2 psi.

Test results of the 4-, 8-, and 12-in. diameter Narmco laminated gaskets are shown in Tables 40 through Table 42. (Test results from previous work conducted on the styrene-butadiene rubber gaskets (Allpax 500) are shown in Tables 24, 26, and 28.)

It should be noted that the gasket flange pressure obtained at -320°F for the Allpax 500 gaskets was obtained by retorquing the bolts at -320°F and the internal pressure was held for only 30 seconds. In addition, the recommendation now in effect for a torquing sequence of bolts, when utilizing the styrene-butadiene copolymer (Allpax 500) gasket, was not used when these tests were conducted, primarily because of the extended length of time required for the torquing sequence.

TABLE 40

NARMCO-LAMINATED GASKETS OF 4-IN. INSIDE DIAMETER TESTED WITH BOLTS

Specimen No.	RT Flange Pressure, psi	-320°F Flange Pressure, psi	Max.* Internal He Pressure @ 75°F, psi	Max.* Internal He Pressure @ -320°F, psi
13	2950	2150	500	500
14	↓	2140	↓	500
15		2290		500
16		2150		493
17		2190		500
18		2240		500
19		2150		500
20	2980	2170		487
21	2980	1930		447
22	2930	2240		495

* Pressure held for a period of 5 minutes after reaching steady state at test temperature.

TABLE 41

NARMCO-LAMINATED GASKETS OF 8-IN. INSIDE DIAMETER
TESTED WITH BOLTS

Specimen No.	RT Flange Pressure, psi	-320°F Flange Pressure, psi	Max.* Internal He Pressure @ 75°F, psi	Max.* Internal He Pressure @ -320°F, psi
11	2939	2210	500	500
12	2882	2130		500
13	2900	2009		500
14	2987	2009		500
15	2996	2200		461
16	2996	2183		500
17	3004	2096		500
18	3022	2074		495
19	3035	2114		500
20	2995	2105		496

* Pressure held for a period of 5 minutes after reaching stready state at test temperature.

TABLE 42

NARMCO-LAMINATED GASKETS OF 12-IN. INSIDE DIAMETER
TESTED WITH BOLTS

Specimen No.	RT Flange Pressure, psi	-320°F Flange Pressure, psi	Max.* Internal He Pressure @ 75°F, psi	Max.* Internal He Pressure @ -320°F, psi
1	2990	2470	500	345
2	2990	2310	500	235
3	3200	2430	500	270
4	4000	2860	500	498
5	4000	2790	500	495

* Pressure held for a period of 5 minutes after reaching steady state at test temperature.

The superiority of the Narmco-developed gasket composite over the gasket product now used appears to be quite significant. Some conclusions that were drawn from the tests results include:

1. No retorquing of the optimum Narnco-developed gasket composite design is required.

2. The internal gas pressures held by this same gasket were normally twice the pressures held by the material now used for Saturn LOX service under identical torquing sequences and test conditions.

3. The Narmco-developed gasket is completely compatible with liquid oxygen.

Physical Property Study

Due to stringent environmental conditions, engineers must have appropriate physical property information on materials being utilized for aerospace application. This is the case of the optimum flange-gasket joint design, or any design utilizing a new material such as the laminated gasket composite developed on the subject contract.

The physical property information reported on the composite gasket material was also utilized in verifying two analytical expressions discussed in the next section.

High-temperature study. — The objective of this study was to determine the upper temperature limit of the newly developed gasket material. Test fixtures were designed and fabricated so that the test specimen could be thermally cycled from some elevated temperature to -320°F. The apparent flange load was measured continuously as the temperature changed, and a continuous monitoring of the internal helium gas pressure was conducted. The test fixtures used to conduct these tests are shown in Figures 68 through 70.

Small (2-in.^{2}) gaskets were fabricated using standard processing techniques developed earlier in the program. Single test specimens were heated to elevated temperatures in increments of 100°F from 200°F to 500°F. It was determined that above 300°F, the FEP Teflon encapsulation material becomes so soft that it readily flows under load. Also, the gasket held 200 psi helium gas pressure at 400°F and 450°F, but would not hold this pressure when thermally cycled down to -320°F.

Upon successive testing of the laminated gasket composite, the gasket performed adequately when thermally cycled from +300°F to -320°F. The -320°F flange pressure used was 2000 psi and the test specimen was held at each test temperature for 5 minutes after the test fixture reached equilibrium. The temperature for 5 minutes after the test fixture reached equilibrium. The test results obtained for five thermal cycles on each of five specimens are shown as Table 43. All of the specimens tested held 200 psi at both test temperatures.

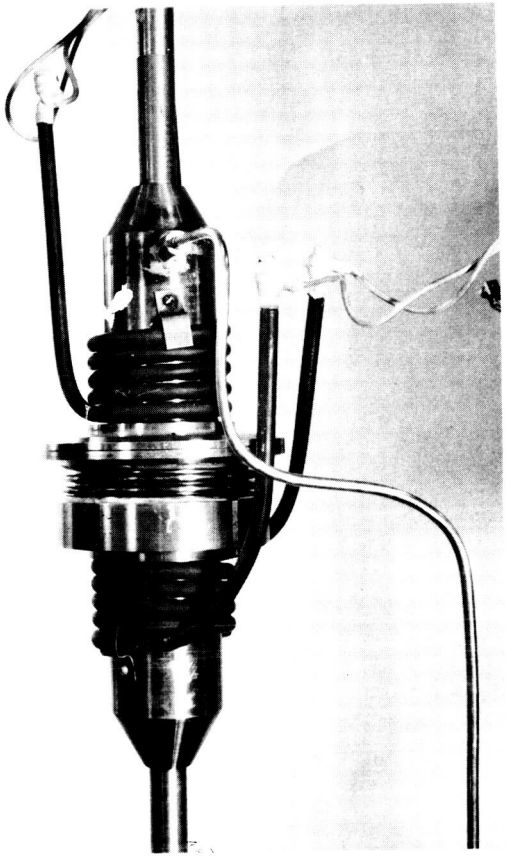

Figure 68. High-Temperature Gasket Test Fixture

Figure 69. High-Temperature Gasket Test Fixture in the Instron Test Machine

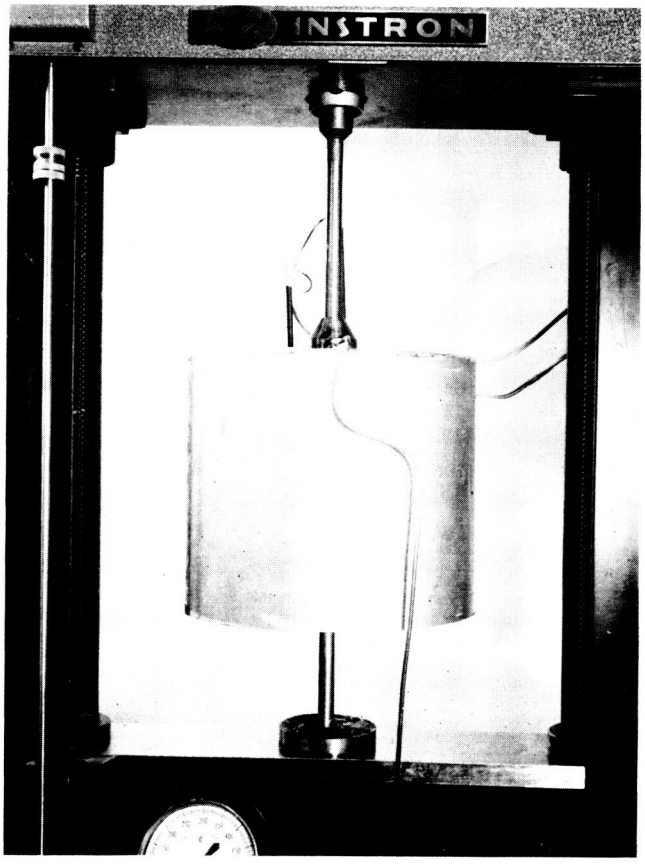

Figure 70. High-Temperature Gasket Test Fixture with Liquid Nitrogen Cryostat

TABLE 43

HIGH-TEMPERATURE 2-IN.^{2} GASKET LEAK TEST

Specimen, ID	Flange Pressure, psi	Test Temp, °F	No. of* Cycles	Internal He Pressure, psi	Leak
A-10	2000	+300°F to -320°F	5	200	No
A-17	2000	+300°F to -320°F	5	200	No
C-2	2000	+300°F to -320°F	5	200	No
C-8	2000	+300°F to -320°F	5	200	No
D-7	2000	+300°F to -320°F	5	200	No

*Note: One thermal cycle – RT to +300°F to -320°F and then to RT. Internal pressure and load maintained at 200 psi and 5860 lb

Linear thermal expansion. — The total linear thermal expansions of five composite laminate specimens from room temperature to approximately 100°F, -320°F, and -423°F were measured using the vertical tube dilatometer shown in Figure 71. To allow the specimens to be held in the 0.090-in jaws, copper "T" tabs were bonded to each end. Results were corrected for the expansion of the copper. It was necessary to grind both ends of each specimen to attain the required parallelism.

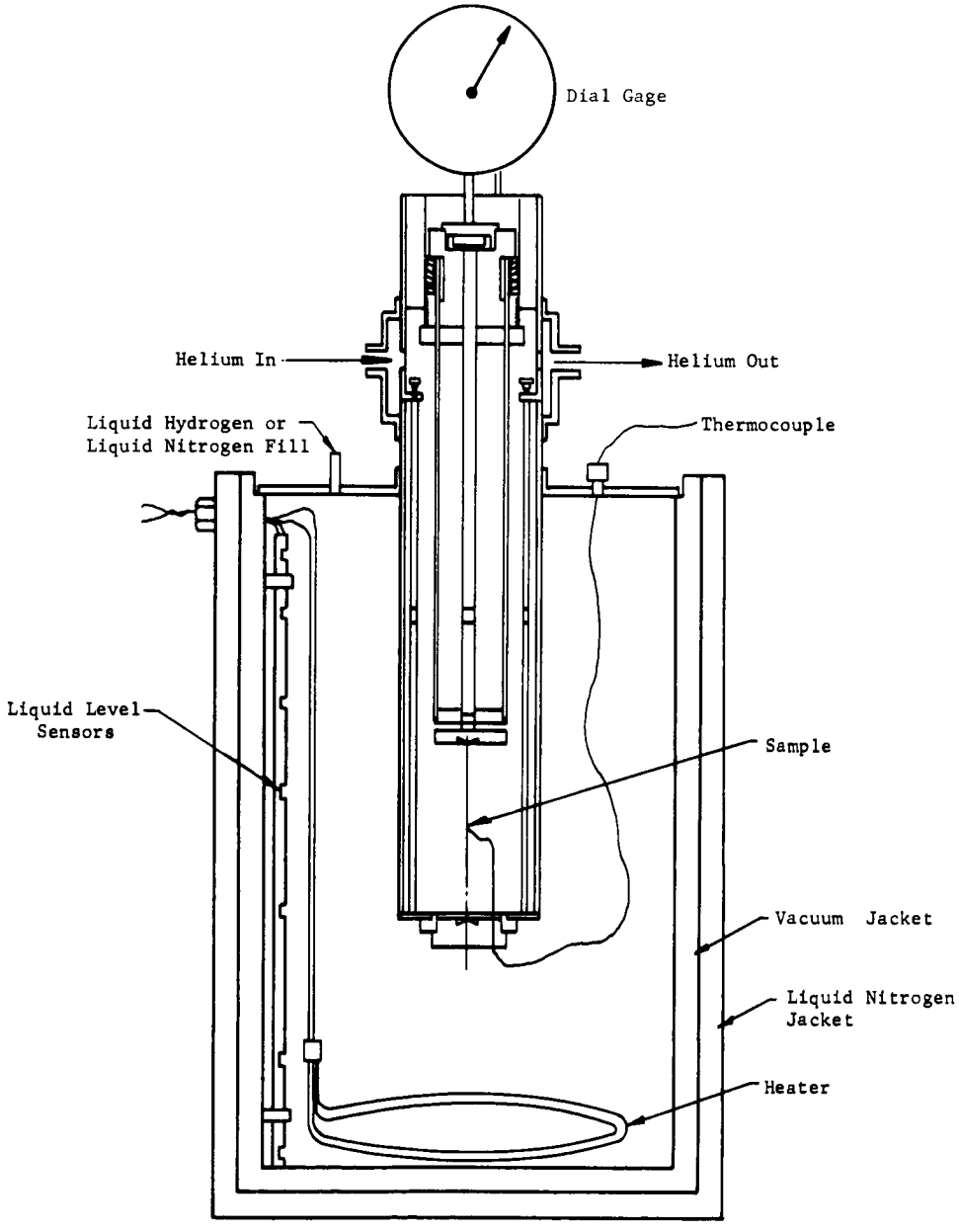

Figure 71. Quartz Tube Dilatometer

The specimens were successively submerged in liquid hydrogen (-423°F), liquid nitrogen (-320°F), and a dry ice and alcohol mixture (about 100°F) and their total expansions from room temperature to each temperature recorded and reduced to $\Delta 1/1$.

Results are tabulated and shown graphically in Table 44 and Figure 72. The curves in Figure 72 were drawn to indicate the probable shape between -100°F and room temperature due to the near room temperature transitions. It should be noted that the curves are based on data points and results of previous measurements on similar compositions, and that the temperature transitions were not recorded.

TABLE 44

LINEAR THERMAL EXPANSIONS OF NARMCO COMPOSITE LAMINATE GASKET MATERIAL

Specimen No.	Length, in.	Temp, °F	$\Delta 1$ in. x 10^{-4}	$\Delta 1/1$ in./in. x 10^{-4}
1	3.196	-423	-41.6	-130.2
		-320	-37.95	-118.7
		- 95.07	-21.80	- 68.2
2	3.211	-423	-42.35	-131.9
		-320	-37.8	-117.7
		- 94.5	-20.5	- 63.8
3	3.165	-423	-39.6	-125.1
		-320	-35.8	-113.1
		- 98.6	-21.4	- 67.6
4	3.177	-423	-49.4	-155.5
		-320	-45.8	-144.2
		-101.25	-31.7	- 99.8
5	3.195	-423	-38.3	-119.9
		-320	-34.1	-106.7
		- 94.67	-19.3	- 60.4

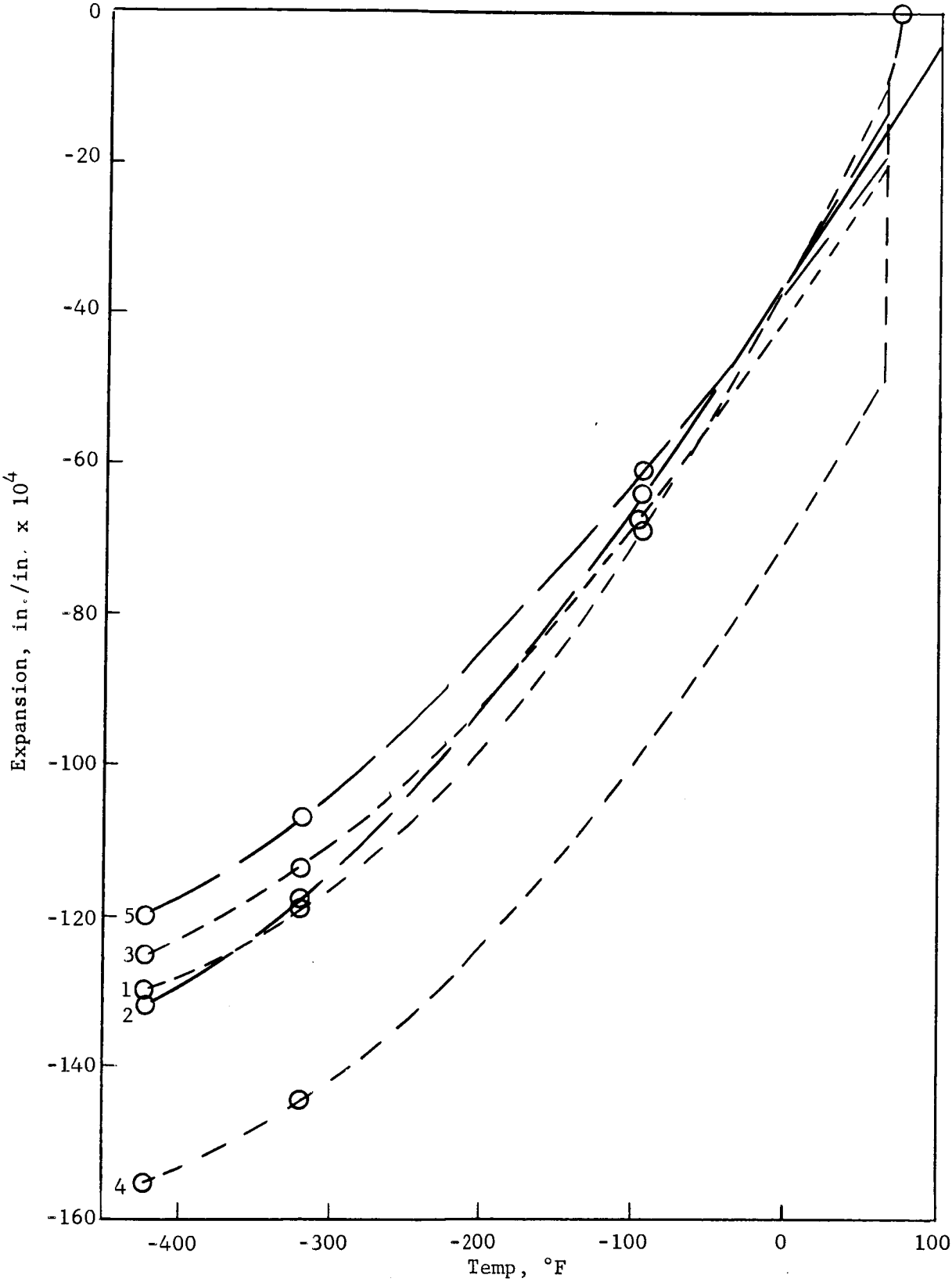

Figure 72. Total Linear Thermal Expansion of Narmco Composite – Laminate Gasket Materials

Poisson's ratio and compressive modulus. – The data obtained for Poisson's ratio and compressive modulus of the laminated gasket composite were obtained by conducting tests in accordance with ASTM-E132-61, "Determination of Poisson's Ratio at Room Temperature." The test setup was adapted to measure and record loads and deflections at cryogenic temperatures utilizing an x-y recorder, a portable cryostat, and cryogenic extensometers. The plots were used to determine these properties utilizing standard test methods.

The values for Poisson's ratio and compressive modulus at room temperature, -320°F, and -423°F are presented in Table 45. Figure 73 is a plot of the compressive modulus and Poisson's ratio as a function of temperature. It should be noted that the actual test data obtained for Poisson's ratio at -320°F were inconsistent with other data presented and the values anticipated. Therefore, to obtain information which could be used to verify the engineering studies discussed later, a straight line interpolation of Figure 73 was used to obtain the values at -320°F (Table 45).

TABLE 45

AVERAGE COMPRESSIVE MODULUS AND POISSON'S RATIO

Temp, °F	Load, psi	Poisson's Ratio	Compressive Modulus, psi x 10^4
75	2000	0.470	9.4
-320	2000	0.375*	11.4
-320	3000	0.270*	10.8
-423	2000	0.224	11.2
-423	3000	0.354	10.7

*Note: These values based on a straight line interpolation of Figure 34.

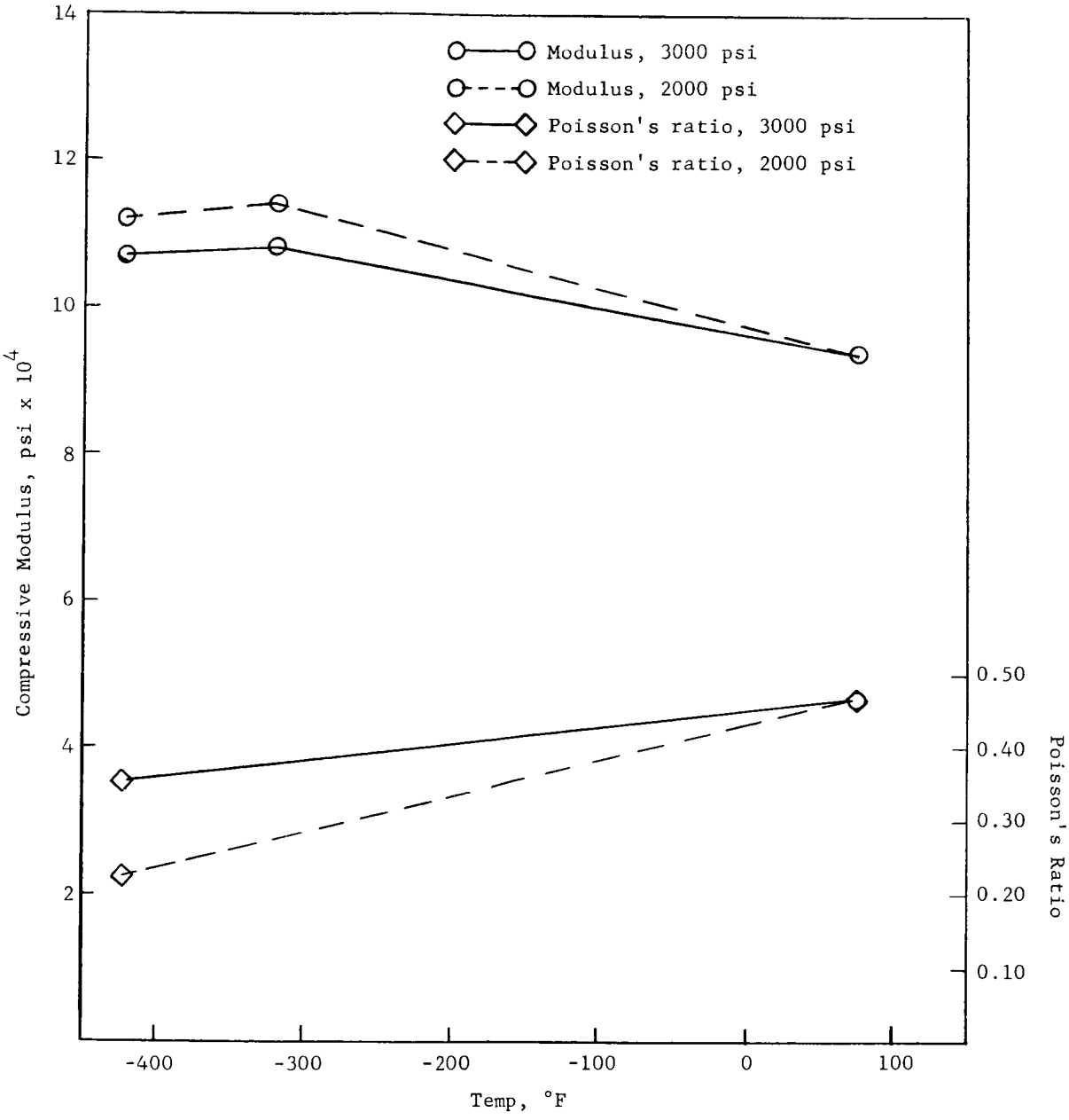

Figure 73. Compressive Modulus and Poisson's Ratio as a Function of Temperature of Narmco Composite Gasket Material

Analytical Studies

The engineering studies conducted on this program resulted in the determination of two analytical expressions which approximate the performance of a gasket-flange joint (Figure 74) when subjected to internal gas pressures at cryogenic temperatures. The first equation to be developed is shown below:

$$T_a^2 \geq + \frac{0.2\,\pi\,\left(g_a - \delta_a\right)\left(b_a^2 - a_a^2\right) d_a}{N_{g_a}} E_{g_c} + \frac{0.4\,\pi\,a_a^2\,d_a\,P_i}{N}\,\mu_c -$$

$$\frac{\pi\left(t_a - t_c\right)\left[2\,h_a\left(\alpha_b^* - \alpha_f^*\right) + \delta_a\left(\alpha_b^* - \alpha_g^*\right)\right] d_a^3}{20\left(2\,h_a + \delta_a\right)} E_{b_c} \qquad (1)$$

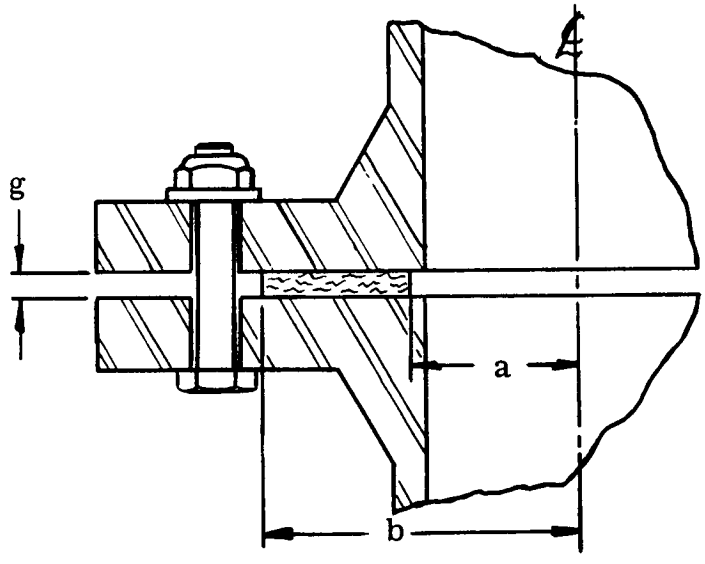

Figure 74. Typical Joint Section

Based on this approach, the primary load to contend with was that caused by the pressure differential between the internal and external conditions (Figure 75). A secondary consideration was the effect of the induced load, which is caused by the temperature differential. This allowed the determination of the normal stresses developed transverse to the gasket. It was then stated that these represented the minimum value of the flange pressure required to contain a predetermined internal pressure.

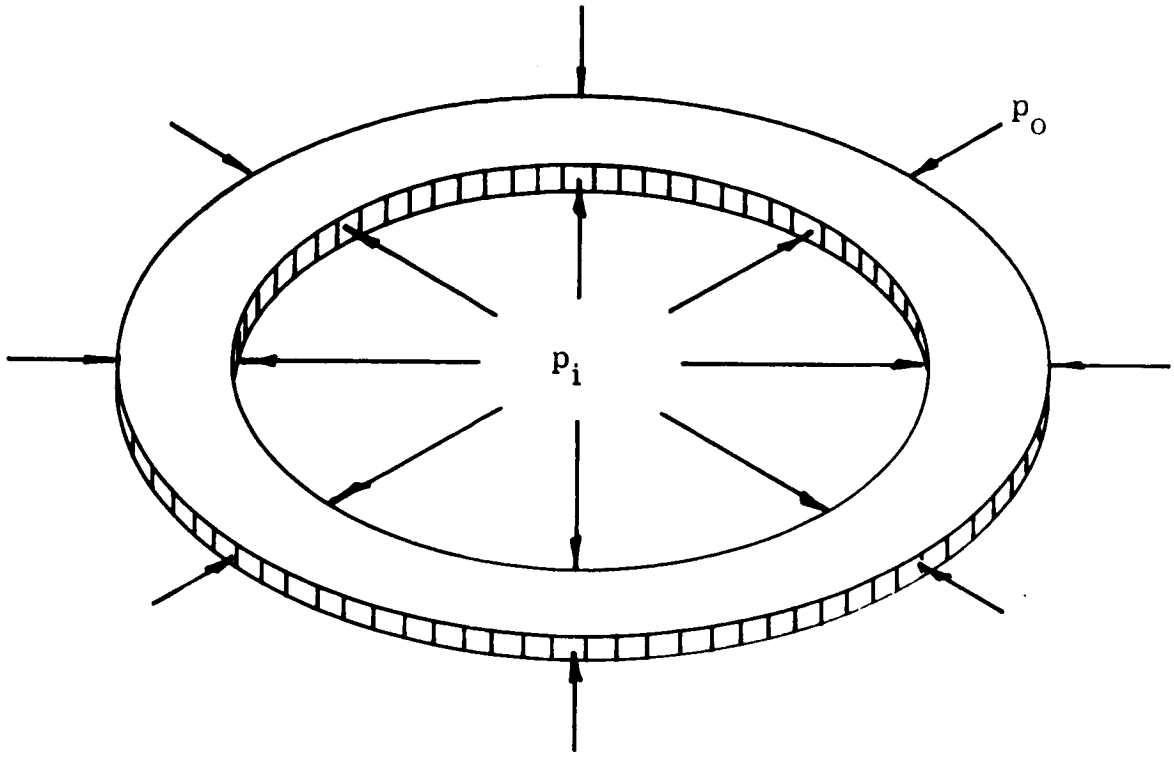

Figure 75. Gasket Loading Less Flange Pressure

Prior to the verification of this analytical expression, certain physical and dimensional properties of the laminated gasket composite were required. These properties are shown in Tables 46 and 47 for the flange joint sizes investigated in this program.

TABLE 46

DIMENSIONAL PROPERTIES FOR THE GASKET-FLANGE JOINT

Size	a, in.	b, in.	A, sq in.	N	ha, in.	d, in.
1	4.0	5.5	11.2	10	1.5	0.375
2	8.0	9.4	19.1	18	1.5	0.375
3	12.0	13.5	29.9	24	1.5	0.375

TABLE 47

PHYSICAL PROPERTIES FOR THE GASKET-FLANGE JOINT

Property	Gasket	Flange	Bolt
Youngs Modulus, E_c	1×10^5 psi	30×10^6 psi	30×10^6 psi
Coefficient of Thermal Expansion α^*	-2.4×10^{-5}	-7.5×10^{-6}	-7.5×10^{-6}
Poisson's Ratio, M_c	0.35	–	–

*Note: Denotes a value from t_a to t_c.

The parameter δ_a compressed gasket thickness was approximated by the following equation:

$$\delta_a = g_a - \frac{NT}{0.2\, d_a}\left(4.45 \times 10^{-7}\right) \tag{2}$$

In equation (2) the compressed gasket thickness was approximated by assuming a linear function of compression versus deflection.

Equation (3) resulted from rearranging equation (1) to obtain the internal pressure as a function of torque.

$$P_i \leq \frac{N}{0.4\,\pi\, a_a^2\, d_a\, \mu_c}\left[T_a - \frac{0.2\,\pi\left(g_a - \delta_a\right)\left(b_a^2 - a_a^2\right) d_a}{N_{g_a}} E_{g_c} + E_{b_c} \frac{\pi\left(t_a - t_c\right)\left[2\, h_a\left(\alpha_b^* - \alpha_f^*\right) + \delta_a\left(\alpha_b^* - \alpha_g^*\right)\right] d_a^3}{20\left(2\, h_a + \delta_a\right)}\right] \tag{3}$$

Equations (4), (5), and (6) for gasket sizes of 4-, 8-, and 12-in. diameters were obtained by substituting the various properties into equation (3).

Gasket Equation (4-in. diameter):

$$P_i \leq \frac{3.79}{K_t}\left[T_a + \frac{10^4}{K_c}\left(-3.36\,\frac{(g_a - \delta_a)}{g_a} + 3.24\,\frac{\delta_a}{60 + 20\,\delta_a}\right)\right] \tag{4}$$

Gasket Equation (8-in. diameter):

$$P_i \leq \frac{1.70}{K_t}\left[T_a + \frac{10^4}{K_c}\left(-3.19\,\frac{(g_a - \delta_a)}{g_a} + 3.24\,\frac{\delta_a}{60 + 20\,\delta_a}\right)\right] \tag{5}$$

Gasket Equation (12-in. diameter):

$$P_i \leq \frac{1.01}{K_t}\left[T_a + \frac{10^4}{K_c}\left(-3.75\,\frac{(g_a - \delta_a)}{g_a} + 3.24\,\frac{\delta_a}{60 + 20\,\delta_a}\right)\right] \tag{6}$$

The two constants, K_c a cryogenic constant and K_t the total constant, were experimentally determined by leak tests conducted on the larger diameter gaskets. These constants have values as tabulated in Table 48.

TABLE 48

GASKET CONSTANTS

Size	K_c	K_t
1 (4 in.)	10	-2.9
2 (8 in.)	10	-3.1
3 (12 in.)	10	-4.5

The constant K_c is believed to depend primarily on the type of cryogenic fluid contained by the gasket-flange joint. The cryogenic fluid utilized for the data investigated was liquid nitrogen. The values for K_c (Table 23) indicate that the constant is independent of gasket and flange diameter, and appears to be only a function of the cryogenic conditions. The constant K_t, however, is believed to be a function of gasket and flange geometry. The data indicate this since the absolute value of the constant K_t increases as the gasket increases.

Repeating the compressed gasket thickness approximation for each particular gasket size yielded the following expressions.

Gasket (4-in. diameter):

$$\delta_a = g_a - 5.93 \times 10^{-5} \left(T_a\right) \tag{7}$$

Gasket (8-in. diameter):

$$\delta_a = g_a - 10.68 \times 10^{-5} \left(T_a\right) \tag{8}$$

Gasket (12-in. diameter):

$$\delta_a = g_a - 14.24 \times 10^{-5} \left(T_a\right) \tag{9}$$

Table 49 shows the results obtained by comparing the theoretically calculated internal pressure and the experimentally determined internal pressure, utilizing the aforementioned analytical expressions.

During the course of work conducted on this program, a second expression was developed which is believed to more closely relate the room temperature sealing pressure to the internal gas pressure held at cryogenic temperatures. This expression was derived by assuming the gasket is loaded in pure compression, with no rotation of flanges and with no significant dimensional changes in the gasket at cryogenic temperatures. The expression was developed utilizing this analytical method (Appendix B).

The equation in Appendix B is based on a stress-strain relationship that is not a simple Hookeian relationship, but instead

$$\epsilon = \frac{1}{K_1} \text{ arc sinh } \left(\frac{\sigma}{E_g}\right)$$

Continued study in this area produced a more valid relationship of

$$\epsilon = \left[\frac{1}{K} \frac{\sigma}{E_g}\right]^{1/5}$$

TABLE 49

THEORETICAL AND EXPERIMENTAL COMPARISON
(Equation 1)

Data* ID	Size ID in.	ga, in.	T, in.-lb	δ, in.	P_i Calculated, psi	P_i Experimental psi	% Deviation of Calculated Pressure From Experimental Test Pressure
1	4	0.074	175	0.064	365	335	+ 9.0
2	4	0.087	250	0.072	425	492	-13.6
3	8	0.112	250	0.085	405	465	-10.8
4	12	0.100	335	0.052	328	325	+ 0.9
5	12	0.103	375	0.050	250	380	-34.2

* Data represent averages of typical groups of leak tests.

Figure 76 graphically reproduces some typical plots of test data for various numerical functions of stress-strain relationships which were considered. The K for curve No. 5 is 5×10^4. Further evaluation approximated K as 4.5×10^4 for curve No. 1, which closely approximated the actual data.

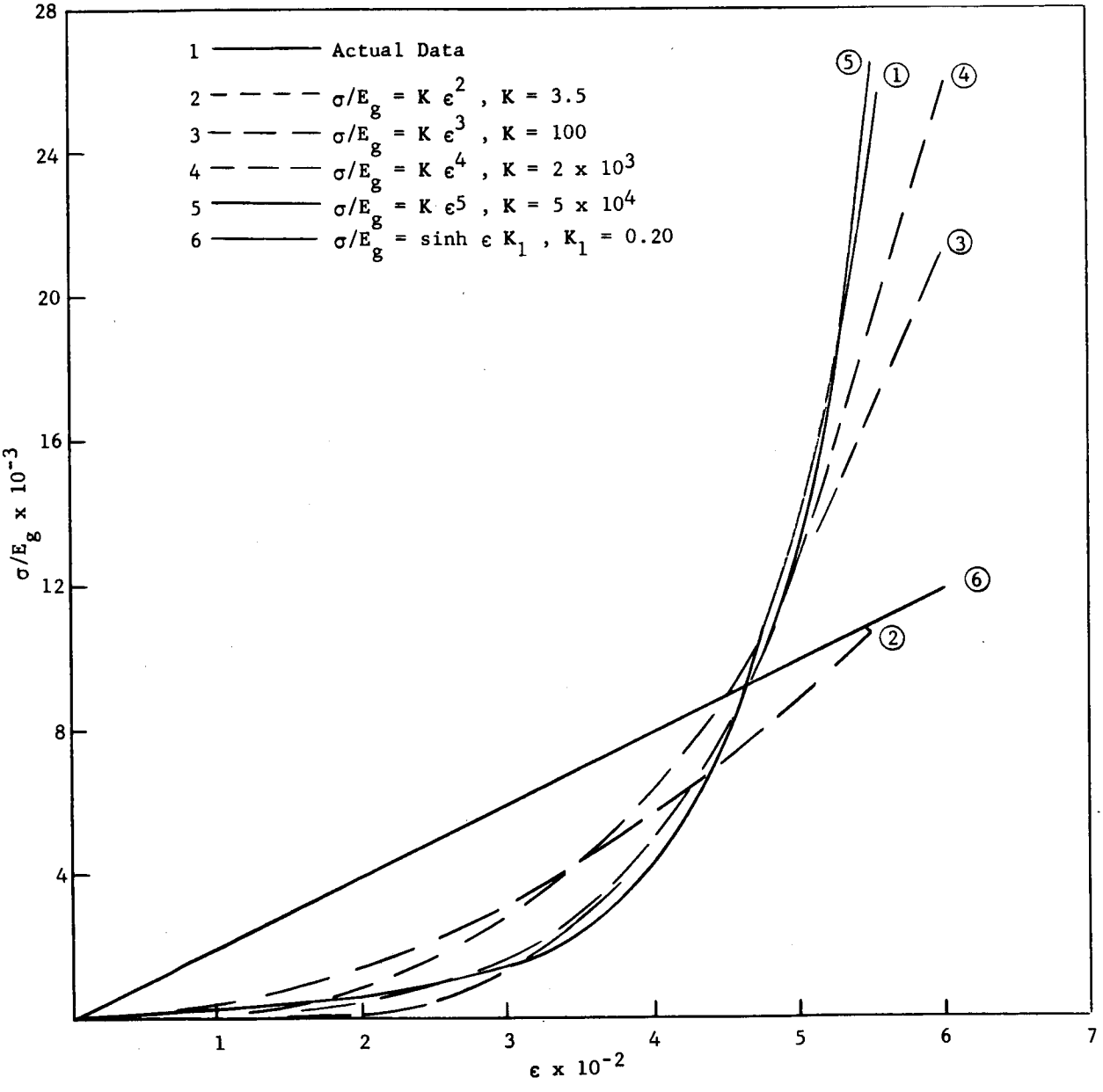

Figure 76. Function Approximations

Completing the analytical expression presented in Appendix B and introducing the latest stress-strain relationship, equation (10), was developed.

$$E_{g_c}\left\{\frac{4\,K_1\left(2\,h_a+\delta_a\right)\left[1+\alpha_b^*\left(t_a-t_c\right)\right]}{\pi\,N\,d_a^2\,\delta_a\left[1+\alpha_g^*\left(t_a-t_c\right)\right]E_{b_c}}\left[K_2\,A_g-N\,B_{b_1}+\pi\,a^2\,P_i\right]\right\}^{1/5}$$

$$=\frac{N}{A_g}\left\{B_{b_1}-\frac{\pi\left(t_a-t_c\right)\left[2\,h_a\left(\alpha_b^*-\alpha_f^*\right)+\delta_a\left(\alpha_b^*-\alpha_g^*\right)\right]E_{b_c}\,d_a^2}{4\left(2\,h_a+\delta_a\right)}\right\}-K_2 \qquad (10)$$

As stated in Appendix B, K_2 is the cryogenic gasket stress after presurization and can be an experimentally determined value for a given gasket material.

Defining the following constants and rearranging the equation, the results were as follows:

$$C_1 \equiv \frac{4\,K_1\left(2\,h_a+\delta_a\right)\left[1+\alpha_b^*\left(t_a-t_c\right)\right]}{\pi\,N\,d_a^2\,\delta_a\left[1+\alpha_g^*\left(t_a-t_c\right)\right]E_{b_c}} \qquad (11)$$

$$C_2 \equiv \frac{\pi\,N\left(t_a-t_c\right)\left[2\,h_a\left(\alpha_b^*-\alpha_f^*\right)+\left(\delta_a\;\alpha_b^*-\alpha_g^*\right)\right]E_{b_c}\,d_a^2}{4\,A_g\,E_{g_c}\left(2\,h_a+\delta_a\right)} \qquad (12)$$

$$\left(C_1\,K_2\,A_g-C_1\,N\,B_{b_1}+C_1\,\pi\,a^2\,P_i\right)^5=\frac{N\,B_{b_1}}{A_g\,E_{g_c}}-C_7-\frac{K_2}{E_{g_c}} \qquad (13)$$

$$\left.\begin{aligned} C_3 &= C_1 K_2 A_g \\ C_4 &= C_1 N \\ C_5 &= C_1 \pi a^2 \\ C_6 &= \frac{N}{E_{g_c} A_g} \\ C_7 &= C_2 + \frac{K_2}{E_{g_c}} \end{aligned}\right\} \qquad (14)$$

$$P_i = \frac{1}{K_j C_5}\left[\left(C_6 B_{b_1} - C_7\right)^{1/5} - C_3 + C_4 B_{b_1}\right] \qquad (15)$$

Introduced into equation (15) is an experimentally determined joint constant, K_j. The variables that effect the value of K_j are not completely known. These variables are believed to include the gasket width and flange diameter.

The values for K_j are as follows:

Gasket Size	
1 (4 in.)	3.0
2 (8 in.)	2.0
3 (12 in.)	1.5

The compressed gasket thickness was obtained with the following relationship:

$$\delta_a = g_a - \frac{g_a}{K_1}\left(\frac{N B_{b_1}}{A_g E_{g_a}}\right) \qquad (16)$$

A solution to equation (15) is shown below, leaving out many of the intermediate analytical steps. (For further detail see Appendix F.)

Given a specific gasket material, K_1 , K_2 , α_g^* , E_{g_a} , and E_{g_c} are known. Given a specific joint, d_a , g_a, N , a , b , h_a , α_b^* , α_f^* , K_j , and E_{b_c} are known and A_g is easily determined. Given a specific application, t_a , t_c , and B_b are known. Thus, δ_a , C_1 , C_2 , C_3 , C_4 , C_5 , C_6 , and then P_i can be determined from equations (11) through (15).

Table 50 presents a comparison of the experimental pressures and the theoretical results obtained utilizing equations (11) through (15). It should be noted that K_2 was taken as 1000 psi, based on the assumed minimum experimentally determined sealing requirements for pressures above 100 psi.

The data shown in Tables 49 and 50 represent the results of leak tests at cryogenic temperature (-320°F) after applying the flange load (torquing bolts) at room temperature. The percent deviations from experimental, obtained utilizing equation (15), are less than those obtained for equation (3). There are several items that could explain the deviations that exist between the experimental results and theoretical results. The method utilizing equation (3) requires two experimental constants and a linear approximation of compression versus deflection to determine the compressed gasket thickness (δ_a). The method utilizing equation (15) requires two simplified experimental constants and utilizes a more precise method of determining the compressed gasket thickness. The constant introduced in the stress-strain relationship,

$$\epsilon = \left[\frac{1}{K} \frac{\sigma}{E_g}\right]^{1/5}$$

utilized in equation (15), and to determine the compressed gasket thickness, is an integral part of the functions. It is not an experimentally determined constant such as K_c , K_t , and K_j , and therefore not subject to experimental errors. It is possible that some experimental error resulted from the repeated use of the bolts which applied load to the gasket-flange joints. The repeated use of these bolts could have caused permanent set or a change in material properties, which would result in experimental error. It should be noted that the conditions which affect the experimentally determined constants could not be determined and controlled during these investigations because of the preliminary nature of the study.

TABLE 50

THEORETICAL AND EXPERIMENTAL COMPARISON
(Equation 15)

Data* ID	Size ID, in.	ga, in.	B_{bl}, lb.	δa, in.	P_i Calculated, psi	P_i Experimental, psi	% Deviation of Calculated Pressure From Experimental Test Pressure
1	4	0.074	2,300	0.070	300	335	-10.4
2	4	0.087	3,300	0.082	470	492	- 4.5
3	8	0.112	3,400	0.105	392	465	-15.7
4	12	0.100	4,500	0.094	320	325	- 1.5
5	12	0.103	5,000	0.097	295	380	-22.4

* Data represent averages of typical groups of leak tests.

Certain 500 psi data were not included in the average values utilized to evaluate the analytical expressions, because it was not known if the 500 psi pressures were the maximum that could be contained for the corresponding bolt loads. More data representing maximum pressures must be obtained for a complete range of flange loads for various gasket sizes. This will allow empirical and graphical data, such as flange pressures versus internal pressure, to be presented as design information.

Conclusions as to which particular solution is most accurate can only be arbitrary. It appears that equation (15) is probably more accurate than equation (3). Equation (15) utilizes two experimental contants which seem to be more simplified than the constants utilized in equation (3). Also, the method of determining the compressed gasket thickness for equation (15) approximates the actual conditions much more precisely than the method used in equation (3).

PROCESSING STUDIES FOR VARIOUS SEAL CONFIGURATIONS AND FLEXIBLE TUBING

A logical follow-on effort to the development of the laminated gasket composite was the application of this concept to seal configurations other than flat gaskets. The objective of this part of the program was to develop processing techniques which are capable of incorporating TFE Teflon film, FEP Teflon film, and laminar woven filament-wound glass reinforcement into such configurations as O-rings; chevron, lip, and ball valve seals; control valve diaphragms and flexible tubing. The developed seals were then evaluated by various types of deflection and leak tests at room temperature and cryogenic temperatures.

The approach taken to meet the above-stated objective was to take the basic fabrication process developed for manufacturing flat gaskets and modify it as required for the various other configurations. The processes were individually evaluated by such means as the dye penetrant test, the compression versus deflection test, and leak testing.

Ball Valve Seals

Methods of construction. — Ball valve seals normally function by having the ball pushed against an opening to seal it. The elasticity of the ball helps ensure a tight seal.

There were no specific design requirements for the prototype ball valve seals. A ball size of 1-in. diameter was chosen, and a maximum leak test pressure of 500 psi was selected as the test pressure to be contained with 100 lb of force acting on the ball. A compression versus deflection test was conducted on the balls to get elasticity data and to determine how each processing method affected the elasticity of the ball valve seal.

Three different fabrication methods were investigated for the manufacturing of ball valve seals. Figure 77 is a schematic of these methods.

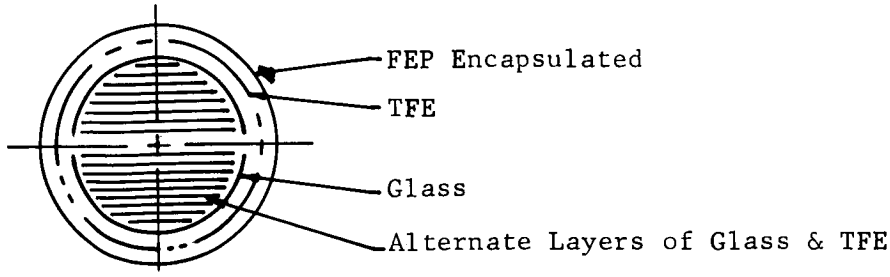

METHOD I

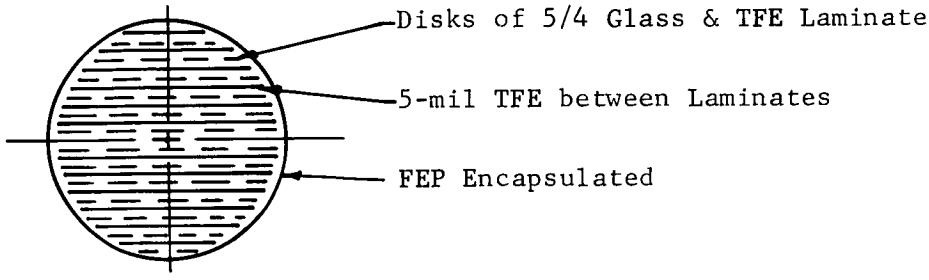

METHOD II

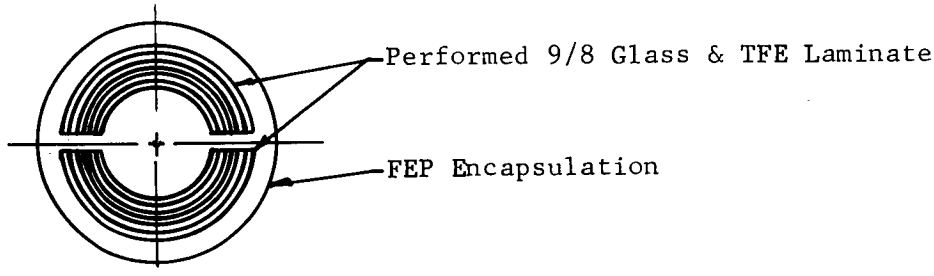

METHOD III

Figure 77. Schematic of Ball Fabrication Methods

The fabrication processes for each type of ball valve seal are described below.

Method I:

1. Plies of 401 heat-cleaned glass cloth and 0.005-in. TFE were separately preformed at 700°F.

2. After preforming, both the preformed TFE and glass cloth were trimmed to the outside of the forming mold.

3. One layer each of the preformed glass cloth and TFE was placed in each half of the forming tool.

4. Alternate plies of 401 glass cloth and TFE were then cut to contour to fit in the remaining volume of the forming tool (see Figure 78).

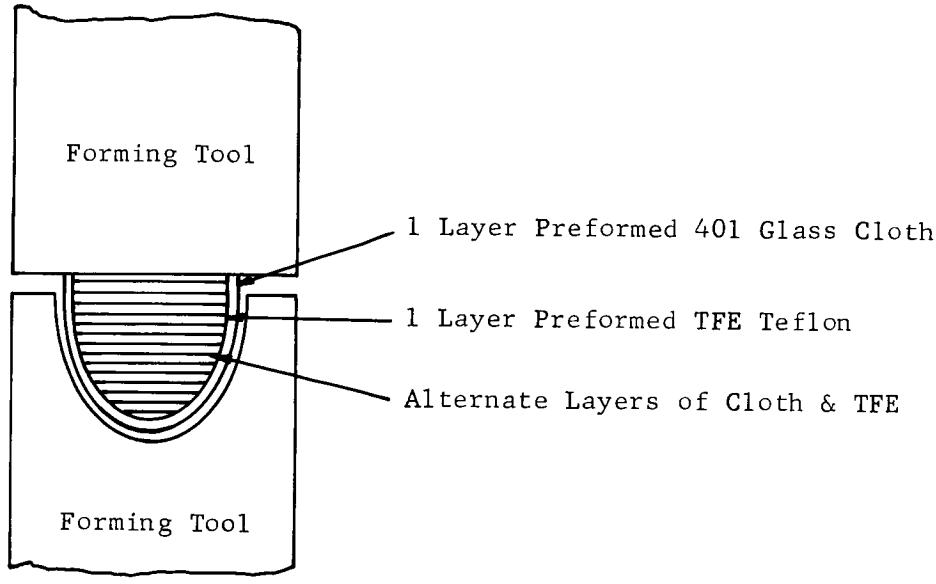

Figure 78. Forming Layup of One-Half of the Ball Valve Seal

5. Each half of the seal was cured at 100 psi for 5 minutes in a 760°F press.

6. After cooling to room temperature, the two halves of the seal were bonded together by adding additional layers of cloth and TFE. The part was then cured for 5 minutes at 760°F and allowed to cool to room temperature.

7. The formed ball valve seal was trimmed and placed in the encapsulation tool surrounded by 0.10-in. thick preformed FEP.

8. The part was encapsulated at 550°F for 3 minutes.

9. The part was cooled to room temperature and the parting line rotated 90° from its original position in the mold.

10. The part was then reheated to 525°F to reseal any possible unencapsulated area about the parting line.

11. The part was cooled to room temperature and submitted to Quality Control for inspection.

Method II:

1. A flat laminate was fabricated per the process specification presented in Appendix F utilizing 5 plies of style 401 glass and 4 plies of 0.005-in. thick TFE.

2. Increasingly smaller diameter circles were trimmed from the laminates and placed in the forming tool shown in Figure 79.

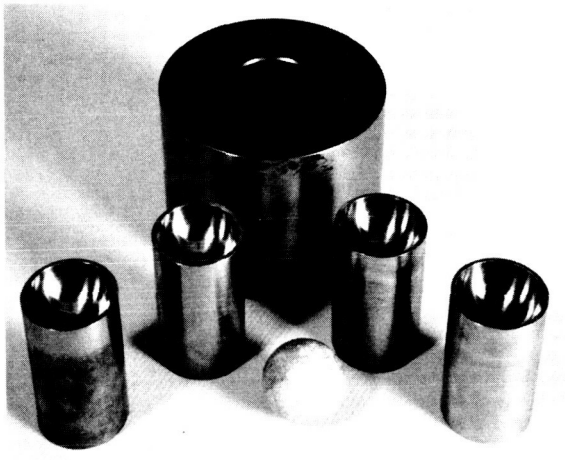

Figure 79. Forming and Encapsulation Tools for Fabrication of Ball Valve Seals Shown with End Item

3. The cut circles were cured in the forming tool at 720°F for 5 minutes.

4. The part was cooled, removed from the forming tool, and placed in the encapsulation tool, also shown in Figure 79, with 0.010-in thick preformed FEP; the part was then cured at 550°F.

5. The completed part was removed and submitted to Quality Control for inspection.

Method III:

1. A flat layup was made utilizing 9 plies of style 401 glass cloth and 8 plies of 0.005-in. thick TFE.

2. The layup was cut into a circle of approximately 2-in. diameter and draped over the forming tool.

3. The tool and laminate were placed in a 760°F press. A 3/4-in. diameter sphere was used to force the laminate to the shape of the cavity in the tool.

4. The formed part was allowed to cool to room temperature; Steps 2 and 3 were then repeated for the other half of the seal.

5. The two halves were placed in the forming tool and bonded together at a temperature of 760°F for 5 minutes, and then allowed to cool to room temperature.

Test methods. — Two tests were conducted on the ball valve seals: the compression versus deflection test, and the helium leak test. Figure 80(a) is a schematic diagram that shows the method of loading and the deflection measurement device, and Figure 80(b) is a photograph of the test equipment.

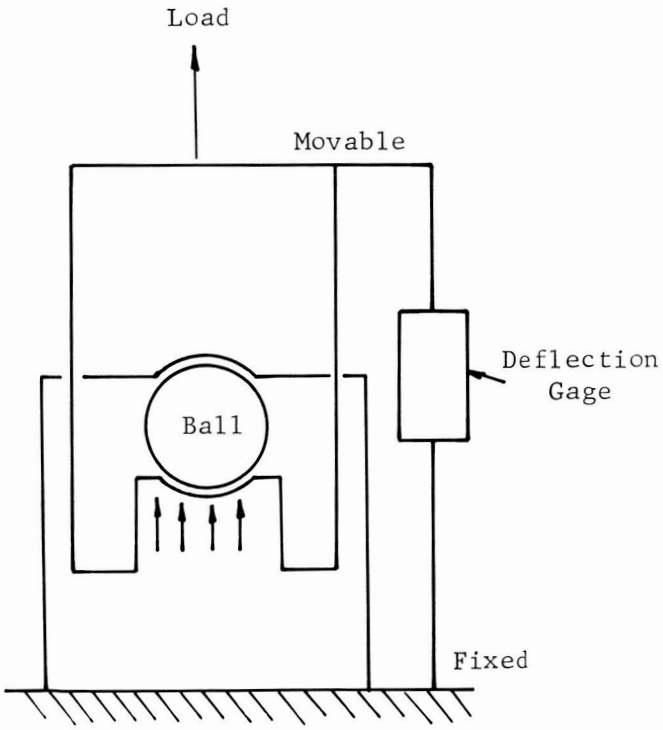

(a)

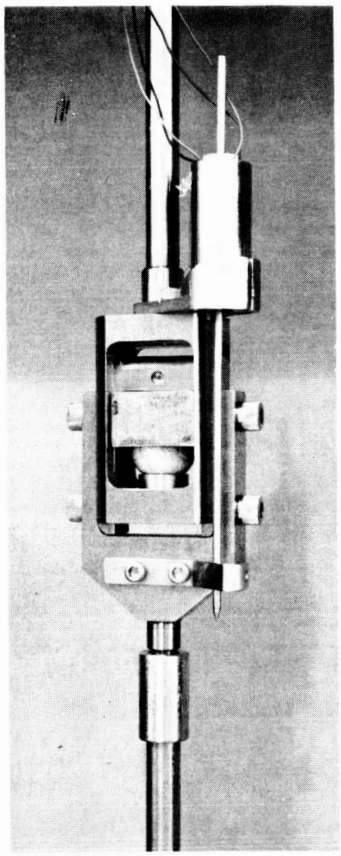

(b)

Figure 80. Compression versus Deflection Test Fixture Used for Ball Valve Seals

The compression versus deflection test is a measure of the compressibility and also of compression set of the item being tested. A x-y plotter records the applied load and the deflection on a strip chart.* Because the product of load times deflection is equal to work, the area under the compression-deflection curve represents the work done upon the item being tested. This area under the curve is therefore a useful standard of comparison for similar objects. Visual inspection of the compression versus deflection curves indicated that any significant changes in the work done upon the item stops by about the third cycle when a number of cycles are run. To illustrate this phenomenon, Figure 81 was prepared from data on a 1-in. diameter ball by plotting the measured area under each of the ten compression-deflection curves. Based on this observation, the areas were measured for the first, second, and tenth cycles of the graphs to determine the effects of short- and long-term cycling.

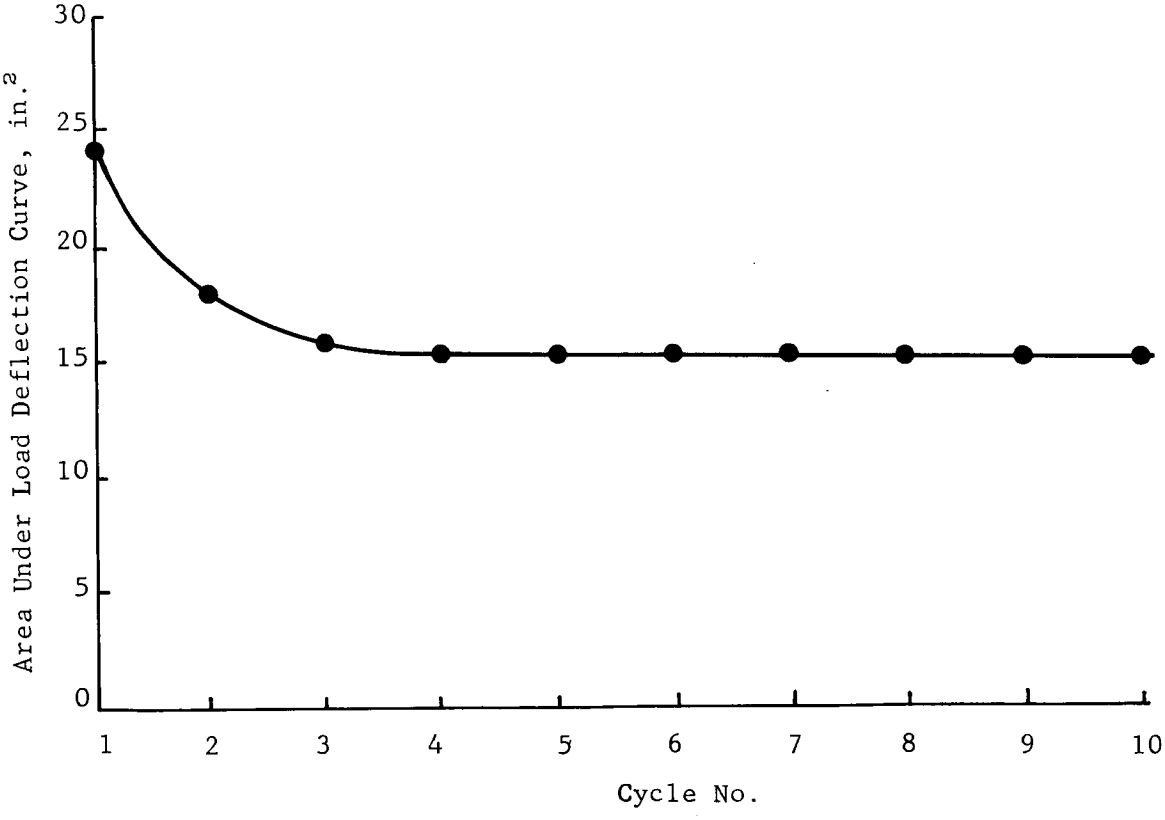

Figure 81. Area Under Compression-Deflection Curve as a Function of Cycle Number (Room Temperature)

* A typical set of output curves is shown as Figure 18.

The leak test was conducted by locating the ball seal in a cavity, which was equal in radius to the radius of the ball seal. Helium gas was introduced through a hole in the seat and the helium pressure contained was measured. The test fixture is shown in Figure 82.

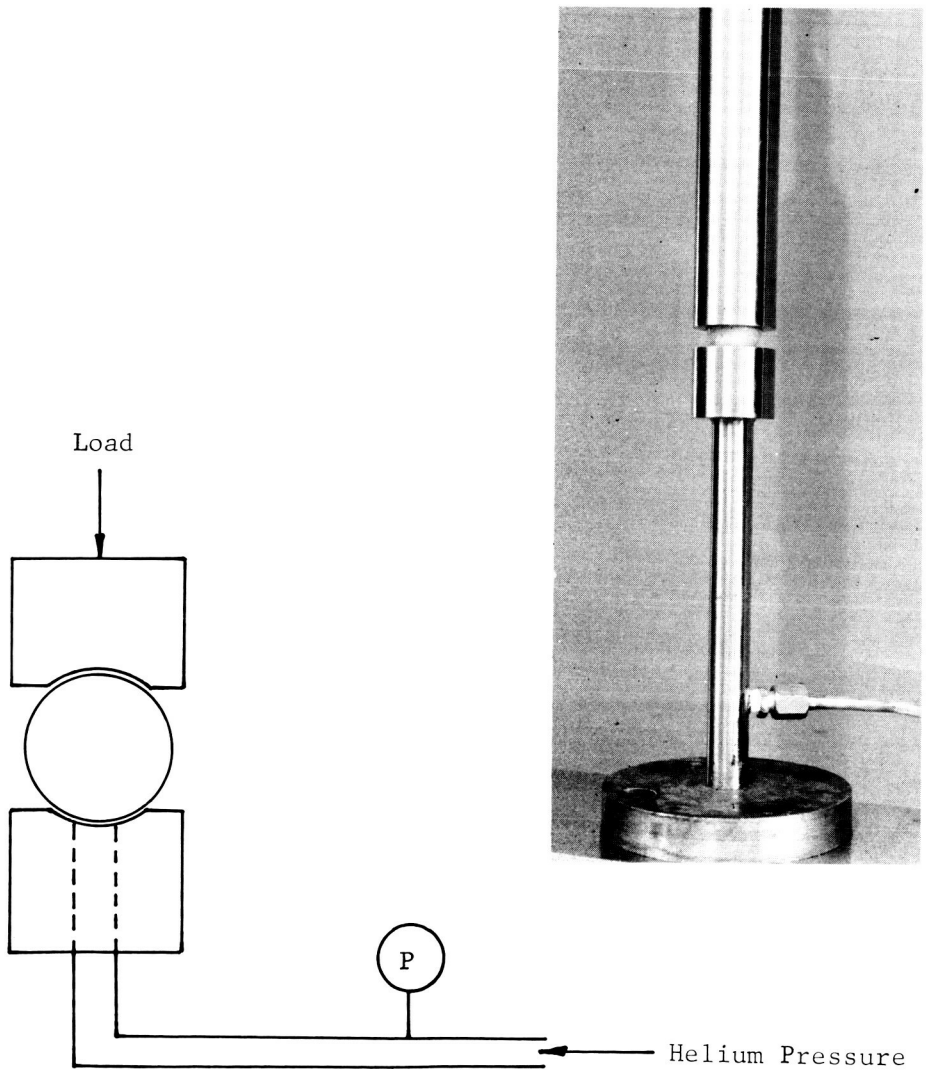

Figure 82. Leak Test Fixture Used for the Ball Valve Seals

The test fixture was placed in a cryostat which was filled with liquid nitrogen to obtain the necessary temperature environment for the -320°F tests. However, the actual test methods were the same as the room temperature tests.

The liquid hydrogen testing was accomplished in the same manner as the liquid nitrogen.*

Test results. — The leak test results of the ball valves are indicated in Table 51. The results and the average value are shown for each test. The results showed that the ball usually did not make an adequate seal even under a 150-lb force at room temperature, and that the balls were completely inadequate as a seal at -320°F. Consequently, testing was not conducted at -423°F because of this poor performance.

TABLE 51

BALL LEAK TEST DATA

Specimen Type	Contained Pressure,* psi			
	100-lb Load		150-lb Load	
	RT	-320°F	RT	-320°F
I	102	10	120	14
	110	10	282	12
	0	10	0	13
II	0	0	0	0
	0	0	365	15
	132	15	345	42
III	114	0	319	0
	69	0	100	0
	200	29	320	65

* Pressure contained after 10 minutes with 500-psi internal pressure.

* The liquid hydrogen cryostat and the liquid hydrogen setup are shown in Figures 59 and 60.

The compression versus deflection test data are given in Tables 52 and 53. Between balls of the same design, the spread in energy absorption on a volume basis was too great to warrant selection of a preferred design. The energy absorption on a mass basis was also calculated in an attempt to find better correlation. Here too, however, the energy absorption spread was too great to make any conclusion.

TABLE 52

BALL COMPRESSION-DEFLECTION TEST DATA AT ROOM TEMPERATURE

Ball	Cycle	Area, $in.^2$	Energy, in.-lb	Energy/Unit Vol $in.-lb/in.^3$	Ball Mass, gm	Energy Unit Mass, in.-lb/gm
I-1	1	--*	--*	--*	12.283	--
I-2	1	20.14	1.610	3.075	13.939	--
	2	14.30	1.145	2.185	--	--
	10	12.24	0.980	0.980	--	0.134
I-3	1	5.45	0.437	0.834	15.574	--
	2	3.78	0.303	0.578	--	--
	3	3.57	0.286	0.546	--	--
	10	3.31	0.265	0.506	--	0.325
II-1	1	--*	--*	--*	15.663	--
II-2	1	15.25	1.221	2.33	17.605	--
	2	7.55	0.605	1.155	--	--
	10	6.32	0.506	0.965	--	0.0548
II-3	1	19.45	1.555	2.97	17.811	--
	2	9.57	0.766	1.461	--	--
	10	7.16	0.574	1.096	--	0.0615
III-2	1	8.48	0.679	1.295	9.298	--
	2	5.94	0.476	0.909	--	--
	10	4.91	0.393	0.750	--	0.0806
III-3	1	11.13	0.891	1.695	9.527	--
	2	9.27	0.743	1.419	--	--
	10	8.25	0.661	1.260	--	0.132
III-6	1	14.92	1.195	2.280	10.320	--
	2	10.85	0.868	1.655	--	--
	10	8.94	0.715	1.365	--	0.132

* Specimen deformed under load.

TABLE 53

BALL COMPRESSION DEFLECTION TEST DATA AT -320°F

Ball	Cycle	Area $in.^2$	Energy, in.-lb	Energy/Unit Vol $in.-lb/in.^3$	Ball Mass, gm	Energy Unit Mass, in.-lb/gm
I-4	1	1.82	0.1325	0.253	14.275	--
	2	1.52	0.1105	0.211	--	--
	10	1.54	0.112	0.213	--	0.0149
I-5	1	2.62	0.191	0.364	14.035	--
	2	2.65	0.193	0.368	--	--
	10	2.24	0.166	0.316	--	0.0225
I-6	1	2.47	0.180	0.343	14.148	--
	2	2.18	0.158	0.301	--	--
	10	2.14	0.156	0.298	--	0.0211
II-4	1	5.72	0.416	0.795	16.714	--
	2	3.10	0.226	0.431	--	--
	3	1.34	0.098	0.187	--	--
	10	1.36	0.099	0.189	--	0.0113
II-5	1	4.62	0.336	0.641	15.243	--
	2	2.98	0.217	0.414	--	--
	10	2.53	0.184	0.351	--	0.231
II-6	1	1.97	0.144	0.275	16.220	--
	2	0.73	0.053	0.101	--	--
	10	0.92	0.067	0.128	--	0.00789
III-7	1	3.70	0.269	0.513	10.175	--
	2	2.93	0.213	0.406	--	--
	10	2.66	0.193	0.368		0.0362
III-8	1	3.34	0.243	0.464	10.703	--
	2	2.10	0.153	0.292	--	--
	10	1.96	0.143	0.273	--	0.0254
III-9	1	8.48	0.616	1.175	10.288	--
	2	4.23	0.308	0.588	--	--
	10	4.20	0.306	0.584	--	0.0569

The weight and therefore the density* of the balls varied, depending on the method of construction. As expected, Type II, fabricated from preliminated glass-TFE laminates, yielded balls with the greatest density; Type III, being hollow, had the lowest density.

The spread in energy absorption values in the balls was probably due to the direction of load application relative to the plies and/or ball equator. Differences in compression would be expected when load is applied either normal or parallel to the ply direction (see Figure 83). Figure 83 was prepared for Type II balls, but the concept can also be applied to Type I balls. The location of the ball equator (determined during fabrication) relative to the load can also affect the ball deflection. Figure 84 is a schematic of the conditions possible.

Figure 83. Schematic of Load Application Relative to Ply Direction

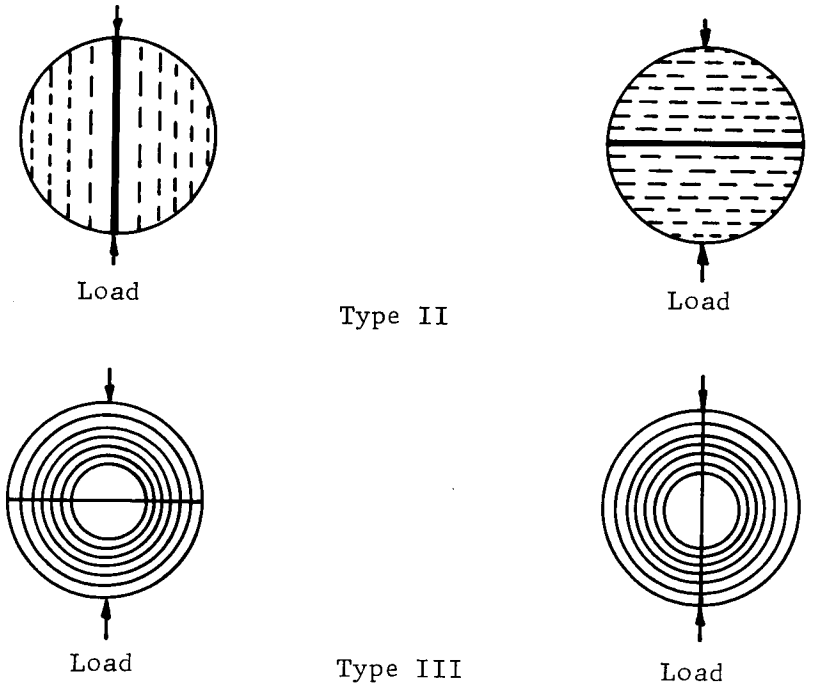

Figure 84. Schematic of Load Application Relative to Ball Equator

* All were of the same volume.

The probability of variations in orientation also applies to the pressure leak test, and may account for the wide spread of results for that test. Based on the results of the energy absorption tests and the leak tests, the ball concept as studied herein cannot be recommended for use as a seal unless there is a reliable method of controlling the ball orientation with respect to the ball equator.

Control Valve Diaphragms

Processing studies were conducted to find methods to produced a control valve diaphragm using the encapsulated glass – Teflon laminate. Figure 85 shows a single diaphragm concept which operates by internal pressure, and Figure 86 illustrates an inflatable membrane concept.

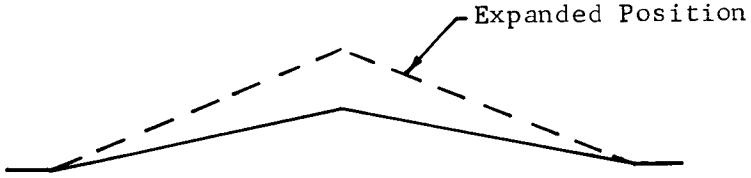

Figure 85. Single Membrane

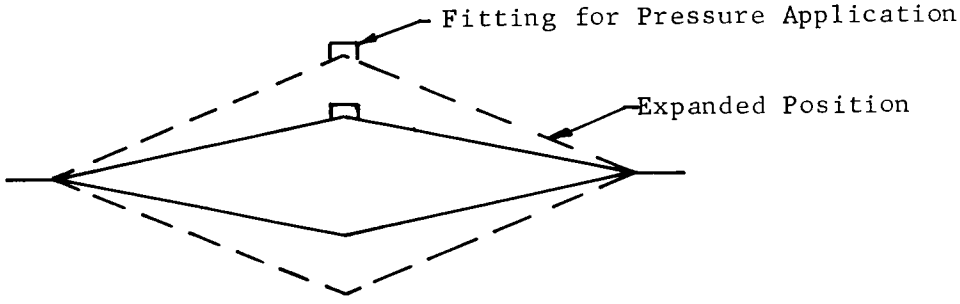

Figure 86. Inflatable Membrane

Processing studies were concerned with the forming and encapsulating of the equivalent of Figure 85, which would lead to the diaphragm of Figure 87. In other words, after the forming and encapsulation of a single diaphragm was developed, the bonding together of two diaphragm "halves," along with any required fittings, would be a routine task.

The following process technique was followed to form the diaphragm.

1. A flat laminate was laid up and cured per the process specification (presented as Appendix F) with the exception that six layers of style 401 glass cloth and five layers of 0.005-in. thick TFE were used. Laminates of three layers of glass cloth and two layers of 0.005-in. thick TFE were also used.

2. The cured laminate was cooled and the thickness recorded.

3. The laminate was trimmed with the trim die shown in Figure 87.

4. The trimmed laminate was placed in the forming tool shown in Figure 88, and the part was cured for 5 minutes at 720°F.

5. The formed part was cooled under pressure, and then the completed part was inspected and measured.

6. The formed part with 0.010-in. thick FEP on each side was placed in the encapsulation fixture, shown in Figure 89, and cured at 550°F.

7. The encapsulated part was then cooled and submitted to Quality Control for inspection.

When the single diaphragms were formed, several attempts were made to bond a double diaphragm with the tools shown in Figure 90. Several diaphragms were fabricated to establish this processing technique. Figure 91 shows some of the double and single diaphragms built.

During the development of these diaphragms, several valve manufacturers were contacted concerning their need for such a diaphragm. A thickness of 0.005 in. to 0.010 in. was specified as a maximum practicable thickness. This thickness limitation and the lack of flexibility of the fabricated diaphragms at room temperature eliminated this particular configuration as a major effort in this program. Some diaphragms were made with fewer layers of glass and Teflon in an attempt to increase flexibility, but this did not lead to any noticeable improvement. Further work to increase flexibility was not conducted because of the above-mentioned thickness limitation.

Figure 87. Valve Diaphragm Cutting Tool

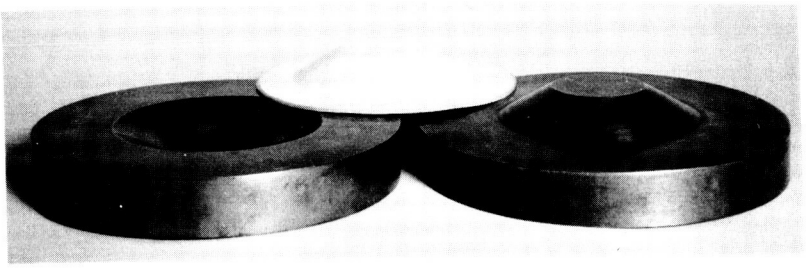

Figure 88. Valve Diaphragm Forming Tool Shown with Formed Laminated Composite

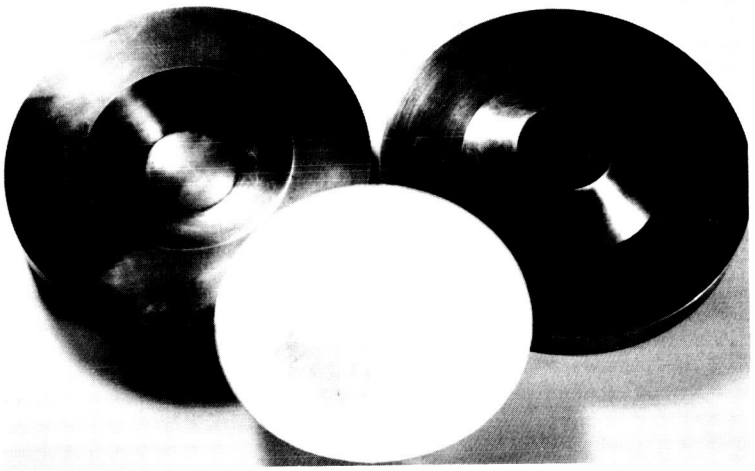

Figure 89. Valve Diaphragm Encapsulation Tool Shown with Completed Part

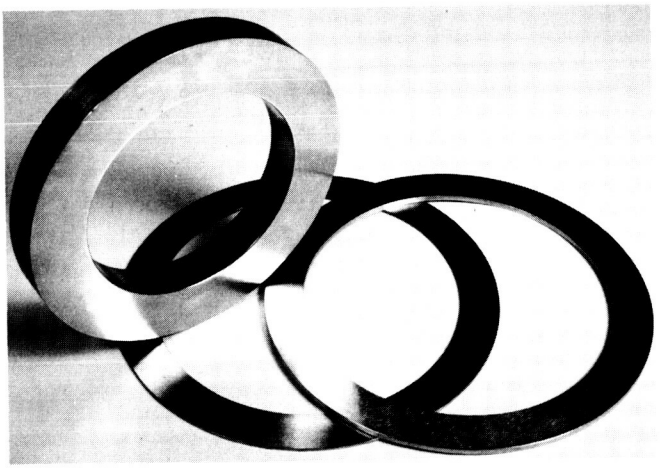

Figure 90. Various Pressure Rings Used in Adhesive-Bonding Two Diaphragm Halves Together

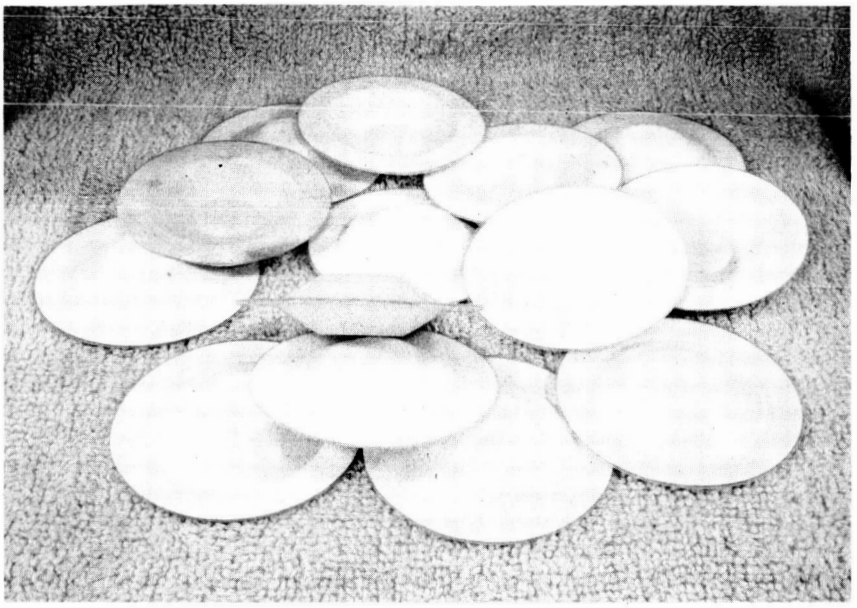

Figure 91. Single and Double Diaphragms

The formed diaphragms were tested for tightness with a penetrant leak check and were found to be satisfactory. Further testing was not conducted, as there is presently no recognizable application for the diaphragms developed under this program.

Flexible Tubing

Currently, the only practical flexible cryogenic tubing is a double-walled stainless steel bellows. Therefore, in an effort to produce a lightweight flexible tubing for cryogenic applications, various methods were investigated utilizing the concept of a glass-TFE composite encapsulated in FEP. Based on the performance requirements of other cryogenic hardware, containment of helium at 200 psi and retention of flexibility were established as general criteria. The requirement of flexibility was not quantified; however, flexibility of the developed tubing was measured in a flexure test.

Fabrication. — Several methods of construction were investigated and are described in Table 54. Prototypes of each method were leak-tested to evaluate the effectiveness of the particular methods of construction. Leaks which occurred in the tubing were considered unsatisfactory and cause for rejection of a particular construction method. Leaks which occurred at the fitting were not considered valid cause for rejection; instead, the ends were reworked and sealed, and then the tubing was retested.

During the test program, some tubes delaminated (see Figure 92). The Type VI method of construction was developed in an effort to solve this problem.

TABLE 54

METHODS OF TUBING FABRICATION

Component	Type I	Type II	Type III	Type IV	Type V	Type VI
Inner layer	FEP multi-filament wrap	FEP multi-filament wrap	FEP shrink-able tubing	FEP shrink-able tubing	FEP shrink-able tubing	FEP shrink-able tubing
Reinforcement	Glass sleeving	Glass sleeving	Glass sleeving	Glass sleeving	Glass sleeving	Glass sleeving + TFE shrink-able tubing + Glass sleeving. All cured into an integral item
Middle layer	FEP multi-filament wrap	TFE multi-filament wrap	TFE multi-filament wrap	TFE shrink-able tubing	TFE shrink-able tubing	
Reinforcement	Glass sleeving	Glass sleeving	Glass sleeving	Glass sleeving	Glass sleeving	
Outer layer	FEP multi-filament wrap	FEP multi-filament wrap	FEP shrink-able tubing	FEP shrink-able tubing	FEP multi-filament wrap	FEP shrink-able tubing

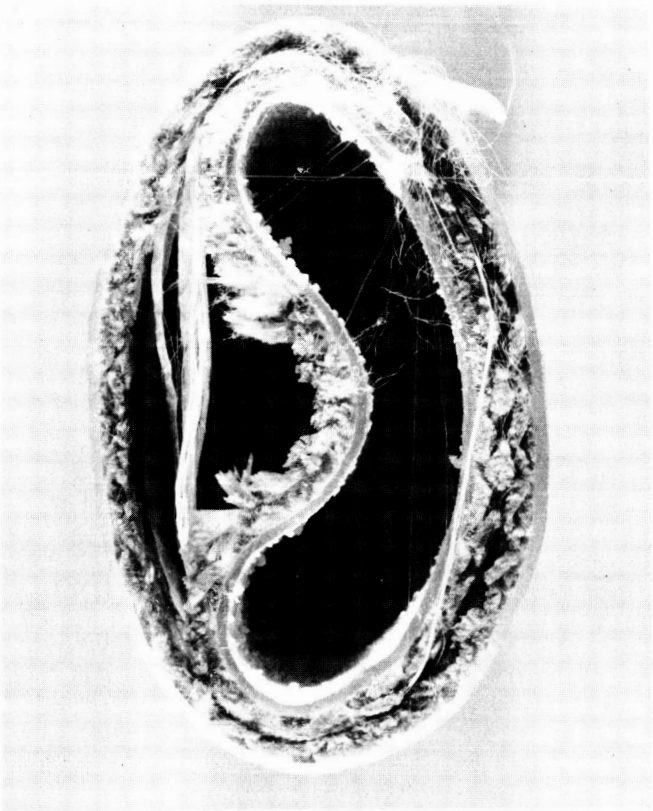

Figure 92. Tubing Type III, Failure after Exposure to -320°F

Type I through Type V flexible tubing were similarly processed, except for the use of various forms of the component materials (individual layers). These methods are described below.

Type I:

1. The mandrel (see Figure 93) was wrapped with 108 glass cloth impregnated with TFE.

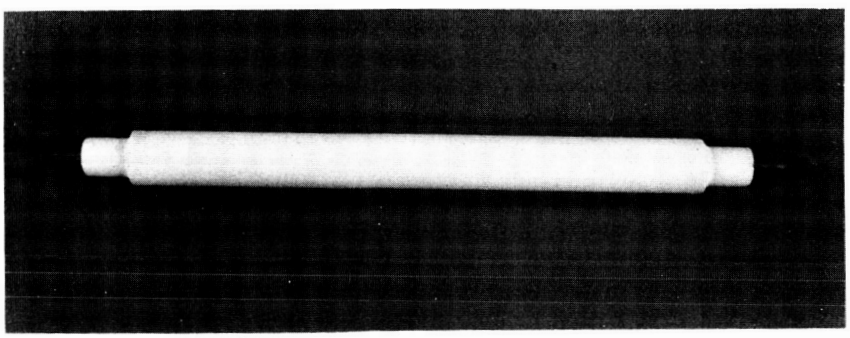

Figure 93. Plaster Laminating Mandrel

2. The cloth was overwrapped with multifilament FEP.

3. Glass sleeving was slip-braided over the multifilament FEP.

4. The sleeving was overwrapped with multifilament FEP.

5. Glass sleeving was slip-braided over the wrapped multifilament FEP.

6. The sleeving was overwrapped with multifilament FEP.

7. 108 glass cloth impregnated with TFE was wrapped over the FEP.

8. This was overwound with a minimum of 10-end roving with maximum tension.

9. The layup was cured in an oven at 550°-560°F for 5 minutes, then cooled to room temperature.

10. The part was then removed from the mandrel.

The Type II through Type V methods of fabrication were similar to the steps described for the Type I method of fabrication except for the particular materials. Where FEP and TFE shrinkable tubing was utilized it was shrunk to the mandrel or layup with a heat gun or a 250°F oven.

Type VI:

1. Glass sleeving was slip-braided on to the laminating mandrel.

2. TFE shrink-fit tubing was slipped over the braided glass and shrunk in a 250°F oven.

3. Glass material was slip-braided over the TFE tubing.

4. 5-end roving was wound from the center toward the end of the mandrel and then wound back toward the center.

5. The layup was cured at 700°±10°F in an oven for 3-4 minutes, and was then cooled to room temperature.

6. The cured laminate was removed from the mandrel.

7. Single filament FEP was overwound on the tube end fittings attached to the encapsulating mandrel.

8. FEP shrink-fit tubing was slipped over the mandrel and shrunk to the mandrel with a heat gun or in a 250°F oven.

9. The glass-TFE laminate was slipped over the shrunk FEP.

10. FEP shrink-fit tubing was slipped over the mandrel and shrunk to the layup with a heat gun or in a 250°F oven.

11. The part was wrapped with 108 glass cloth impregnated with TFE.

12. The part was overwound with a minimum of 10-end roving with maximum tension.

13. The part was cured in a 550°F oven for 3 minutes, then cooled to room temperature.

14. The mandrel was removed from the part, the overwound roving, and the 108/TFE glass cloth.

Test Methods. — Leak tests, burst tests, and flexibility tests were conducted on the flexible tubing. Leak and burst tests were conducted with water at room temperature and with helium gas at room temperature and -320°F.

A schematic of the test setup is shown in Figure 94. The pressure source for the water tests was a 1000-psi Blackhawk handpump. This pump was adequate because of the low volume of water required for the test. The pressure source for the room temperature and -320°F helium tests was a standard K bottle.

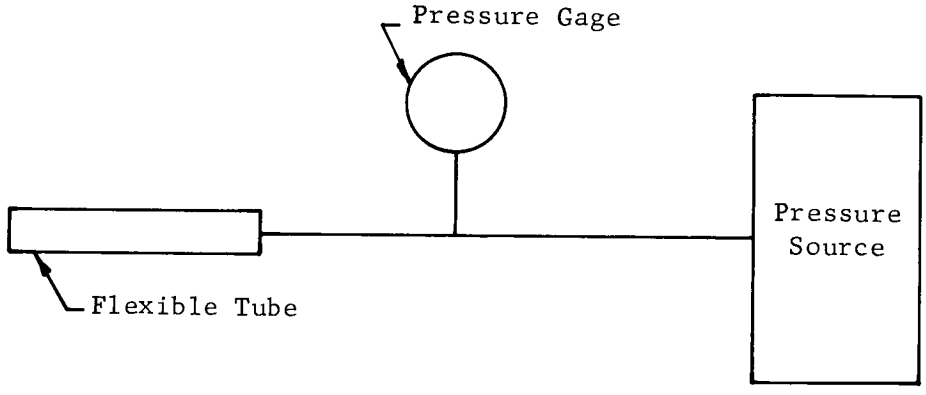

Figure 94. Leak and Burst Test Setup

The leak test was conducted by pressurizing the flexible tube to 200 psig. The pressure after 10 minutes was recorded and was the basis for the leak evaluation.

The burst tests were conducted by pressurizing the flexible tubing until failure. The rate of pressurization was approximately 5 psig per second for the helium tests and approximately 10 psig for the water tests.

Besides being capable of containing 200 psig, the tubing also had to be flexible. A test was devised to indicate the inherent flexibility of the tubing. Figure 95 shows a tube undergoing the flexibility test. Figure 96, a schematic of the load application points and tubing placement, contains the data obtained from the flexibility test.

The point at which a slight ripple occurred in the tubing (see Figure 95) was considered to be the maximum angle of deflection.

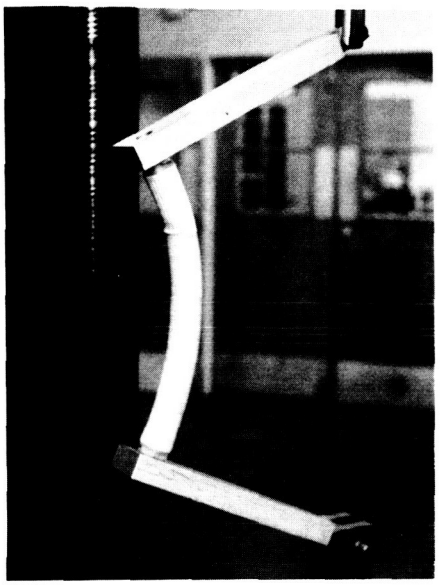

Figure 95. Tubing Undergoing Flexibility Test

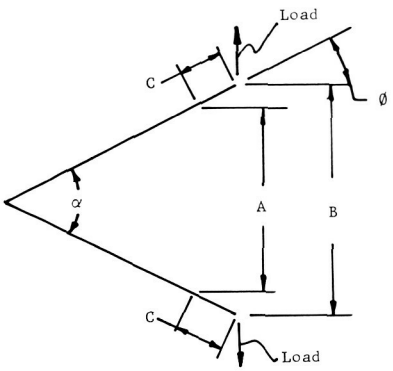

A = length of tubing, in.

B = distance between upper and lower load arms at position when tube collapses, in.

C = length of load arm, in.

$\alpha = 2\,\emptyset$

$\emptyset = \sin^{-1} \frac{B - A}{2C}$

S/N	A	B	C	α	Load lb
2	12.375	16.290	10.25	22°	--
6	12.125	18.675	10.25	37°	18
8	12.375	20.375	10.25	46°	21.5

Figure 96. Flexibility Test on 1-in. Diameter Type VI Flexible Tubing

Test results. — Table 55 presents leak test data which was utilized to evaluate the various methods of tubing fabrication. It appears that the combination of materials that comprised the Type IV tubing is more suitable for containing 200-psig pressure.

As previously discussed, delaminations occurred during the leak testing of the Type I through Type V tubes (see Figure 92). To eliminate these delaminations, the Type VI method of construction was developed utilizing the leak-sealing capabilities of the Type IV tubing.

TABLE 55

LEAK TEST DATA FOR FLEXIBLE TUBING

(Process Evaluation)

Specimen Identification		Pressure after 10 min, psig		
		H_2O	He @ RT	He @ -320°F
Type I	1	20	No test	No test
	2	15	No test	↓
Type II	1	80	0	
	2	40*	No test	
	3	100	0	
	4	120	3	↓
Type III	1	200**	85	38
Type IV	1	200**	200	200
Type V	1	180	No test	No test
	2	160	↓	↓
	3	180	↓	↓

* Leakage occurred in end fittings

** No leak.

Table 56 presents the leak and burst pressure data obtained on the Type VI tubing. The 1-in. diameter tubing yielded results which indicate good leak-sealing ability and adequate burst strengths. The 2-in. diameter tubing leak and burst test results were lower than the test results for the 1-in. diameter tubing. A cursory analysis shows that the wall thicknesses were substantially the same for both the 1-in. and 2-in. diameter tubing. The basic formula for the stress (S) in the wall of the tubing is

$$S = \frac{pD}{2t}$$

where P is the internal pressure, D is the diameter, and t is the wall thickness.

TABLE 56

LEAK AND BURST PRESSURE DATA FOR TYPE VI TUBING

Specimen No.	Dia, in.	Pressure Media (Temp)	Leak Pressure after 10 min, psig	Burst Pressure, psig
1	1	H_2O (RT)	66	430
4		H_2O (RT)	158	475
7		H_2O (RT)	192	480
2		He (RT)	196	No test
6		He (RT)	198	
8		He (RT)	196	
3*		He (-320°F)	200**	970
5*		He (-320°F)	200**	950
9*		He (-320°F)	200**	900
10	2	H_2O (RT)	--***	--
11		H_2O (RT)	45†	100†††
13		H_2O (RT)	148	275
12		He (RT)	186	290
14		He (RT)	--††	--
16		He (RT)	50	280†††
15*		He (-320°F)	40	400
17*		He (-320°F)	170	700
18*		He (-320°F)	50	780

* Hose clamps utilized on both ends of tube for leak and burst tests @ -320°F.

** No leak.

*** Failed at 130 psi.

† Reading after 2 minutes.

†† Serious leak at 150 psi.

††† Maximum pressure attainable.

This formula shows that as the diameter of the tube increases, the internal failing pressure decreases for a particular allowable stress and wall thickness.

Analysis of the processing techniques indicates that Method VI is the most practical. Method VI reduces the man-hours required to fabricate the part by 30% and the reproducibility of the fabricated tubing is significantly higher. The test results also indicate this process method eliminates the previous delamination failures. Examination of the test results indicates that this concept for the fabrication of lightweight flexible tubing is worthy of consideration for future optimization studies.

O-Rings

Methods of fabrication. — Static O-rings are classified as gasket-type seals. Narmco had demonstrated that flat gaskets fabrication from the FEP encapsulated glass — TFE composite exhibited outstanding performance, and suggested that this concept, when applied to other gasket configurations, would also exhibit improved cryogenic performance. Thus, this concept was applied to the O-rings. The following methods of fabricating the internal glass-TFE composite were studied:

Method A. Formed laminating

Method B. Toroidal winding on steel wire

Method C. Toroidal winding on laminate

Method D. Circumferential winding

These methods are shown schematically in Figure 97 and the process technology developed to obtain the various types of gaskets are explained in the following paragraphs.

Method A. Formed Laminate:

1. In accordance with the process specification presented in Appendix F, six pieces of 0.005-in. thick TFE were laminated with seven pieces of Style 401 glass cloth, at 720°F for 5 minutes under 500 psi, into a flat sheet.

2. The laminate was trimmed to the desired O-ring size.

3. The trimmed laminate was placed in the forming tool shown in Figure 98 and formed at 720°F for 5 minutes.

4. The formed laminate was placed in the encapsulation tool (also shown in Figure 98) with four pieces of 0.010-in. thick FEP, using two layers on each side. A layer of 0.005-in. FEP was placed on the inside and outside diameters. The mold was closed and the part encapsulated at 550°F for 3 minutes.

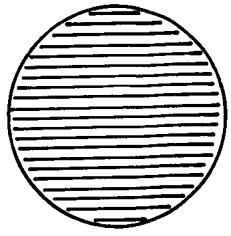

Laminate formed to circular cross section and encapsulated

(A) Formed Laminate

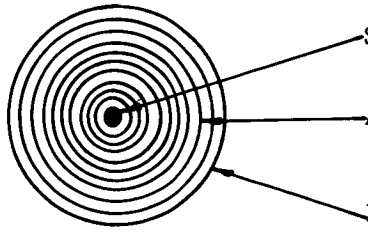

(B) Toroidal Winding on Steel Wire

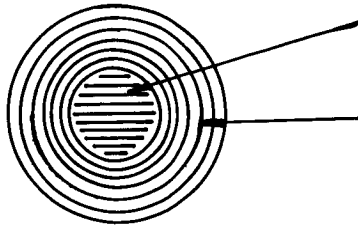

(C) Toroidal Winding on Laminate Core

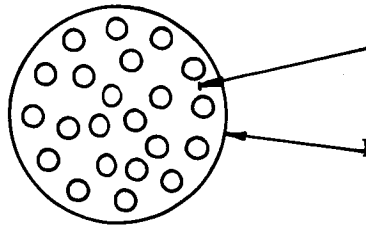

(D) Circumferential Winding

Figure 97. O-Ring Cross Sections for Various Methods of Fabrication

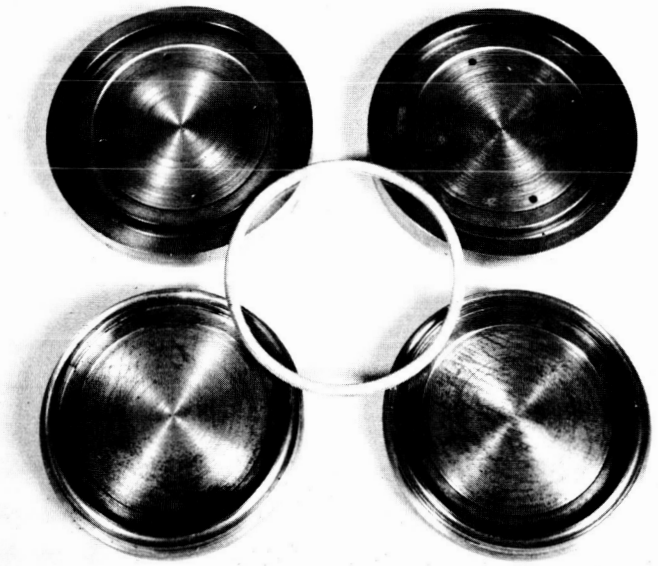

Figure 98. O-Ring Forming Tool and Encapsulation Tool Shown with a Fabricated O-Ring

5. The encapsulated O-rings were cooled, checked for leaks, and delivered to Quality Control for inspection of the O-ring cross section and the overall diameter of the part.

Method B — Toroidal Winding on Steel Wire:

1. A steel wire core was placed in a toroid winding machine (see Figure 99) and the spools of heat-cleaned S-glass roving and TFE were attached to the machine.

2. A layer of glass was wound around the steel wire core (see Figure 100).

3. A layer of TFE was wound over the layer of cloth.

4. Steps 2 and 3 were then repeated until the diameter of the O-ring was approximately 3/16 in.

5. The number of plies of glass and TFE used were recorded.

6. The wound O-ring was placed in the forming tool (shown in Figure 98) and formed at a temperature of 720°F for 30 minutes.

7. The formed part was cooled to room temperature.

8. The formed O-ring was placed back in the toroid winder, and two layers of FEP multifilament were wound over the O-ring.

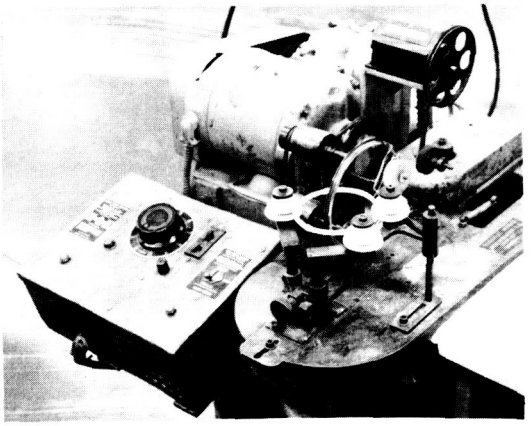

Figure 99. Toroid Winding Machine with Glass Spools Attached to the Revolving Platform

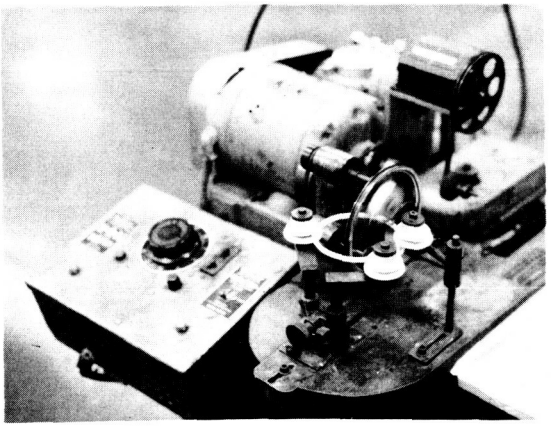

Figure 100. S-Glass Filament Being Wound over the Steel Core

9. The wound laminate was then placed in the encapsulation tool (shown in Figure 98) and cured for 3 minutes at 550°F.

10. The encapsulated O-rings were cooled, checked for leaks, and delivered to Quality Control for inspection of the O-ring cross section and the overall diameter of the part.

Method C — Toroidal Winding on Laminate Core:

1. In accordance with the process specification presented in Appendix F, six pieces of 0.005-in. thick TFE were laminated with seven pieces of style 401 glass cloth, at 720°F for 5 minutes under 500 psi, into a flat sheet. The laminate was cooled to 400°F maximum, under pressure.

2. The laminate was trimmed to the desired O-ring size and the corners trimmed as shown in the following sketch:

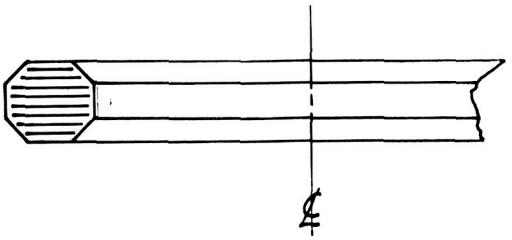

3. The trimmed laminate was placed in the forming tool shown in Figure 98, formed at 720°F at 500 psi for 5 minutes, and cooled to 400°F under pressure before being removed from the tool.

4. The formed ring was placed in a toroid winding machine and a spool of FEP was set up for winding.

5. Two layer of FEP multifilament yarn (0.010 thickness) were over-wound on the laminated core.

6. The formed O-ring was placed in the encapsulation tool, the tool closed, and the part encapsulated at 550°F at 100 psi for 3 minutes.

Method D — Circumferential Winding:

1. A split-ring winding mandrel was set up in the lathe (see Figures 101 and 102) and alternate layers of heat-cleaned glass roving and TFE multifilament yarn wound as shown in the folllowing sketch:

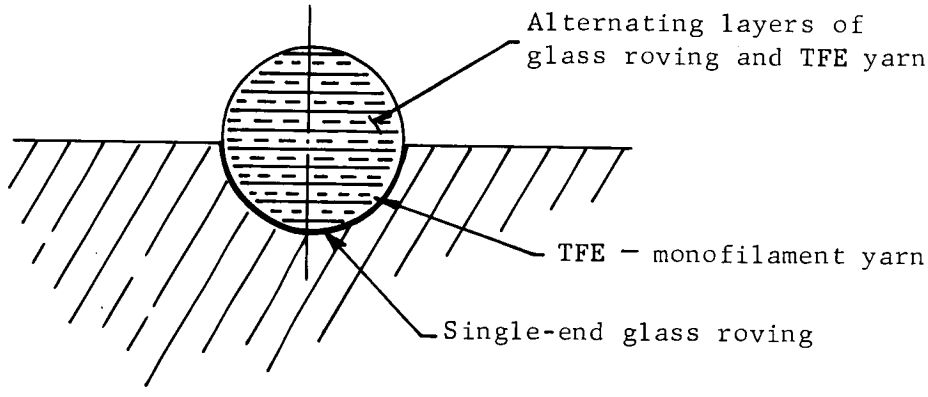

2. The split-ring clamp forming tool (shown in Figure 103 and 104) was placed over the winding and secured tightly.

3. The assembly was cured in an oven at 720°F for 5 minutes, cooled to a maximum of 400°F, and trimmed and cleaned.

4. To encapsulate the cured O-rings, a layer of 0.010-in. FEP film was placed in the bottom of the encapsulating mold shown

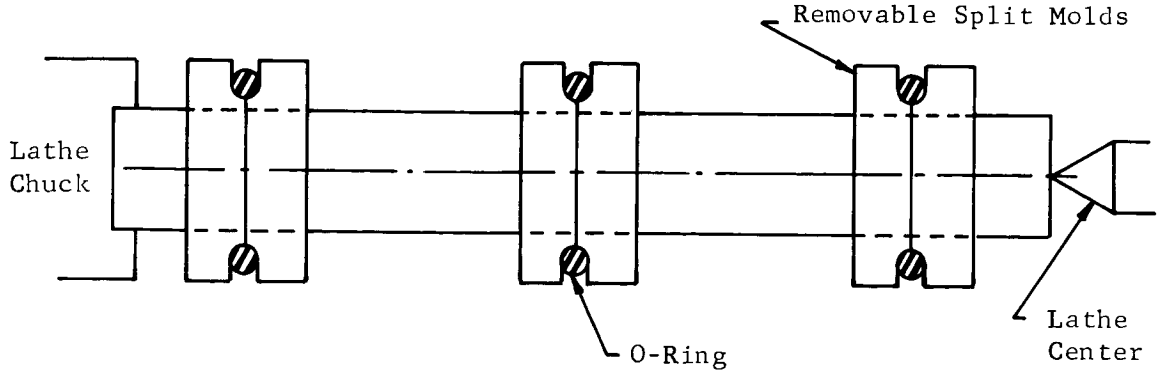

Figure 101. Split-Ring Winding Mandrel Setup

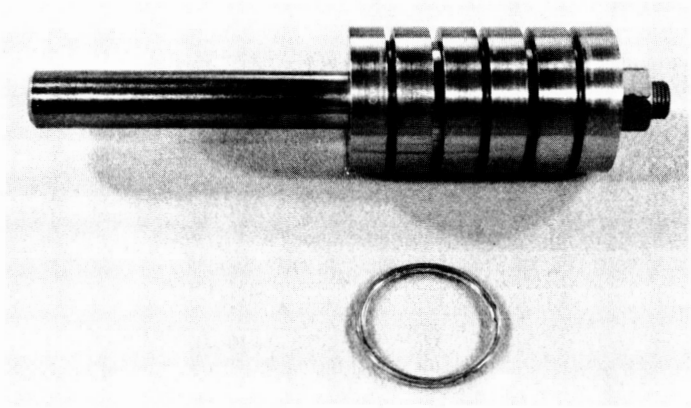

Figure 102. Split-Ring Winding Mandrel

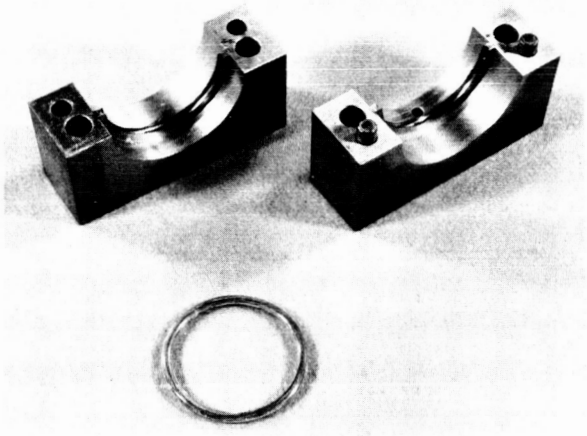

Figure 103. Split-Ring Clamp Forming Tool

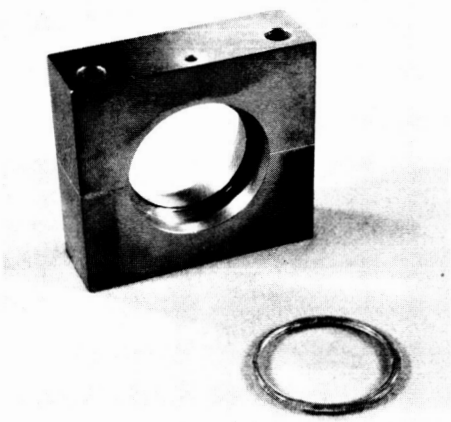

Figure 104. Split-Ring Clamp Forming Tool

in Figure 105. The O-ring was placed over the film and another layer of FEP film added on top of the O-ring. The mold was closed and cure took place at 550°F at 100 psi for 3 minutes.

5. The part was cooled under pressure to 400°F maximum temperature, removed from the mold, and cleaned and trimmed.

6. The part was subjected to dye penetrant, leak inspection, then delivered to Quality Control for inspection of the cross section and overall dimensions.

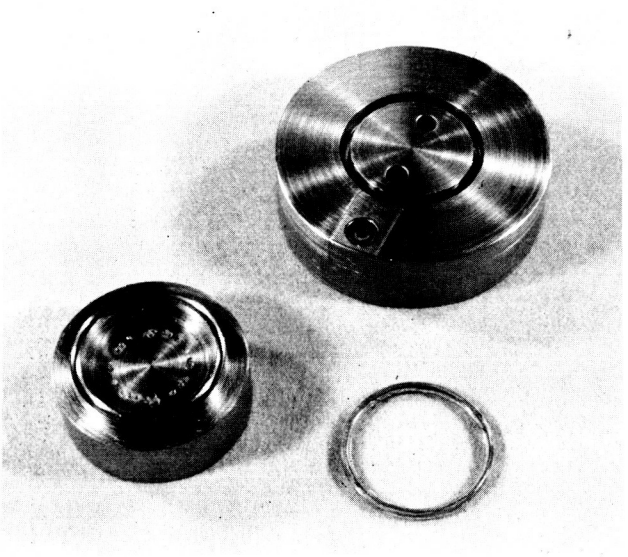

Figure 105. Encapsulating Mold for the Circumferentially Wound O-Rings

Test methods. — Two types of tests were conducted on the O-rings to evaluate the performance of the particular methods of construction. The tests performed were the leak test and the compression versus deflection test, conducted at room temperature, -320°F, and -423°F. The -423°F tests were performed on O-rings fabricated by what appeared to be the most promising method of construction, Method C.

The compression versus deflection test was similar to that used for the ball valve seals. The test fixture, which was modified for this test, is shown in Figure 58. The fixture was modified in such a manner that the developed O-rings could be tested utilizing the previous fixture shown in Figure 27.

The data were obtained by measuring the area under the compression-deflection curves. (See Figure 18 for a typical set of curves.) The areas

under the first, second, and tenth cycles were measured and considered sufficient indication of the performance of the O-ring over short- and long-time cycling.

The leak tests were conducted by loading an O-ring between two flanges with the outer diameter restrained by a metal ring. The assembly is shown in Figure 106, and the actual components are shown in Figures 107 and 108. The annular space captivated by the O-ring and flanges was pressurized with helium to 200 psi or 500 psi. The pressure was recorded 10 minutes after the initial pressurization.

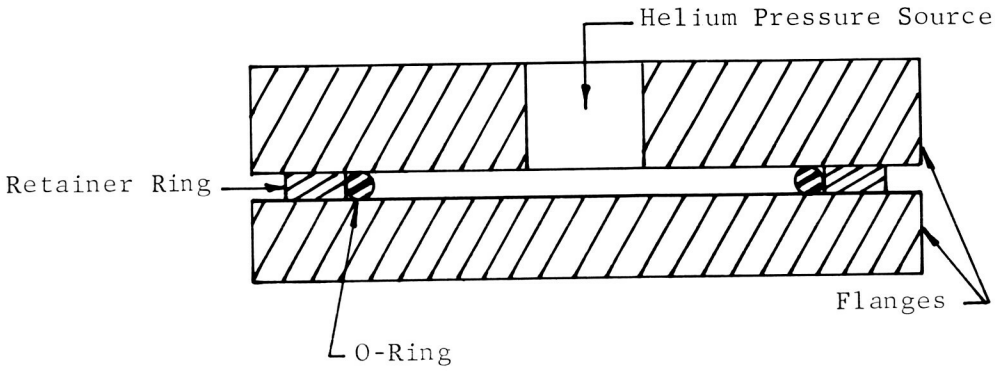

Figure 106. Cross Section of O-Ring Leak Test Setup

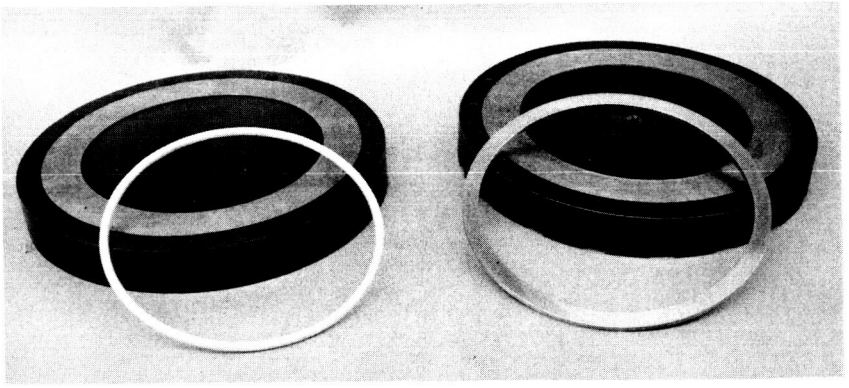

Figure 107. O-Ring Leak Test Flanges, Backing Ring, and Test Specimens

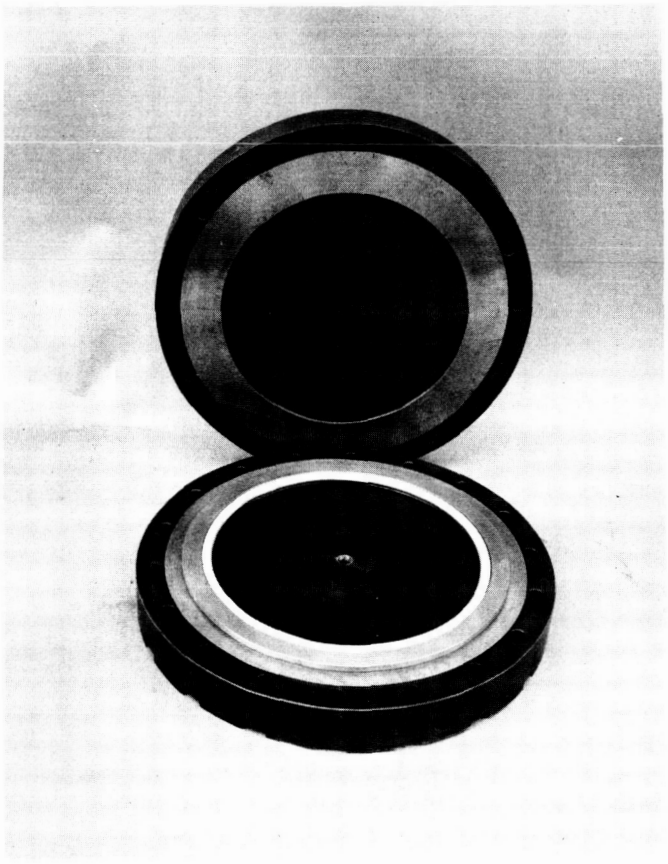

Figure 108. O-Ring Leak Test Fixture Partially Assembled

Test results. — The 4-in. and the 1-1/2 in. diameter O-ring compression versus deflection data are presented in Tables 57 and 58 respectively. Preliminary data and the appearance of the test specimens indicated that Method D does not provide an O-ring with compressibility and the ability to return to its original dimensions.

The 4-in. and 8-in. O-ring leak test data are presented in Table 59. The 8-in. diameter O-rings were fabricated utilizing Method A, the formed laminate method, because the capabilities of the toroidal winder did not permit winding of the 8-in. diameter O-rings.

The leak test data in Table 59 indicated that Method C, toroidal winding on a laminate core, had the best leak-sealing performance of all the investigated fabrication methods. This fabrication method is most practical, considering processing and fabrication criteria such as simplicity of processing, reproducibility, guaranteed quality, and man-hours expended.

TABLE 57

4-IN. DIAMETER O-RING COMPRESSION VERSUS DEFLECTION DATA

Specimen No.	Temp, °F	Cycle	Area, in.	Energy, in.-lb	Energy Per Unit Vol, in.-lb/in.^{3}
A-1	RT	1	26.80	18.51*	48.1
		2	8.13	5.61	14.5
		10	5.79	4.00	10.4
A-4		1	8.50	5.87	17.55
		2	6.04	4.17	12.50
		10	5.17	3.57	10.70
A-7		1	12.40	8.56	25.30
		2	7.61	5.25	15.50
		10	6.30	4.36	12.50
A-2	-320	1	2.13	1.47	4.22
		2	2.30	1.59	4.45
		10	2.41	1.66	4.76
A-5		1	3.00	2.19	6.10
		2	2.93	2.14	5.95
		10	2.81	2.05	5.70
A-8		1	1.68	1.23	3.42
		2	1.54	1.13	3.14
		10	1.49	1.09	3.03
B-1	RT	1	7.70	5.31	14.92
		2	5.21	3.60	10.12
		10	4.85	3.35	9.52
B-4		1	8.91	6.15	17.30
		2	6.80	4.70	13.21
		10	5.57	3.85	10.73
B-7		1	9.10	6.28	17.86
		2	6.31	4.36	12.40
		10	5.40	3.73	10.60
C-1		1	10.70	7.39	21.7
		2	5.96	4.12	12.1
		10	4.83	3.33	9.8
C-2		1	10.07	6.95	20.60
		2	5.62	3.88	11.50
		10	4.46	3.08	9.10
C-3		1	9.00	6.21	18.4
		2	5.76	3.98	11.8
		10	4.50	3.11	9.2

* 1540-lb load rather than 1000 lb.

TABLE 58

1-1/2 IN. DIAMETER O-RING COMPRESSION VERSUS DEFLECTION DATA

Specimen No.	Temp, °F	Cycle	Area, $in.^2$	Energy, in.-lb	Energy Per Unit Vol, $in.-lb/in.^3$
D-1	RT	1	6.19*	0.46	8.96
		2	4.65	0.34	6.63
		10	3.59	0.27	5.26
D-4		1	0.80	0.059	1.11
		2	0.78	0.058	1.09
		10	0.60	0.045	0.85
D-7		1	1.40	0.104	2.06
		2	0.02	0.068	1.35
		10	0.69	0.051	1.01
D-2	-320	1	0.16	0.013	0.254
		2	0.13	0.010	0.195
		10	0.10	0.008	0.156
D-5		1	0.13	0.010	0.198
		2	0.12	0.009	0.179
		10	0.10	0.008	0.159
D-8		1	0.16	0.013	0.261
		2	0.11	0.009	0.181
		10	0.09	0.007	0.141
D-3	-423	1	1.13	0.0902	1.44
		2	0.97	0.774	1.24
		10	0.70	0.0558	0.89
D-6		1	0.40	0.0319	0.510
		2	0.38	0.0303	0.475
		10	0.36	0.0287	0.460
D-9		1	0.23	0.0184	0.295
		2	0.19	0.0152	0.244
		10	0.15	0.0119	0.191

* Loaded to 148 lb rather than 100 lb.

TABLE 59

4- AND 8-IN. DIAMETER O-RING LEAK TEST DATA

Specimen No.	Temp, °F	Initial Pressure, psi	Pressure after 10 min, psi	Backing Ring Dia, in.	Pressure under 550-lb Load, psi
4-in. Dia Ring					
A-1	RT	500	140	0.150	--
-4	↓	↓	210	↓	--
-7	↓	↓	285	↓	--
A-2	-320	↓	18	0.175	--
-5	↓	↓	20	↓	--
-8	↓	↓	30	↓	--
B-2	RT	↓	90	0.150	--
-5	↓	↓	140	↓	--
-8	↓	↓	110	↓	--
C-4	↓	↓	410	↓	--
-5	↓	↓	500	↓	--
-6	↓	↓	115	↓	--
D-1	↓	200	62	--	950
-4	↓	↓	125	--	934
-7	↓	↓	94	--	958
D-2	-320	↓	48	--	950
-5	↓	↓	35	--	958
-8	↓	↓	15	--	977
D-2	-423	↓	0 (3 min)	--	950
-6	↓	↓	0 (2 min)	--	↓
-9	↓	50 max	0 (10 sec)	--	↓
8-in. Dia Rings					
1	RT	500	270	0.200	--
2	↓	↓	265	↓	--
3	↓	↓	320	↓	--
4	-320	↓	85	↓	--
5	↓	↓	110	↓	--
6	↓	↓	470	↓	--

Lip Seals

The concept of encapsulating a glass-TFE composite with FEP was utilized for the fabrication of lip seals. The lamination was formed on a truncated cone and cut to the desired size with a trimming tool. The trimmed laminate was then encapsulated with FEP. Two methods of fabrication are described in the following paragraphs.

Method 1:

1. A cutting template was utilized to cut six pieces of 0.005-in. thick TFE and seven pieces of style 401 glass cloth. The materials were in accordance with the specification presented in Appendix F.

2. The material (glass and TFE) was laid so that the glass cloth was oriented 45° to the prior layer of glass cloth. The TFE was placed between the glass layers.

3. The TFE-glass layup was assembled in the lamination mold (Figure 109) and cured at 720°F and 500 psi for 5 minutes.

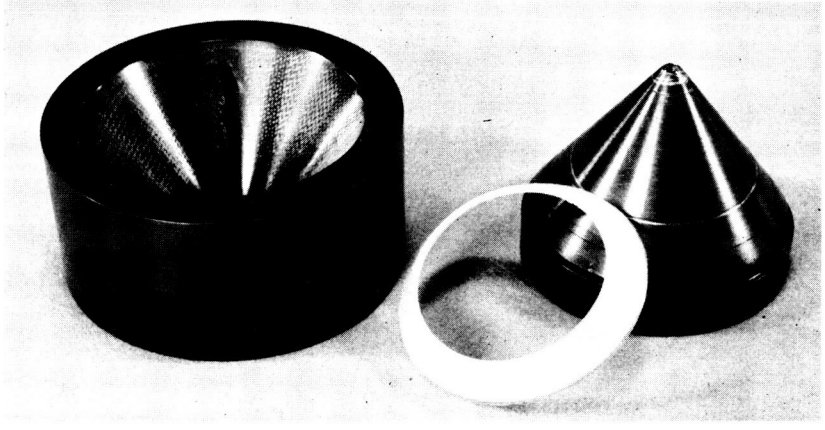

Figure 109. Lip Seal Laminating Tool Shown with Finished Lip Seal

4. The laminate was cooled to room temperature and the thickness recorded.

5. The laminate was trimmed to the desired size, utilizing the trim tool (shown in Figure 110).

6. The trimmed laminate, with 0.010-in. thick FEP on each side, was assembled in the encapsulation fixture (Figure 111).

7. Encapsulation was accomplished at 550°F at 500 psi for 3 minutes and cooled to room temperature.

Figure 110. Lip Seal Trim Tool Shown with Finished Lip Seal

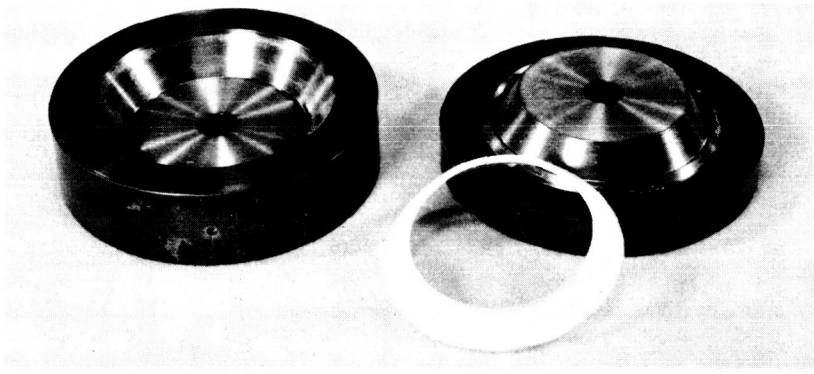

Figure 111. Lip Seal Encapsulation Tool Shown with Finished Lip Seal

8. The finished part was removed, trimmed of excess flash, and delivered to Quality Control for inspection.

Method 2:

1. A cutting template was utilized to cut six pieces of 0.005-in. thick TFE and seven pieces of style 401 glass cloth in accordance with the specification presented in Appendix F.

2. The glass and TFE was laid up so that the glass cloth was oriented 45° to the prior layer of glass cloth. The TFE was placed between the glass layers.

3. The TFE-glass layup was assembled in the lamination mold (Figure 109), cured at 760°F and 500 psi for 5 minutes, and cooled under pressure to 400°F or lower.

4. The formed lip seal laminate was placed between the two layers of 0.010-in. FEP and assembled in the lamination tool.

5. The laminate was then encapsulated at 550°F for 3 minutes with the male tool closed to the stops required for the desired thickness.

6. The encapsulated laminate was cooled under pressure to below 450°F and removed when the temperature was ambient (room temperature).

7. The encapsulated laminate was placed in the encapsulation tool (Figure 111) with strips of 0.010-in. thick × 0.060-in. wide FEP placed at the bottom and top edges.

8. Encapsulation was accomplished at 550°F and 100 psi for 3 minutes, and the part was then cooled under pressure to 450°±15°F and removed at ambient temperature (room temperature).

9. The encapsulated lip seal was removed of flash, leak-checked, and submitted to Quality Control for inspection.

Test method. — The most important parameter to be considered for the lip seal is its leak-sealing ability. To test this capability, a standard fitting was adapted to perform leak tests on the developed lip seals.

To check for the leak-sealing ability of a lip seal, the seal was assembled into the fitting shown in Figure 112 and attached to the helium pressure source (regulated standard K bottle). Figure 113 shows the leak test setup. The fitting-seal assembly was pressurized to 200 psi and the pressure was recorded 10 minutes after the initial pressurization.

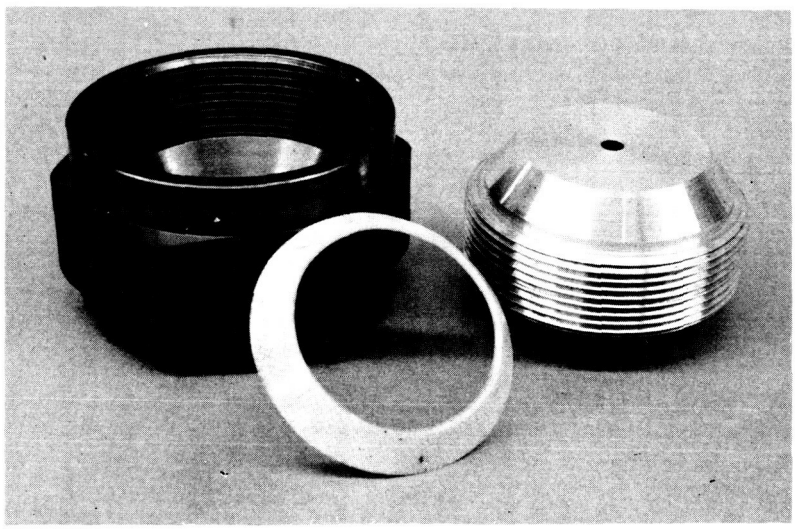

Figure 112. Lip Seal Leak Test Fixture and Sample Lip Seal

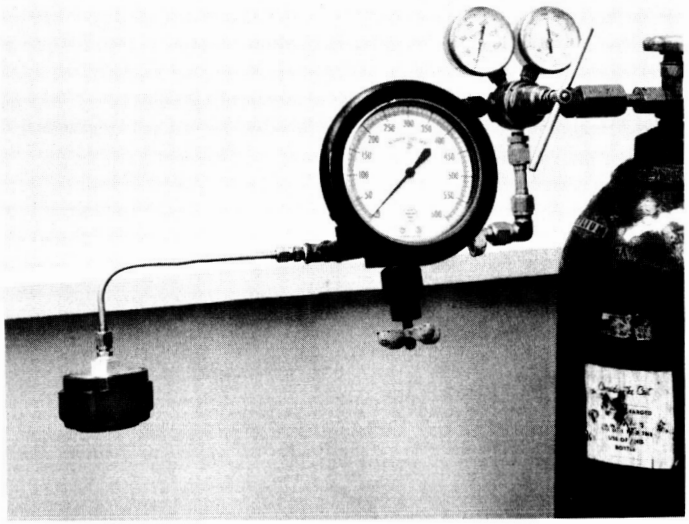

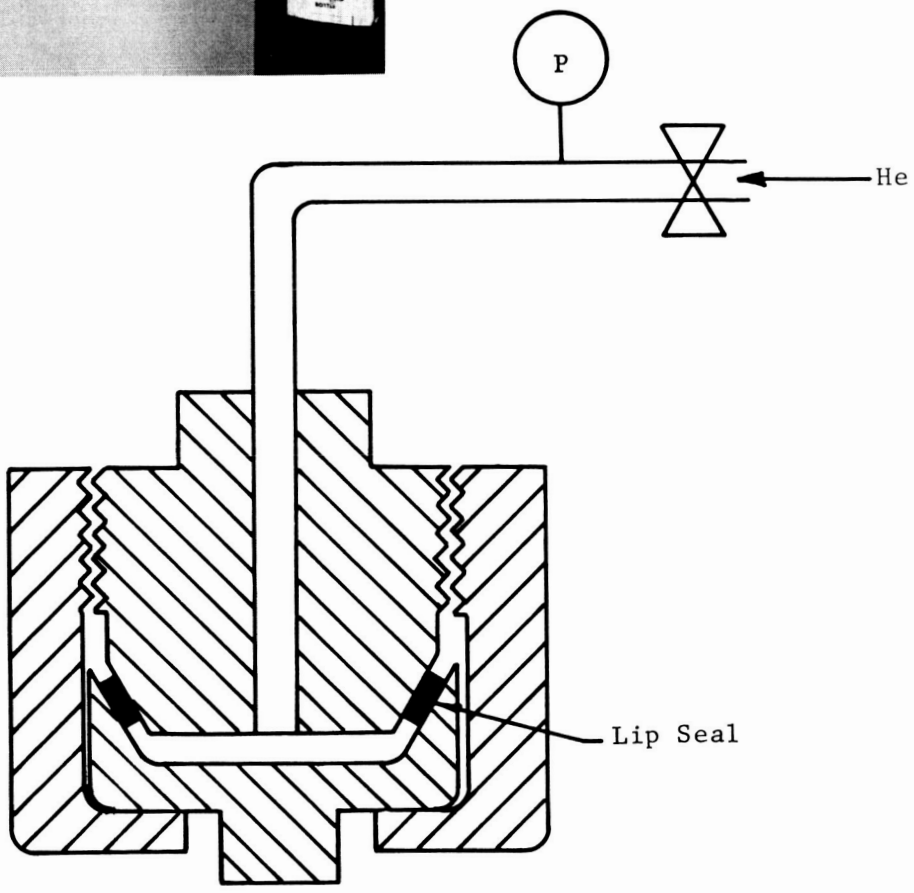

Figure 113. Lip Seal Test Fixture

Test results. — The leak test data for the 1/2-, 1-, and 2-in. diameter lip seals are shown in Table 60. The data are presented for Method 2 only.

Lip seals fabricated by Method 1 could not pass the dye penetrant test. This leak test was a check to ensure encapsulation. Also, the lip seal fabricated with Method I appeared to be less compressible and had considerably more flash than the seals fabricated with Method 2.

Fabrication Method II was found to be reproducible, low in cost, and the seals developed had adequate sealing capabilities. Future optimization studies would improve the sealing capability of the seal and possibly reduce the cost per item even further.

TABLE 60

LIP SEAL LEAK TEST RESULTS

Lip Seal Size, in.	Test Temp					
	RT		-320°F		-423°F	
	Initial He Pressure psi	Pressure after 10 min, psi	Initial He Pressure psi	Pressure after 10 min, psi	Initial He Pressure psi	Pressure after 10 min, psi
1/2	200	200	200	0**	200	0†
↓	200	0*	200	45	200	0††
	200	70	200	0***	200	0***
1	600	600	200	188	--	--
↓	600	600	200	176	600	600
	600	600	200	184	600	315
2	200	45	200	0	200	0†
↓	200	70	200	0	200	50
	200	195	200	55	200	40

Time to final pressure reading:
* 2-1/2 minutes
** 3 minutes
*** 1-1/2 minutes
† 2 minutes
†† 1 minute

Chevron Seals

The concept of encapsulating a glass — TFE composite with FEP was also utilized in the fabrication of chevron seals. Fabrication processes investigated included such methods as postforming a laminate to the required chevron shape or laminating the required part in a formed lamination tool. The encapsulation in FEP was performed in a standard encapsulation tool which was constructed to the required chevron shape. The methods of fabrication are described below.

Type A:

1. A flat laminate was laid up, per the process specification presented in Appendix F, utilizing 5 plies of style 401 glass and 4 plies of 0.005-in. thick TFE. A washer-shaped piece was cut from the uncured laminate and placed in the forming tool shown in Figure 114.

2. The laminate was then press-cured in the forming tool at 760°F for 5 minutes.

3. The cured laminate was placed in the trimming tool and cut to the required size for encapsulation (see Figure 115).

4. Two layers of 0.010-in. thick FEP were preformed in the forming tool by being heated to 350°F for 5 minutes.

5. A layup was made by placing one layer of preformed FEP on each side of the cured laminate in the encapsulation tool.

6. The part was then cured for 3 minutes at 540°F under 100-psi pressure.

7. After cooling to room temperature, the part was cleaned, trimmed, and submitted to Quality Control for inspection.

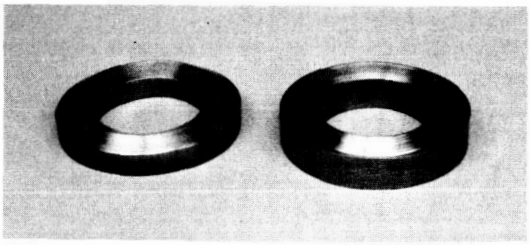

Figure 114. Chevron Seal Forming and Encapsulation Tool

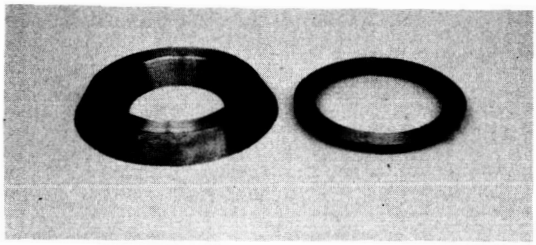

Figure 115. Chevron Seal Trimming Tool

Type B:

1. A flat laminate was laid-up per the process specification presented in Appendix F, utilizing 4 plies of style 401 glass and 3 plies of 0.005-in. thick TFE. A washer-shaped piece was cut from the uncured laminate and placed in the forming tool.

2. The laminate was then cured in the forming tool to the required shape in a press at 760°F for 5 minutes.

3. A pre-encapsulated laminate was made by placing one layer of 0.005-in. thick FEP and one layer of 0.010-in. thick FEP in the female half of the forming tool, followed by the preformed laminate, and then two layers of 0.010-in. thick FEP.

4. This new layup was cured in the forming tool at 550°F for 3 minutes.

5. This laminate, after cooling, was trimmed with the trimming tool.

6. The final encapsulation was made by placing the trimmed pre-encapsulated laminate in the encapsulation tool with two layers of 0.010-in. thick FEP on each face, and curing at 550°F for 3 minutes.

7. After cooling to room temperature, the part was cleaned, trimmed, and submitted to Quality Control for inspection.

Type C:

1. A flat laminate was laid up in accordance with the process specification presented in Appendix F, utilizing 4 plies of style 401 glass and 3 plies of 0.005-in. thick TFE. A washer-shaped piece was cut from the uncured laminate and placed in the forming tool.

2. The laminate was then cured in the forming tool to the required shape in a press at 760°F for 5 minutes.

3. Three layers of 0.010-in. thick FEP and one layer of 0.005-in. thick FEP were preformed in the forming tool by being heated to 350°F for 5 minutes.

4. A pre-encapsulated laminate was made by placing one layer of preformed 0.005-in. thick FEP and one layer of preformed 0.010-in. thick FEP in the female half of the forming tool, followed by the preformed laminate, and then two layers of preformed 0.010-in. thick FEP.

5. This new layup was cured in the forming tool at 550°F for 3 minutes.

6. This laminate, after cooling, was trimmed with the trimming tool.

7. The final encapsulation layup was made by placing the trimmed pre-encapsulated laminate in the encapsulation tool with two layers of 0.010-in. thick FEP on each face, and curing at 550°F for 3 minutes.

8. After cooling to room temperature, the part was cleaned, trimmed, and submitted to Quality Control for inspection.

Test methods. — To evaluate the performance of the particular methods of construction for the chevon seals, leak tests and the compression versus deflection tests were conducted at room temperature, -320°F, and -423°F. These tests were conducted in a manner similar to that for O-rings.

The compression versus deflection test fixture is shown in Figure 116. The flanges match the shape of the chevron seal. The configuration of the compression versus deflection flange and the leak test flanges are shown in Figure 117.

The compression versus deflection data were obtained by measuring the area under the compression-deflection curves (see Figure 18 for a typical set of curves). The areas under the first, second, and tenth cycles were measured and considered sufficient indication of the test results for the set of 10 cycles.

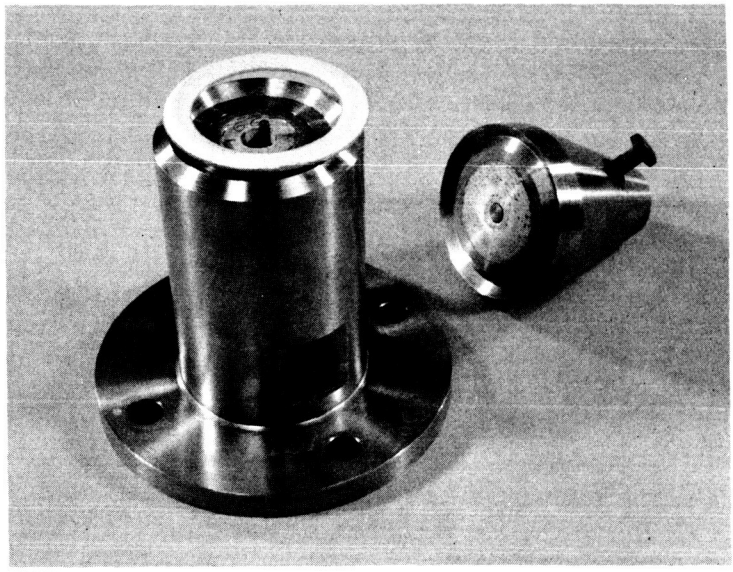

Figure 116. Chevron Seal Compression versus Deflection Test Fixture

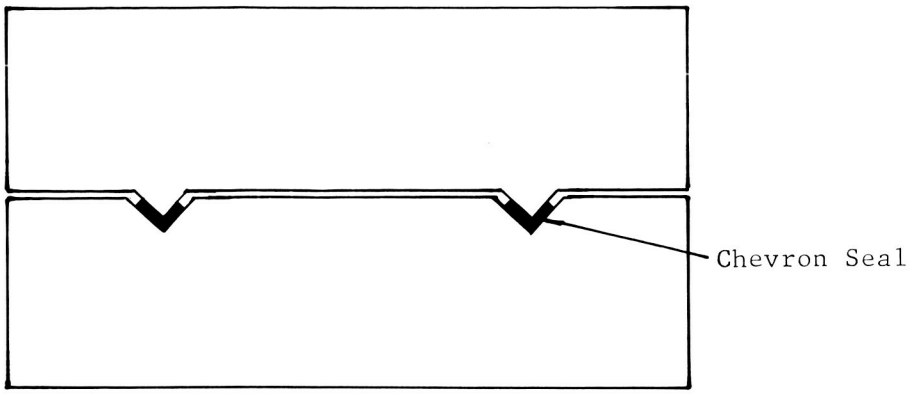

Figure 117. Configuration of the Compression versus Deflection and Leak Test Flange Setup

The leak test was conducted by loading a chevron seal between two flanges as shown in Figure 117 and Figure 118. The 2-in. chevron seal test fixture utilized a test machine for the load application. The 4-in. chevron seal test fixture utilized bolted mating flanges for the load application. The annular space captivated by the chevron seal and the flanges was pressurized with helium to 600 psi. The pressure was recorded 10 minutes after the initial pressurization.

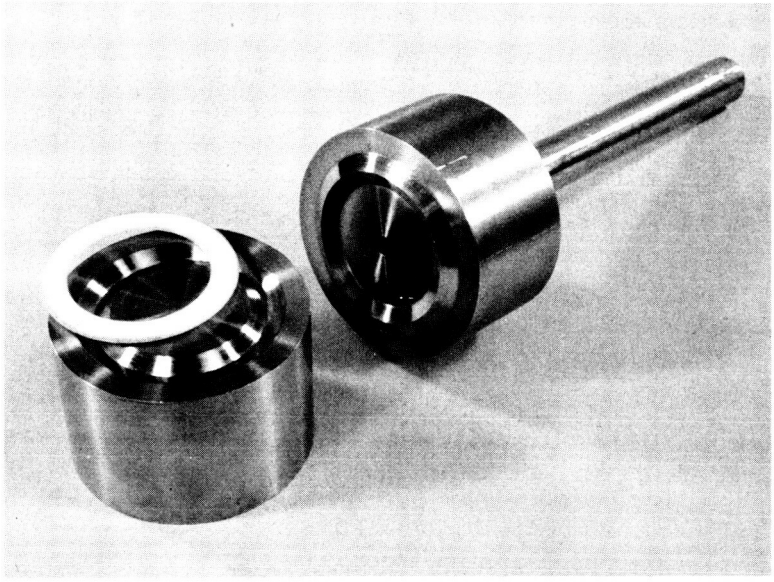

Figure 118. Chevron Seal Leak Test Fixture

Test results. — The compression versus deflection tests and the leak tests were conducted on chevron seals fabricated by the Type B method. The other fabrication methods resulted in chevron seals with wrinkles in the encapsulation, incomplete encapsulation, and improper formation of the V-shape.

Table 61 presents compression versus deflection test data for the 2-in. diameter chevron seals, and indicates that the developed seal had good compressibility.

TABLE 61

COMPRESSION VERSUS DEFLECTION DATA FOR 2-IN. CHEVRON SEALS

Specimen No.	Temp, °F	Cycle	Area, $in.^2$	Energy, in.-lb (Area × K)*	Energy per Unit Vol, $in.-lb/in.^3$
NR-277-1	RT	1	5.53	21.12	165.5
		2	3.50	13.41	105.0
		10	2.78	10.65	83.3
-2		1	3.31	12.68	99.0
		2	2.42	9.27	72.5
		10	1.99	7.63	59.8
-3		1	3.04	11.65	91.0
		2	2.07	7.93	61.9
		10	1.27	4.87	38.0
-4	-320	1	1.20	5.02	39.2
		2	1.18	4.93	38.5
		10	1.03	4.30	33.6
-5		1	1.14	4.76	37.2
		2	1.13	4.72	36.8
		10	1.00	4.18	32.6
-6		1	1.61	6.73	52.5
		2	1.35	5.64	44.0
		10	1.18	4.93	38.5
-7	-423	1	1.38	5.46	42.7
		2	1.36	5.38	42.0
		10	1.01	5.99	31.2
-8		1	1.09	4.31	33.7
		2	1.05	4.15	32.4
		10	0.99	3.91	30.6
-9		1	1.64	6.49	50.6
		2	1.42	5.62	43.9
		10	1.39	5.50	43.3

Table 62 presents preliminary leak test data for the 2- and the 4-in. diameter chevron seals. The data indicate good leak-sealing capabilities for chevron seals in a matched flange.

The performance in cryogenic environments indicates further tests are necessary to determine the maximum internal pressure that the chevron seal is capable of containing.

It is apparent from the test results and an examination of the fabrication criteria that the lamination of plies in the forming tool (Type B) shows great promise for a solution to the serious current sealing problems and those which may be encountered in future designs.

TABLE 62

CHEVRON SEAL LEAK TEST DATA

Specimen No.	Temp, °F	Initial Pressure, psi	Pressure after 10 min	Remarks
2-in. Seals				
NR-277-1	RT	600	600	6000-lb load
-2	↓	↓	↓	↓
-3	↓	↓	↓	↓
-4	-320	↓	↓	↓
-5	↓	↓	95	↓
-6	↓	↓	575	↓
-7	-423	↓	175	3000-lb load
-8	↓	↓	535	↓
-9	↓	↓	350	↓
4-in. Seals				
4	RT	600	600*	270 in./lb
5	↓	↓	↓	240 in./lb
6	↓	↓	↓	240 in./lb
8	-320	↓	↓	270 in./lb
9	↓	↓	↓	↓
11	↓	↓	↓	↓

* After 5 minutes.

REPRODUCIBILITY OF GASKETS

A study was conducted to determine the adequacy of the process specification presented in Appendix F in satisfactorily defining the techniques required to manufacture flat cryogenic gaskets for LOX service. Two fabrication technicians were selected; one who had prior gasket experience and a recently hired technician who had never before worked on gaskets. Both were given the assignment of making three each of four flat gaskets covering an outside diameter range from 2.06 in. to 9.5 in.

Each gasket was inspected by fluorescent penetrant and by a leak test to determine its ability to retain 500 psi of helium at room temperature. The test results are summarized in Table 63.

TABLE 63

TECHNIQUE FOR TEST RESULTS OF GASKET REPRODUCIBILITY

Gasket Description			Penetrant Leak Test		RT, 500 psi Pressure Test*	
Narmco Part No.	OD, in.	ID, in.	Inexperienced Technician	Experienced Technician	Inexperienced Technician	Experienced Technician
228-27	2.06	1.375	All satisfactory	All satisfactory	No leaks	No leaks
228-11	3.95	2.62	All failed	All satisfactory	1 failed 2 no leaks	No leaks
228-15	5.5	4.0	All failed	All satisfactory	All failed	No leaks
228-17	9.5	8.0	1 failed** 2 satisfactory	All satisfactory	1 failed 2 no leaks	No leaks

* Test requirement is to hold pressure 10 minutes without a pressure drop.

** Visual delamination observed.

From the test data in Table 63, the following conclusions can be made:

1. Gaskets that fail the penetrant test will probably fail in a leakage test.

2. An experienced technician following the process specification can make satisfactory flat gaskets at a low rejection rate.

3. An inexperienced technician following the process specification can make gaskets that are satisfactory but at a high rejection rate.

It is therefore believed that the process specification sufficiently defines production techniques and is satisfactory for use without further modification. Fabrication experience is necessary, however, if a low rejection rate is to be maintained.

PRODUCTION GASKETS AND GASKET APPLICATIONS

While the work performed under this contract was directed toward the development of a LOX gasket, the newly developed laminated gasket material has already found applications outside of this program.

Whittaker Controls and Guidance, a sister division of Narmco Research & Development in Whittaker Corporation, is currently developing a series of controls valves for the Saturn V launch vehicle. Some of these valves are for LOX service. Difficulties have been encountered in minimizing the leakage through the valve.

Because of the experience gained from this program, Narmco was asked to help reduce the leakage. Although the application is quite different from that for the flat gasket, it appears that the Teflon-glass laminate can provide an effective seal. Narmco has designed a seal for the 17-in. valve (see Figures 119 and 120) and has fabricated seals for 4- and 10-in. valves (see Figures 121 through 126).

The compressibility of the Teflon-glass laminate at the cryogenic condition should improve the seal because it allows more deflection of critical parts, such as the visor, while still maintaining a seal.

Preliminary testing has been very encouraging, and leakage rates approaching zero now appear within reach.

Another application already found for the Teflon-glass laminate is the valve seal of a liquid hydrogen dewar (see Figure 127). This seal previously was solid Teflon which, after short service, fractured. The new seal, with its superior strength, has not yet failed.

The newly developed gasket was used to seal several camera windows in the liquid hydrogen tank of a Saturn S-IV vehicle. Motion pictures were taken in space of the liquid hydrogen under a condition of weightlessness.

An application which was evaluated by the Chrysler Corporation Space Division on the Saturn S-IB launch vehicle is the sealing of the LOX sump tank with the newly developed gasket material. The gasket evaluated is of approximately 28-in. diameter, 0.125-in. thickness, and 0.500-in. width, as shown in Figure 128.

The fabrication processes, as developed during the subject program, were modified slightly for the larger gasket. After the first few attempts to fabricate the large diameter gaskets, it became apparent that either further modification of the existing process specification must be made or a brand new process specification would have to be developed. Further process development improved the gaskets to the point that the laminate would hold together through the encapsulation phase of the fabrication process, which had not been possible before; however, the gaskets still were not fully encapsulated. During further process development, it was determined that the entire gasket could be

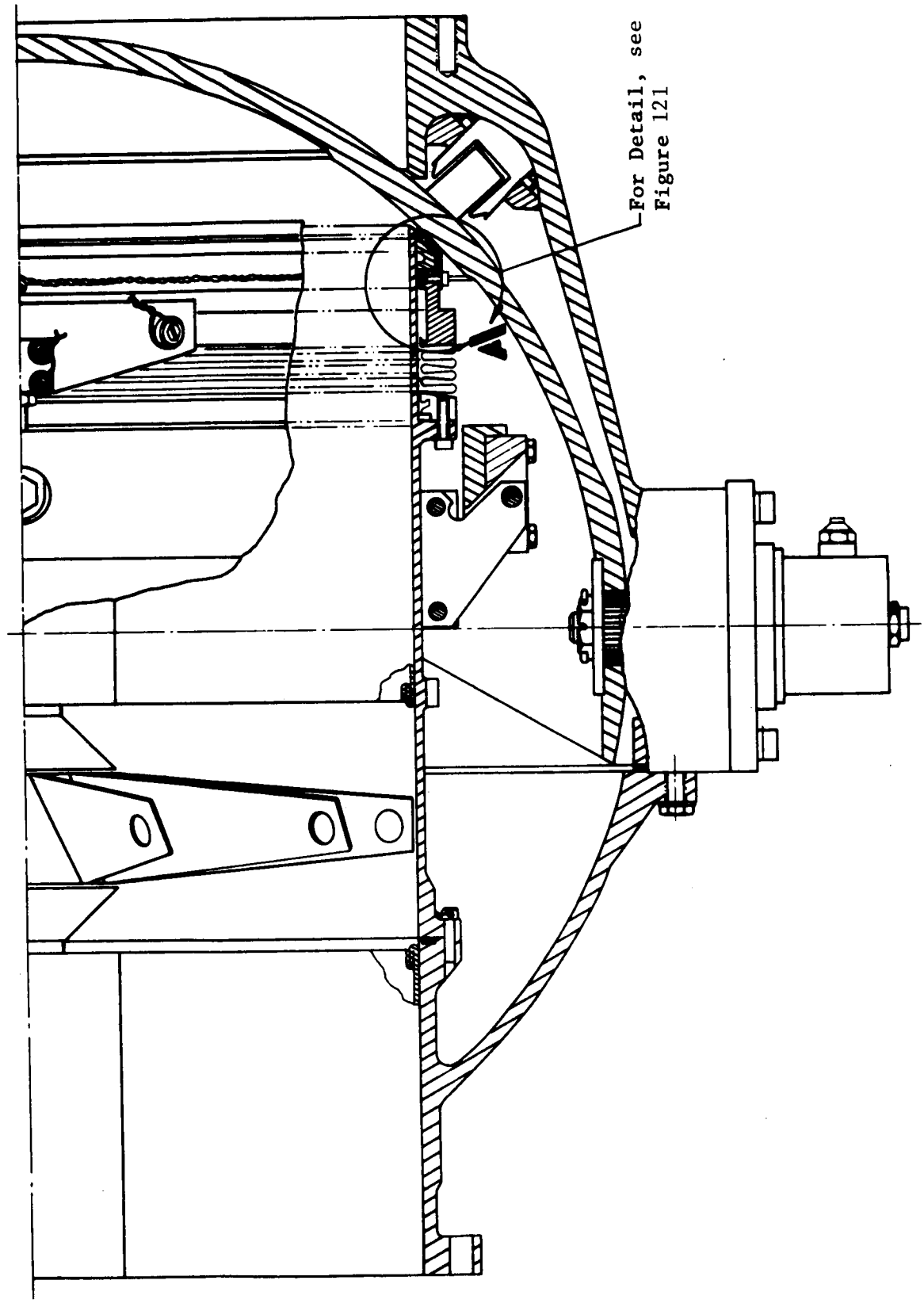

Figure 119. 17-in. LOX Valve

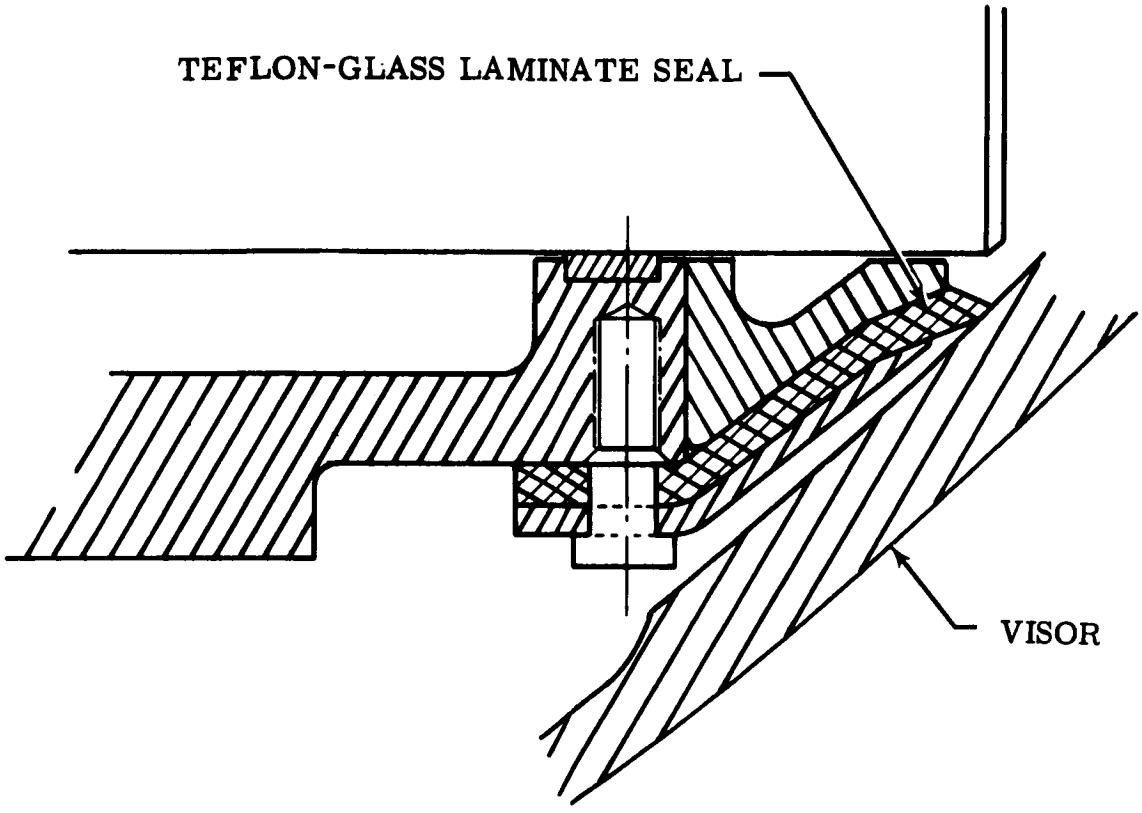

Figure 120. Section "A" Wiper Seal Detal

Figure 121. 4-in. Valve Visor with Groove

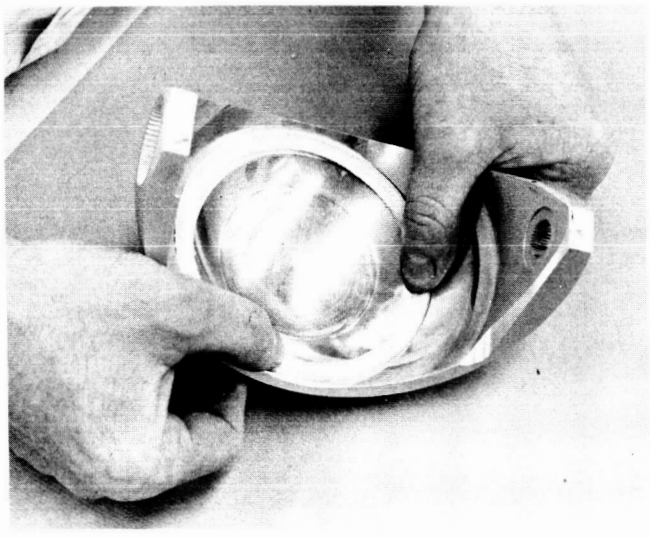

Figure 122. Installation of Laminated Seal

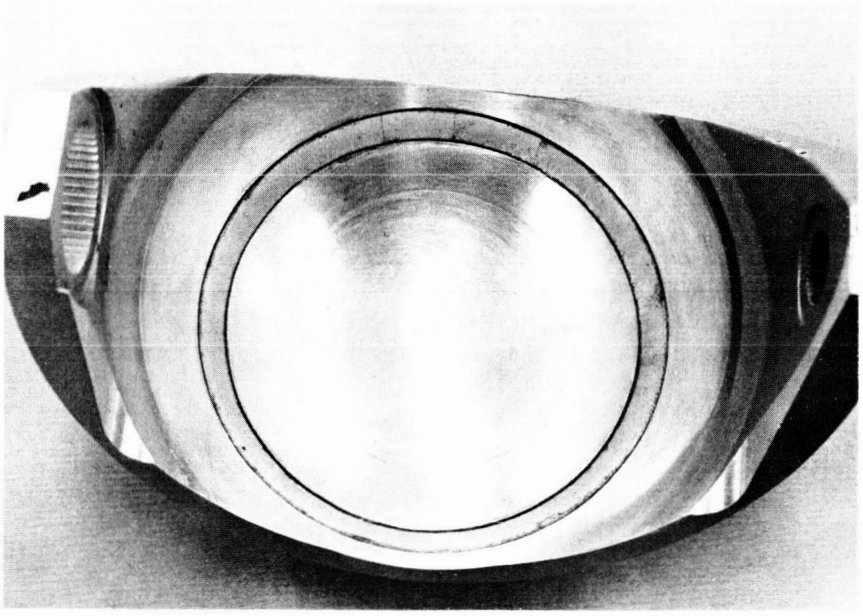

Figure 123. Seal Encapsulated in Visor

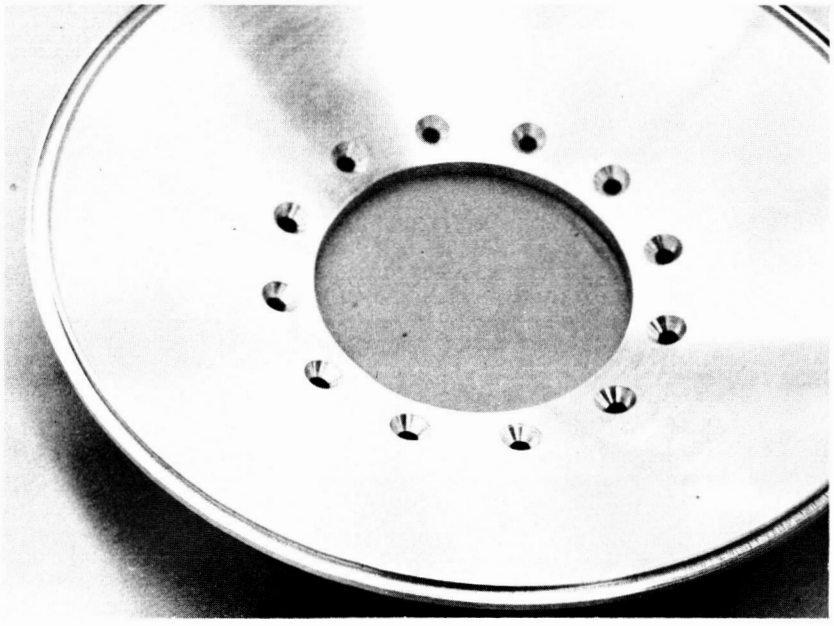

Figure 124. 10-in. Valve Visor Bowl with Groove

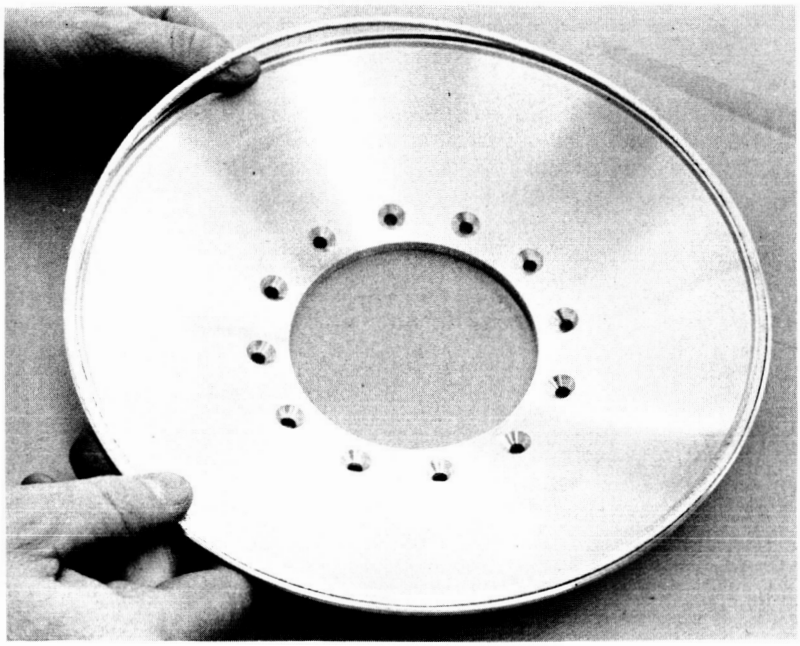

Figure 125. Installation of Laminated Seal

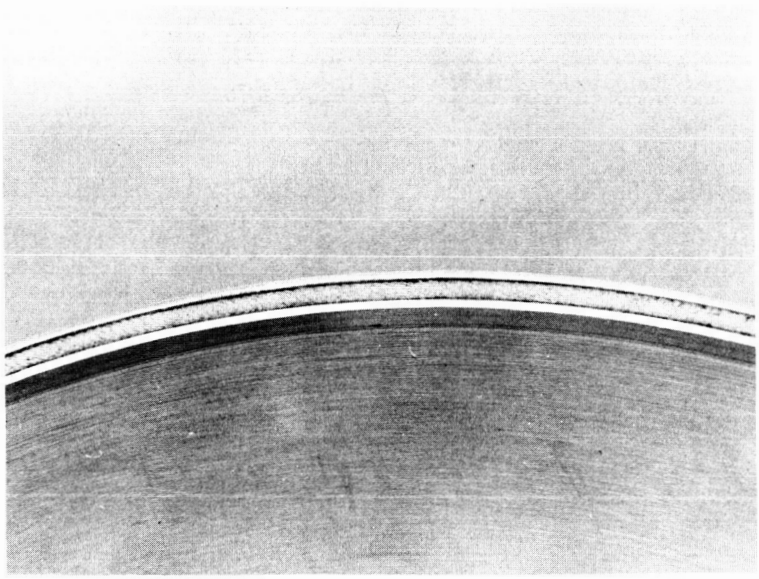

Figure 126. Seal Encapsulated in Visor Bowl

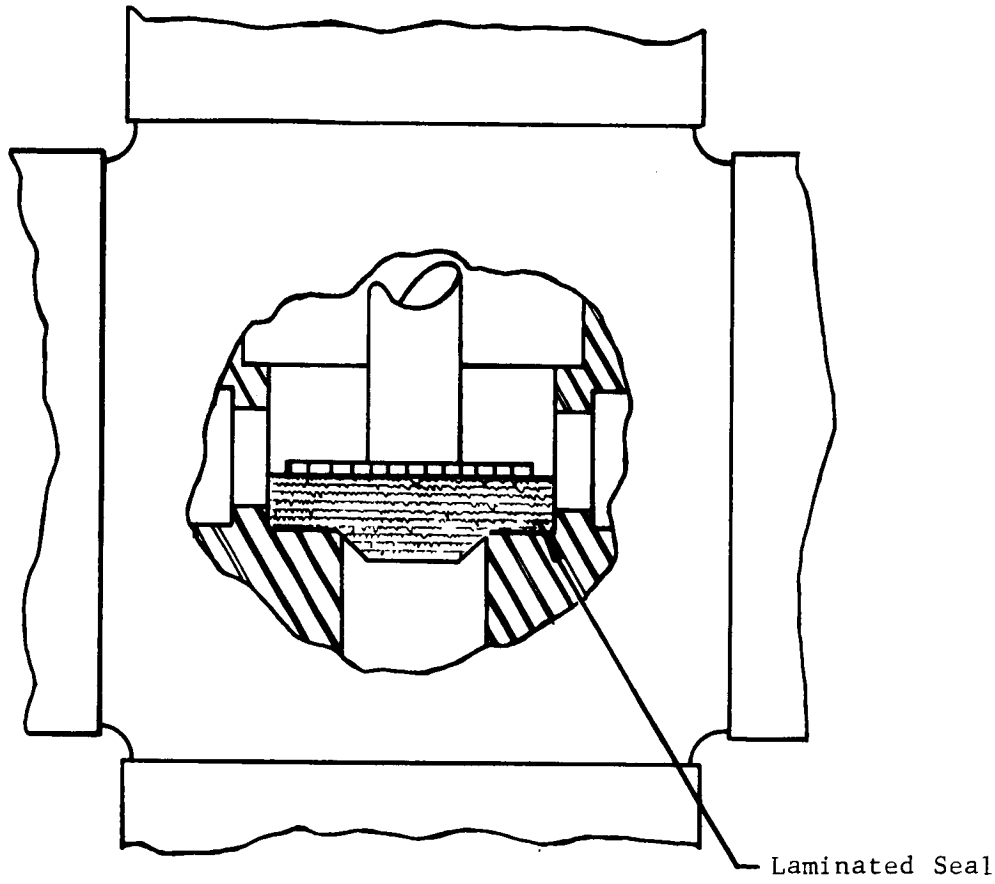

Figure 127. Liquid Hydrogen Dewar Valve Seal

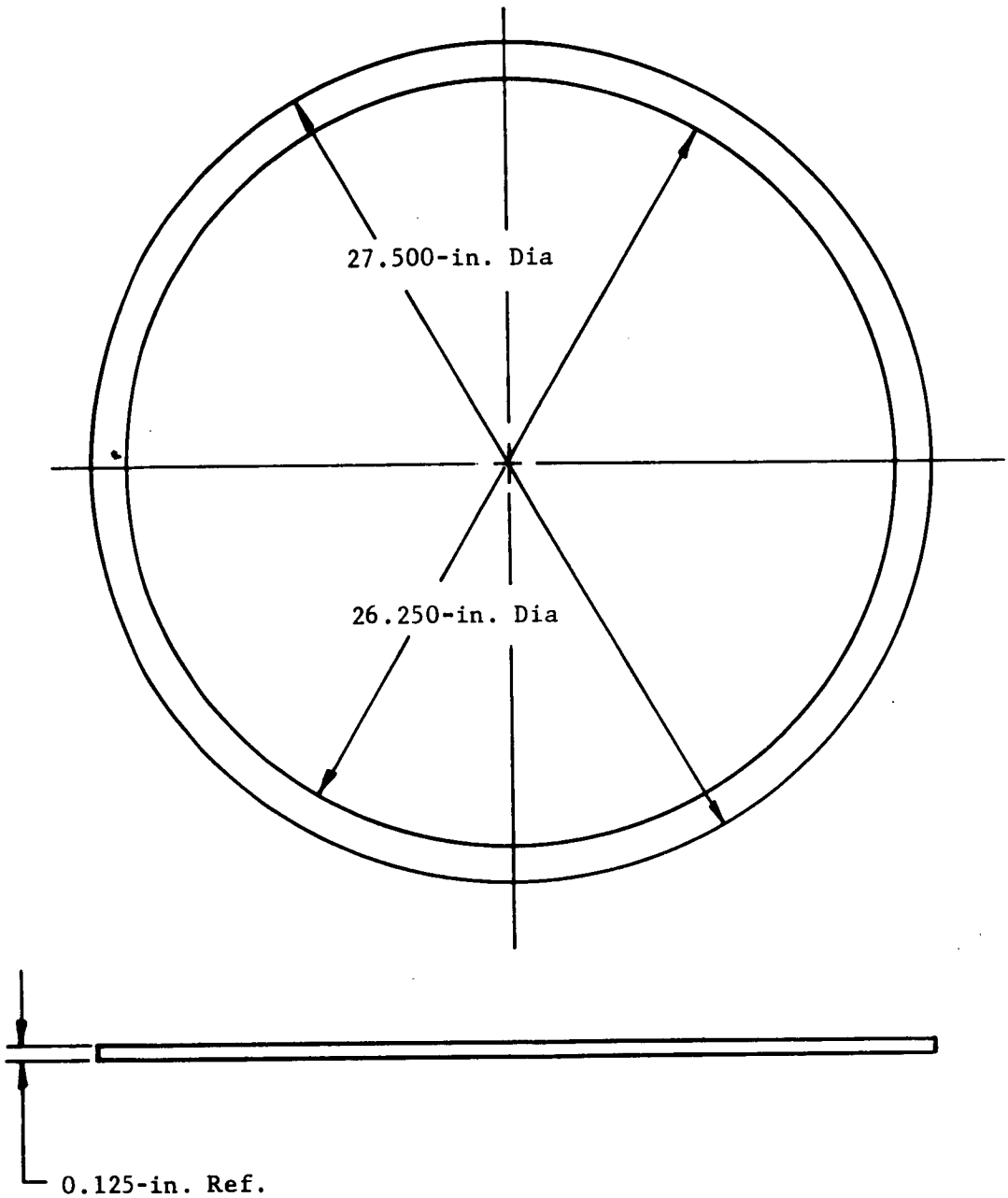

Figure 128. Chrysler Saturn S-IB Gasket

encapsulated by placing the partially encapsulated gasket in a press at 550°F with two pieces of FEP on each side of the gasket. At this temperature, the FEP melts and flows over the unrestrained gasket.

On 17 May 1965, the following test program started at Chrysler, Michoud:

1. 1 hour at -320°F at an internal pressure of 40 psi
2. 1 hour at -320°F at an internal pressure of 60 psi
3. 1 hour at -320°F at an internal pressure of 80 psi
4. Steps 1 and 2 were repeated.
5. The full-size test fixture was then warmed to room temperature and the above test program repeated 10 times.
6. After completion of the full 10 cycles, the gasket was then tested with water at 115 psi at room temperature.

The first gasket tested did not complete this six-step test program. A leak occurred during the first cycle after 30 minutes at 60 psi. The pressure was increased to 85 psi in an attempt to force liquid through the sealed joint. The seal prevented leakage of liquid nitrogen from the test fixture, and the remaining portion of the test cycle was completed.

While the test was being conducted at Chrysler, further process development was being conducted. A gasket was fabricated which closely resembled the previously fabricated small gaskets in both appearance and structure. This gasket was air-freighted to Michoud for Chrysler personnel.

The second test gasket closely resembled previously fabricated gaskets of smaller diameter in both appearance and physical properties. It was placed in the same stand, and the same test procedure as stated before was followed. The gasket completed 20 cycles with no gas or liquid leaks and no bolt retorquing.

A fourth application presently being evaluated by the Chrysler Space Division on the Saturn S-IB space booster is the sealing of a 4-in. LOX valve. In this particular application, the newly developed gasket material is being used as a dynamic seal which has point-contact loading. Test results obtained to date indicate that the seal, in this particular application, is far superior to any other type evaluated. A reliability endurance test which the dynamic seal was subjected to included 500 cycles at room temperature, 500 cycles at 260°F, and 1000 cycles at -375°F. The pressure containment requirement is 45 psig.

CONCLUSIONS AND RECOMMENDATIONS

Effective reinforcement and restriction to cold flow have been achieved in a laminated structure which utilizes a LOX-compatible fabric, such as glass, and a fluorocarbon resin binder. The materials have been laminated into a unique system which does not involve complete impregnation of the fiber bundle. This feature provides a springlike compressibility which is not subject to drastic changes in flexibility when the temperature is decreased, as is a resin binder. The laminates can be prepared with LOX compatability. Other desirable features include good tensile strength and low compression set.

Shortcomings of several other gasketing materials have been demonstrated in the areas of cryogenic compressibility, ambient cold flow, and compression set.

Optimization of the laminate approaches to cryogenic gasket materials has been accomplished in the following areas:

1. Resin selection
2. Pressing time and temperature
3. Laminating pressure
4. Interlaminar separation and resin content
5. Fabric composition and style
6. Encapsulation of laminates

The developed laminate gasket material has demonstrated its superiority over the currently available gasket material, Allpax 500, and other commercially available flat LOX gasket materials.

The specimen-to-specimen variations indicated by the preliminary test data are inevitable in a relatively new concept and are present even in the Allpax 500 gasket, which is a production material.

The typical laminated gasket exhibited sealing properties superior to the Allpax 500 material at room temperature and noticeably better liquid hydrogen sealing performance. The laminate gasket composite performance indicates great promise for this severe application.

The optimized Narmco-developed laminate gasket composite exhibited properties which surpassed all other currently available nonmetallic cryogenic gaskets. The optimization studies and the corresponding test data and engineering studies provided the following information:

1. A time-consuming torque sequence is not required for the laminate gasket composite.

2. The developed gasket composite has less variation in compression versus deflection properties than the gasket material presently being used for Saturn LOX applications.

3. The developed laminated gasket composite can be thermally cycled from 300°F to -320°F without affecting the sealing properties of the gasket.

4. The internal gas pressures held by the newly developed laminated gasket composite were normally twice the pressures held by the material now used for Saturn LOX service under identical torquing sequences and test conditions.

5. The second analytical expression indicates that the room temperature flange pressure required to seal at cryogenic temperatures can normally be predetermined within ±10%.

The Narmco-developed gasket composite has been utilized in various actual applications. Every properly processed laminated gasket tested in an actual application exhibited superior performance when compared with all other non-metallic type cryogenic gaskets tested under identical conditions.

The use of cryogenic propellants in today's space vehicles has brought about the definite requirement for a good, all-purpose cryogenic seal. The Narmco-developed laminated gasket composite concept which was developed for flat gasket applications was also applied to the development of other seal configurations. Concepts for the processing of chevron seals, lip seals, ball seals, diaphragms, and O-rings have been developed utilizing TFE-FEP and glass materials. The laminated concept has also been employed in the development of flexible cryogenic tubing.

The lip seals, chevron seals, O-rings, and flexible tubing developed indicate that promising performance may be obtained with further investigation.

It is apparent from the leak test data that the small annular spaces which were utilized to contain the gas pressures seriously affect the performance of the seals investigated. A minor leak would be magnified by the loss of gas volume in the small annular space. Future work should be conducted which would simulate actual sealing conditions and provide a better response to optimization of processing variables such as winding speed, laminating pressures and temperatures, and forming conditions.

The following processing methods for the listed seals appear to be the most practible when considering such processing and fabrication criteria as simplicity of processing, reproducibility, quality, and man-hours expended:

1. Flexible Tubing: Type VI

2. Lip Seals: Lamination of plies in the forming tool

3. Chevron Seals: Lamination of plies in the forming tool

4. O-Rings: Toroidal winding on a laminate core

Further optimization of these processes and others which show promise are required along with additional test data. This will result in methods to produce reliable, LOX compatible cryogenic seals and the performance criteria required for the design of cryogenic systems which are reliable and leak-free.

Other areas of interest may also be investigated, such as applying the laminated gasket composite to the fabrication of high-temperature gaskets. This may be accomplished by utilizing other material combinations such as metal fabrics and high-temperature polymers or coatings.

The utilization of the laminated composite of Teflon and glass could possibly be used as an energy-absorbing cryogenic shock-absorbing material.

APPENDIX A

THEORETICAL RELATIONSHIP FOR PREDICTING ROOM TEMPERATURE FLANGE LOADS FOR SEALING AT CRYOGENIC TEMPERATURE (DERIVATION NO. I)

1. Theoretical Analysis

Desired: An equation giving the required torquing for a gasketted joint at a given internal pressure

General solution:

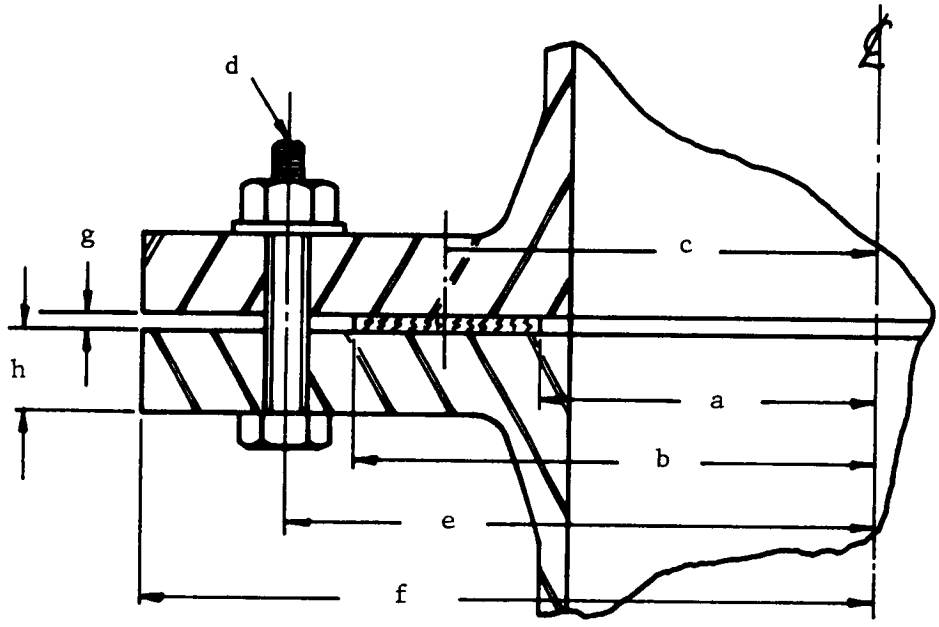

Figure 129. Typical Joint Section

Nomenclature (See Figure 129):

a = Gasket inside radius
b = Gasket outside radius
c = Gasket mean radius = $\frac{1}{2}$ (a + b)
d = Nominal bolt diameter
e = Bolt circle radius
f = Flange outside radius
g = Gasket thickness (uncompressed)
h = Flange thickness (assumed the same for both flanges)
p = Pressure (i, inside; o, outside), psia
t = Temperature, °F

Nomenclature (Continued):

A = Area, $in.^2$

B = Bolt force per unit circumference, lb/in.

E = Modulus of elasticity, $lb/in.^2$

F = Force applied to gasket per unit circumference, lb/in.

L = Length, in.

N = Number of bolts

T = Torque on bolt, in.-lb

α = Coefficient of linear expansion, in./in./°F

δ = Compressed gasket thickness, in.

ε = Strain, in./in.

μ = Poisson's ratio

σ = Normal stress, $lb/in.^2$

Subscripts:

a = Ambient

b = Bolt

c = Cryogenic

f = Flange

g = Gasket

a. Basic Relationship

The approach taken is to look at the gasket only, ignoring for the moment the flange pressure and consider the pressure differential between the inside and outside conditions as the only loading (see Figure 130). This allows the determination of the normal stresses developed transverse to the gasket. It is then stated that this represents the minimum value of flange pressure required to contain the internal pressure.

Using the cylindrical coordinates r, θ, z:

$$\sigma_r = \frac{a^2 b^2 (p_o - p_i)}{b^2 - a^2} \cdot \frac{1}{r^2} + \frac{p_i a^2 - p_o b^2}{b^2 - a^2} \quad \ldots\ldots (1)$$

$$\sigma_\theta = -\frac{a^2 b^2 (p_o - p_i)}{b^2 - a^2} \cdot \frac{1}{r^2} + \frac{p_i a^2 - p_o b^2}{b^2 - a^2} \quad \ldots\ldots (2)$$

(Solution from Lamé; Reference 16)

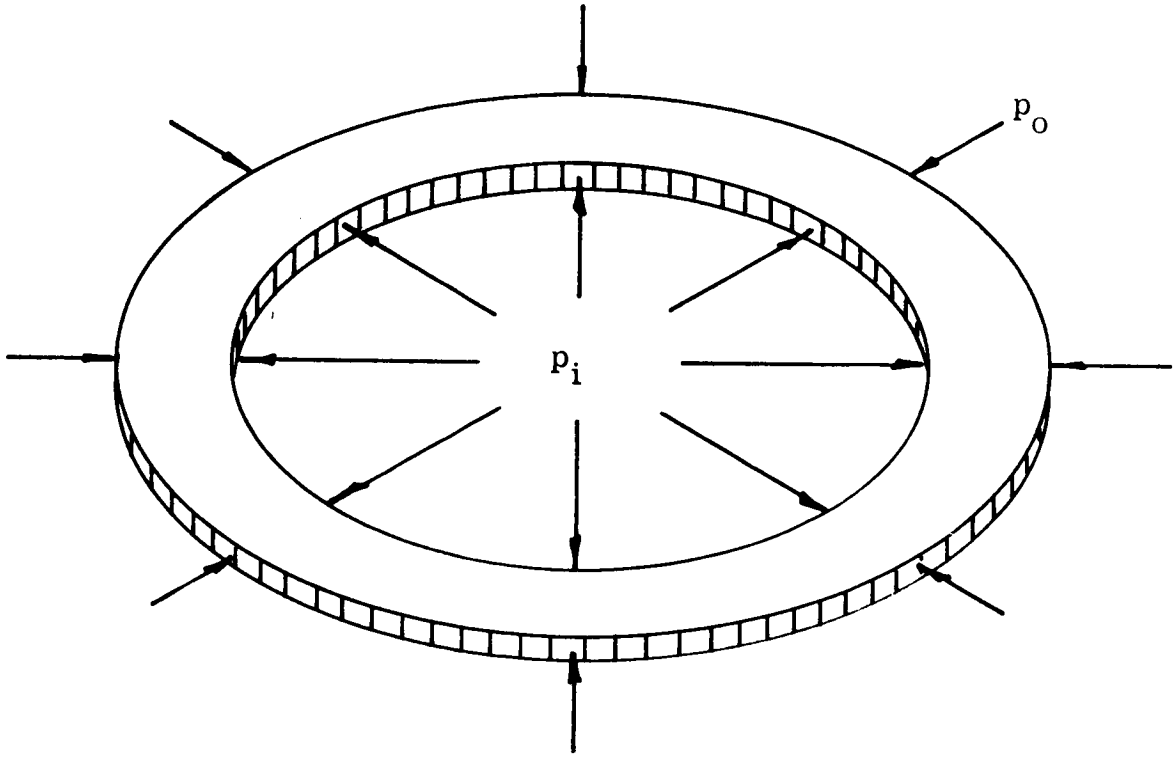

Figure 130. Gasket Loading Less Flange Pressure

For the launch vehicle application, p_o will be zero psig at launch and zero psia in space. At all times $p_i \gg p_o$ so that p_o may be taken as zero at all times. Equations (1) and (2) then simplify to

$$\sigma_r = \frac{a^2 p_i}{b^2 - a^2}\left(1 - \frac{b^2}{r^2}\right) \qquad \ldots\ldots (3)$$

$$\sigma_\theta = \frac{a^2 p_i}{b^2 - a^2}\left(1 + \frac{b^2}{r^2}\right) \qquad \ldots\ldots (4)$$

Inserting Equations (3) and (4) into Hooke's Law:

$$\epsilon_z = \frac{1}{E}\left[\sigma_z - \mu\left(\sigma_r + \sigma_\theta\right)\right] \qquad \ldots\ldots (5)$$

yields

$$\epsilon_z = \frac{1}{E_g}\left[\sigma_z - \mu\frac{a^2 p_i}{b^2 - a^2}\left(1 - \frac{b^2}{r^2} + 1 + \frac{b^2}{r^2}\right)\right]$$

$$= \frac{1}{E_g}\left[\sigma_z - \frac{2\mu a^2 p_i}{b^2 - a^2}\right]$$

or

$$\sigma_z = E_g \epsilon_z + \frac{2\mu a^2 p_i}{b^2 - a^2} \qquad \ldots\ldots (6)$$

Now impose the condition that the strain be equal to the change in gasket thickness divided by the original thickness:

$$\epsilon_z = \frac{g - \delta}{g} \qquad \ldots\ldots (7)$$

Substituting Equation (7) into (6):

$$\sigma_z = E_g \frac{g - \delta}{g} + \frac{2\mu a^2 p_i}{b^2 - a^2} \qquad \ldots\ldots (8)$$

The flange pressure must at least equal this normal stress to maintain a seal.

$$p_f \geq \sigma_z \qquad \ldots\ldots (9)$$

It is therefore seen from Equations (8) and (9) that the required flange pressure is a function of the gasket dimensions (a, b, g), the gasket properties (E, δ, μ), and the loading (p_i).

b. Gasket Loading vs. Bolting (See Figure 131)

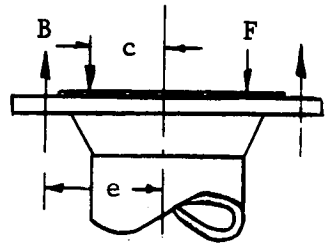

Figure 131. Flange Free-Body Diagram

The moments due to the bolt force and the gasket force must be in equilibrium so

$$Fc = Be \qquad \ldots\ldots (10)$$

but

$$p_f = \frac{F\,\pi\,2\,c}{\pi\,b^2 - \pi\,a^2} = \frac{2\,c\,F}{b^2 - a^2} \qquad \ldots\ldots (11)$$

therefore

$$p_f = \frac{2\,c\left(\frac{Be}{c}\right)}{b^2 - a^2} = \frac{2\,Be}{b^2 - a^2} \qquad \ldots\ldots (12)$$

c. Temperature Effects (See Figure 132)

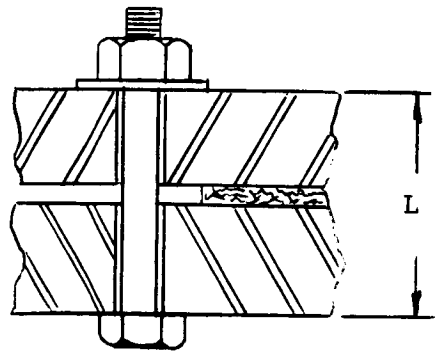

Figure 132. Joint Detail

Assume that all parts are initially at the same temperature t_a and later at the same cryogenic temperature t_c. This is an approximation because it is known that there is a temperature gradient radially as well as transversely throughout the joint.

$$\text{Let} \quad \Delta t = t_c - t_a < o$$

At t_1:

Figure 46 joint thickness $L = h + \delta + h = 2h + \delta$ . . . (13)

At t_2:

Change in bolt length $= \alpha_b L \Delta t$

Change in gasket thickness $= \alpha_g \delta \Delta t$

Change in flange thickness $= \alpha_f h \Delta t$

Because both flanges and gasket are all changing thicknesses, the joint thickness changes

$$\Delta L = 2 \alpha_f h \Delta t + \alpha_g \delta \Delta t = (2 \alpha_f h + \alpha_g \delta) \Delta t \quad . . . (14)$$

However, the bolt length change due to temperature only is $\alpha_b L \Delta t$. Therefore, there is an induced change in bolt length of

$$\Delta t \left(\alpha_b L - 2 \alpha_f h - \alpha_g \delta\right) =$$

$$\left(t_c - t_a\right) \left[\alpha_b (2h + \delta) - \left(2 \alpha_f h + \alpha_g \delta\right)\right] =$$

$$\left(t_c - t_a\right) \left[2h \left(\alpha_b - \alpha_f\right) + \delta \left(\alpha_b - \alpha_g\right)\right] \quad . . . . (15)$$

This results in an induced strain in the bolt of

$$\hat{\epsilon}_b = \frac{\Delta L}{L} = \frac{\left(t_c - t_a\right) \left[2h \left(\alpha_b - \alpha_f\right) + \delta \left(\alpha_b - \alpha_g\right)\right]}{2h + \delta} \quad . . . . (16)$$

This causes a change in the bolt stress of

$$\hat{\sigma}_b = -E_b \hat{\epsilon}_b = - \frac{\left(t_c - t_a\right)\left[2h\left(\alpha_b - \alpha_f\right) + \delta\left(\alpha_b - \alpha_g\right)\right]E_b}{2h + \delta} \quad \ldots\ldots (17)$$

(Negative sign because of a relative lengthening of the bolt, resulting in a positive strain, has the effect of decreasing the bolt load and stress and vice versa.)

Which corresponds to a change in bolt load of

$$\tilde{B} = \hat{\sigma}_b \, N \, \frac{\pi}{4} d^2 = \frac{-\pi\left(t_c - t_a\right)\left[2h\left(\alpha_b - \alpha_f\right) + \delta\left(\alpha_b - \alpha_g\right)\right]E_b \, N \, d^2}{4\,(2h + \delta)}$$

To avoid confusion regarding the temperature at which the various properties are measured, additional subscripts for ambient and cryogenic temperatures are included:

$$\tilde{B}^* = \frac{\pi\left(t_a - t_c\right)\left[2\,h_a\left(\alpha_b^* - \alpha_f^*\right) + \delta_a\left(\alpha_b^* - \alpha_g^*\right)\right]E_{b_c} \, N \, d_a^{\,2}}{4\left(2\,h_a + \delta_a\right)} \quad \ldots\ldots (18)$$

where * indicates value is from t_a to t_c.

The change in bolt load per unit circumference would be

$$\hat{B}^* = \frac{\left(t_a - t_c\right)\left[2\,h_a\left(\alpha_b^* - \alpha_f^*\right) + \delta_a\left(\alpha_b^* - \alpha_g^*\right)\right]E_{b_c} \, N \, d_a^{\,2}}{8\left(2\,h_a + \delta_a\right)e_a} \quad \ldots\ldots (18a)$$

d. Combination of Above

Combining Equations (8), (9), (12), and (18a) and using subscript "a" to denote ambient temperature value and "c" to denote cryogenic, with * to indicate that the value is from t_a to t_c:

$$p_f \geq \sigma_z$$

$$\frac{2 B_c e_c}{b_c^2 - a_c^2} \geq + E_{g_c} \frac{g_c - \delta_c}{g_c} + \frac{2 \mu_c a_c^2 p_i}{b_c^2 - a_c^2}$$

$$B_c \geq + E_{g_c} \frac{\left(g_c - \delta_c\right)\left(b_c^2 - a_c^2\right)}{2 g_c e_c} + \mu_c \frac{a_c^2 p_i}{e_c}$$

but $B_c = B_a + \hat{B}^*$

$$B_a + \frac{\left(t_a - t_c\right)\left[2 h_a \left(\alpha_b^* - \alpha_f^*\right) + \delta_a \left(\alpha_b^* - \alpha_g^*\right)\right] E_{b_c} N d_a^2}{8 \left(2 h_a + \delta_a\right) e_a} \geq$$

$$- E_{g_c} \frac{\left(g_c - \delta_c\right)\left(b_c^2 - a_c^2\right)}{2 g_c e_c} + \mu_c \frac{a_c^2 p_i}{e_a}$$

$$B_a \geq + E_{g_c} \frac{\left(g_c - \delta_c\right)\left(b_c^2 - a_c^2\right)}{2 g_c e_c} + \mu_c \frac{a_c^2 p_i}{e_c} -$$

$$\frac{\left(t_a - t_c\right)\left[2 h_a \left(\alpha_b^* - \alpha_f^*\right) + \delta_a \left(\alpha_b^* - \alpha_g^*\right)\right] E_{b_c} N d_a^2}{8 \left(2 h_a + \delta_a\right) e_a} \quad \ldots (19)$$

$$\Delta L = L \alpha \Delta t$$

$$L_2 - L_1 = L_1 \alpha \left(t_2 - t_1\right)$$

$$L_2 = L_1 \left[1 + \alpha \left(t_2 - t_1\right)\right]$$

$$\therefore L_c = L_a \left[1 + \alpha \left(t_c - t_a\right)\right]$$

But second term $\ll 1$ so that $L_c \approx L_a$ for Δt and α's to be used.

Therefore, $\delta_c \approx \delta_a$, $g_c \approx g_a$, $b_c \approx b_a$, $a_c \approx a_a$, $e_c \approx e_a$ so Equation (19) can be rewritten:

$$B_a \geq + E_{g_c} \frac{\left(g_a - \delta_a\right)\left(b_a^2 - a_a^2\right)}{2 g_a e_a} + \mu_c \frac{a_a^2 p_i}{e_a} -$$

$$\frac{\left(t_a - t_c\right)\left[2 h_a \left(\alpha_b^* - \alpha_f^*\right) + \delta_a \left(\alpha_b^* - \alpha_g^*\right)\right] E_{b_c} N d_a^2}{8 \left(2 h_a + \delta_a\right) e_a} \quad \ldots \quad (19a)$$

In this form, the required bolt force at ambient temperature (t_a) to contain internal pressure (p_i) at cryogenic temperature (t_c) is a function of cryogenic material properties (E_{g_c}, μ_c, E_{b_c}), coefficients of linear expansion in the temperature range desired (α_b^*, α_f^*, α_g^*), and physical dimensions at the ambient temperature (δ_a, g_a, b_a, a_a, e_a, h_a, d_a) as well as the number of bolts (N).

Remember that B is the total bolt force per unit circumference. Using B_b for bolt force per individual bolt,

$$B \left(2 \pi e\right) = N B_b$$

$$B = \frac{N B_b}{2 \pi e} \quad \ldots \ldots \quad (20)$$

Applying Equation (20) to Equation (19a) yields:

$$B_{b_a} \geq + \frac{\pi \left(g_a - \delta_a\right)\left(b_a^2 - a_a^2\right)}{N g_a} E_{g_c} + \frac{2 \pi a_a^2 p_i}{N} \mu_c -$$

$$\frac{\pi \left(t_a - t_c\right)\left[2 h_a \left(\alpha_b^* - \alpha_f^*\right) + \delta_a \left(\alpha_b^* - \alpha_g^*\right)\right] d_a^2}{4 \left(2 h_a + \delta_a\right)} E_{b_c} \quad \ldots \quad (21)$$

e. Bolt Load vs. Torque

It has been shown (Reference 9) that

$$T = r_t W \left[\frac{\cos \theta_n \tan \alpha + \mu_1}{\cos \theta_n - \mu_1 \tan \alpha} + \frac{r_c}{r_t} \mu_2\right] \quad \ldots \ldots \quad (22)$$

where

T = Required torque

W = Load in bolt

r_t = Thread pitch radius

r_c = Mid-radius of washer contact area

θ_n = Angle between resultant force normal to the thread surface and the tangential plane

α = Helix angle

μ_1 = Coefficient of friction for threads

μ_2 = Coefficient of friction of washer on flange

For most cases (60-degree angle threads and coefficient of friction of 0.15), this can be approximated by

$$T = 0.2\, d\, W \qquad \ldots\ldots (23)$$

where d = nominal or outside diameter of the bolt.

Inasmuch as the accuracy obtainable with a torque wrench is quite limited, and the expression previously derived (Equation 21) is an inequality anyway, the more precise Equation (22) is not needed: Equation (23) is sufficient. In the nomenclature used previously:

$$T = 0.2\, d\, B_b \qquad \ldots\ldots (23a)$$

f. Final Expression

Combining Equations (21) and (23a):

$$T_a \geq + \frac{0.2\,\pi \left(g_a - \delta_a\right)\left(b_a^{\,2} - a_a^{\,2}\right) d_a}{N\, g_a} E_{g_c} + \frac{0.4\,\pi\, a_a^{\,2}\, d_a\, P_i}{N}\,\mu_c - \frac{\pi \left(t_a - t_c\right)\left[2\, h_a \left(\alpha_b^* - \alpha_f^*\right) + \delta_a \left(\alpha_b^* - \alpha_g^*\right)\right] d_a^{\,3}}{20 \left(2\, h_a + \delta_a\right)} E_{b_c} \qquad (24)$$

The derivation of Equation (8), and therefore Equation (24), was based on the theory of elasticity which requires materials that are elastic, isotropic, and homogeneous. However, it has been shown (Reference 7) that "substantial plastic flow of at least one of the materials at the seal interface is necessary for zero leakage." It is therefore desirable that the gasket be loaded beyond its yield

point (the gasket rather than the flanges because plastic flow of material interfers with reusability and replacing a gasket rather than the flanges is certainly preferred). This would mean that theory of plasticity, rather than elasticity, would apply. However, it is felt that using the inequality sign in Equation (24) would place the gasket in the plastic range. Therefore, disregard the equality sign in the equation, resulting in an expression giving the minimum value for torque.

Most gasket materials, including those developed by Narmco Research & Development, are neither isotropic nor homogeneous. Nevertheless, it was believed that effective E_g's and μ's could be determined in the appropriate directions so that Equation (24) could still be applied.

APPENDIX B

THEORETICAL RELATIONSHIP FOR PREDICTING ROOM TEMPERATURE FLANGE LOADS FOR SEALING AT CRYOGENIC TEMPERATURE (DERIVATION NO. II)

Because the experimental verification of the theoretical relationship for sealing that was developed earlier in the program was not as conclusive as desired, a more conventional approach to that problem has also been considered and is presented in the subsequent section. It is anticipated that the subsequent experimental phases of this program may be used to determine which of these two approaches more closely represents the actual situation.

1. Cryogenic Gasketing Analysis

   Consider a gasket in a flanged connection. When initially tightened, the total gasket force equals the total bolt force.

$$F_t = B_t = NB_b \qquad (1)$$

   where N is the number of bolts and B_b is the force per bolt.

Now allow a cryogenic fluid to pass through the pipeline containing this flanged connection.

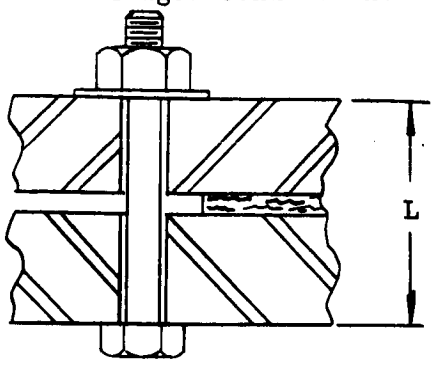

Assume that all parts are initially at the same temperature t_a and later at the same cryogenic temperature t_c. This is an approximation because a temperature gradient is known to exist radially as well as transversely throughout the joint.

Let $\Delta t = t_c - t_a < 0$

At t_1:

Joint thickness $L = h + \delta + h = 2h + \delta$ (2)

At t_2:

Change in bolt length $= \alpha_b L \Delta t$

Change in gasket thickness $= \alpha_g \delta \Delta t$

Change in flange thickness $= \alpha_f h \Delta t$

Because both flanges and gasket are all changing thicknesses, the joint thickness changes

$$\Delta L = 2 \alpha_f h \Delta t + \alpha_g \delta \Delta t = \left(2 \alpha_f h + \alpha_g \delta\right) \Delta t \qquad (3)$$

However, the bolt length change due to temperature only is $\alpha_b L \Delta t$. Therefore, there is an induced change in bolt length of

$$\Delta t \left(\alpha_b L - 2\alpha_f h - \alpha_g \delta\right) = \left(t_c - t_a\right) \left[\alpha_b (2h + \delta) - \left(2\alpha_f h + \alpha_g \delta\right)\right] =$$

$$\left(t_c - t_a\right) \left[2h\left(\alpha_b - \alpha_f\right) + \delta\left(\alpha_b - \alpha_g\right)\right] \qquad (4)$$

This results in an induced strain in the bolt of

$$\hat{\epsilon}_b = \frac{\Delta L}{L} = \frac{\left(t_c - t_a\right) \left[2h\left(\alpha_b - \alpha_f\right) + \delta\left(\alpha_b - \alpha_g\right)\right]}{2h + \delta} \qquad (5)$$

This causes a change in the bolt stress of

$$\hat{\sigma}_b = -E_b\hat{\epsilon}_b = -\frac{\left(t_c - t_a\right)\left[2h\left(\alpha_b - \alpha_f\right) + \delta\left(\alpha_b - \alpha_g\right)\right]E_b}{2h + \delta} \tag{6}$$

(Negative sign because a relative lengthening of the bolt, resulting in a positive strain, has the effect of decreasing the bolt load and stress and vice-versa.)

which corresponds to a change in bolt load of

$$\tilde{B} = \hat{\sigma}_b N \frac{\pi}{4} d^2 = \frac{-\pi\left(t_c - t_a\right)\left[2h\left(\alpha_b - \alpha_f\right) + \delta\left(\alpha_b - \alpha_g\right)\right]E_b N d^2}{4\left(2h + \delta\right)}$$

To avoid confusion regarding the temperature at which the various properties are measured, additional subscripts for ambient and cryogenic temperatures are included:

$$\tilde{B}^* = -\frac{\pi\left(t_c - t_a\right)\left[2h_a\left(\alpha_b^* - \alpha_f^*\right) + \delta_a\left(\alpha_b^* - \alpha_g^*\right)\right]E_{b_c} N d_a^2}{4\left(2h_a + \delta_a\right)} \tag{7}$$

where * indicates the value is from t_a to t_c .

From equations (1) and (7), the new gasket force is

$$F_t = NB_b + \tilde{B}^* = N\left\{B_b - \frac{\pi\left(t_c - t_a\right)E_{b_c} d_a^2}{4\left(2h_a + \delta_a\right)}\left[2h_a\left(\alpha_b^* - \alpha_f^*\right) + \delta_a\left(\alpha_b^* - \alpha_g^*\right)\right]\right\} \tag{8}$$

When the cryogenic fluid is pressurized to p_i internal pressure, the hydrostatic end force causes the bolt stress to increase to a new value σ_{b_2} and the bolts increase in length by an amount Δ. Simultaneously, the gasket increases in thickness by the same amount Δ , and the gasket compressive stress is reduced to σ_{g_2} . The bolts should follow Hooke's law

$$\sigma_{b_2} - \sigma_{b_1} = E_{b_c}\epsilon = E_{b_c}\frac{\Delta}{L_2} \tag{9}$$

where L_2 is $L_1 + \Delta L$ or

$$L_2 = \left(2h_a + \delta_a\right)\left[1 + \alpha_b^*\left(t_c - t_a\right)\right] \tag{10}$$

or

$$\sigma_{b_2} = E_{b_c} \frac{\Delta}{\left(2h_a + \delta_a\right)\left[1 + \alpha_b^* \left(t_c - t_a\right)\right]} + \sigma_{b_1}$$

$$= E_{b_c} \frac{\Delta}{\left(2h_a + \delta_a\right)\left[1 + \alpha_b^* \left(t_c - t_a\right)\right]} + \frac{B_{b_1}}{A_b} \qquad (11)$$

The new force equilibrium requires that

$$\sigma_{g_2} A_g + p_i A_i = N \sigma_{b_2} A_b \qquad (12)$$

where A_i is πa^2 and A_b is $\frac{\pi}{4} d^2$.

Substituting equation (11) into (12):

$$\sigma_{g_2} A_g = \frac{\pi N d_a^2}{4} \left\{ E_{b_c} \frac{\Delta}{\left(2h_a + \delta_a\right)\left[1 + \sigma_b^* \left(t_c - t_a\right)\right]} \right\}$$

$$+ N B_{b_1} - \pi a^2 p_i \qquad (13)$$

from the definition of strain

$$\Delta = \delta_c \epsilon = \delta_a \left[1 + \alpha_g^* \left(t_c - t_a\right)\right] \epsilon \qquad (14)$$

The gasket material in general is not a simple Hookeian one but rather follows

$$\sigma = E_g f(\epsilon) \qquad (15)$$

where $f(\epsilon)$ is a function of stress to be experimentally determined for the material.

For the Teflon-glass laminate material, it has been found that

$$f(\epsilon) = \sinh (K_1 \epsilon) \qquad (16)$$

Substituting equation (16) into (15):

$$\epsilon = \frac{1}{K_1} \text{ arc sinh } \left(\frac{\sigma}{E_g}\right) \tag{17}$$

and then equation (17) into (14)

$$\Delta = \delta_a \left[1 + \alpha_g^* \left(t_c - t_a\right)\right] \frac{1}{K_1} \text{ arc sinh } \left(\frac{\sigma_{g_1} - \sigma_{g_2}}{E_{g_c}}\right) \tag{18}$$

and finally equation (18) into (13)

$$\sigma_{g_2} A_g = \frac{\pi N d_a^2}{4} \left\{ E_{b_c} \frac{\delta_a \left[1 + \alpha_g^* \left(t_c - t_a\right)\right] \text{ arc sinh} \left(\frac{\sigma_{g_1} - \sigma_{g_2}}{E_{g_c}}\right)}{K_1 \left(2h_a + \delta_a\right)\left[1 + \alpha_b^* \left(t_c - t_a\right)\right]} \right\} + NB_{b_1} - \pi a^2 p_i \tag{19}$$

The cryogenic gasket stress after pressurization $\left(\sigma_{g_2}\right)$ appears on both sides of this transcendental equation. For a given gasket material, this can be an experimentally determined reasonable arbitrary value, K_2

$$\frac{4}{\pi N d_a^2}\left[K_2 A_g - NB_{b_1} + \pi a^2 p_i\right] = \frac{\delta_a \left[1 + \alpha_g^* \left(t_c - t_a\right)\right] E_{b_c}}{K_1 \left(2h_a + \delta_a\right)\left[1 + \alpha_b^* \left(t_c - t_a\right)\right]} \times \text{ arc sinh } \left(\frac{\sigma_{g_1} - K_2}{E_{g_c}}\right)$$

$$\frac{4K_1 \left(2h_a + \delta_a\right)\left[1 + \alpha_b^* \left(t_c - t_a\right)\right]}{\pi N d_a^2 \delta_a \left[1 + \alpha_g^* \left(t_c - t_a\right)\right] E_{b_c}} \left[K_2 A_g - NB_{b_1} + \pi a^2 p_i\right] = \text{ arc sinh } \left(\frac{\sigma_{g_1} - K_2}{E_{g_c}}\right)$$

(continued)

$$E_{g_c} \sinh \left\{ \frac{4K_1 \left(2h_a + \delta_a\right)\left[1 + \alpha_b^* \left(t_c - t_a\right)\right]}{\pi N d_a^{\,2} \delta_a \left[1 + \alpha_g^* \left(t_c - t_a\right)\right] E_{b_c}} \right.$$

$$\left. \times \left[K_2 A_g - N B_{b_1} + \pi a^2 p_i\right] \right\} = \sigma_{g_1} - K_2 \qquad (20)$$

The initial gasket stress σ_{g_1} is

$$\sigma_{g_1} = \frac{F_{t_1}}{A_g} \qquad (21)$$

Substituting equations (8) and (21) into (20):

$$E_{g_c} \sinh \left\{ \frac{4K_1 \left(2h_a + \delta_a\right)\left[1 + \alpha_b^* \left(t_c - t_a\right)\right]}{\pi N d_a^{\,2} \delta_a \left[1 + \alpha_g^* \left(t_c - t_a\right)\right] E_{b_c}} \left[K_2 A_g - N B_{b_1} + \pi a^2 p_i\right] \right\} =$$

$$\frac{N}{A_g} \left\{ B_{b_1} - \frac{\pi \left(t_c - t_a\right)\left[2h_a \left(\alpha_b^* - \alpha_f^*\right) + \delta_a \left(\alpha_b^* - \alpha_g^*\right)\right] E_{b_c} d_a^{\,2}}{4\left(2h_a + \delta_a\right)} \right\} - K_2 \qquad (22)$$

For a given application, the only variables in this equation are the initial bolt load $\left(B_{b_1}\right)$ and the internal pressure (p_i).

Defining two constants

$$C_1 \equiv \frac{4K_1 \left(2h_a + \delta_a\right)\left[1 + \alpha_b^* \left(t_c - t_a\right)\right]}{\pi N d_a^{\,2} \delta_a \left[1 + \alpha_g^* \left(t_c - t_a\right)\right] E_{b_c}} \qquad (23)$$

$$C_2 \equiv \frac{\pi N \left(t_c - t_a\right)\left[2h_a \left(\alpha_b^* - \alpha_f^*\right) + \delta_a \left(\alpha_b^* - \alpha_g^*\right)\right] E_{b_c} d_a^{\,2}}{4 A_g E_{g_c} \left(2h_a + \delta_a\right)} \qquad (24)$$

equation (22) becomes

$$\sinh\left(C_1K_2A_g - C_1NB_{b_1} + C_1\pi a^2 p_i\right) = \frac{NB_{b_1}}{E_{g_c}A_g} - C_2 - \frac{K_2}{E_{g_c}} \qquad (25)$$

Defining some additional constants

$$\left.\begin{aligned} C_3 &\equiv C_1K_2A_g \\ C_4 &\equiv C_1N \\ C_5 &\equiv C_1\pi a^2 \\ C_6 &\equiv N/E_{g_c}A_g \\ C_7 &\equiv C_2 + \frac{K_2}{E_{g_c}} \end{aligned}\right\} \qquad (26)$$

Substituting equation (26) into (25)

$$\sinh\left(C_3 - C_4B_{b_1} + C_5p_i\right) = C_6B_{b_1} - C_7$$

$$C_3 - C_4B_{b_1} + C_5p_i = \text{arc sinh}\left(C_6B_{b_1} - C_7\right)$$

$$p_i = \frac{1}{C_5}\left[\text{arc sinh}\left(C_6B_{b_1} - C_7\right) - C_3 + C_4B_{b_1}\right] \qquad (27)$$

Equation (27) gives the maximum possible pressure that can be contained in a given joint for any initial bolt load.

Requiring the compressed gasket thickness (δ_a) to determine constants is inconvenient; equations (15) and (16) should be used, instead, to get them in terms of the uncompressed thickness (g_a).

$$\sigma_{g_a} = E_{g_a} \sinh \left(K_1 \epsilon\right)$$

$$= E_{g_a} \sinh \left(K_1 \frac{g_a - \delta_a}{g_a}\right) \tag{28}$$

$$\sigma_{b_a} NA_b = \sigma_{g_a} A_g$$

$$\sigma_{g_a} = \frac{NA_b \sigma_{b_a}}{A_g} = \frac{NB_{b_1}}{A_g}$$

Therefore

$$\frac{NB_{b_1}}{A_g} = E_{g_a} \sinh \left(K_1 \frac{g_a - \delta_a}{g_a}\right)$$

$$\text{arc sinh} \left(\frac{NB_{b_1}}{A_g E_{g_a}}\right) = K_1 \left(\frac{g_a - \delta_a}{g_a}\right)$$

or

$$\delta_a = g_a - \frac{g_a}{K_1} \text{ arc sinh} \left(\frac{NB_{b_1}}{A_g E_{g_a}}\right) \tag{29}$$

2. Method of Application

a. Given a specific gasket material

K_1, K_2, α_g*, E_{g_a} and E_{g_c} are known

b. Given a specific joint

d_a, g_a, N, a, b, h_a, α_b*, α_f* and E_{b_c} are known

and A_g is easily determined from

$$A_g = \pi \left(b^2 - a^2\right)$$

(Note: This analysis has not considered changes in gasket diameters with either load or changing temperatures, so that a and b are considered always constant.)

c. Given a specific application

$$t_a,\ t_c \text{ and } B_{b_1} \text{ are known}$$

d. From the above

$$\delta_a \text{ and then } C_1,\ C_2,\ C_3,\ C_4,\ C_5,\ C_6 \text{ and } C_7$$

can be determined from equations (29), (23), (24), and (26)

e. From c and d above, equation (27) then yields the theoretical internal pressure that can be contained.

APPENDIX C

PRODUCT SPECIFICATION FOR INCOMING TFE TEFLON MATERIAL FOR LOX-COMPATIBLE GASKETS

1.0 Material

1.1 This specification covers sintered, unfilled, unpigmented polytetrafluoroethylene (TFE-fluorocarbon resin) film normally made by casting.

2.0 Application

2.1 Material conforming to this specification is for the fabrication of gaskets.

3.0 General Requirements

3.1 Form

The material shall consist of a translucent film made of polytetrafluorethylene (TFE-fluorocarbon resin) without pigment or filler.

3.2 Dimensions

Rolls shall be supplied in minimum lengths of 10 yd.

4.0 Quality Assurance Provisions

4.1 Visual Examination

Incoming material shall be visually inspected for defects of workmanship, material, and color. The material shall be of uniform quality and condition, free from defects detrimental to the fabrication or performance of parts.

4.2 Color

The color shall be that characteristic of unpigmented film which ranges from cloudy to milky transparents dependent upon the thickness.

4.3 Thickness

The thickness at any point of the film shall be 0.005 in. ±0.001 in.

4.4 Transition Point

One specimen shall be prepared to the dimensions specified in ASTM Method D1457-56T, except that the thickness shall be that of the film. The specimen shall require no conditioning. The transition point shall be 621°±10°F.

4.5 Specific Gravity

One specimen of any convenient size shall be conditioned for a minimum of 1 hour at a temperature of 23°±1.1°C (73.4°±2°F) and shall be tested either in a specific gravity gradient column or by determining whether the specimen floats in a liquid of the maximum specific gravity and sinks in one of the minimum specific gravity specified. The density shall then be 2.15-2.20.

4.6 Rejections

Material not meeting above requirements shall be subject to rejection and return to vendor for credit.

4.7 Packaging

Packaging shall be accomplished in such a manner as to ensure that material will not be damaged during normal handling.

4.8 Marking

Each roll shall be legibly marked to give the following information:

Material Designation _____

Roll No. _____

Yards _____

Narmco's P.O. _____

4.9 Certification

The vendor shall furnish with each shipment certification that the material meets the requirements of this specification.

APPENDIX D

PRODUCT SPECIFICATION FOR INCOMING TEFLON FLUORINATED ETHYLENE-PROPYLENE MATERIAL FOR LOX-COMPATIBLE GASKETS

1.0 Material

1.1 This specification covers sintered, unfilled, fluorinated ethylene-propylene (FEP-fluorocarbon resin) film normally made by casting.

2.0 Application

2.1 Material conforming to this specification is for the fabrication of gaskets.

3.0 General Requirements

3.1 Form

The material shall consist of a translucent film made of fluorinated ethylene-propylene (FEP-fluorocarbon resin) without pigment or filler.

3.2 Dimensions

Rolls shall be supplied in minimum lengths of 10 yd.

4.0 Quality Assurance Provisions

4.1 Visual Examination

Incoming material shall be visually inspected for defects of workmanship, material, and color. The material shall be of uniform quality and condition, free from defects detrimental to the fabrication or performance of parts.

4.2 Color

The color shall be that characteristic of unpigmented film which ranges from cloudy to milky transparents, depending upon the thickness.

4.3 Thickness

The thickness at any point of the film shall be 0.005 in. ±0.001 in.

4.4 Specific Gravity

One specimen of any convenient size shall be conditioned for a minimum of 1 hour at a temperature of 23°±1.1°C (73.4°±2°F) and shall be tested either in a specific gravity gradient column or by determining whether the specimen floats in a liquid of the maximum specific gravity and sinks in one of the minimum specific gravity specified. The density shall then be 2.15-2.20.

4.5 Rejections

Material not meeting above requirements shall be subject to rejection and return to vendor for credit.

4.6 Packaging

Packaging shall be accomplished in such a manner as to ensure that material will not be damaged during normal handling.

4.7 Marking

Each roll shall be legibly marked to give the following information:

Material Designation _____

Roll No. _____

Yards _____

Narmco's P.O. _____

4.8 Certification

The vendor shall furnish with each shipment certification that the material meets the requirements of this specification.

APPENDIX E

PRODUCT SPECIFICATION FOR INCOMING GLASS FABRIC FOR LOX-COMPATIBLE GASKETS

1.0 Material

1.1 This specification covers a satin-weave, silicone-treated glass material.

2.0 Application

2.1 Material conforming to this specification is for the fabrication of glass fabric laminates for structural and nonstructural parts.

3.0 General Requirements

3.1 Form

The material shall consist of single ply woven glass material.

3.2 Dimensions

Rolls shall be supplied in width of 38 in. ±3 in. and standard lengths of 125 yd, unless otherwise requested.

4.0 Quality Assurance Provisions

4.1 Visual Examination

Incoming material shall be visually inspected for defects of workmanship, material, and color. The material shall be of uniform quality and condition, clean and free from defects detrimental to fabrication or performance of parts.

4.2 Thickness

The nominal thickness of material shall be 0.0096 in. ±0.001 in. A minimum of ten readings shall be taken across the length of roll.

4.3 Yarn Construction

The yarn construction shall be

Warp: 150-1/2

Fill: 150-1/2

4.4 Weight

One 6-in. square specimen shall be measured to the nearest 0.01 in. and weighed to the nearest 0.01 gm. Weight should be 8.60 oz/yd^2.

4.5 Tensile

The minimum breaking strength when tested per ASTM Method D579-49 shall be

Warp: 350 lb/in.

Fill: 330 lb/in.

4.6 Rejections

Material not meeting above requirements shall be subject to rejection and return to vendor for credit.

4.7 Packaging

Packaging shall be accomplished in such a manner as to ensure that material will not be damaged during normal handling.

4.8 Marking

Each roll shall be legibly marked to give the following information:

Fabric Designation _____

Roll No. _____

Yards _____

Narmco's P.O. _____

4.9 Certification

The vendor shall furnish with each shipment, certification that the material meets the requirements of this specification.

APPENDIX F

PROCESS SPECIFICATION FOR THE FABRICATION OF GASKET, CRYOGENIC FOR LIQUID OXYGEN SERVICE

SCOPE: This specification covers the general requirements in the fabrication of cryogenic gasket for liquid oxygen service.

1.0 Objective

1.1 The objective of this specification is to set forth the fabrication processes and controls applicable for the fabrication of NRD glass-Teflon gaskets.

1.2 This specification is applicable to all work performed by Narmco Research & Development and/or any subcontractor that may fabricate cryogenic gaskets for LOX service.

2.0 References

2.1 "Elastomeric gasket materials development for cryogenic application," Contract No. NAS 8-5053, F. Wilson and J. Feldmann.

2.2 DuPont technical data for fluorocarbon resins.

2.3 ASTM Method D579-49.

2.4 ASTM Method D1457-56T.

2.5 Narmco Drawing No. 63-077.

3.0 General

3.1 At processing temperature Teflon TFE and FEP fluorocarbon film liberates vapor that may be harmful. Provide adequate ventilation during processing of TFE or FEP film. For more information refer to polychemicals Department Information Bulletin No. X-59d.

3.2 High degree of cleanliness must be maintained throughout the process of manufacturing the gaskets.

4.0 Materials

4.1 Materials used under this specification shall be ordered to the following callouts:

4.1.1 (TFE) Tetrafluoroethylene (0.005 in. thick).

4.1.2 (FEP) Fluorinated ethylene-propylene (0.005 in. thick).

4.1.3 Glass fabric: #401 Crawfoot satin weave glass cloth Greige goods 38 in. wide.

5.0 Receiving Inspection

5.1 TFE Film

5.1.1 Visual Examination

Incoming material shall be visually inspected for defects of workmanship.

5.1.2 Color Appearance

The color shall be characteristic of unpigmented film which ranges from cloudy to milky transparent, depending upon thickness.

5.1.3 Thickness

The thickness shall be measured and tolerance shall be within ±0.005 in. of specified thickness.

5.1.4 Transition Point

The transition point shall be 327°±10°C. Each batch of TFE shall be qualified for production use per ASTM method D1457-56T.

5.1.5 Specific Gravity

The density shall be 2.15 – 2:20 g/cc a specimen cut to a convenient size shall be conditioned at 23°C±1.1°C for 1 hour. Tests shall be conducted by either a specific gradient column or by determining whether the specimen will float or sink at the maximum or minimum specific gravity, respectively.

5.1.6 Packaging

Packaging shall be accomplished in such a manner that material will be free of damage under normal handling conditions. The following marking shall appear on the package:

Material Designation _____

Roll No. _____ Lot No. _____

Yards _____ Wt. _____

N.R.D. P.O. _____

5.2 Glass Fabric

5.2.1 Each roll of glass shall be inspected for the following:

5.2.1.1 Damage, visually.

5.2.1.2 Thickness shall be 0.0096 in. ±0.001 in. A minimum of ten readings shall be taken along the length of the roll.

5.2.1.3 Yarn construction shall be:

Warp: 150-1/2

Fill: 150-1/2

5.2.1.4 Weight shall be 8.60 oz/yd. A 6-in. square specimen shall be cut off the roll and weighed to the nearest 0.01 gram.

5.2.2 Material of Rejection

5.2.2.1 Materials not meeting the above requirement shall be subject to rejection. It is the responsibility of the Inspection Department to inform the project officer of the degree of nonconformity of the material.

5.2.3 Materials Review Board

5.2.3.1 The Material Review Board shall convene as required to render disposition of discrepant material. Disposition shall be "use as is," "return to vendor," or "scrap."

5.2.4 Marking

5.2.4.1 Each roll shall be legibly marked to give the following information:

Fabric Designation _____

Roll No. _____ Lot No. _____

Yardage _____

N.R.D. P.O. _____

6.0 Certification

6.1 Certification of conformance shall fully and completely identify material. Batch and/or lot number, applicable specifications and to NRD purchase order number.

7.0 Process Control

7.1 Only qualified TFE material shall be used. Each roll of TFE material shall be identified as to qualification, date roll and lot number.

7.1.2 FEP material must be wrapped in a polyethylene bag as soon as possible, after use.

7.2 FEP

7.2.1 Only qualified FEP film shall be used. Each roll of FEP shall be identified as to qualification date, roll and lot number.

7.2.2 FEP material must be wrapped in a polyethylene bag as soon as possible, after use.

7.3 Glass Fabric

7.3.1 Only qualified #401 Crowfoot weave glass shall be used. Each roll shall be identified as to qualification data, roll and batch number.

7.3.2 Glass fabric shall be heat cleaned. Heat cleaning shall be accomplished by transferring the roll of glass cloth to an 8 in. transite tube, loosely, up to 50 yards/roll. Place in oven at 650°F for 8 hours.

7.3.3 Rolls of glass fabric (#401 Crowfoot weave) shall be wrapped in polyethylene bag after use, also rolls of glass fabric that have been heat cleaned shall be identified as to the date and batch number.

7.4 Control Process

7.4.1 All cure times and temperatures shall be logged on the job traveler.

7.4.2 Laminating temperatures shall be controlled by iron-constantan thermocouple wire and potentiometer.

8.0 Fabrication

8.1 TFE and #401 glass laminate

8.1.1 Cut TFE 0.005 in. film to the required size and quantity.

8.1.2 Cut #401 heat cleaned glass to the required sizes as follows:

3 pieces 90° to warp

2 pieces 45° to warp

8.2 Lamination Procedure

8.2.1 Lay-up #401 glass and Teflon TFE between clean aluminum caul plates as follows:

8.2.1.1 First a 90° glass

8.2.1.2 5 mils TFE

8.2.1.3 A 45° glass

8.2.1.4 5 mils TFE

8.2.1.5 A 90° glass

8.2.1.6 5 mils TFE

8.2.1.7 A 45° glass

8.2.1.8 5 mils TFE

8.2.1.9 And finally 90° glass. Orientate 45° layers as shown below. This is a typical laminating sequence of glass-to-TFE laminate.

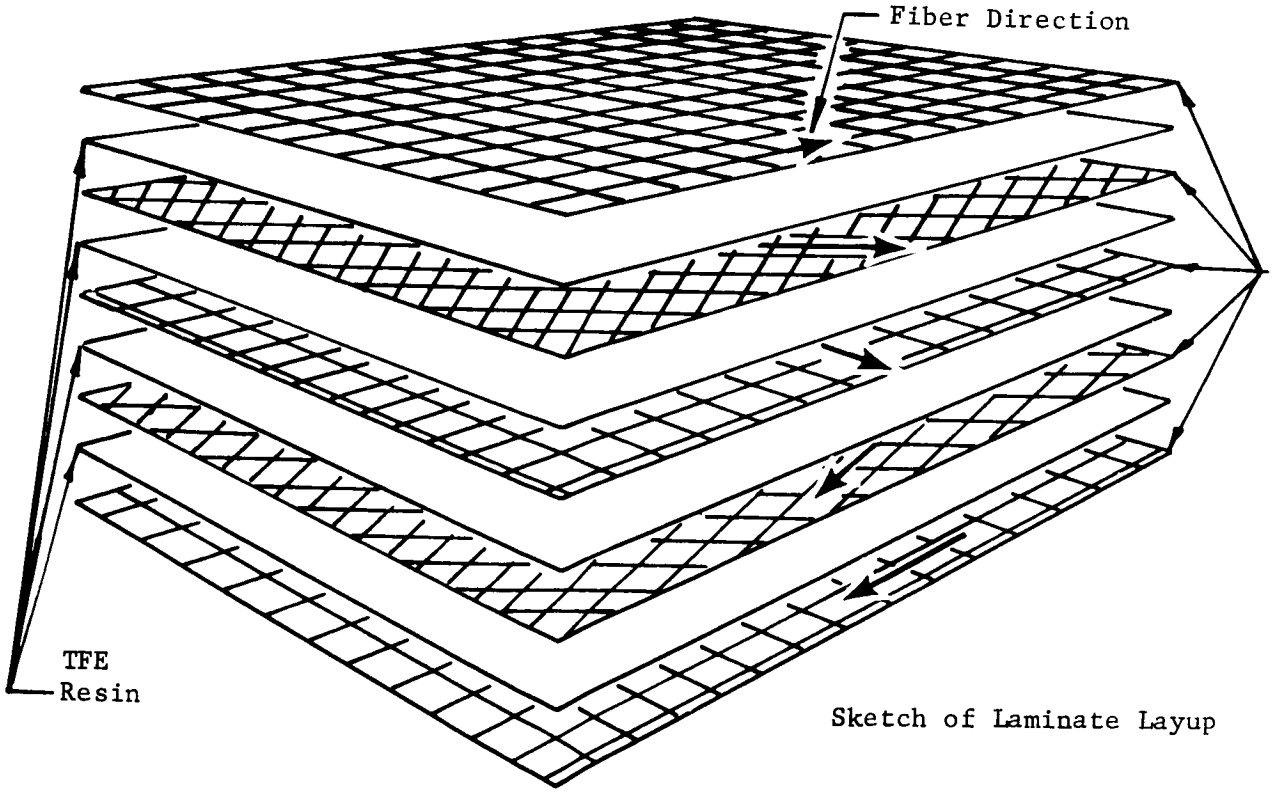

Sketch of Laminate Layup

8.3 Laminating Conditions

8.3.1 Place the multiaxial layup between clean aluminum caul plates, insert a thermocouple in the layup and put in a 720°F press platen.

8.3.2 Apply 500 psi pressure as soon as the laminate is placed in the press.

8.3.3 Lamination time at 720°F shall be .5 minutes. Desired laminating time shall start when thermocouple has reached 720°F.

8.3.4 Upon completion of lamination time the heat shall be turned off and the pressure maintained at 500 psi until thermocouple indicates 400°F. Remove the laminate from the press and cool rapidly with tap water. Caution must be taken that laminate is kept dry during the cooling operation. To insure this, run tap water on surface of aluminum caul only.

8.4 Encapsulation of Laminate

8.4.1 Cut two pieces of FEP the same size as the laminate. Place 0.005 in FEP film on each side of the laminate and cure between clean aluminum caul plates.

8.4.2 Cure 0.005 in. thick FEP on the laminate at 550°F±5°F with 100 psi pressure, for 1-1/2 minutes.

8.5 Trimming of Gasket Laminates

8.5.1 Use approved laminate trim die.

8.5.2 Use a flat lead sheet for a back-up plate.

8.5.3 Place laminate on the back-up plate, position the trim die and apply cutting pressure.

8.6 Trimming of gasket incapsulating material (5 mil FEP).

8.6.1 Trim per paragraph 8.5 utilizing the FEP die cutter.

8.6.2 Trim 1/16 inch and 1/32 inch strips sufficient in length to cover the periphery of the gasket, both inside and outside.

8.7 Gasket Encapsulation

8.7.1 Use only approved encapsulating die.

10.0 Packaging

10.1 The completed gaskets shall be wrapped and packaged in a suitable container for shipment

11.0 All applicable certifications and records shall be enclosed in the shipping container.

8.7.2 Encapsulate as Follows:

8.7.2.1 Place 5 mil FEP in mold (trimmed per paragraph 8.5).

8.7.2.2 Position the trimmed gasket laminate.

8.7.2.3 Wrap the 1/16 in. 10-mil FEP around and against the wall of the encapsulating die.

8.7.2.4 Wrap the 1/32 in. 10-mil FEP strip around and against the gasket material to be encapsulated.

8.7.2.5 Position one layer of 5 mil FEP (trimmed per paragraph 8.5).

8.7.2.6 Assemble the male and the female dies.

8.7.3 Encapsulating Conditions

8.7.3.1 Place encapsulating die in a press, set platen temperature at 550°F.

8.7.3.2 Insert an iron-constantan thermocouple in the fixture. Heat to 500°F, apply a 100 psi pressure.

8.7.3.3 Temperature must be carefully watched not to exceed 560°F. The sealing temperature is 550°F ±5°F, for 1-1/2 minutes.

8.7.3.4 Remove encapsulating die from the press, cool rapidly with tap water.

8.7.3.5 Remove gasket from encapsulating die. Care must be exercised in the removal of the encapsulated gasket from the tool to prevent damage.

8.7.3.6 Take six random readings of thickness and record.

8.7.3.7 Check for leaks, using a die penetrant.

8.7.3.8 The above operation sequence is mandatory to obtain the optimum gasket encapsulation.

9.0 Final Inspection

9.1 The encapsulated gaskets shall be inspected for compliance to this specification and applicable engineering drawing. Final inspection shall be witnessed by the project engineer.

APPENDIX G

GEORGE C. MARSHALL SPACE FLIGHT CENTER
NATIONAL AERONAUTICS AND SPACE ADMINISTRATION

SPECIFICATION
(PROPOSED)
GASKET, CRYOGENIC, LAMINATED, LOX COMPATIBLE

This proposed specification, dated June 15, 1966, prepared by the George C. Marshall Space Flight Center has not been approved and is subject to modification. DO NOT USE FOR PROCUREMENT PURPOSES.

1. SCOPE

1.1 This specification covers the requirements for a laminated gasket suitable for use with liquid oxygen and liquid hydrogen in space vehicles.

2. APPLICABLE DOCUMENTS

2.1 The following documents form a part of this specification to the extent specified herein. Unless otherwise indicated, the issue in effect on date of invitation for bids or request for proposals shall apply.

SPECIFICATIONS

George C. Marshall Space Flight Center

MSFC-SPEC-106	Testing Compatibility of Materials for Liquid Oxygen Systems.

STANDARDS

Military

MIL-STD-105	Sampling Procedures and Tables for Inspection by Attributes.

MIL-STD-129 Marking for Shipment and Storage.

MIL-STD-202 Test Methods for Electronic and Electrical Component Parts.

(Copies of specifications, standards, drawings, and publications required by contractors in connection with specific procurement functions should be obtained from the procuring activity or as directed by the contracting officer.)

2.2 Other publications. - The following documents form a part of this specification to the extent specified herein. Unless otherwise indicated, the issue in effect on date of invitation for bids or request for proposals shall apply.

The Consolidated Classification Committee

Uniform Freight Classification Rules

(Application for copies should be addressed to the Consolidated Classification Committee, One Part Avenue at 33rd Street, New York, N.Y. 10016.)

American Trucking Association, Inc.

National Motor Freight Classification Rules

(Application for copies should be addressed to the American Trucking Association, Inc., 1616 P Street N.W. Washington, D.C. 20036.)

3. REQUIREMENTS

3.1 Samples.

3.1.1 Preproduction. - The preproduction sample, when required, shall be capable of meeting the requirements of this specification.

3.1.2 Quality assurance. - The quality assurance sample, when required (see 6.2), shall be capable of meeting the requirements of this specification.

3.2 Materials. - Except as otherwise specified, the selection of materials shall be at the discretion of the contractor. Materials shall be such that the finished product is chemically inert to liquid oxygen and can seal between flanges.

3.3.1 Chemical requirements. - The gasket material shall be chemically inert to liquid oxygen.

3.3.2 Dimensional requirements. - The finished gasket shall meet the following requirements:

(a) The nominal thickness shall be 0.055 to 0.250 inches.

(b) The thickness tolerance shall be ±0.005 inch from average nominal thickness measured at any point.

(c) The width of the gasket shall be as specified ±0.050 inch.

3.4 Construction.

3.4.1 Lamination. - The lamination shall consist of alternate single layers of number 401 heat cleaned glass cloth and 0.005-inch TFE.

3.4.1.1 Orientation of laminates. - Each ply of glass cloth shall be oriented so that the warp direction of each ply is 45° from the one previous. Each ply of TFE shall be oriented 90° from the one previous. The angular rotation shall always be in the same direction. A finished 1/16-inch thick gasket shall have five plies of glass and four plies of TFE. A finished 1/8-inch thick gasket shall have nine plies of glass and eight plies of TFE.

3.4.1.2 Preparation of cutting. - The laminate layup shall be stapled together and marked for cutting into a circle of the specified size for the pressure laminated cure.

3.4.1.3 Curing. - The laminate layup after cutting shall be cured as follows:

(a) Place the layup between clean aluminum caul plates.

(b) Insert an iron-constanstan thermocouple in the layup and place in 382°C press platen.

(c) Lamination time shall be 5 minutes at 382°C. The layup shall then be allowed to cool to 326°C under 500 psi pressure.

3.2.1 Glass cloth. - Number 401 crowfoot satin weave heat cleaned glass cloth shall be used as one of the laminations and shall meet the following requirements:

(a) Nominal range thickness .007 to .010 inch.

(b) Thickness tolerance ±.001 inch from nominal measured at any point on a single roll.

3.2.1.1 Yarn construction. - The yarn shall weigh approximately 8.60 ounces per yard for 38-inch wide material and shall meet the following requirements:

(a) Warp shall be 150 - 1/2.

(b) Fill shall be 150 - 1/2.

(c) Material shall be free from visible defects.

3.2.2 TFE film. - TFE film shall be used as one of the laminations and shall meet the following requirements:

(a) The nominal thickness shall be 0.005 inch.

(b) The thickness tolerance shall be ±10 percent from nominal, measured at any point on a single roll.

(c) Specific gravity shall be 2.15 to 2.20.

3.2.3 FEP film. - The finished laminated gasket shall be encapsulated in FEP film. The FEP film shall meet the following requirements:

(a) The nominal thickness shall be 0.005 to 0.010 inch.

(b) The thickness tolerance shall be ±10 percent from nominal, measured at any point on a single roll.

(c) Specific gravity shall be 2.15 to 2.20.

3.3 Design. - The gasket material shall be designed to conform to the requirements of this specification.

(d) The layup shall then be allowed to cool to room temperature without pressure.

3.4.2 Encapsulation. - The laminate shall be encapsulated in FEP film. 0.005-inch thick FEP film shall be cured on the laminate at 288°C, under 100 psi for 3 minutes and allowed to cool to room temperature under pressure.

3.4.3 Cutting. - The encapsulated laminate shall be cut to final size using a cutter in conjunction with the laminating press. A lead plate shall be used between the press platen and the laminate. Thin sheets of polyethylene shall be used between the laminate and the cutter and the teflon plate.

3.4.4 Trimming. - The laminate shall be trimmed with surgeons scissors to remove any frayed edges or strings. If cutter is sharp and laminate is properly encapsulated this will not occur.

NOTE

The laminate at this time shall be approximately 0.060 inch narrower (inner to outer perimeter), and approximately 0.020 inch thinner (top to bottom) than the nominal size of the finished gasket.

3.4.5 Final encapsulation. - The laminated composite shall be encapsulated as follows:

(a) A layer of TFE impregnated glass cloth shall be placed on the bottom of the female half of the die.

(b) Two layers of 0.005-inch FEP shall be placed on top of the glass cloth.

(c) The laminated composite shall be placed on the FEP.

(d) One strip of 0.010-inch and one strip of 0.005 inch FEP shall be placed on the inside and also the outside perimeter of the laminated composite.

(e) Two layers of 0.005-inch FEP and one layer of TFE impregnated glass shall be placed on top of the laminated composite.

(f) The male half of the die shall be mated to the female half of the die.

(g) The die shall be placed in the press and the press shall be closed to a predetermined distance so that there is a 1/8-inch cavity with the tool. This gives the finished gasket a nominal 1/8-inch thickness. Encapsulating time shall be 3 minutes at 288°C.

3.4.5 Encapsulating tool. - There shall be a chemically nickeled encapsulating die for each size gasket. The inside diameter of the female part shall always be greater than the inside diameter of the finished gasket. (See examples 1 through 3)

Example 1 — For an 8-inch nominal inner diameter gasket the die shall have an inner diameter of 8.010 inches.

Example 2 — For a 12-inch nominal inside diameter gasket the die shall have an inside diameter of 12.015 inches.

Example 3 — For a 26.5 inch nominal inside diameter gasket the die shall have an inside diameter of 26.6 inches.

3.5 Workmanship. - The surface of the completed gasket must be free of flashing, cracks, and radial scoring. The completed gasket must lie flat without evidence of wrinkling, warping, or waviness when under uniform vertical restraint.

4. QUALITY ASSURANCE PROVISIONS

4.1 Responsibility for inspection. - Unless otherwise specified in the contract or purchase order (see 6.2), the supplier is responsible for the performance of all inspection requirements as specified herein. Except as

otherwise specified, the supplier may utilize his own facility or any commercial laboratory acceptable to MSFC. The procuring activity or its designated representative reserves the right to perform any or all of the inspections set forth in the specification where such inspections are deemed necessary to assure supplies and services conform to prescribed requirements.

4.2 Lot size. - Lot size shall be determined by the quantity manufactured as indicated in table I.

Table I. Lot and sample size.

Quantity manufactured	Lot size	Sample quantity
10 or less	All	All
11 to 50	All	10
51 to 100	50	10 each lot
100 to 200	100	20 each lot
over 200	100	20 each lot

4.3 Samples. - Samples will be selected in accordance with table I and Standard MIL-STD-105.

4.3.1 Preproduction sample. - When preproduction tests are required, the preproduction sample shall consist of the contractually stated number of gaskets representative of the identical material and manufacturing process to be used in production. Preproduction sample examinations and tests shall be performed by the contractor under MSFC surveillance, or as directed by the procuring activity at the installation designated by the contract or order (see 6.2).

4.3.1.1 Preproduction rejection. - If any specimen of the preproduction sample fails to meet the requirements of any inspection specified herein, the preproduction sample shall be rejected. Before a new preproduction sample is submitted, a detailed report shall be forwarded to the procuring activity covering the rejection and the action taken to prevent recurrence of the defect causing failure. A reworked preproduction sample shall not be submitted. Production lots will not be considered for acceptance until the preproduction sample has been approved.

4.3.2 Quality assurance. - The quality assurance sample shall be selected at random from the lot submitted for MSFC acceptance at any one time. The number of quality assurance samples to be submitted shall be specified in the contract or order (see 6.2).

4.3.2.1 Quality assurance rejection. - If any specimen of the quality assurance sample fails any inspection specified herein, the entire lot represented by the sample shall be rejected. Before the rejection lot can be resubmitted for acceptance, a detailed report shall be forwarded to the procuring activity covering the rejection and the action taken to prevent recurrence of the defect causing failure. The defect causing failure and the corrective action taken will be the basis for permitting resubmittal. Any reworked lot must be accompanied by a detailed report covering previous rejection and corrective action taken.

4.3.3 Acceptance inspection. - Unless otherwise specified by the procuring activity, an acceptance inspection shall be performed on all items submitted for acceptance at any one time. The acceptance inspection shall consist of all examinations and acceptance tests specified herein.

4.3.3.1 Acceptance inspection rejection. - Any item that fails any acceptance inspection shall be rejected. Rejected items may be resubmitted at the discretion of the procuring activity, after corrective action has been taken. The number and type of defects shall be the basis for permitting resubmittal. Any reworked items shall be accompanied by a detailed report concerning previous rejection and corrective action taken.

4.4 Examination. - The gasket shall be examined to determine conformance to 3.2, 3.3, 3.4, and 3.5. Upon completion of testing, examine preservation, packaging, packing, and marking for conformance to the requirements of section 5.

4.5 Test procedures. - Unless otherwise specified by the contract, detailed test procedures including schematic diagram of test setups and a list of equipment to be utilized for test shall be submitted by the contractor and approved by the procuring activity prior to accomplishment of tests.

4.5.1 Test conditions. - Testing of the gasket shall be accomplished as specified herein. Each gasket submitted for testing shall have passed the examination specified in 4.4.

4.5.2 Preproduction tests. - The preproduction tests, when required, shall consist of all the acceptance tests specified herein. Gaskets subjected to these tests shall be considered unserviceable but may be retained for examination by the procuring activity.

4.5.3 Quality assurance tests. - The quality assurance tests, when required, shall consist of all the preproduction and acceptance tests specified herein. Gaskets subjected to the quality assurance tests shall be considered unserviceable but may be retained for examination by the procuring activity.

4.5.4 Acceptance tests. - Unless otherwise specified by the procuring activity, acceptance tests shall be conducted on all gaskets submitted for MSFC acceptance.

4.5.4.1 Proof pressure. - Proof pressure tests are not necessary for pressures less than 600 psi. For applications where pressures may exceed 600 psi, the procurer shall establish test setup and test procedures to ensure proof pressure exceeds by 50 percent anticipated maximum in-use pressure.

4.5.4.2 LOX compatibility. - Gaskets shall be tested for LOX compatibility in accordance with Specification MSFC-SPEC-106.

4.5.4.3 Liquid hydrogen compatibility. - The gasket shall be compatible with liquid hydrogen except in the presence of oxygen.

4.5.4.4 Vibration. - The gasket shall be vibrated, while assembled between flanges, in accordance with its intended use arrangement, as specified in method 201 of Standard MIL-STD-202, except the following conditions shall apply:

(a) Vibration in the plane parallel to the diameter of the gasket shall be 4 hours.

(b) Vibration in the plane perpendicular to the diameter of the gasket shall be 4 hours.

After vibration the gasket shall meet the requirements of 4.4.

5. PREPARATION FOR DELIVERY

5.1 Unless otherwise specified, the preservation, packaging, and packing may be equivalent to the contractor's best commercial practice, provided that this practice is sufficient to protect the gasket against damage during shipment. Exterior containers shall conform to Uniform Freight Classification Rules for rail shipment or National Motor Freight Classification Rules for truck shipment, as applicable.

5.2 Marking. - Interior and exterior containers shall be marked in accordance with Standard MIL-STD-129.

6. NOTES

6.1 Intended use. - The gasket covered by this specification are intended for use in liquid oxygen, liquid nitrogen, and liquid hydrogen systems of space vehicle's and space vehicle launch complexes.

6.2 Ordering data. - Procurement documents should specify:

(a) Title, number, and date of specification.

(b) Whether preproduction sample is required (see 3.1.1).

(c) Number of gaskets required for preproduction sample (see 4.3.1).

(d) Where the preproduction sample test will be accomplished (see 4.3.1).

(e) Whether quality assurance sample is required (see 3.1.2).

(f) Number of gaskets required for quality assurance sample (see 4.3.2).

(g) Where quality assurance test will be accomplished (see 4.3.3).

(h) Whether special preservation, packaging, packing, and marking is required.

6.3 Changes, deviations, or waivers. - No technical changes, deviations, or waivers will be made to the requirements of this document without the approval of the cognizant design engineering activity of MSFC. All changes, deviations, or waivers will be submitted to the Technical Writing and Editing Section of the Propulsion and Vehicle Engineering Laboratory (R-P&VE-VNW) for coordination with the cognizant design activity.

Notice. - When Government drawings, specifications, or other data are used for any purpose other than in connection with a definitely related Government procurement operation, the United States Government thereby incurs no responsibility nor any obligation whatsoever; and the fact that the Government may have formulated, furnished, or in any way supplied the said drawings, specifications, or other data is not to be regarded by implication or otherwise as in any manner licensing the holder or any other person or corporation, or conveying any rights or permission to manufacture, use, or sell any patented invention that may in any way be related thereto.

Custodian:	Preparing activity:
NASA - George C. Marshall Space Flight Center	George C. Marshall Space Flight Center

CITED REFERENCES

1. "(Proposed) Compatibility Testing, Liquid Oxygen System Materials, Specification for," NASA Specification MSFC-SPEC-106, 14 Aug 1961

2. "Teflon," DuPont Information Bulletin No. X-60d, p. g

3. ASTM D1147-61T, June 1961

4. L. H. Gillespie et al., "New Design for Teflon," Machine Design, 21 Jan 1960, 18 Feb 1960 (reprint)

5. R. F. Robbins et al., Elastomeric Seals and Materials at Cryogenic Temperatures, Quarterly Report 7918, National Bureau of Standards, 15 July 1963

6. R. E. Mowers et al., Program of Testing Nonmetallic Materials at Cryogenic Temperatures, Final Report, Contract AF 04(611)6354, Rocketdyne Division of North American Aviation, Inc., Canoga Park, Calif., 30 Dec 1962

7. T. P. Goodman et al., Design Criteria for Zero-Leakage Connectors for Launch Vehicles, Contract NAS 8-4012, Advanced Technology Laboratories, Schenectady, New York, 15 Mar 1963

8. W. G. Scheck and D. Marano, Development of Improved LOX-Compatible Laminated Gasket Composite, Annual Summary Report, Contract NAS 8-5053, Narmco Research & Development, San Diego, Calif., 15 Aug 1965

9. M. F. Spotts, Design of Machine Elements, Prentice-Hall, Inc., Englewood Cliffs, New Jersey, 1958

10. L. S. Marks, Mechanical Engineers' Handbook, McGraw-Hill, New York, 1956

11. K. H. Lenzen, "Strength and Clamping Force of Bolts," Product Engineering, Dec 1947

12. I. G. Nolt and E. M. Smoley, Techniques for Evaluating Gasket Loads in Flanged Joints, Armstrong Cork Company

13. E. M. Smoley and F. J. Kessler, Retaining Tension in Gasketed Joints, Armstrong Cork Company

14. Gasket Design Manual, Armstrong Cork Company

15. E. M. Smoley, "Design Criteria for Sealing Gasketed Joints," Machine Design, 21 Nov 1963

16. Timoshenko and Goodier, Theory of Elasticity, second edition, Engineering Society Monographs, McGraw-Hill, New York, 1957

UNCITED REFERENCES

1. Irving Roberts, "Gaskets and Bolted Joints," Pressure Vessel and Piping Design; Collected Papers 1927 – 1959, American Society of Mechanical Engineers

2. Ralph H. Sonneborn et al., Fiberglas Reinforced Plastics, first edition, Reinhold Publishing Corporation, New York, 1954

3. MIL-HDBK-17, Plastics for Flight Vehicles, Part I, Reinforced Plastics

4. Poisson's Ratios for Glass-Fabric-Base Plastic Laminates, FPL Report No. 1860, Forest Products Laboratory, Madison, Wis., Jan 1957

5. R. B. Gosnell, Elastomeric Gasket Materials Development for Cryogenic Temperatures, Annual Summary Report, Contract NAS 8-5053, Narmco Research & Development, San Diego, Calif., 15 Apr 1963

6. C. F. Key and W. A. Riehl, Compatibility of Materials with Liquid Oxygen, NASA, George C. Marshall Space Flight Center, Huntsville, Ala., 23 Oct 1963

7. C. F. Key and L. J. Moore, Treatment of Allpax Gasket Material for LOX Service, NASA, George C. Marshall Space Flight Center, Huntsville, Ala., 20 June 1960

8. F. Wilson and J. W. Feldmann, Elastomeric Gasket Materials Development for Cryogenic Temperatures, Annual Summary Report, Contract NAS 8-5053, Narmco Research & Development, San Diego, Calif., 15 June 1964

Distribution List

Contract No. NAS 8-5053

NASA
George C. Marshall Space Flight Center
Huntsville, Alabama
Attn: PR-RC (1 copy)

NASA
George C. Marshall Space Flight Center
Huntsville, Alabama
Attn: MS-IL (1 copy)

NASA
George C. Marshall Space Flight Center
Huntsville, Alabama
Attn: MS-T (1 copy)

NASA
George C. Marshall Space Flight Center
Huntsville, Alabama
Attn: MS-I (2 copies)

NASA
George C. Marshall Space Flight Center
Huntsville, Alabama
Attn: R-P&VE-RI (1 copy)

NASA
George C. Marshall Space Flight Center
Huntsville, Alabama
Attn: R-P&VE-MG (14 copies)

NASA
Manned Spacecraft Center
Houston, Texas
Attn: Dr. Richard Downs (1 copy)

The Boeing Company
Saturn Booster Branch
Aero-Space Division
P.O. Box 26088
New Orleans 26, Louisiana
Attn: Donald R. Glenn (M/S LC-17)
Senior Test Engineer (1 copy)

Douglas Aircraft Corporation
1000 Ocean Park Boulevard
Santa Monica, California
Attn: Mr. J. E. Waisman, Chief
Materials Research &
Production, Methods Section,
Department A-260 (1 copy)

General Dynamics/Astronautics
Post Office Box 1128
San Diego, California 92112
Attn: Louis Canter, Manager
Library and Information
Services 128-00 (2 copies)

Picatinny Arsenal
Plastics Technical Evaluation Center
Dover, New Jersey 07801
Attn: SMUPA-VP3 (1 copy)

US Department of Commerce
National Bureau of Standards
Cryogenic Engineering Laboratory
Boulder, Colorado
Attn: Mr. P. R. Ludtke (1 copy)